WNK1-dependent osmoregulation in $CD4^+$ T cell activation

Joshua Biggs O'May

University College London
and
The Francis Crick Institute
PhD Supervisor: Victor Tybulewicz

A thesis submitted for the degree of
Doctor of Philosophy
University College London
March 2021

Declaration

I, Joshua Biggs O'May confirm that the work presented in this thesis is my own. Where information has been derived from other sources, I confirm that this has been indicated in the thesis.

Abstract

$CD4^+$ T cell activation is critical for the initiation of the adaptive immune response. In particular, through the provision of help to B cells, $CD4^+$ T cells are essential for the generation of high-affinity, class-switched antibodies specific for epitopes on invading pathogens. $CD4^+$ T cells also augment the activation of $CD8^+$ cytotoxic T lymphocytes and modulate the effector function of innate immune cells. These features of the immune response are essential for the clearance of many pathogens and are conditional on the ability of a small population of antigen-specific $CD4^+$ T cells to rapidly expand in response to antigenic challenge. In this study we show that this expansion is strongly dependent on the activity of the WNK1 kinase, and that in the absence of WNK1, $CD4^+$ T cells are unable to support a class-switched antibody response. WNK1 has been extensively studied in the distal nephron of the kidney, where it regulates ion transport, and consequently blood pressure, via the STK39 and OXSR1 kinases and the SLC12A-family of ion co-transporters. Here we show that this osmoregulatory function of WNK1 is required for TCR signalling in $CD4^+$ T cells and the subsequent entry of these cells into G1 phase of the cell cycle. Furthermore, having entered the cell cycle, WNK1-deficient T cells show a reduced rate of DNA replication and activate the ATR-mediated cell cycle checkpoint, resulting in a G2/M blockade. $CD4^+$ T cells carrying mutations in both *Oxsr1* and *Stk39* phenocopy WNK1-deficient T cells, although the defects in TCR-induced proliferation are less severe. Taken together, these data suggest that WNK1 regulates cell cycle progression via the OXSR1 and STK39 signalling pathways, as well as via another, non-canonical pathway. Importantly, the defective TCR signalling and G1 entry exhibited by WNK1-deficient $CD4^+$ T cells can be rescued by activating the cells in hypotonic medium. These novel findings reveal fundamental roles for WNK1 activity and transmembrane water movement in antigen receptor signalling and cell cycle dynamics.

Impact Statement

The discovery that WNK1-dependent signalling regulates many aspects of $CD4^+$ T cell activation has immunological implications for diseases or therapeutics that influence the WNK1 signalling pathway. Pseudohypoaldosteronism type II (PHA-II), for example, is a disease caused by hyperactivation of the WNK signalling pathway. Loop diuretics, such as Bumetanide and Azosemide, are used to treat various edematous conditions and exert their effects by inhibiting NKCC channels, which are core components of the WNK1 signalling pathway. My research suggests that $CD4^+$ T cell proliferation, activation marker expression, cytokine expression, survival and differentiation in patients with dysregulated or therapeutically modulated WNK1 signalling should be investigated. The finding that osmoregulation in particular is critical for so many aspects of $CD4^+$ T cell activation means this investigation should also be extended to any conditions in which $CD4^+$ T cell water transport is affected. For example, hyperglycaemia in diabetic patients increases plasma tonicity and thus will almost certainly affect $CD4^+$ T cell water transport.

The profound effects of WNK1-deficiency on class-switched, antigen-specific antibody responses shows that the WNK1 signalling pathway is critical for this process. This finding could have implications for the design of vaccines, most of which primarily function to generate a robust antibody response to a given antigen. The requirement of WNK1 during ZAP-70 activation, first reported here, may be a universal mechanism present in $CD8^+$ T cells, $\gamma\delta$ T cells and NK cells, all of which depend on ZAP-70 signalling for their function and all of which express WNK1. This would have implications for any therapeutics that manipulate signalling via ZAP-70, such as CAR T-cell therapy.

WNK1 is ubiquitously expressed in mammals and orthologues are present in many different organisms. Therefore, the findings described in this thesis may be relevant in a range of biological contexts outside of the mammalian immune system. The role of WNK1 signalling during cell cycle progression and ATR checkpoint activation, for example, may be a common mechanism to multiple cell types. This could be of interest clinically as WNK1 has been implicated in tumorigenesis as well as metastasis.

In conclusion, by defining the role of the WNK1-OXSR1/STK39 signalling axis during an adaptive immune response and highlighting the fundamental role of osmoregulation during this process I have provided a subject for further study in a range of disease/therapeutic contexts. The mechanistic information presented in this thesis, particularly relating to WNK1-dependent ZAP-70 signalling and WNK1-dependent cell cycle progression, could be important for the understanding of these processes in a range of biological contexts and potentially for the development of novel therapeutics.

Acknowledgements

Thanks very much to Victor for giving me such a fascinating project to work on for my PhD and for all the immunological insight and brilliant ideas you've given me over the years. It has also been a great pleasure to teach you so much about statistical methods and to see how passionate you have become about the subject. I'd also like to say a big thank you to all the members of the Tybulewicz lab for putting up with me for 4.5 years, I look forward to one final year with you all. In particular thank you to Robert for all the great work he had already done characterising the role of WNK1 in $CD4^+$ T cells that really set my project up so nicely and for helping me get started in the lab. Thank you to Lesley for your help making all those chimeras and all the other bits and bobs you've helped me with. Thank you to Darryl and Leon for all the WNK1 chat – it's been great to have other people around me who actually care. Your help in the lab has also been amazing. Thank you to Edina for all your help with the molecular biology and the constant optimism. You would have come higher up the list but the years of BAFF presentations took their toll. Thanks to Daisy for teaching me all her Western blot wizardry.

Thanks also to the members of my thesis committee – Lucy Walker, George Kassiotis, and Erik Sahai for keeping me on the straight and narrow over the course of the project. Thanks Louisa, Jack, Tinashe, and all the BRF staff for looking after my mice over the years. Thanks to mum, dad and grandma for nodding along at all those dinners where I wittered on about science. Finally, thanks to Gems and Tobs for helping me get through the thesis writing process by providing a good old giggle at the end of the day.

Table of Contents

Table of figures

List of tables

Abbreviations

AB-IMDM	Air-buffered Iscove's modified Dulbecco's medium
ACK	Ammonium-chloride-potassium
ADAP	Adhesion- and degranulation-promoting adaptor protein
AE	Anion exchanger
AICD	Activation-induced cell death
AIRE	Autoimmune regulator
AKT	RAC-α serine/threonine-protein kinase/Protein
AP-1	Activator protein 1
APAF-1	Apoptotic protease activating factor 1
APC	Antigen presenting cell
AR	Aldose reductase
ARP	Actin related protein
ASCL2	Achaete-scute homologue 2
ASK3	Apoptosis signal-regulating kinase 3
ATF	Activating transcription factor
ATM	Ataxia telangiectasia mutated
ATR	ATM- and Rad3-related
BCL6	B cell lymphoma 6
BGT-1	Betaine/GABA transporter 1
BLIMP1	B lymphocyte-induced maturation protein 1
BLM	Bloom syndrome protein
BRCA2	Breast cancer 2
BSA	Bovine Serum Albumin
c/p/dSMAC	Central/peripheral/distal supramolecular activation complex
CBL-B	Casitas B-lineage lymphoma proto-oncogene-b
CCL	Chemokine (C-C motif) Ligand
CCR	Chemokine (C-C motif) Receptor
CCT	Conserved C Terminal
CDC	Cell division cycle

CDK	Cyclin-dependent kinase
CFTR	Cystic fibrosis transmembrane conductance regulator
cGAMP	Cyclic guanosine monophosphate-adenosine monophosphate
cGAS	cGAMP synthase
CGG	Chicken gamma globulin
CHK1	Checkpoint kinase 1
CLIP	Class II-associated invariant chain peptide
CMG	CDC45-MCM-GINS
CREB	cAMP response element-binding protein
CSK	C-terminal SRC kinase
CTLA4	Cytotoxic T-lymphocyte associated protein 4
CTV	CellTrace Violet
CUL3	Cullin 3
CXCL	C-X-C motif chemokine ligand
CXCR	C-X-C motif chemokine receptor
DAG	Diacyl glycerol
DAMP	Damage-associated molecular pattern
DC	Dendritic cell
DMSO	Dimethyl sulphoxide
DN	Double negative
DNA	Deoxyribonucleic acid
DSB	Double strand break
dsRNA	Double stranded RNA
DUSP	Dual specificity phosphatase
E2F	E2 factor
EBI2	Epstein-Barr virus-induced G protein coupled receptor 2
EDTA	Ethylenediaminetetraacetic acid
EdU	5’-Ethynyl-2’-deoxyuridine
EGF	Epidermal growth factor
EGR-1	Early growth response 1
ELISA	Enzyme-linked immunosorbent assay

ENSA	α-endosulfine
ER	Endoplasmic reticulum
ERK	Extracellular signal-regulated kinase
ERT2	Estrogen receptor T2
ETP	Early thymic progenitors
ETS	E26 transformation-specific
FACS	Fluorescence-activated cell sorting
FADD	FAS-associated protein with death domain
FANCD2	Fanconi anemia complementation group D2
FCS	Foetal calf serum
FLIP	FLICE (FADD-like IL-1β-converting enzyme)-inhibitory protein
FOXO3A	Forkhead box protein 3A
FOXP3	Forkhead box protein P3
FRC	Fibroblastic reticular cell
FRET	Förster resonance energy transfer
GABA	γ-aminobutyric acid
GADD45β	Growth arrest and DNA-damage-inducible β
GADS	GRB2 related adaptor protein downstream of SHC
GAP	GTPase activating protein
GDP	Guanosine diphosphate
GEF	Guanine nucleotide exchange factor
GRB2	Growth factor receptor-bound protein 2
GSK-3	Glycogen synthase kinase 3
GTP	Guanosine triphosphate
GWL	Greatwall
HRR	Homologous recombination repair
HSC	Haematopoietic stem cell
HU	Hydroxyurea
IAP	Inhibitor of apoptosis
ICAM-1	Intercellular adhesion molecule 1
ICOS(L)	Inducible costimulator (ligand)
IFN	Interferon

Ig	Immunoglobulin
IGF	Insulin-like growth factor
IL	Interleukin
iNOS	Inducible nitric oxide synthase
IP_3	Inositol-1,4,5-triphosphate
ITAM	Immunoreceptor tyrosine-baswed activation motif
ITK	IL-2-inducible T-cell kinase
KAP-1	KRAB-associated protein 1
KCC	Potassium-chloride cotransporter
KLF2	Krüppel-like factor 2
KLHL3	Kelch-like protein 3
LAT	Linker for activation of T cells
LCK	Lymphocyte-specific protein tyrosine kinase
LFA-1	Lymphocyte function-associated antigen 1
MACS	Magnetic-activated cell sorting
MAPK	Mitogen-activated protein kinase
MCM	Minichromosome maintenance
MEF2	Myocyte enhancer factor 2
MEK	MAP/ERK kinases
MEKK	MEK kinase
MFI	Median fluorescence intensity
MHC	Major histocompatibility complex
mLN	Mesenteric lymph nodes
MRN	MRE11, RAD50, NBS1 complex
mTEC	Medullary thymic epithelial cells
mTORC1	Mammalian target of rapamycin complex 1
MYC	Myelocytoatosis oncogene
MYT1	Membrane-associated tyrosine- and threonine-specific cdc2-inhibitory kinase
NCC	Sodium-chloride symporter
NCK	Non-catalytic region of tyrosine kinase
NEDD4L	E3 ubiquitin-protein ligase NEDD4-like
NFAT	Nuclear factor of activated T cells

NFκB	Nuclear factor kappa-light-chain-enhancer of activated B cells
NHE	Sodium-hydrogen antiporter
NHEJ	Non-homologous end joining
NKCC	Sodium-potassium-chloride cotransporter
NLRP3	NOD-, LRR- and pyrin domain containing protein 3
NMR	Nuclear magnetic resonance
NO	Nitrtic oxide
NP	4-hydroxy-3-nitrophenylacetyl
NRDP1	Neuregulin receptor degradation protein 1
ORC	Origin recognition complex
OTUD7B	OTU domain-containing protein 7B
OVA	Ovalbumin
OXSR1	Oxidative stress responsive 1
p-MHC	Peptide-MHC
PAMPs	Pathogen-associated molecular pattern
PANX	Pannexin 1
PBC	Peptide-binding cleft
PBS	Phosphate buffered saline
PD-1	Programmed cell death protein 1
PD-L1	Programmed death ligand 1
PDK1	Phosphoinositide-dependent kinase-1
PFA	Paraformaldehyde
PH	Pleckstrin homology
PHA-II	Pseudohypoaldosteronism type II
PI3K	Phosphoinositide 3-kinase
PIP_2	Phosphatidylinositol-4,5-bisphosphate
PIP_3	Phosphatidylinositol-3,4,5-triphosphate
PKCθ	Protein kinase C θ
PKD1	Protein kinase D
PLCγ1	Phospholipase C γ1
PP2A	Protein phosphatase 2A
PP6	Protein phosphatase 6

PRR	Pattern recognition receptor
PSGL-1	P-selectin glycoprotein ligand 1
PTPN	Protein tyrosine phosphatases non-receptor type
PVDF	Polyvinylidene difluoride
qPCR	Quantitative polymerase chain reaction
RAC	RAS-related C3 botulinum substrate
RAF-1	Rapidly accelerated fibrosarcoma
RAG	Recombination activating gene
RAP1	RAS-related protein 1
RAPL	Regulator for cell adhesion and polarization enriched in lymphoid tissues
RAPTOR	Regulatory-associated protein of mammalian target of rapamycin
RASGRP1	RAS guanyl-releasing protein 1
RB	Retinoblastoma
RCE	Gt(ROSA)26Sor$^{tm1(Cre/ESR1)Thl}$
RHEB	Ras homolog enriched in brain
RHEB	Ras homolog enriched in brain
RHO	Ras homologous
RIAM	RAP1-GTP-interacting adapter molecule
RIF1	RAP1-interacting fator 1
RNA	Ribonucleic acid
ROMK	Renal outer medullary potassium channel
RORγt	RAR-related orphan receptor γt
RPA	Replication protein A
RPMI+	Roswell Park Memorial Institute
RSK	Ribosomal S6 kinase
RT-qPCR	Reverse transcription – quantitative polymerase chain reaction
RVD	Regulatory volume decrease
RVI	Regulatory volume increase
S1K	Schedule 1 killing
S1PR1	Sphingosine-1-phosphate receptor 1

SDS	Dodium dodecyl sulfate
SGK1	Serum and glucocorticoid-regulated kinase 1
SH2/3	SRC homology 2/3
SHP1	SRC homology region 2 domain-containing phosphatase-1
SKAP	SRC kinase associated protein
SLC	Solute carrier
SLP-76	SH2 domain-containing protein of 76 kDa
SMARCAL1	SWI/SNF-related matrix-associated actin-dependent regulator of chromatin subfamily A-like protein 1
SMIT	Na^+-dependent myo-inositol transporter
SOS	Son of sevenless homologue 1
SP1	Specificity protein 1
SRC	Sarcoma
SREBP	Sterol regulatory element binding proteins
STAT	Signal transducer and activator of transcription
STIM	Stromal interaction molecule
STK39	Serine/threonine kinase 39
STS	Supressor of T cell signalling
T-BET	T-box expressed on T cells
TauT	Taurine transporter
TBS-T	Tris-buffered saline + 0.05% tween
TCF-1	T cell factor 1
TCR	T cell receptor
TdT	Terminal deoxynucleotidyl transferase
T_{FH}	T follicular helper
TGFβ	Transforming growth fator β
T_H	T helper
TIRF	Total internal reflection fluorescence
TLR	Toll-like receptor
TNFα	Tumour necrosis factor α
TNFR	TNF receptor
TOPBP1	Topoisomerase IIβ-binding protein 1

T_{reg}	T regulatory
TSC1/2	Tuberous sclerosis 1/2
TSP	Thymus-seeding progenitor
UBA	Ubiquitin-associated
WASP	Wiskott-Aldrich Syndrome protein
WAVE	WAS Family verprolin-homologous protein
WNK	With-no-lysine
WRN	Werner syndrome helicase
WT	Wild type
XPA	Xeroderma Pigmentosum group A
XRCC2	X-ray repair cross complementing 2
ZAP-70	Zeta chain-associated protein kinase 70

Chapter 1. Introduction

Living organisms have to defend against many different types of pathogen including bacteria, viruses, fungi and eukaryotic parasites, which seek to exploit the rich environment provided by a host. To control and eliminate these pathogens jawed vertebrates have evolved an immune system consisting of two arms – innate and adaptive – which are able to communicate and together facilitate the clearance of this multitude of pathogens. The immune system is also capable of facilitating clearance of transformed cells although this tumour surveillance function of the immune system will not be discussed. Immune cells known as leukocytes mediate the innate and adaptive immune responses via both cellular and humoral mechanisms.

1.1 Innate immune system

The innate immune system is comprised of many phagocytic cell types which patrol the tissue environment and are the first immune cells to encounter a pathogen once the epithelial layer is breached. Innate immune cells are able to recognise pathogens via structures known as PAMPs – pathogen associated molecular patterns. These structures are highly conserved and often indispensable for pathogen survival. Examples include lipopolysaccharide which is required to build the outer membrane of gram-negative bacteria and double stranded RNA (dsRNA) sequences which make up the genome of some viruses. Innate immune cells are also able to recognise DAMPs – damage associated molecular patterns – which are endogenous molecules released during tissue damage and are a sign that infection is taking place (Hou et al., 2013). One example would be histones which are released from the intracellular compartment during cell damage. PAMPs and DAMPs are recognised by germline-encoded pattern recognition receptors (PRRs) present in the cytosol, endosomal compartments, plasma membrane or secreted into the extracellular milieu (Takeuchi and Akira, 2010). There are many different types of PRR, each of which recognises a different PAMP. Examples include cGAMP synthase (cGAS), toll-like receptors and collectins.

The complement system is also able to specifically target foreign microorganisms resulting in their opsonization and/or lysis. This proteolytic cascade involves ~20 proteins present in the blood and extracellular fluid and can be triggered by antibodies or fluid-phase PRRs bound to the surface of pathogens. Alternatively, the cascade can be initiated by the spontaneous formation of a C3 convertase complex at the surface of a pathogen. The presence of Factor H on host cells blocks C3 convertase assembly, whereas assembly is uninhibited at the surface of pathogens to which Factor H is not bound. This allows the complement pathway to distinguish between foreign and host cells (Ricklin et al., 2010). Opsonisation is achieved through the enzymatic formation of the C3b complement protein fragment which covalently binds to the surface of foreign pathogens via an ester bond and can be recognised by complement receptors on the surface of innate immune cells.

Activation of PRRs or complement receptors by ligand-binding induces innate immune cell effector functions, such as phagocytosis, and the expression of a variety of host genes, the identity of which can depend on the type of PAMP/DAMP, and therefore pathogen, encountered (Guha and Mackman, 2001; Moretti and Blander, 2014). These genes encode proteins such as pro-inflammatory chemokines, cytokines, antimicrobial proteins and costimulatory molecules.

Chemokines mediate the recruitment of leukocytes to the site of infection. These molecules diffuse through the extracellular space and bind and activate chemokine receptors expressed on the surface of immune cells to change their migratory behaviour. For example, neutrophils, which are the first innate immune cell types recruited to the site of infection, detect the presence of chemokines produced at the site of injury such as CXCL1, CXCL2 and CXCL8 via CXCR1 and CXCR2 chemokine receptors (Rajarathnam et al., 2019).

Cytokines are soluble secreted proteins that have a range of autocrine and paracrine functions and can exert their effect at both the local and systemic level. For example, IFNα and IFNβ are produced in the presence of viral nucleic acids and induce an antiviral state in infected and neighbouring cells rendering them refractory to viral replication (Gautier et al., 2005). Acute phase cytokines such as IL-1β, IL-6 and TNFα exert their activity at the systemic level by acting on the hypothalamus to increase body temperature and on hepatocytes to secrete soluble PRRs (Dinarello, 1989). IL-1β, IL-6 and TNFα can also act locally on the endothelium inducing

vasodilation, an increase in endothelial permeability, and the expression of adhesion factors required for the recruitment of leukocytes (Dinarello, 1989; Smith et al., 1989).

The specific cytokine environment is determined by the type of invading pathogen and elicits an immune response appropriate for that pathogen. For example, IL-4 is produced in the presence of extracellular parasites such as *Nippostrongylus brasiliensis*, whereas IL-12 and IFNγ are produced in the presence of intracellular pathogens such as *Listeria monocytogenes* or *Toxoplasma gondii* (Bancroft et al., 1991; Reis e Sousa et al., 1997; Shinkai et al., 2002). These cytokines direct the type of effector functions employed by both innate and adaptive immune cells. For example, IFNγ activates the cytoplasmic enzyme iNOS in innate immune cells to produce NO free radicals capable of directly killing intracellular pathogens, but also instructs B cells to produce the IgG2a antibody isotype.

Additional to the cytokine environment they produce, early responding innate immune cells present at the site of infection are also responsible for communicating supplementary information about the invading pathogen to the adaptive arm of the immune system. This information is in the form of pathogen-derived peptides presented on major histone compatibility (MHC) molecules at the cell surface. MHC molecules are extremely polymorphic and are expressed on the surface of cells even in the absence of infection. In general MHC class I (MHC-I) molecules present peptides of cytoplasmic or nuclear origin generated by the endogenous pathway of antigen processing, whereas MHC class II (MHC-II) molecules present peptides of extracellular origin generated by the exogenous pathway of presentation (Blum et al., 2013). However, crossover between the pathways does occur when exogenous antigens escape the endosomal compartment into the cytoplasm and are loaded onto MHC-I molecules in a process known as cross-presentation. Additionally, autophagy can deliver endogenous antigens to the MHC-II pathway (Dengjel et al., 2005).

MHC-II proteins are assembled in the endoplasmic reticulum where their peptide binding cleft (PBC) is occupied by an invariant peptide (CLIP). These complexes are subsequently trafficked to lysosomes which are then fused with phagosomes containing phagocytosed material. Lysosomal fusion results in acidification and triggers that activity of acid hydrolases and cathepsis which cleave the phagocytosed proteins via proteolysis to generate peptides. Displacement of CLIP by these exogenous peptides is mediated by H-2M in mice and the resulting

peptide-MHC-II (p-MHC-II) complex is trafficked to the plasma membrane (Vyas et al., 2007). PRR signalling enhances the efficiency of peptide loading and presentation by promoting MHC expression, phagosome maturation and the formation of endolysosomal tubules which transport peptide-MHC-II complexes to the plasma membrane (Inaba et al., 2000; Vyas et al., 2007).

Dendritic cells (DCs) and macrophages, both myeloid cell lineages, are particularly efficient at antigen presentation and are designated as professional antigen presenting cells (APCs), although it is thought that DCs are the most potent in terms of initiating an adaptive immune response (Banchereau et al., 2000). Activation of certain PRRs, such as TLR4, or the presence of inflammatory cytokines, such as TNFα, induces a program of maturation in these cells (Shen et al., 2008; Chabot et al., 2016). DC maturation is a complex developmental pathway which involves changes to antigen capture and processing efficiency as well as T cell priming capacity. It is widely accepted that a transient increase in antigen capture and processing efficiency during maturation is followed by a dramatic attenuation of this function involving the downregulation of antigen uptake receptors such as FcγRIIB (Liu et al., 2006). This change is associated with an increase in T cell priming capacity attributed to the upregulation of MHC, adhesion and costimulatory molecules by mature DCs (Cella et al., 1997; Manickasingham and Reis e Sousa, 2001; Larsen et al., 1992). Costimulatory molecules such as CD40, CD80 and CD86 are thought to mark DCs which have encountered pathogen and are therefore presenting pathogen-derived peptides on their surface. This distinguishes these cells from those which are presenting self-peptides to which an adaptive immune response should not be mounted.

DCs are continuously recirculating from peripheral tissues to secondary lymphoid tissues (Huang et al., 2000). Maturation results in the upregulation of the CCR7 chemokine receptor which increases mature DC responsiveness to CCL21 and CCL19. These proteins are chemokines constitutively produced in the T cell area of secondary lymphoid organs by fibroblastic reticular cells (FRCs). CCR7 signalling skews mature DC migration towards higher concentrations of CCL21 and CCL19 and ultimately results in their homing to the T cell zone of secondary lymphoid tissues (Asselin-Paturel et al., 2005; Jarrossay et al., 2001). Through this mechanism antigens acquired in the periphery are thus concentrated in the T cell zone of secondary lymphoid organs where they can be efficiently identified by adaptive

immune cells. This dramatically increases the likelihood that the adaptive immune system is able mount a response to the invading pathogen.

1.2 Adaptive immunity

T cells are able to provide specificity for the invading pathogen by distinguishing between self and non-self peptides presented on MHC molecules via their antigen receptor known as the T cell receptor (TCR). This specificity allows the immune system to target a foreign pathogen while limiting immunopathology against the host. Innate immune cells rely on conserved PAMPs present in many species to identify foreign agents whereas T cells are able to provide specificity for novel protein sequences unique to the invading pathogen. This function expands the repertoire of determinants which can be used to identify the foreign agent and allows the host immune response to recognise pathogens despite their continuing evolution. Additionally, long-term persistence of antigen-specific adaptive immune cells generates immune memory which facilitates a rapid adaptive immune response to re-infection.

1.3 T cell development

Thymus seeding progenitor (TSPs) cells derived from haematopoietic stem cells (HSCs) in the bone marrow migrate to the thymus where they undergo a complex developmental program producing naive T cells. The predominant function of this developmental pathway is to generate naïve T cells with a broad repertoire of self-tolerant TCRs capable of binding p-MHC molecules.

Upon entering the thymus, TSPs receive signals from Notch ligands which enforce an early T lineage gene expression programme by inducing the expression of TCF-1 and GATA-3 transcription factors (Germar et al., 2011; Hosoya et al., 2009). Notch signalling promotes proliferation and differentiation into early thymic progenitors (ETPs) characterised as $CD4^{-}CD8^{-}CD25^{-}CD44^{+}KIT^{hi}$ cells (Figure 1). C-KIT is the receptor for stem cell factor (Godfrey et al., 1993).

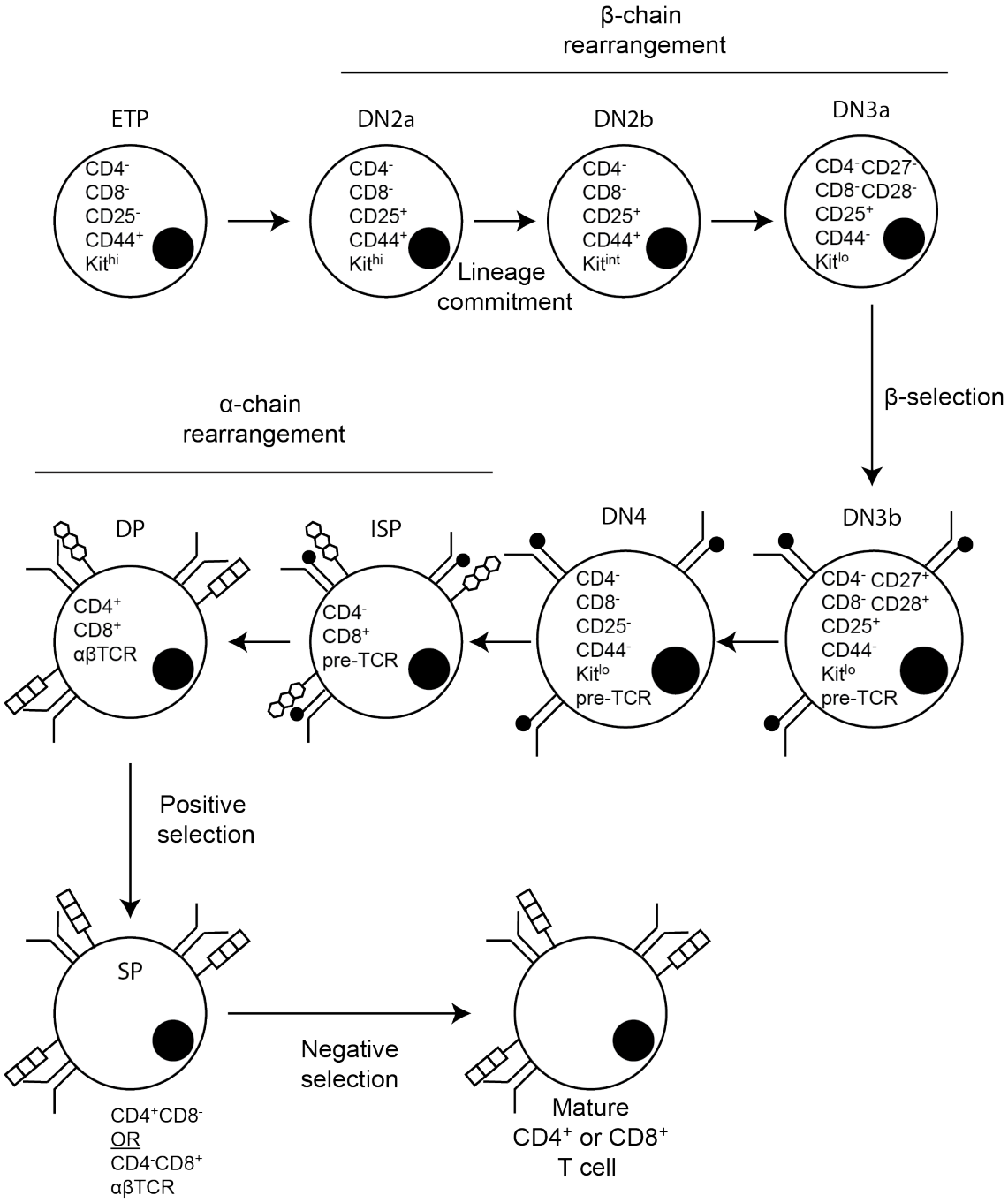

Figure 1. T cell development in the thymus. Multipotent early thymic progenitor (ETP) cells enter the thymus where they undergo a lengthy developmental program to produce mature $CD4^+$ or $CD8^+$ T cells. ETPs transit through a large number of intermediates which are characterised by cell surface expression of markers such as CD25, CD27, CD28, CD44 and C-KIT as well as CD4 and CD8. During this process rearrangement of the α and β TCR chains takes place to generate a diverse repertoire of receptors. Subsequently cells undergo positive selection and negative selection during which cells expressing TCRs incapable of binding to p-MHC molecules and those expressing self-reactive TCRs are eliminated.

Under the influence of continuing Notch stimulation ETPs differentiate further into $CD4^-CD8^-CD25^+CD44^+KIT^{hi}$ DN2a cells and subsequently $CD4^-CD8^-CD25^+CD44^+KIT^{int}$ DN2b cells which are fully committed to the T cell lineage due to an increase in the activity of the BCL11B transcription factor (Yui et al., 2010). After differentiating through the $CD4^-CD8^-CD25^+CD44^-KIT^{lo}CD28^-CD27^-$ DN3a stage, the β-selection-checkpoint is reached. Cells can only transit through this checkpoint to become $CD4^-CD8^-CD25^+CD44^-KIT^{lo}CD28^+CD27^+$ DN3b cells if a successful pairing between the rearranged β-chain and the pre-TCRα chain is achieved (Williams et al., 2005; Ciofani et al., 2006). Alternatively, DN3 cells can express the γδ TCR chains and divert to a parallel developmental pathway to become γδ T cells whereas pre-TCR-expressing cells differentiate further to become αβ T cells (Lauritsen et al., 2009).

Successful rearrangement of the TCR β chain locus during DN2 and DN3 stages of development is required for successful negotiation of the β-selection checkpoint and progression to the DN4 stage of T cell development (Mallick et al., 1993). β chain rearrangement occurs through the activity of the RAG1/RAG2 recombinase which mediates site-directed rearrangement of variable (V), diversity (D) and joining (J) gene segments within this locus (Shinkai et al., 1992). Diversity in rearranged β chain coding sequences is generated mainly through differences in the precise combination of V, D and J segments used and augmented by the activity of the terminal deoxynucleotidyl transferase (TdT) which adds nucleotides in the junctions between recombined gene segments (Cabaniols et al., 2001).

Following successful β chain rearrangement and pre-TCR expression, DN3 cells differentiate into DN4 cells. The β-selection signal is thought to be driven by pre-TCR oligomerisation at the cell surface and is accompanied by upregulation of CD27 and CD28, downregulation of CD25, and successive rounds of proliferation mediated by hyperphosphorylation of retinoblastoma protein (RB) and an increase in CDK activity (Yamasaki et al., 2006; Hoffman et al., 1996; Godfrey et al., 1993). In fact, pre-TCR-dependent proliferation is a pre-requisite for DN4 differentiation in this case (Kreslavsky et al., 2012). DN4 cells transiently progress through an immature single positive (ISP) $CD8^+CD4^-$ stage before becoming double positive (DP) cells characterised by dual expression of CD4 and CD8 co-receptor molecules (Shinkai et al., 1993). At this phase of development rearrangement of V and J

segments at the α chain locus takes place, again mediated by the activity of the RAG1/RAG2 recombinase and TdT, generating further diversity in the TCR. This process continues until the cell successfully navigates the positive selection checkpoint or dies due to neglect (Petrie et al., 1993; Brändle et al., 1992). Productive α chain rearrangement is followed by surface expression of the αβ TCR and positive and negative selection checkpoints (Wilson et al., 1996).

The TCR pairs with both CD4 and CD8 co-receptor molecules at the surface of DP cells. The CD4 and CD8 co-receptors determine specificity for either peptide-MHC-II or peptide-MHC-I complexes, respectively, as they bind to the base of MHC molecules near the plasma membrane stabilising the interaction (König et al., 1992; Sun et al., 1995). The presence of both CD4- and CD8-associated TCRs on the surface of DP cells allows them to practice antigen recognition by scanning p-MHC-I and -II molecules presented mainly on cortical thymic epithelial cells. Peptides presented on these cells are mainly generated through macroautophagy and are thus self-antigens (Aichinger et al., 2013). A positive selection signal is delivered to the cell when TCR complexes successfully engage peptide-MHC complexes with sufficient affinity resulting in enhanced survival and cessation of further α chain rearrangements (Starr et al., 2003). Partial downregulation of CD8 allows the cell to determine whether the TCR is MHC-I or MHC-II restricted. A drop in the signal strength during CD8 downregulation reveals that the TCR is MHC-I restricted and induces $CD8^+$ cytotoxic T cell differentiation whereas sustained TCR signalling during CD8 downregulation shows that the TCR is MHC-II restricted and results in $CD4^+$ T helper (T_H) cell differentiation (Singer et al., 2008).

These $CD4^+$ and $CD8^+$ T cells must also undergo negative selection during which self-reactive T cells are deleted from the population. $CD4^+$ and $CD8^+$ T cells scan DCs in the thymic cortex presenting ubiquitous self-antigens and medullary thymic epithelial cells (mTECs) presenting tissue specific self-antigens, the expression of which is driven by the extremely promiscuous transcription factor AIRE (Gotter et al., 2004). mTECs are also able to handover antigens to thymic DCs for cross-presentation (Hubert et al., 2011). TCR binding to a self p-MHC complex presented by one of these cell types with affinity above a certain threshold results in apoptosis, although negative selection is not a perfect process and some self-reactive T cells do escape deletion (Gascoigne et al., 2016). Nonetheless, in general,

naïve T cells emerging from the thymus are capable of binding p-MHC complexes and are self-tolerant.

1.4 $CD4^+$ T cell migration

After exiting the thymus naïve T cells continuously recirculate between the vasculature and secondary lymphoid organs including the spleen, lymph nodes and mucosa-associated lymphoid tissue. In these secondary lymphoid tissues they scan p-MHC complexes presented by APCs to identify those to which their TCR is specific. The likelihood that a naïve T cell encounters its cognate p-MHC complex is inherently small and it is estimated that a unique p-MHC-II molecule can be recognised by only 1:1,000,000 $CD4^+$ T cells (Jenkins et al., 2010). Continuous recirculation between secondary lymphoid organs and rapid migration within them greatly enhances the likelihood that a T cell will encounter a cognate p-MHC complex identifying it as foreign and initiate an adaptive immune response towards the antigen.

Naïve $CD4^+$ T cells use a “random walk” pattern of migration within the T cell zone of secondary lymphoid tissues (Textor et al., 2011). Their motility is supported by the network of FRCs which produce chemokines such as CCL21, CCL19 and CXCL12 that further enhance migration speed (Bajenoff et al., 2006; Worbs et al., 2007). Interstitial migration of naïve $CD4^+$ T cells in the T cell zone is dependent on actomyosin dynamics and largely occurs in an integrin-independent manner (Woolf et al., 2007). Ligand-binding to chemokine receptors stimulates polarity establishment and motility via Rho GTPases. RAC1 and RAC2 polarise to the leading edge of the cell where they mediate extension of pseudopodia structures by stimulating actin polymerisation into filamentous actin (F-actin) (Faroudi et al., 2010). The trailing edge, known as the uropod, is a rigid structure stabilised by interactions between the plasma membrane and actomyosin cortex, a stable actin-rich structure proximal to the membrane. This interaction is mediated by ERM proteins which bind to the C-terminal of F-actin and the N-terminal domains of transmembrane proteins polarised to the uropod, such as CD44 (Lee et al., 2004). Pseudopodia extension coupled to uropod contraction, a process which is facilitated by RhoA-dependent regulation of Myosin-IIA activity, leads to rapid forward motion (Lammermann et al.,

2008; Soriano et al., 2011). This migration mechanism allows naïve $CD4^+$ T cells to migrate at ~10-12μm/min and interact with ~100 DCs per hour (Beltman et al., 2007).

When naïve T cells encounter cognate-antigen presented on the surface of an APC, TCR signalling results in an increase in the frequency of Ca^{2+} fluxes into the cell, an increase in the basal concentration of intracellular calcium, arrest of movement, and the formation of a stable integrin-mediated contact with the APC (Wei et al., 2007b). This contact is maintained for several hours and mediated by a specialised structure known as the immunological synapse.

1.5 $CD4^+$ T cell activation

1.5.1 Immunological synapse

The immunological synapse (IS) is a highly compartmentalised structure consisting of a central supramolecular activation cluster (cSMAC) surrounded by two radial rings known as the peripheral SMAC (pSMAC), the distal SMAC (dSMAC) as well as stable TCR microclusters. The IS is stabilised by interactions between the integrin - LFA-1 – expressed on the surface of T cells and its ligand – ICAM-1 – expressed on the surface of APCs. These LFA-1-ICAM-1 complexes are organised to form the pSMAC (Monks et al., 1998). TCR-p-MHC complexes continuously form microclusters in a phosphorylation-independent but actin-dependent manner at the periphery of the IS (Campi et al., 2005). These structures are several hundred nanometres in diameter and contain a vast array of downstream signalling molecules including LCK, ZAP-70, SLP-76 and LAT (Bunnell et al., 2002). While initially being associated with active downstream signalling, microcusters subsequently undergo actin-mediated transport to the cSMAC, during which downstream signalling molecules such as ZAP-70 and SLP-76 dissociate (Yokosuka et al., 2005). This relocalisation results in interruption of signalling and ubiquitin-dependent TCR degradation (Varma et al., 2006).

1.5.2 TCR triggering

TCRs are able to interact with a range of p-MHC complexes, including those presenting self-peptides, at a wide range of affinities (K_D = 1-200μM). Additionally,

agonist p-MHC complexes are present on the surface of APCs at vanishingly low frequencies (Mazza et al., 2007). Despite these unusual receptor-ligand binding characteristics T cells are able to distinguish between self and non-self p-MHC ligands with high selectivity and even a single agonist p-MHC molecule is enough to induce T cell activation exemplifying the exquisite sensitivity of the TCR (Huang et al., 2013).

The TCRs inherent affinity for some self p-MHC molecules means that activation of TCR signalling cannot proceed via the “occupancy model”. This model stipulates that signalling is induced if the T cell engages a threshold number of TCRs at any given time. Because the number of low affinity TCR interactions with highly abundant self p-MHC molecules could easily match, or even surpass, the number of high affinity interactions with rare agonist p-MHC molecules this mechanism would not allow for discrimination between self and non-self p-MHC complexes. The “kinetic proofreading” model offers a possible mechanism by which the TCR could discriminate between self and non-self ligands (McKeithan, 1995). It proposes that the T cell determines the TCRs affinity for a ligand by measuring the lifetime, or half-life, of the interaction. This binding characteristic is directly related to the receptor’s affinity for a ligand. Lifetime measurements would require there to be series of enzymatic steps before a second messenger is generated and disseminated to the rest of the cell to provide a time delay between ligand-binding and output, in this case T cell activation. This model also requires these enzymatic steps to be reversible, for example through the action of phosphatases. Fast dissociation from self p-MHC molecules would therefore occur during this time delay preventing productive signalling downstream. An elegant study from Yousefi *et al.* using optogenetic control of the TCR binding kinetics showed that Ca^{2+} flux only occurred if a threshold half-life of 8 seconds was reached and that this was relatively independent of ligand concentration (Yousefi et al., 2019). This model however cannot account for the range of individual receptor-ligand interaction lifetimes that occur for a given half-life. It may be the case that repeated p-MHC sampling is required to provide lifetime measurements with high confidence. In fact, aggregate dwell times are the best predictor of TCR ligand potency as they can account for the existence of highly stimulatory ligands that have a short $T_{1/2}$ but a fast K_{on} (Govern et al., 2010).

Another “mechanical proofreading” model postulates that the TCR acts as a mechanosensor. This model was prompted by the seminal observation by Kim *et al.*

that TCR triggering requires pN forces applied perpendicularly to the membrane with cognate, but not irrelevant, p-MHC molecules (Kim et al., 2009). This model is made more compelling by evidence showing that the TCR transmits >12pN forces to p-MHC molecules, and this is required for antigen specificity (Liu et al., 2016). An interesting observation which may shed light onto the mechanism for mechanical proofreading is that interaction between TCRs and non-cognate p-MHC complexes have “slip bond” characteristics meaning they exhibit reduced lifetimes under force, whereas interactions with cognate p-MHC complexes have “catch bond” characteristics meaning they increase in life-time under tension (Liu et al., 2014a). This would align with the previous model described as cognate p-MHC interactions would therefore have longer half-lives, enhancing the cell’s ability to carry out kinetic proofreading. Mechanical proofreading may also be achieved by a “strain test” in which the TCR would undergo a conformational change but only if ligand-binding was of a sufficient affinity.

The TCR is associated with CD3ε,γ,δ and ζ polypeptides forming a multimeric receptor complex with a stoichiometry of TCR$\alpha\beta$-CD3$\varepsilon\gamma$-CD3$\varepsilon\delta$-CD3$\zeta\zeta$. TCR α and β chains contain no cytoplasmic signalling motifs, whereas CD3 molecules provide a multitude of immunoreceptor tyrosine-based activation motifs (ITAMs) which are responsible for transmission of the signal into the cytoplasm. Ligand-binding induces an intracellular tyrosine phosphorylation cascade. One of the earliest events in this signalling pathway is the phosphorylation of tyrosine residues in the ITAMs present in the cytoplasmic domains of CD3 molecules. This process is mediated by the constitutively active LCK tyrosine kinase which is constitutively bound to the cytoplasmic tail of the CD4 co-receptor (Love and Hayes, 2010; Nika et al., 2010a). Phosphorylated ITAMs act as a scaffold for ZAP-70 recruitment which binds via its SH2-domain. LCK is then able to phosphorylate and activate ZAP-70 which in turn phosphorylates LAT and SLP76 (Wardenburg et al., 1996; Zhang et al., 1998). These ZAP-70 mediated phosphorylation events lead to the nucleation of a membrane-bound signalling complex, known as the LAT signalosome, which is membrane-anchored via LAT and acts to activate a myriad of downstream signalling pathways discussed below in Chapter 0.

Although these early signalling events are well established there are multiple models that attempt to explain the mechanism by which the TCR signalling complex transmits signals across the plasma membrane to initiate this phosphorylation

cascade. One prominent model proposes that ligand-binding induces a conformational change in the TCR-CD3 signalling complex that transmits information across the plasma membrane, similar to most germline-encoded cell surface receptors. CD3ε and ζ polypeptide chains contain highly basic regions in their intracellular domains which are buried in the negatively charged phospholipids on the inner leaflet of the plasma membrane. Upon TCR engagement, a conformational change is thought to release these polybasic motifs from the membrane, a process which would render the associated ITAMs susceptible to phosphorylation by LCK (Gagnon et al., 2012; Zhang et al., 2011a). The CD3ε cytoplasmic domains also contains a proline-rich sequence which is inaccessible under unstimulated conditions but is exposed upon TCR activation facilitating the recruitment of NCK via its SH3 domain, although it is unclear whether this interaction is required for T cell activation (Szymczak et al., 2005; Tailor et al., 2008).

The mechanism by which conformational changes that occur in the TCR α and β chains could be transmitted to the CD3 cytoplasmic tails remains unclear. NMR spectroscopy studies revealed that ligand-binding induces allosteric changes to the TCRα and β chains at multiple sites (Rangarajan et al., 2018; Natarajan et al., 2017). Interestingly this includes changes to the CαAB loop and Cβ FG loop which are in contact with, or highly proximal to, the CD3εδ and CD3γε dimers respectively (Dong et al., 2019). Deletion of these loops reduces T cell sensitivity to activation by p-MHC while preserving expression of TCR-CD3 receptor complexes supporting the theory that they are required for signal transmission (Beddoe et al., 2009; Touma et al., 2006).

Another prominent model for TCR signal transduction is the molecular segregation model. This model stipulates that upon triggering the TCR redistributes with respect to phosphatases such as CD45 and CD148 which dephosphorylate ITAMs. It has been proposed that this may occur because interactions between the relatively small TCR and p-MHC complexes can only occur when the plasma membranes of the T cell and DC are in close proximity. This would serve to exclude molecules with large extracellular domains, including CD45 and CD148, from these close contact regions by sterically hindering their diffusion and thus skewing the phosphorylation/dephosphorylation equilibrium of ITAMs towards phosphorylation inducing signalling. This model is supported by studies in which the ectodomain of

CD45 and CD148 were truncated leading to suppression of TCR signalling (Cordoba et al., 2013). An additional point of interest is that CD45 is excluded from TCR microclusters distal to the cSMAC where signalling occurs but is enriched at the cSMAC where TCR signalling is quenched (Varma et al., 2006).

TCR aggregation has also been proposed to provide antigen-specificity as well as a mechanism for the initiation of downstream cytoplasmic signalling. However, a recent FRET-based study has shown that TCR signalling propagates from monomeric TCR-CD3 receptor complexes suggesting that oligomerisation is not in fact the mechanism that supports antigen recognition and TCR activation (Brameshuber et al., 2018).

The author prefers a combination of a number of these models to describe TCR ligand discrimination and triggering as they are by no means mutually exclusive. As previously mentioned, aggregate dwell time is the best predictor of ligand potency and therefore the cell must somehow record this parameter in order to identify agonist ligands. Kinetic proofreading provides a mechanism by which the cell could achieve this. Because mutation of the polybasic sequence of CD3ε does not augment ITAM phosphorylation it is unlikely that release of this motif from the membrane initiates signalling (Deford-Watts et al., 2009; Fernandes et al., 2010). A preferrable explanation is that increased dwell time, which would be augmented by force-dependent formation of catch-bonds, results in prolonged exclusion of the CD45 phosphatase due to the proximity of opposing membranes. This would tip the equilibrium towards LCK-dependent phosphorylation of CD3 inducing downstream signalling. The paradox presented by this model is that CD45 is also required to activate LCK (discussed below). However recent evidence shows that although CD45 is segregated from signalling TCRs it is initially localised within a few hundred nanometres and thus could maintain LCK in its active conformation while failing to quench TCR signalling (Razvag et al., 2018) (Figure 2).

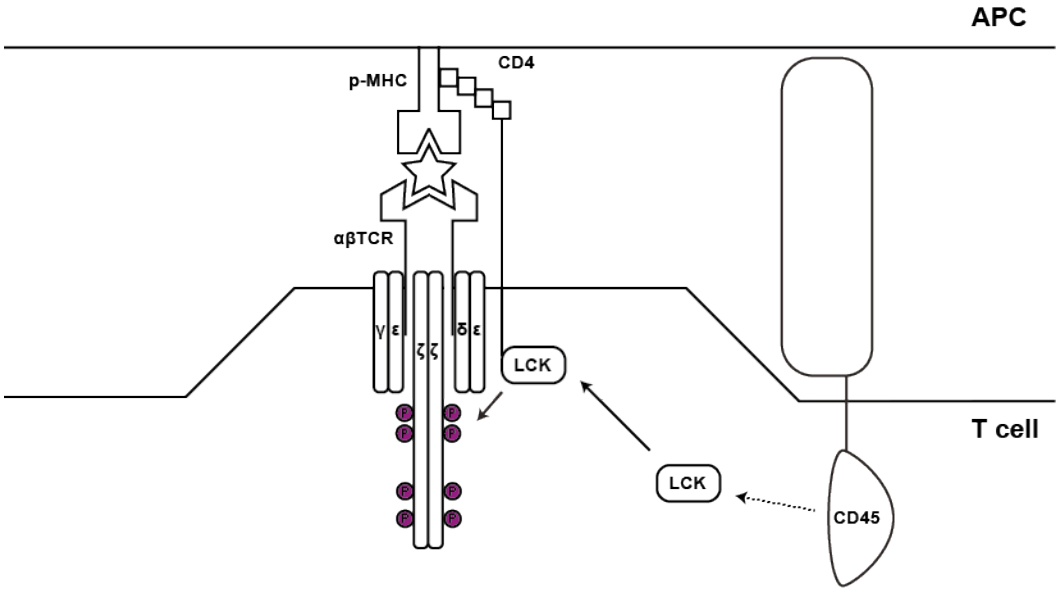

Figure 2. Kinetic segregation model of TCR triggering. The small intermembrane distance stabilised by the TCR-p-MHC interaction excludes the large rigid extracellular domain of CD45. This allows activated LCK to phosphorylate CD3 and induce downstream signalling which would otherwise be inhibited due to CD45-dependent dephosphorylation.

Regardless of the mechanism, TCR activation results in phosphorylation of ITAMs in the intracellular tails of CD3ε and CD3ζ molecules by SRC-family kinases - LCK and FYN (Samelson et al., 1990; Samelson et al., 1986). However, there seems to be only an absolute requirement for LCK (Appleby et al., 1992; Molina et al., 1992). LCK activity is regulated by phosphorylation of Y394 and Y505 (Figure 3). Autophosphorylation or transautophosphorylation of Y394, which is located in the activation loop, stabilises the active conformation of the kinase domain whereas the C-terminal tyrosine Y505 is phosphorylated by CSK and promotes an inactivating conformational change which is mediated by an interaction between this site and the SH2 domain of LCK (Xu et al., 1999; Hardwick and Sefton, 1995). Intramolecular interactions between an SH3 domain, polyprotein helix and “linker” region of LCK stabilise the closed conformation further (Xu et al., 1997). Both phosphorylation sites are substrates for CD45 dephosphorylation, which can thus act as a positive and negative regulator of LCK, although Y394 is a poorer affinity substrate (Zikherman et al., 2010). Y394 can also be dephosphorylated by an array of other phosphatases which are thus negative regulators of TCR signalling and include: PTPN2, PTPN12, PTPN22, SHP1, and DUSP22.

Dephosphorylation of Y505 by CD45 results in an open, “primed” conformation that may possess some catalytic activity although this remains a controversial topic as *in vitro* analyses yielded different results (Hui and Vale, 2014; Oro et al., 1996). A study using LCK-deficient JCaM 1.6 cells derived from the Jurkat T cell leukaemia cell line showed that expression of a Y394F/Y505F mutant was not able to reconstitute downstream ERK activation or Ca^{2+} fluxes suggesting the unphosphorylated form of LCK is not sufficient for productive signalling (Philipsen et al., 2017). Using a FRET biosensor, the authors also clarified that in addition to the conformational change, Y394 phosphorylation is indeed required for catalytic activity.

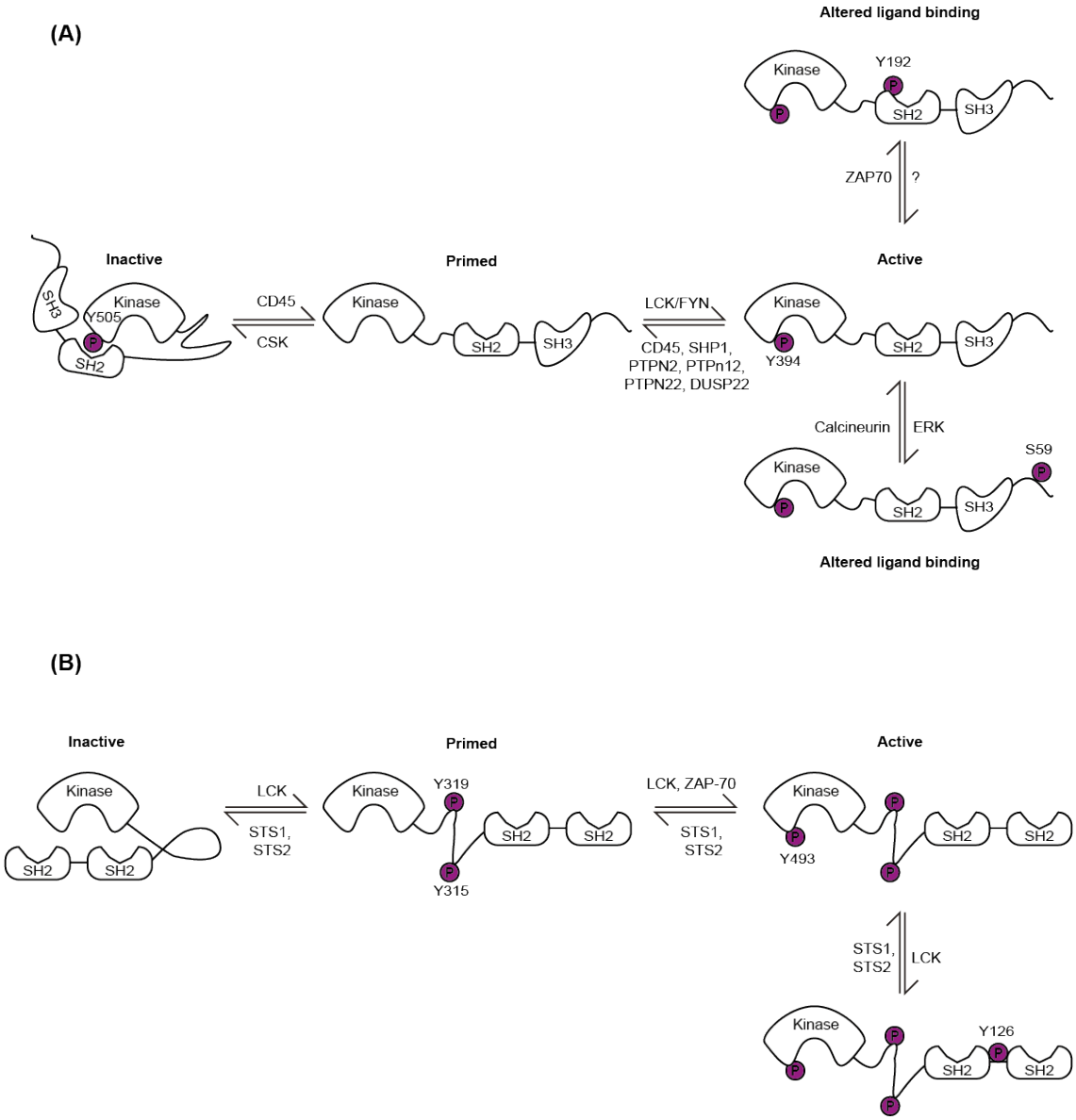

Figure 3. LCK and ZAP-70 regulation. LCK (A) and ZAP-70 (B) mediate the earliest steps during TCR signal transduction. They can exist in multiple phosphorylation states which determine their activity and substrate specificity. A range of kinases and phosphatases can regulate each of these phosphorylation events thereby modulating TCR signalling. Adapted from (Gaud et al., 2018).

A pool of constitutively active, Y394-phosphorylated LCK (pY394) is present in T cells, although there are contradicting reports on the size of this pool ranging from 2-40% of total intracellular LCK (Ballek et al., 2015; Nika et al., 2010b). Similarly, there is controversy over whether TCR activation leads to an increase in this percentage, with some studies reporting an increase in the pY394 form upon TCR stimulation and others finding no evidence of this (Philipsen et al., 2017; Nika et al.,

2010b). It is widely accepted however that LCK non-covalently associates with CD4 and CD8 coreceptors (Veillette et al., 1988).

A third site on LCK (S59) is phosphorylated by ERK in a feedback loop (Winkler et al., 1993). This phosphorylation event was shown to change the substrate specificity of LCK (Joung et al., 1995). A separate study later found this site to participate in a feedback loop facilitating ligand discrimination by the T cell (Štefanová et al., 2003). The authors of this study proposed a mechanism by which TCR antagonists induce LCK-dependent phosphorylation of SHP-1, binding of SHP-1 to LCK, SHP-1-dependent dephosphorylation of LCK Y394 and thus the formation of a negative feedback loop. In contrast, agonist-binding would result in ERK-dependent phosphorylation of LCK S59, which blocks SHP-1 recruitment, preventing the formation of the negative feedback loop and thus facilitating productive TCR signalling and activation. This mechanism is at odds with *in vivo* data as a S59A substitution in mice had no effect on ligand discrimination and in fact slightly enhanced activation, suggesting an inhibitory role of S59 phosphorylation during T cell activation (Paster et al., 2015). The authors of another study found that expression of the LCK mutant S59A augmented TCR signalling, including LCK Y394 phosphorylation, whereas expression of the phosphomimetic mutant S59E had the reverse effect in LCK-deficient JCam1.6 cells (Dutta et al., 2017). These results align with the previous *in vivo* finding that pS59 has an inhibitory role. Surprisingly, the authors were also able to show that calcineurin, which is activated by Ca^{2+} release, is recruited to ZAP-70 during activation and can dephosphorylate LCK S59. Pharmacological inhibition of this phosphatase reduced the TCR-dependent phosphorylation of multiple signalling molecules, including the Y493 residue of ZAP-70, whereas phosphorylation of CD3ζ Y83 and ZAP-70 Y319 were unaffected. This change in TCR-induced phosphorylation pattern did not perfectly match that of the S59E mutant suggesting calcineurin was performing multiple roles proximal to the TCR.

Y192, which is in the LCK SH2 domain, is another tyrosine phosphorylated in a negative feedback loop downstream of the TCR. Complementary studies using Jurkat cells found that phosphorylation of this residue is dependent on ZAP-70 and ITK activity, although the authors note that other kinases are likely to play a role (Sjölin-Goodfellow et al., 2015; Granum et al., 2014). Initially it was proposed that this post-translational modification inhibtited LCK activity to all substrates. This is

supported by evidence that phosphorylation of Y192 inhibits dephosphorylation of Y505 by CD45, thus locking the kinase in the inactive conformation (Courtney et al., 2017). However, contrary to its negative role in TCR signalling, another study showed that Y192 phosphorylation alters LCK substrate specificity and is in fact required for cell-cell adhesion although the mechanism was not fully elucidated (Granum et al., 2014).

Phosphorylated ITAMs of the intracellular tails of CD3ζ molecules act as a scaffold for ZAP-70 binding via its SH2 domain, thus localising the protein to the membrane (Katz et al., 2017; Chan et al., 1991). The current model for ZAP-70 activation elucidated using hydrogen-deuterium exchange mass spectrometry, states that CD3ζ binding induces a conformational change from the closed, autoinhibited state to the open, "primed" state promoting phosphorylation of Y315 and Y319 in interdomain B by LCK or autophosphorylation (Brdicka et al., 2005; Di Bartolo et al., 1999a; Klammt et al., 2015; Neumeister et al., 1995). This stabilises the "primed" conformation as well as the interaction with pCD3ζ resulting in increased dwell time, phosphorylation of the activation loop at Y493, and downstream signalling. pY315 and pY319 also act as docking sites for signalling molecules, for example, pY319 is a well-documented binding site for LCK (Pelosi et al., 1999). In fact, mutation of this residue to phenylalanine exerts a dominant negative effect on TCR signalling (Di Bartolo et al., 1999b).

ZAP-70 Y319 can be dephosphorylated by the non-canonical family of phosphatases – STS-1 and -2 – which are unique in that they have a ubiquitin association (UBA) domain paired with a SH3 domain at their N-terminus (Mikhailik et al., 2007). Deletion of both these phosphatases results in enhanced SLP76 and LAT phosphorylation as well as TCR-induced proliferation showing they have a negative regulatory effect on ZAP-70-dependent signalling *in vivo* (Carpino et al., 2004). STS2 requires intact UBA and SH3 domains to supress TCR signalling, suggesting a mechanism by which ZAP-70 is recognised via a ubiquitin moiety along with a poly-proline motif (Mikhailik et al., 2007). Recently it has been shown that ZAP-70 poly-ubiquitination at K578 is carried out by NRDP1 in $CD8^+$ T cells, although the ligase responsible for ZAP-70 ubiquitination in $CD4^+$ T cells has not been identified. Interestingly, NRDP1-deficiency did not affect CD3ζ or LCK phosphorylation but dramatically increased ZAP-70 Y319 phosphorylation (Yang et al., 2015). OTUD7B,

on the other hand, has been found to deubiquitinate ZAP-70 predominantly at K544 in both $CD4^+$ and $CD8^+$ T cells, blocking STS1- and 2-binding and thus positively regulates TCR signalling, including ZAP-70 Y319 phosphorylation (Hu et al., 2016). The authors of these studies found that these effects were independent of ubiquitin-dependent protein degradation. Another study by Huang et al. showed that poly-ubiquitination of CD3ζ at K54 by CBL-B and ITCH E3 ligases supresses ZAP-70 recruitment and activation, however this pathway also results in reduced CD3ζ phosphorylation (Huang et al., 2010).

Following phosphorylation of Y315 and Y319, residue Y493, located within the activation loop of ZAP-70, is phosphorylated by LCK or via autophosphorylation resulting in complete activation of ZAP-70 kinase activity (Wang et al., 2010). PTPN22 is able to dephosphorylate ZAP-70 at Y493, but not Y319, thus inhibiting its kinase activity (Wu et al., 2006a). Stable association with the TCR also results in phosphorylation of Y126, possibly through trans-autophosphorylation. This reduces the affinity of ZAP-70 for the phosphorylated ITAMs on CD3 proteins and results in diffusion of ZAP-70 away from the TCR complex in the plane of the membrane suggesting a possible “catch-and-release” mechanism for ZAP-70 regulation that would facilitate signal amplification and dispersal (Katz et al., 2017).

Activated ZAP-70 goes on to phosphorylate a number of proteins including LAT and SLP76 which are able to induce nucleation of the signalosome at the membrane which acts as a signalling platform (Figure 4). This process is essential for TCR signal transmission (Zhang et al., 1999). LAT is phosphorylated on 9 tyrosine residues which act as docking sites for multiple adaptor and effector proteins containing SH2 domains (Zhang et al., 2000). These include GRB2, PLCγ1 and GADS.

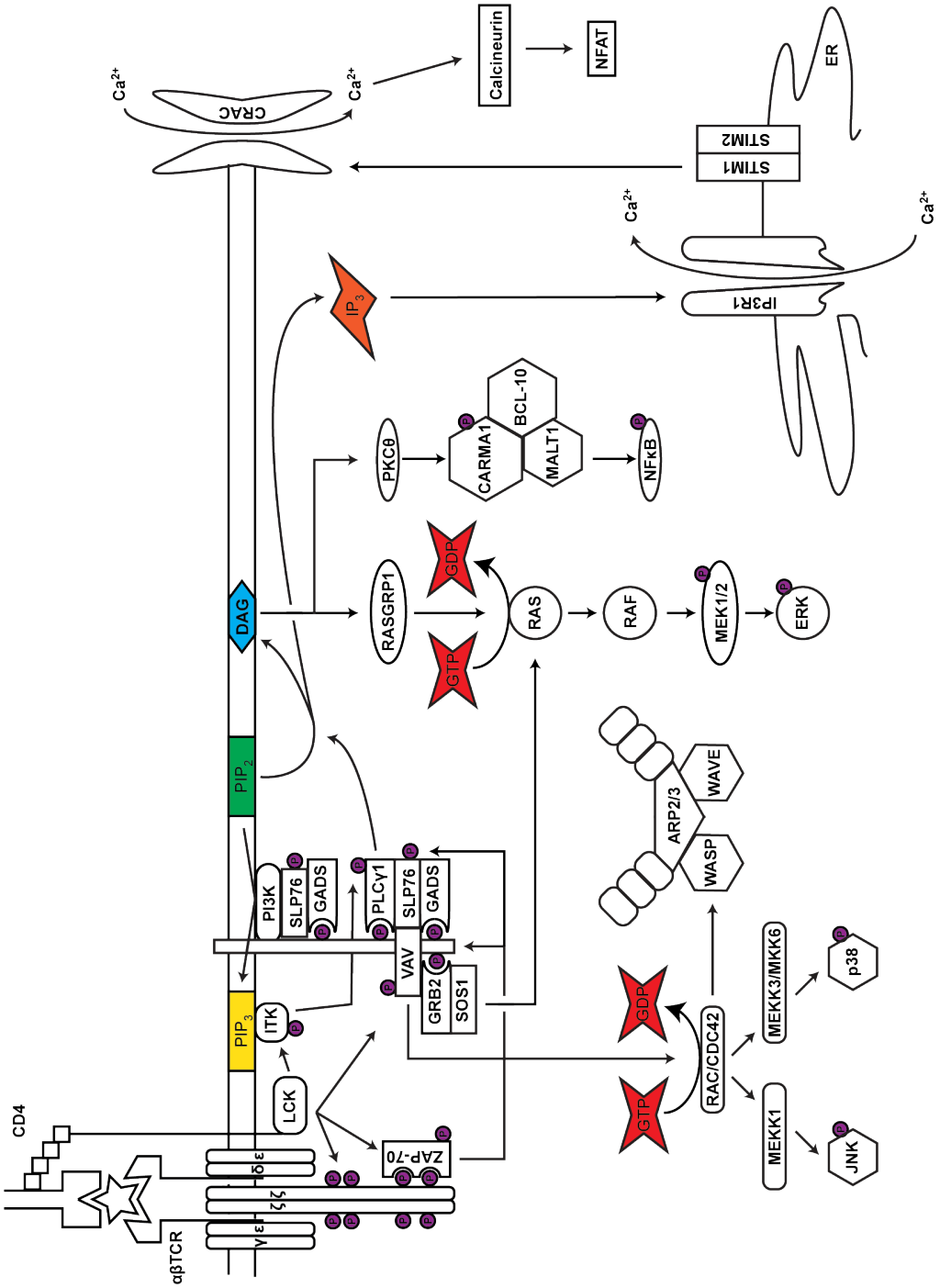

Figure 4. TCR signalling pathway. Stimulation of the TCR elicits a myriad of signalling pathways. The most TCR proximal event required for signal transduction is the LCK-dependent phosphorylation of ITAM domains on the intracellular tails of CD3 molecules associated with the αβTCR. This results in the recruitment and activation of ZAP-70 which is then able to mediate the nucleation of the LAT signalosome which serves as a signalling platform for downstream pathways. LCK also activates ITK which in turn activates PLCγ1 at the LAT signalosome. From here PLCγ1 catalyses the conversion of PIP_2 into DAG and IP_3 which induce the RAS, PKCθ and Ca^{2+} signalling pathways. SOS1, which is also recruited and activated at the LAT signalosome, augments RAS signalling further. In parallel, VAV1 activates RAC1/RAC2/CDC42 signalling. These pathways are collectively responsible for T cell activation.

GADS acts as an adapter molecule to recruit SLP-76, which in turn recruits ITK, VAV1 and NCK. GRB2 contributes to the recruitment of VAV1 and SOS1, a RAS guanine nucleotide exchange factor (RAS-GEF) (Lowenstein et al., 1992). It is likely that the assembly of the LAT signalosome is in fact a far less linear process than described here and involves a stunningly complex array of protein-protein interactions and post-translational modifications. For example, each SOS1 molecule is able to bind 2 GRB2 molecules, facilitating the assembly of higher order LAT oligomers at the cell surface (Douglass and Vale, 2005; Houtman et al., 2006; Su et al., 2016b). This higher order assembly was required for signal amplification under limiting stimulation conditions. Subsequently its was shown that these LAT assemblies are required for optimal PLCγ1 activation downstream of the TCR (Kortum et al., 2013). The same goes for ERK kinase activation (Su et al., 2016a). This may be related to the fact that LAT assemblies are required for extended SOS1 recruitment to the membrane which is necessary for SOS1 activation (Huang et al., 2016). Additionally, these LAT assemblies exclude CD45 suggesting that they could contribute to kinetic segregation of phosphatases during productive TCR signalling.

The LAT signalosome structure not only recruits effector molecules to the membrane for activation via post-translational modification, but also acts to enhance their activity by stabilising their active conformations. This is illustrated by the mechanism of PLCγ1 activation, which requires ITK-dependent phosphorylation but also interaction with VAV1, SLP76 and LAT to generate full phospholipase activity (Beach et al., 2007; Saveliev et al., 2009). ITK activity is also regulated via post-translational modifications and protein-protein interactions. Initially ITK is recruited to the membrane via its pleckstrin homology (PH) domain, which binds to phosphatidylinositol-3,4,5-triphosphate (PIP_3) produced by phosphoinositide 3-kinase (PI3K) (Ching et al., 1999). Here it is phosphorylated by LCK and subsequently recruited to SLP76 where it phosphorylates PLCγ1. An NMR-based study showed that ITK activity requires not only LCK-dependent phosphorylation but also conformational changes induced upon binding to p-SLP76 via its SH2 domain (Pletneva et al., 2006).

PLCγ1 is a major effector molecule responsible for signalling downstream of the signalosome. PLCγ1 is a phospholipase that hydrolyses phosphatidylinositol-4,5-

bisphosphate (PIP_2) to produce inositol-1,4,5-trisphosphate (IP_3) and diacylglycerol (DAG), essential second messengers in the TCR signalling pathway. DAG is responsible for activating both RAS and PKCθ signalling pathways. DAG recruits PKCθ to the membrane where it signals primarily via the NFκB pathway but is also known to contribute to the activity NFAT and RAS signalling pathways (Sun et al., 2000).

DAG also inducibly recruits RASGRP1 to the membrane where it is phosphorylated and activated by PKCθ. RASGRP1 is a RAS-GEF which stimulates the release of GDP from RAS to allow binding of GTP. RAS is active in the GTP-bound form and activates RAF-1, which activates MEK1 and MEK2, which in turn activate ERK1 and ERK2 mitogen activated protein kinases (MAPKs). SOS1 is another RAS-GEF and directly regulates guanine nucleotide exchange of membrane-bound RAS when recruited to the LAT signalosome by GRB2. These two RAS-GEFs play partially-redundant, complementary roles in activation of the RAS signalling pathway. RASGRP1 appears to play a dominant role in RAS activation whereas SOS1 acts as a RAS rheostat (Roose et al., 2007). SOS1 activity is augmented by binding to RAS-GTP via an allosteric pocket. Therefore, maximal SOS1 activity requires accumulation of RAS-GTP, which is initially mediated via RASGRP1 activity. As RAS-GTP levels increase a positive feedback loop is formed and SOS1 becomes highly activated and enhances RAS signalling. An interesting characteristic of TCR-mediated ERK signalling is that it converts an analogue TCR signal into a digital response. This can be predicted *in silico* by modelling the interaction between RASGRP1 and SOS1 signalling (Das et al., 2009). RASGRP1 provides an analogue signal which is transformed into a digital signal by the SOS1 feedback loop. This signalling circuit also provides a form of “memory” for previous TCR engagement as it results in dramatically augmented ERK signalling during subsequent antigen encounters experienced within a set period of time. ERK itself also participates in a feedback loop with the membrane proximal signalling apparatus by phosphorylating LCK at S59 as discussed earlier in the chapter.

IP_3, the second second messenger generated by PLCγ1 activity, activates Ca^{2+}-permeable ion channels in the endoplasmic reticulum (ER). Ca^{2+} ions move down the electrochemical gradient into the cytoplasm. Ca^{2+} depletion in the ER induces the aggregation of STIM1 and STIM2 ER proteins which trigger the store-

operated Ca^{2+} channel at the plasma membrane to generate an even larger influx of Ca^{2+} into the cytoplasm (Oh-hora et al., 2008). Cytoplasmic Ca^{2+} activates many signalling proteins including the phosphatase calcineurin and the CaMK kinase. These proteins in turn activate the transcription factors NFAT, CREB, and MEF2.

VAV1 is another GEF activated downstream of the TCR which is specific for RHO-family GTPases. Upon recruitment to the LAT signalosome VAV1 undergoes a two-step activation program in which phosphorylation of VAV1 Y142 and Y160 provides a binding site for LCK and makes Y174 accessible for phosphorylation by LCK. This relieves autoinhibition and rapidly stimulates downstream signalling (Yu et al., 2010). VAV1 activates actin cytoskeletal dynamics by converting RAC1, RAC2 and CDC42 to their GTP-bound state. These GTP-bound RHO GTPases then activate WASP and WAVE2 which bind ARP2/3 proteins and act as actin-nucleation factors generating a complex actin network that ultimately supports IS formation. VAV1 GEF activity is also required for AKT and TEC kinase activation, most likely by stimulating PI3K activity via RHO GTPases (Reynolds et al., 2002; Saveliev et al., 2009).

LFA-1 integrin activity, and interaction with the actomyosin cytoskeleton, is also essential for IS formation. LFA-1 undergoes a conformational change to a high affinity state in response to TCR stimulation, a process known as inside-out signalling (Springer and Dustin, 2012). Signalling from the TCR influences clustering and anchoring to the F-actin cytoskeleton resulting in high-affinity binding to ICAM-1 and stable conjugate formation. The RAP1 GTPase is a critical regulator of TCR-induced adhesion, particularly by increasing the avidity of LFA-1 interactions (Sebzda et al., 2002; Shimonaka et al., 2003). Pharmacological inhibition showed that RAP1 activation downstream of the TCR is highly dependent on PLCγ1 and PKCθ signalling in primary T cells, although the latter was revealed using PMA stimulation and thus may not be relevant for TCR-dependent RAP1 activation (Katagiri et al., 2004; Ghandour et al., 2007). ADAP is an adaptor molecule that is recruited to the LAT signalosome and is critical for TCR-induced RAP1 activation and adhesion but does not influence other TCR proximal signalling events (Katagiri et al., 2000; Griffiths et al., 2001; Wu et al., 2006b). Its activity is dependent on SLP-76 binding and is required for augmenting LFA-1 avidity by inducing clustering at the membrane, a pre-requisite for productive cell-cell adhesion (Wang et al., 2004). To achieve this change in adhesive behaviour, ADAP recruits RAP1 to the membrane via SKAP55

and RIAM where it is activated by RAP GEFs (Ménasché et al., 2007; Kliche et al., 2006). The PKCθ effector PKD1 also is important for RAP1 recruitment to the membrane and activation, possibly by recruiting the RAP-GEF C3G (Medeiros et al., 2005).

RAP1 binds to both RIAM and RAPL effector protein which in turn promote the binding of TALIN to the β subunit of LFA-1 (Lee et al., 2009; Katagiri et al., 2006). This complex promotes a conformational change in LFA-1 to the extended-closed low-affinity conformation, clustering and nucleates further factors to facilitate anchoring of LFA-1 to the actin cytoskeleton. Mechanical forces generated from cortical actin flows in the pSMAC actin network generates a conformational change to the open-extended high-affinity conformation and stable ICAM-1 binding (Comrie et al., 2015). Accordingly, VAV1-mediated cytoskeletal rearrangements are required for this process (Ardouin et al., 2003; Krawczyk et al., 2002). These stable interactions increase the sensitivity of T cells to antigens by 100-fold (Bachmann et al., 1997). Inversely, outside-in signalling via LFA-1 is thought to also mediate de-adhesion from APCs by inducing phosphorylation of LAT at Y171 and recruiting GRB2-SKAP1 complexes to the LAT signalosome (Raab et al., 2017).

Another major signalling node in T cell activation are the class 1 PI3Ks which catalyse the phosphorylation of phosphatidylinositol-4,5-bisphosphate (PIP_2) to phosphatidylinositol-3,4,5-triphosphate (PIP_3). These kinases are heterodimeric and contain a p85α, p85β or p55γ regulatory subunit that constitutively associates with a p110α, p110β, p110δ or p110γ catalytic subunit, which exhibit some level of redundancy. P110δ in complex with p85α or p85β produces most PIP_3 in mature T cells and has been shown to be critical for T cell function *in vivo* (Lucas et al., 2016; Okkenhaug et al., 2002). Interestingly, this critical role for PI3Kδ was later found to be at least in part mediated by its ability to induce cell-cell adhesion though regulation of RAP1, cofilin and ERM (Garçon and Okkenhaug, 2016). This explained the observation that cells expressing a kinase-dead form of PI3Kδ were able to proliferate normally in response to beads coated in anti-CD3 and anti-CD28 antibodies whereas the response to antigen presented on APCs was severely compromised. The δ isoform is known to be activated downstream of the TCR, cytokine receptors and costimulatory receptors. A number of pathways have been reported to be required for PI3Kδ activation by these various stimuli. It has been

shown that TCR-dependent recruitment of PI3Kδ to the membrane requires LAT and SLP-76 (Shim et al., 2011). The RAS signalling pathway has also been shown to play a role in PI3K activation in peripheral primary T cells (Wabnitz et al., 2006). Saveliev et al. show that VAV1 GEF activity is required for AKT activation in naïve $CD4^+$ T cells providing indirect evidence that VAV1 may also contribute to PI3K activation (Saveliev et al., 2009). Although it is clear that CD28 signalling also augments PI3K activity, the mechanism by which signals are transmitted between these proteins is unclear as mutation of the YxxM motif abrogates PI3K binding but not CD28-dependent activity (Garçon et al., 2008; Prasad et al., 1994).

Synthesis of PIP_3 at the membrane results in the recruitment of pleckstrin homology (PH) domain containing proteins including PDK1, its downstream target AKT, TEC tyrosine kinases, such as ITK, and RHO-GEFs. PIP_3-binding induces a conformational change in AKT that converts it into a substrate for PDK1 which is co-localised to the PIP_3-rich membrane domain via its PH domain (Milburn et al., 2003). ITK localisation to the membrane is thought to be essential for LCK-mediated phosphorylation and activation (Shan et al., 2000). The PIP_3-dependent localisation of RHO-GEFs to the membrane seems to regulate their exchange activity by bringing them into the proximity of LCK (Han et al., 1998).

AKT signalling plays a major role in regulating T cell activation. Signalling through this pathway regulates survival, metabolism, cytokine production and division by inducing an array of post-translational modifications and transcriptional changes. A particularly important regulatory function of the AKT pathway is to activate mTORC1 activity which subsequently regulates many processes including lipid metabolism and protein synthesis (Inoki et al., 2002). This pathway and its role in the cell cycle is discussed further in Chapter 1.9.1.

1.5.3 Costimulation

As posited by the “two signal model” of activation, T cells require a second costimulatory signal, supplementary to the TCR signal, in order to become activated. This signal is supplied by costimulatory receptors expressed on the T cell which bind to costimulatory molecules expressed on the surface of APCs. As previously mentioned, DCs upregulate costimulatory molecules in the presence of PAMPs or

certain inflammatory cytokines (Chapter 1.1). DCs without costimulatory molecules on their surface are therefore unlikely to be presenting pathogen derived p-MHC molecules. TCR engagement in the absence of costimulation results in T cell anergy, which refers to a broad range of functionally inactivated states in which cytokine secretion and proliferative responses are commonly suppressed (Schwartz, 2003). This process contributes towards peripheral tolerance by inactivating self-reactive T cells which have escaped deletion in the thymus. If the T cell receives both TCR and costimulatory signals this leads to activation.

There are many costimulatory receptors expressed on the surface of T cells, however CD28 is the most well studied and T cells are strongly reliant on its activity to mount an immune response (Dodson et al., 2009; Lucas et al., 1995). CD28 interacts with CD80 and CD86 costimulation molecules on the surface of APCs. It competes for these ligands with the inhibitory receptor – CTLA-4 – which is also expressed on the surface of T cells and can form a higher affinity interaction (Krummel and Allison, 1995). ICOS, which is highly related to CD28, is another major costimulatory receptor. ICOS binds to ICOS-ligand (ICOSL) which can also act as a ligand for CD28 (Yao et al., 2011). The pro- and anti-inflammatory activities of this receptor-ligand family are thus regulated in a complex manner but ultimately act as a rheostat for the immune response.

One major function of CD28 signalling is to dramatically increase *Il2* expression by increasing its transcription and stabilising *Il2* RNA (Fraser et al., 1991; Lindstein et al., 1989). Another well documented function of CD28 signalling is to promote T cell survival by inducing the expression of Bcl-Xl, an anti-apoptotic factor. Interestingly, CD28 also seems to be able to increase the sensitivity of a T cell to lower abundance or lower affinity antigen (Bachmann et al., 1997).

Proteomics studies have shown that CD28 costimulation mainly acts to enhance signalling pathways induced downstream of CD3 (Kim and White, 2006). CD28 has a cytoplasmic tail which can act as a signalling scaffold for SH2- and SH3-domain containing proteins upon stimulation. In particular the YXXM motif and the distal proline motif (PYAP) play major but partially redundant roles in signal transduction as mutation of both these sites results in profound defects in T cell cytokine production, survival and proliferation (Boomer et al., 2014). The PYAP motif seems to have the most profound role in immune responses *in vivo*. GRB2 and

GADS recruitment to CD28 upon stimulation is well documented and augments VAV1 and NFκB activation respectively.

1.5.4 Activation marker expression

Cell surface activation markers such as IL-2Rα, CD44 and CD69 are rapidly transcriptionally upregulated in response to TCR stimulation and can be used to determine the activation state of the cell but also carry out essential roles in effector T cell function. *Il2rα* is expressed in response to TCR stimulation and encodes the IL-2Rα chain (CD25) which generates a high-affinity IL-2 receptor when it forms a heterotrimer with the constitutively expressed IL-2Rβ and γ_c subunits. IL-2 receptor-induced JAK-STAT signalling promotes T cell proliferation by mediating an array of transcriptional changes, in particular the expression of cyclin D2, cyclin D3 and CDK6 (Moriggl et al., 1999). However, *in vivo* this role of CD25 signalling seems to be redundant and in fact *Il2rα*$^{-/-}$ mice develop lethal lymphoproliferative and autoimmune syndrome (Willerford et al., 1995). It transpires that IL-2 signalling has an essential function during the development and survival of regulatory T (T_{reg}) cells which constitutively express high levels of CD25 and supress autoreactive peripheral T cells (Fan et al., 2018; Almeida et al., 2002). TCR-mediated expression of *Cd25* is regulated via a vast array of transcription factors that bind to 5 positive regulatory regions located upstream and downstream of the transcriptional start site. These transcription factors include members of AP-1, NFAT, NFκB and ETS families of transcription factors (Kim, 2002; Schuh et al., 1998). CD28 signalling enhances *Cd25* expression via CREB/ATF transcription factors, which cooperate with AP-1 transcription factors, and also via NFκB transcription factors (Yeh et al., 2001; Kahn-Perles et al., 1997). IL-2 binding to the IL-2R is not only responsible for transcription of pro-proliferative genes but also *Cd25* itself, forming a positive feedback loop. IL-2-dependent *Cd25* expression is mainly mediated via the STAT5 signalling pathway (John et al., 1999). STAT5 directly binds to positive regulatory regions to enhance *Cd25* transcription in concert with HMG-I(Y) (Kim, 2002). Other cytokines such as IL-1, IL-7, IL-12, IL-15, TGF-β and TNFα have been found to induce CD25 signalling via SMAD and NFκB transcription factors (Kim et al., 2006; Kim et al., 2005; Pimentel-Muinos et al., 1994).

CD44 and CD69 proteins are involved in adhesion and migration. The primary ligand for CD44 is the extracellular matrix component hyaluronic acid (HA) and via this interaction CD44 can mediate tethering and rolling interactions with vascular endothelial cells that express HA (Ponta et al., 2003). CD44 also interacts with the VLA-4 integrin to mediate extravasion and thus upregulation of CD44 promotes recruitment of activated, effector T cells to sites of infection (Nandi et al., 2004). CD44 has also been found to bind to LCK as well as the TCR signalling complex and augment TCR-dependent function *in vitro* (Dianzani et al., 1999). This function of CD44 was not observed *in vivo*, although a clear role in regulating T helper (T_H) 1 T cell differentiation and survival *in vivo* has been established (Baaten et al., 2010; Guan et al., 2009). CD44 seems to be a sensitive reporter of mTORC1 activity in $CD4^+$ T cells (Daley et al., 2013). Several transcription factors have been found to bind to the *cd44* promoter and regulate transcription including SP1, EGR1, TCF4, AP-1, NFκB, ETS-1, 3, KLF4 and FOXP3 (Chen et al., 2018). However, these studies were carried out in a range of cell types under different conditions.

CD69 is one of the earliest activation markers to appear on the cell surface subsequent to T cell activation. *In vivo* CD69 appears to supress T_H1 and T_H17 responses, while promoting differentiation into T_{reg} cells (Radulovic et al., 2012). One of the best characterised ligands of CD69 is GAL-1, a carbohydrate-binding protein expressed on APCs. CD69 binding to Gal-1 on DCs has been shown to supress T_H17 differentiation *in vitro* (de la Fuente et al., 2014). CD69 also engages in cis interactions at the cell surface with Sphingosine 1-phosphate receptor 1 (S1PR1) and SLC7A5. The interaction with SLC7A5 is required to mediate SLC7A5/CD98-mediated amino acid uptake in γδ T cells (Cibrian et al., 2016). The interaction with S1PR1 supresses its activity by triggering degradation. This enforces tissue retention of $CD4^+$ T cells as S1PR1 signalling regulates tissue egress by mediating migration in response to S1P present in the blood (Shiow et al., 2006). Induction of *Cd69* expression during T cell activation is known to be heavily dependent on ERK signalling to the AP-1 family of transcription factors (D'Ambrosio et al., 1994). Additional contributions from EGR, ATF/CREB and RUNX families of transcription factors have been identified (Laguna et al., 2015; Castellanos Mdel et al., 2002). However, many of these experiments have been done using PMA/ionophore-mediated stimulation and so do not reflect physiological TCR stimulation.

1.6 Cytokine expression and differentiation

Upon activation, $CD4^+$ T cells differentiate into a specific T effector cell subset. Each subset has a different set of effector functions required for either the elimination of a specific type of pathogen or suppression of the immune response. The best characterised $CD4^+$ T cell subsets generated during activation in the periphery are T_H1, T_H2, T_H17, induced T regulatory (iT_{reg}) and T follicular helper (T_{FH}). In general, T_H1 cells are generated in response to intracellular pathogens, T_H2 cells in response to extracellular bacteria and metazoan parasites and T_H17 in response to extracellular bacteria and fungi. iT_{reg} cells are produced to dampen immune responses, particularly towards self-peptide-MHC-II complexes, and T_{FH} cells are produced to provide “B cell help” in order to generate antigen-specific antibodies of an isotype relevant to the class of invading pathogen.

The cytokine environment produced by early responding innate immune cells polarises $CD4^+$ T cell differentiation towards a specific subset. The affinity of the TCR for its cognate p-MHC-II ligand is also thought to direct this cell fate decision. Differentiation into each subset is driven by a master transcription factor, unique to each subset, in combination with a specific STAT transcription factor. T_H1 cell differentiation is mediated by T-bet and STAT4, T_H2 by GATA-3 and STAT5, T_H17 by RORγT and STAT3, iT_{reg} by FOXP3 and STAT5, and T_{FH} by BCL-6 and STAT3 (Figure 5) (Zhu et al., 2010). The resulting differentiation program determines $CD4^+$ T cell effector function, and in particular the precise cytokine profile produced by these cells. This means each subset can be characterised by its production of hallmark cytokines.

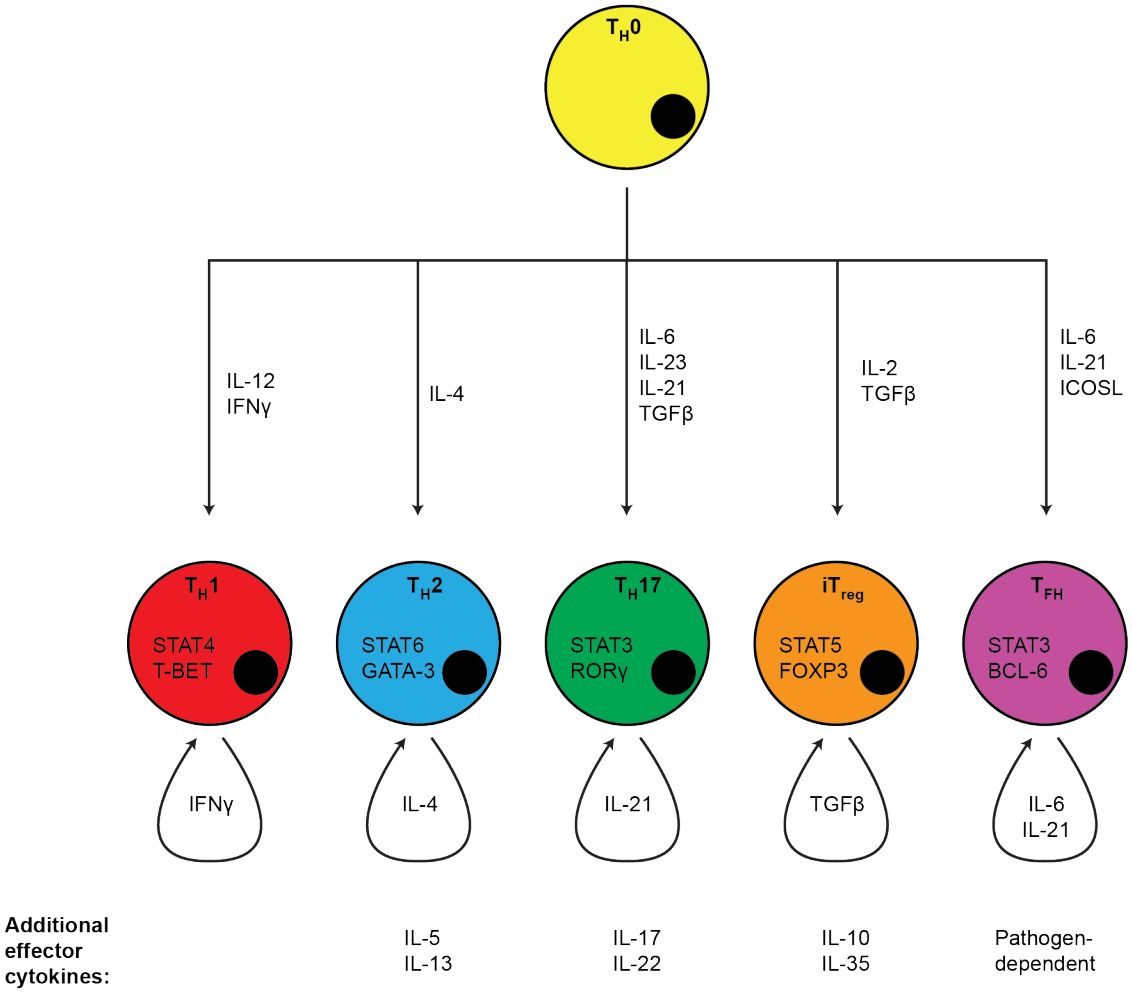

Figure 5 CD4$^+$ T cell differentiation. Upon activation in the periphery, naïve CD4$^+$ T cells are capable of differentiating into a number of different subtypes, each of which has a range of effector functions appropriate for a specific type of invading pathogen. The cytokine environment determines which differentiation program will be selected. Each differentiation program is driven by a master transcription factor in combination with a specific STAT transcription factor. Each subtype is able to reinforce its differentiation through autocrine and paracrine signalling as well as antagonising alternative differentiation pathways.

IFNγ rapidly induces T-bet expression via STAT1 *in vitro* to generate T_H1 cells. There is a complete requirement for T-bet for IFNγ expression, forming a positive feedback loop, however STAT4 strongly synergises with T-BET to induce high levels of IFNγ expression (Thieu et al., 2008). T-BET also induces IL-12Rβ2 expression, sensitising these cells to IL-12, which in turn induces STAT4-dependent expression of IFNγ (Afkarian et al., 2002). IL-12 signalling via STAT4, in concert with IL-18 signalling via MAPKs, also enforces TCR-independent IFNγ production (Yang et al., 2001).

STAT6-dependent IL-4 signalling upregulates GATA-3 expression, which in turn upregulates IL-4 expression, forming a positive feedback loop promoting T_H2 differentiation (Yamane et al., 2005). A second positive feedback loop is formed by IL-4-dependent upregulation of IL-4Rα, increasing the sensitivity of the cell to IL-4 (Liao et al., 2008). However *in vivo* this seems to mainly affect bystander antigen-inexperienced cells rather than activated cells suggesting a mechanism by which T_H2 polarisation can propagate through the $CD4^+$ T cell population during infection (Perona-Wright et al., 2010). Interestingly, IL-2-dependent activation of STAT5 is also required for expression of the *Il4* gene. In fact, STAT5 or GATA3 alone is insufficient to induce *Il4* expression (Cote-Sierra et al., 2004; Zhu et al., 2004). A study has also reported that STAT5 can mediate IL-4Rα expression but this is contradictory to subsequent findings that IL-4Rα expression was limited to $CD25^-$ cells and blockage of IL-2 signalling using antibodies did not affect IL-4Rα (Liao et al., 2008; Perona-Wright et al., 2010). This discrepancy may reflect the different *in vitro* culture systems used. However, the study by Perona-Wright et al. showed that IL-4Rα expression was strictly dependent on IL-4 signals and independent of CD25 expression *in vivo* in response to *H. polygyrus* infection (Perona-Wright et al., 2010). Another point of cross-talk between these two pathways occurs in differentiated T_H2 cells as GATA3 has been shown to be required to maintain *Cd25* expression (Guo et al., 2009).

RORγt and RORα are induced in response to TCR stimulation in concert with TGFβ and IL-6. These cytokines act via STAT3 signalling to induce RORγt and RORα, expression. The importance of this pathway in T_H17 differentiation is illustrated by the fact that deletion of *Stat3* results in a complete loss of T_H17 cells (Harris et al., 2007). There is a complete requirement for RORγt and RORα for IL-17 and IL-23R expression (Yang et al., 2008). Expression of IL-21 and IL-22, which are hallmark T_H17 cytokines, is also heavily dependent on these transcription factors. IL-6, 21 and 23 then signal via STAT3 to enforce RORγt, RORα, IL-17, IL-21 and IL-23R expression forming a positive feedback loop (Chen et al., 2006; Wei et al., 2007a).

BCL-6 is required for T_{FH} differentiation and for the provision of B cell help and is induced in response to IL-6 an IL-21 cytokine signalling. In particular this transcription factor induces expression of CXCR5 *in vivo* as well as downregulating

expression of CCR7. This change in chemokine receptor expression promotes migration of $CD4^+$ T cells to the B cell follicle (Yu et al., 2009). BCL-6 is also necessary and sufficient for the expression of other T_{FH}-related molecules such as IL-6 and IL-21R forming a positive feedback loop, however the T_{FH} differentiation program is much more dependent on migratory behaviour and will be discussed further below in Section 1.7 (Nurieva et al., 2009b).

TGFβ signalling via SMAD and TCR signalling via NFAT, CREB, AP-1 and C-REL respectively, is required for the expression of FOXP3 and thus iT_{reg} differentiation (Kanamori et al., 2016; Ruan et al., 2009; Tone et al., 2008). IL-2 signalling via STAT5 is also essential for iT_{reg} differentiation as deletion of IL-2Rβ results in a dramatic loss of these cells and constitutively active STAT5 drives their differentiation (Burchill et al., 2008).

As well as the positive feedback loops which enforce differentiation into specific subsets, there are multiple mechanisms by which $CD4^+$ differentiation signalling pathways interact to suppress one another. This can occur at the level of the master transcription factor, STAT signalling or cytokine expression. For example, T-bet supresses GATA3 expression, whereas GATA3 downregulates STAT4 expression, which is essential for IL-12 signalling in T_H1 differentiation. Additionally, STAT5 signalling during T_H2 differentiation supresses T-bet expression. This also explains how overlapping sets of cytokines can induce very distinct differentiation programs. For example, TGFβ blocks BCL-6 production promoting T_H17 or iT_{reg} differentiation over T_{FH} despite the fact that both T_{FH} and T_H17 depend heavily on IL-6 signalling (Nurieva et al., 2009b). Bifurcation of the T_H17 and T_{reg} lineages is dependent on the amount of TGFβ each pathway requires. A low concentration of TGFβ is sufficient for RORγt expression whereas FOXP3 requires large amounts (Zhou et al., 2008). At low TGFβ concentrations RORγt is then able to interact with FOXP3, blocking its function and polarising differentiation towards the T_H17 subset.

As previously mentioned TCR signal strength is also thought to contribute to $CD4^+$ T cell fate determination. Relatively early during the studies of $CD4^+$ T cell differentiation it was discovered that stimulation of the TCR with high affinity agonists *in vitro* and *in vivo* favours T_H1 polarisation, whereas low affinity agonists favour T_H2 polarisation (Pfeiffer, 1995). Jorritsma et al. found that stimulation of AND TCR-transgenic $CD4^+$ T cells with their cognate ligand -moth cytochrome c (MCC) – *in*

vitro resulted in sustained ERK activation and high levels of IFNγ production, whereas stimulation with the low affinity altered peptide ligand (K99R) resulted in transient ERK activation and high levels of IL-4 production (Jorritsma et al., 2003). Pharmacological inhibition of ERK confirmed that indeed a low level of ERK signalling results in preferential IL-4 expression over IFNγ. This group dissected the mechanism further to show that reduced ERK signalling decreases the ratio of fos-jun/jun-jun AP1 dimer DNA binding activity whereas high ERK signalling flux increased this ratio. Jun homodimers are known to be a required for *Il4* transcription this suggesting that low ERK signalling facilitates early IL-4 expression and subsequent T_H2 differentiation (Li et al., 1999). Another group found that K99R stimulation of AND $CD4^+$ T cells *in vitro* resulted in a decrease in the ratio of NFAT1/NFAT2 DNA binding activity, whereas MCC stimulation resulted in high DNA binding from both NFAT paralogues (Brogdon et al., 2002). A low NFAT1/NFAT2 ratio is required for *Il4* gene expression as NFAT1 is thought to downmodulate the activity of NFAT2 which is required for *Il4* expression (Ranger et al., 1998). This provides another mechanism by which TCR signal strength influences T_H1 vs. T_H2 fate decision. It seems that TCR signal strength can also influence T_H17 differentiation as citrullination of an agonist peptide enhanced T_H17 differentiation over other lineages in the presence of pro-T_H17 cytokines *in vitro* (Tibbitt et al., 2016). The authors concluded this was due to reduced TCR affinity for the ligand, although other possibilities cannot be excluded. The reported polarisation towards T_H17 cells was due to reduced IL-2 signalling which in turn increased the ratio of phosphorylated STAT3/STAT5 in these cells. Interestingly CD28 signalling via AKT has been reported to suppress T_H17 differentiation in response to polarising cytokines *in vitro* (Revu et al., 2018).

The physiological relevance of TCR/CD28 signal strength in determining differentiation into effector T cells is unclear, particularly as activation *in vivo* is likely to take place in an environment already rich in polarising cytokines. Indeed, naïve T cells must be exposed to both IL-23 and IL-1β to differentiate into T_H17 cells, regardless of signal strength. As previously mentioned, the elegant study from Perona-Wright et al. also showed that T_H2 cells cells communicate with bystander naïve cells to induce IL-4Rα expression via IL-4 signalling showing that cells can be primed for certain developmental pathways prior to activation *in vivo* (Perona-Wright

et al., 2010). For many years it was thought that high TCR signal strength also favoured T_{FH} differentiation as T cells expressing high affinity TCRs were found to be enriched in the T_{FH} compartment (Fazilleau et al., 2009). These data were supported by limiting-dilution adoptive transfer experiments that showed responses derived from individual $CD4^+$ T cells expressing unique TCRs had strong inter-clonal variation (Tubo et al., 2013). However, a more recent study showed that this variation between in behaviour of T cell clones was not actually dependent on TCR affinity, but in fact was determined by other probabilistic events that occurred during the lifetime of the T cell (Cho et al., 2017). However, at the population level the response patterns between T effector cells and T_{FH} cells were closely related to TCR signal quality. iT_{reg} cells can be induced in the presence of low affinity or high affinity ligands *in vivo*, however only those responding to high affinity antigen are able to persist (Gottschalk et al., 2010).

Some cytokines are produced by $CD4^+$ T cells before a specific differentiation program has been induced. For example, TNFα is induced within hours of TCR stimulation (Yang et al., 1998). TNFα expression is induced both at the transcriptional and post-transcriptional level. Induction of *Tnfa* transcription upon TCR engagement is mediated by calcineurin-dependent NFAT1 activation as well as the activity of ATF-2, JUN and SP1 transcription factors (Tsytsykova and Goldfeld, 2000; Falvo et al., 2000). Yang et al. found that TNFα expression was also regulated at the post-transcriptional level. This group found that TCR stimulation actually increases the efficiency of immature *Tnfa* RNA splicing and translocation of mature RNA to the cytoplasm which facilitated rapid translation (Yang et al., 1998). CD28 signalling has also been shown to enhance expression of TNFα (Thompson et al., 1989).

IL-2 is also expressed early during T cell activation. This is thought to occur in two phases. The initial phase encompasses the first 12 hours of activation when very few naïve T cells express IL-2, and a late phase, when there is a massive burst of expression (McKarns and Schwartz, 2008). Transcriptional induction through multiple cis-acting elements at the *Il2* locus is well characterised and requires members of the AP-1, NFκB, NFAT and OCT families of transcription factors as well as the architectural protein HMGI(Y) (Liao et al., 2013). TCR signalling alone is able to induce expression of IL-2 but CD28 signalling enhances enhancer activity five-fold

by increasing the recruitment of AP-1, NFκB and NFAT transcription factors (Fraser et al., 1991). More recently it has been shown that the late phase expression is also highly dependent on TNFRII suggesting a possible interaction between the two cytokine signalling pathways (McKarns and Schwartz, 2008).

1.7 T_{FH} cells and the germinal centre

The transcriptional repressor BCL6 is regarded as the master transcription factor for T_{FH} development as it is necessary and sufficient for this process (Johnston et al., 2009). BCL6 expression is rapidly induced in naïve $CD4^+$ T cells in response to TCR stimulation by DCs whereas interactions with cognate B cells are required to maintain BCL6 expression (Baumjohann et al., 2011; Fukuda et al., 1995). Nurieva et al. showed that T_{FH} development is also highly dependent on IL-6 and IL-21 signalling via STAT3 as deletion of these proteins results in severely impaired T_{FH} development *in vivo* as measured by CXCR5 expression (Nurieva et al., 2008). Furthermore, this group showed that these cytokines are sufficient for the induction of BCL6 and CXCR5 *in vitro*. This is a controversial finding as whole animal deletion of IL-21 or IL-6 was shown to have no effect or modest effects on T_{FH} development *in vivo* (Poholek et al., 2010). This may be because both signal via STAT3 and thus they are able to compensate for each other's absence. However, a further study showed no effect of STAT3-deficiency on T_{FH} development (Eddahri et al., 2009). Dendritic cells are potent producers of IL-6 in response to immune challenge (Chakarov and Fazilleau, 2014). IL-6 is necessary and sufficient for IL-21 expression *in vitro* and *in vivo* and BCL6 contributes to IL-21R, IL-6 and IL-21 expression in these cells forming a number of positive feedback loops (Dienz et al., 2009; Nurieva et al., 2009a; Suto et al., 2008).

Conversely, IL-2 is a potent inhibitor of T_{FH} differentiation as it induces the expression of BLIMP1 - a BCL6 antagonist - via STAT5 signalling (Johnston et al., 2009). Interestingly it appears that IL-2-producing $CD4^+$ T cells are precursors for T_{FH} cells as they are able to evade autocrine effects of IL-2 but supress T_{FH} differentiation in other $CD4^+$ T cells through paracrine IL-2 signalling (DiToro et al., 2018). DCs at the T-B border are also able to augment T_{FH} development in this region

by quenching IL-2 signalling through the expression of soluble and membrane-bound CD25 (Li et al., 2016).

T_{FH} development is intimately linked to the cell's migratory behaviour which is mediated by a dramatic change in the expression of chemokine receptors at the cell surface. CXCR5 upregulation is highly correlated with, and partially dependent on, BCL6 expression throughout T_{FH} development and allows the cell to respond to CXCL13 produced in the B cell follicle (Baumjohann et al., 2011; Nurieva et al., 2009a). The transcription factor ASCL2, which is selectively upregulated in T_{FH} cells, has also been found to mediate CXCR5 upregulation as well as CCR7 downregulation in a BCL6-independent manner (Liu et al., 2014b). BCL6 activity has been shown to result in the downregulation of PSGL1 chemokine receptor which is able to respond to CCL19 and CCL21 cytokines and, in concert with CCR7 activity, traps the cell in the T cell zone of the secondary lymphoid tissue (Poholek et al., 2010). These changes collectively allow the T_{FH} cell to migrate to the T-B border where there is a low concentration of IL-2. Here T_{FH} cells can scan B cells to identify those which are antigen specific by detecting the presence of antigenic p-MHC-II molecules on their surface.

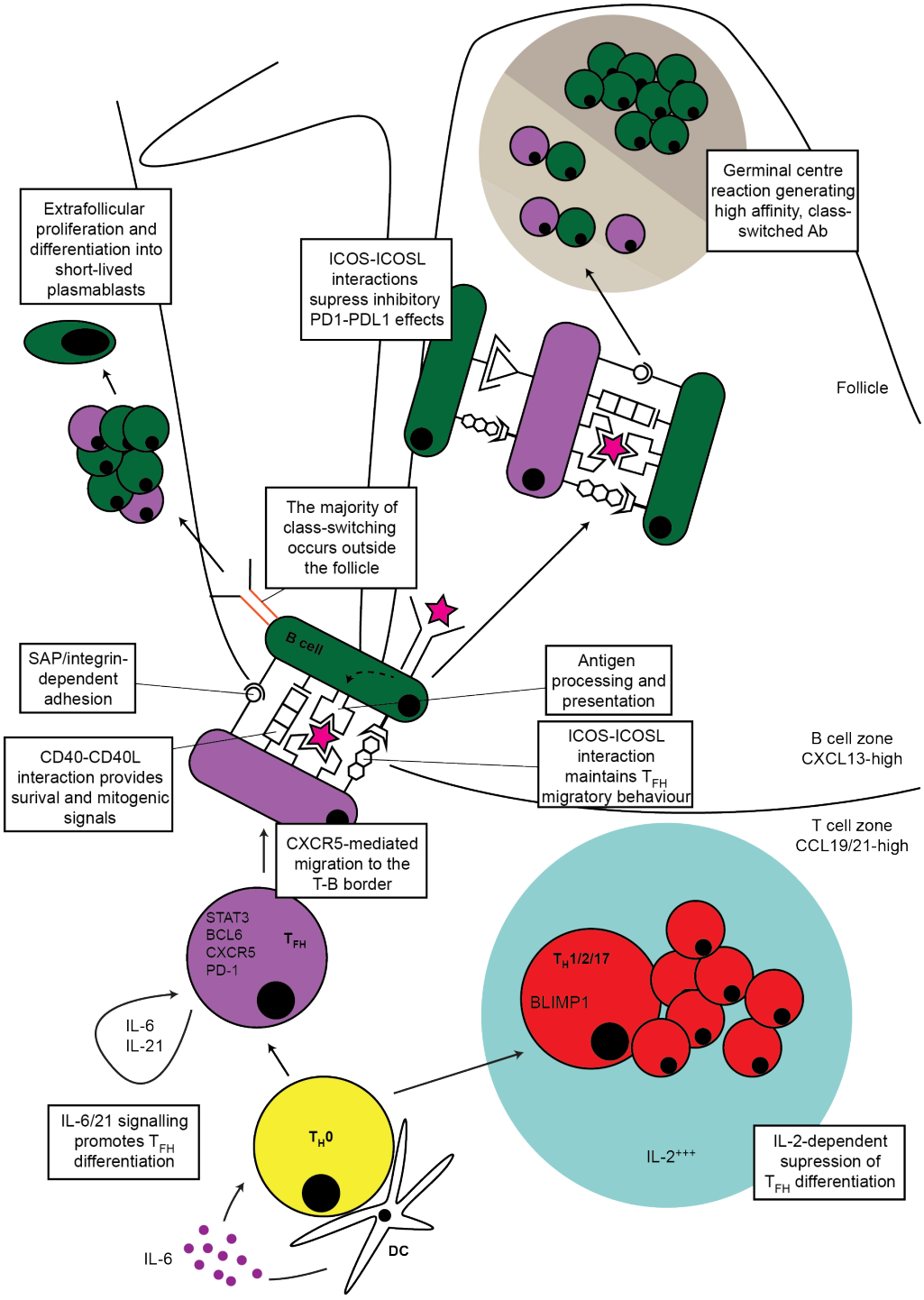

Figure 6. T_{FH} differentiation. Like other CD4$^+$ T cell subsets T_{FH} cells undergo a unique differentiation program mediated by a master transcription factor and STAT protein pair. In this case BCL6 and STAT3, which are induced by IL-6 and IL-21 signalling. However, the T_{FH} differentiation program is also intimately linked to the cell's migratory behaviour and ability to interact with B cells. In particular, upregulation of CXCR5 drives migration to the B cell follicle and reciprocal signals between T_{FH} and B cells through ICOS-ICOSL and CD40-CD40L interactions are essential for both extrafollicular and geminal centre responses. Additionally, it is now evident that T_{FH} differentiation is not necessarily a parallel program of differentiation to the other lineages but can in fact overlap significantly with them.

B cells in the B cell follicle scan the extracellular milieu for antigen using their B cell receptors (BCRs). Small soluble antigens drain into the secondary lymphoid organs via the afferent vessels, whereas large antigens coated in complement proteins are sequestered by subcapsular sinus macrophages via complement receptor 3 (CR3) and relayed into the follicle where they are presented by follicular dendritic cells, macrophages or DCs (Roozendaal et al., 2009). Antigen binding by the BCR leads to initiation of an intracellular signalling cascade, analogous to that of downstream of the TCR, and B cell activation (Burkhardt et al., 1991). One consequence of this is the internalisation of the antigen-bound BCR in clathrin-coated pits driven by myosin IIA contractility (Natkanski et al., 2013). The B cell then acts as an APC by degrading the antigen, loading it onto an MHC-II molecule, and presenting it at the cell surface for recognition by T_{FH} cells. Another consequence of B cell activation is a change in migratory behaviour mediated by the upregulation of CCR7 which results in homing to the T-B border where there is a higher concentration of CCL19 and CCL21 (Reif et al., 2002). This means that activated B cells and T_{FH} cells are concentrated in a confined area which increases the chance that antigen-specific cells will encounter one another.

Interactions with cognate B cells are essential for the maintenance of T_{FH} identity and/or survival (Baumjohann et al., 2011). Interaction with a cognate B cell results in the formation of a stable synapse between the cells mediated by binding of SAP and integrins to their respective ligands expressed on the surface of the B cell (Cannons et al., 2010). This stable synapse facilitates the delivery of reciprocal signals between the two cell types and ensures that only B cells expressing a B cell receptor (BCR) specific for the invading pathogen are recruited into the immune response. As well as presenting p-MHC-II molecules to T_{FH} cells, activated B cells express high levels of ICOSL which is recognised by ICOS expressed on T_{FH} cells. T_{FH} cells are highly dependent on signalling from ICOS as deletion of ICOS or ICOSL results in a dramatic loss of T_{FH} cells (Akiba et al., 2005). This dependence on ICOS signalling is at least in part due to its effect on the expression of chemokine receptors and thus retention of the T_{FH} cell in the B cell follicle. ICOS was shown to signal via the transcription factor KLF2 to maintain the chemokine receptor pattern of CXCR5, CCR7, PSGL-1 and S1PR1 (Weber et al., 2015). This is exemplified by the fact that ICOS-ICOSL blockade results in the migration of fully differentiated T_{FH} cells back into the T cell zone. ICOSL signals provided by non-cognate bystander B cells

facilitate T_{FH} migration up the CXCL13 gradient into the follicle by counteracting the suppressive effects of PD-L1 molecules expressed on the surface of the same bystander B cells, thus selecting for $ICOSL^{hi}$ T_{FH} cells. PD-L1 is the ligand for PD-1 which is expressed early during the T_{FH} differentiation program and is used as a marker for these cells.

CD40-CD40L interactions also play a key role in T-B communication and initially promote survival and migration of T-B conjugates to the perimeter of the follicle, via EBI2 (Kelly et al., 2011). From this point B cells can undergo extrafollicular proliferation and differentiation into short-lived plasmablasts, which are responsible for initial antibody response (Lee et al., 2011; Coffey et al., 2009). T_{FH} cell migration up the CXCL13 gradient into the follicle is supported by ICOSL signals provided by non-cognate, bystander B cells (Shi et al., 2018). These signals counteract the suppressive effects of PD-L1 ligands expression on the surface of these same bystander B cells, thus selecting for ICOS high Tfh cells.

The CD40-CD40L interaction is also essential for the formation and maintenance of germinal centres illustrated by the fact that blockade of this interaction results in dissolution of pre-existing germinal centres (Han et al., 1995). Germinal centre B cells migrate into the follicle and undergo cyclic migration between the light and dark zones of the germinal centre under the control of CXCR4 and CXCR5 chemokine receptors (Allen et al., 2004). In the dark zone these cells undergo clonal expansion and somatic hypermutation, predominantly of IgV genes, after which they migrate to the light zone. T_{FH} cells form consecutive, transient interactions with cognate B cells in the GC in a process known as serial entanglement (Liu et al., 2015; Shulman et al., 2014). TCR-mediated Ca^{2+} fluxes and ICOS signalling during these interactions results in rapid recycling of CD40L to the cell surface and thus the provision of ‘help’ signals to antigen-specific B cells. An intriguing parallel axis for T-B communication is mediated by dopamine which is released from T cells during a cognate interaction with B cells (Papa et al., 2017). This was found to reciprocally upregulate ICOSL on the surface B cells further augmenting CD40-CD40L interactions. Serial entanglement therefore favours the survival and expansion of antigen-specific B cells, particularly those with high affinity BCRs which are able to present antigen more efficiently to T_{FH} cells on their surface. In fact, the amount of proliferation and hypermutation each B cell undergoes in the dark zone is directly proportional to the amount of antigen captured and presented

to T_{FH} cells in the light zone (Gitlin et al., 2014). TCR-dependent Ca^{2+} fluxes also enhance expression of IL-21 and IL-4 by T_{FH} cells. IL-21 promotes B cell proliferation and differentiation into plasma cells, whereas IL-4 promotes B cell survival (Zotos et al., 2010; Wurster et al., 2002).

T_{FH} cells are also responsible for providing signals that direct BCR class-switching. This is the process by which the isotype of the BCR is selected to reflect the type of invading pathogen. T_{FH} cells are in fact able to express all of the hallmark cytokines of the different effector T cell subsets including IFNγ, IL-4 and IL-17 (Reinhardt et al., 2009; Lu et al., 2011; Hirota et al., 2013). These cytokines induce the expression of different BCR isotypes. For example, IFNγ drives IgG2a/c class switching which is required for the clearance of intracellular pathogens, whereas IL-4 drives IgG1 and IgE class switching which is required for the clearance of helminths (Toellner et al., 1998). Signalling via these cytokines determine the BCR isotype selected. Until recently class-switching was thought to take place inside the germinal centre, but a paradigm-challenging paper by Roco *et al*. showed that this process predominantly occurs during the extrafollicular stage of the response (Roco et al., 2019).

The apparent plasticity of T_{FH} cell cytokine secretion agrees with reports that T_{FH} cells share differentiation programs with other effector CD4+ T cell subsets and harbour positive epigenetic markings on T_H1, T_H2 and T_H17-related loci (Lu et al., 2011). For example, IFNγ and IL-12 signalling not only induces T-BET expression and accompanying T_H1 differentiation but can also induce the expression of BCL6 and IL-21 (Fang et al., 2018). Fate tracking experiments confirmed that cells which initially have the same levels of T-BET expression as T_H1 cells , are able to differentiate into T_{FH} cells while maintaining IFNγ expression in a STAT4-dependent manner even once T-BET expression is lost. This feature of T_{FH} cells therefore allows them to communicate the nature of the invading pathogen to B cells. In conclusion, T_{FH} cells are essential for the selection of antigen specific B cells, induction of somatic mutation and class-switching, and B cell differentiation to generate a high affinity, antigen-specific, class-switched antibody response.

1.8 Survival

A balance between T cell proliferation and cell death is crucial during an immune response to allow the generation of a pool of antigen-specific T cells large enough to ensure the clearance of the pathogen but restricted enough to prevent overactivation of the immune system which leads to cytokine storms and immune pathology. T cell death is mainly mediated through apoptosis, a form of controlled cell death. This process can be activated via two main routes but is ultimately mediated by activation of caspase effector proteins. The first route, known as the intrinsic pathway, is induced by pro-apoptotic, BH3-only BCL-2 family proteins that promote permeabilization of the mitochondrial outer membrane resulting in cytochrome c release which stimulates APAF-1 leading to caspase activation (Riedl et al., 2005). The second route, known as the extrinsic pathway, is mediated by cell surface receptors which, upon ligation, are capable of activating caspases directly in a cytochrome c-independent manner.

Naïve T cell survival is mediated by MHC-dependent tonic signals from the TCR as well as signalling via γ_c-chain containing cytokine receptors. In particular, IL-7 signalling has been shown to play an essential role for naïve T cell survival *in vivo* (Martin et al., 2006; Vivien et al., 2001). Signals from the TCR, costimulation receptors and cytokine receptors support survival during activation. Once the T cell pool reaches a certain size, or antigen levels are successfully depleted, cytokines and TCR signals become limiting and so activated T cells undergo apoptosis in a process known as passive cell death. Cytokine signals promote survival by inducing the expression of the pro-apoptotic members of the BCL-2 family as overexpression of these proteins can rescue passive cell death upon cytokine withdrawal (Deng and Podack, 1993). Upregulation of the pro-apoptotic protein BIM counteracts these cytokine signals during activation, increasing the cells sensitivity to withdrawal from cytokine signals. This finding is supported by the fact that deletion of the anti-apoptotic BCL-2 family member BIM, which induces cytochrome c release, results in enhanced survival of activated T cells *in vivo* (Hildeman et al., 2002).

Another apoptotic programme known as activation-induced cell death (AICD) plays a major role in limiting T cell population size and preventing an excessive immune response. This process is pre-programmed from the onset of activation and depends on death receptor-ligand binding at the cell surface. In $CD4^+$ T cells the

principal death receptor ligand pair is FAS-FASL, but TNFR-TNFα also play a role. FAS, FASL and TNFα are expressed in response to TCR stimulation and augmented by IL-2-mediated expansion (Zheng et al., 1998). FASL and TNFα can induce T cell AICD by ligating FAS or TNFαR respectively, in an autocrine or paracrine manner (Refaeli et al., 1998a; Zheng et al., 1995; Dhein et al., 1995). The pro-apoptotic activity of FAS signalling is counterbalanced by the high levels of FLIP in recently activated T cells, particularly in the presence of costimulation which inhibits FAS signalling (Ueffing et al., 2008). However, FLIP levels decrease during IL-2-mediated expansion increasing the propensity of these cells to undergo AICD in the presence of FAS (Refaeli et al., 1998a). This form of cell death cannot be rescued by overexpression of anti-apoptotic BCL-2 family members suggesting that it is independent of cytochrome c release (Van Parijs et al., 1998). However, this interpretation may be too simplistic as the pro-apoptotic BCL-2 protein BIM is upregulated upon TCR re-stimulation and deletion of this protein results in reduced sensitivity to AICD suggesting that there is an overlap between the two pathways (Snow et al., 2008). Increases in the expression of death receptors and their ligands is not the only reason activated T cells have a higher propensity to undergo AICD. In fact, downstream signalling from these receptors is augmented by more efficient recruitment of caspase-8 and FADD, sensitising these cells further to death ligands (Scaffidi et al., 1998).

A number of signalling networks are responsible for this multifaceted regulation of T cell survival. The NFκB family transcription factor proteins – C-REL and RELA – which are activated in response to TCR and CD28 signalling have been shown to be instrumental in mediating T cell survival during activation *in vitro* as dual deletion of these two proteins results in a ~8-fold decrease in viability (Grumont et al., 2004). This profound survival defect could be rescued by overexpression of BCL-2 suggesting that NFκB signalling promotes survival by inducing the expression of anti-apoptotic factors *in vitro*. These findings were supported by a study by Marinari et al. who found that stimulation of CD28 alone resulted in upregulation of BCL-X_L expression in an NFκB-dependent manner (Marinari et al., 2004). Specifically, nuclear translocation of RELA and p52 members of the NFκB family and recruitment to the *Bcl-xl* promoter was induced by CD28 ligation. Additional anti-apoptotic BCL-2 factors regulated by NFκB-dependent transcription have also been described in T

cells, such as BFL-1 (Zong et al., 1999). NFκB also regulates the expression of non-BCL-2 anti-apoptotic proteins such as IAPs and GADD45β. These proteins are capable of inhibiting both the extrinsic and intrinsic pathways of cell death, in the case of IAPs by directly binding and inhibiting caspases. Interestingly the transient translocation of RELA into the nucleus during activation is associated with increased *Bcl-xl* and GADD45β expression, whereas its subsequent export from the nucleus coincides with increased susceptibility to AICD (Mittal et al., 2006). Only overexpression of GADD45β reverses this increased susceptibility. This gives a possible mechanism by which AICD sensitivity is regulated temporally via the NFκB pathway. Not only does NFκB upregulate anti-apoptotic factors, but it has also been found to downregulate the pro-apoptotic factor p73, a member of the p53 protein family during T cell activation (Wan and DeGregori, 2003). $p73^{-/-}$ T cells exhibit enhanced survival during activation *in vitro* and deletion of *p73* rescued the survival defect resulting from NFκB inhibition and massively reduced the cells sensitivity to AICD (Lissy et al., 2000). Interestingly p73-mediated cell death required the activity of CDKs as transduction of the cells with $p16^{TAT}$ rescued the cells from antigen-induced apoptosis resulting from the inhibition of NFκB activity. p73 is a known target of E2F transcription factors suggesting that these transcription factors have pro-proliferative and pro-apoptotic functions but in the presence of NFκB activity the latter is blocked.

As previously mentioned, cytokine signalling via the shared γ_c-chain can also promote T cell survival, and cytokine withdrawal subsequently leads to passive cell death. IL-2 has been shown to induce BCL-2 expression by activating the AKT signalling pathway, whereas attenuation of AKT signalling during cytokine withdrawal results in the activation of the FOXO3A transcription factor resulting in increased BIM expression and cytochrome c release (Lindemann et al., 2003; Dijkers et al., 2000). IL-2-signalling in concert with TCR signalling is also responsible for sensitisation of activated T cells towards AICD by upregulating FASL and downregulating FLIP. IL-2 induces CD95L expression via SP1 and NFAT transcription factors (Xiao et al., 1999). TCR and CD28 costimulation is also capable of inducing FASL expression through NFAT signalling suggesting a convergence between IL-2 and TCR signalling during this process. In addition, TCR-induced nuclear translocation of NFκB and

EGR-1 has also been reported to play a role in the upregulation of FASL expression (Holtz-Heppelmann et al., 1998; Matsui et al., 1998).

The metabolic reprogramming of T cells upon stimulation is also linked to FASL expression as activation in the presence of 2-DG, an inhibitor of glucose uptake, completely bocks FASL expression and caspase cleavage (Larsen et al., 2017). A feature unique to AICD is the requirement for TCR re-triggering in addition to elevated death receptor signalling (Lenardo, 1991). The reason for this dependency has yet to be fully elucidated but a recent study using mathematical modelling has shown that amplified NFAT signalling during secondary TCR triggering could be required to induce FASL to levels high enough to induce AICD (Shin et al., 2019). FLIP downregulation is mediated, at least in part, via C-MYC which directly binds and represses the FLIP, providing another link between metabolic reprogramming and AICD (Ricci et al., 2004). Again, there is no clear mechanistic basis for the dependence of FLIP downregulation on IL-2 signalling.

In conclusion, TCR, CD28 and cytokine signals provide both pro-apoptotic and anti-apoptotic signals to the cell. These signals seem to be predominantly mediated by NFκB, NFAT and AKT signalling. As clonal expansion progresses the balance is tipped towards the pro-apoptotic signals due to stimulation-dependent changes to the expression of proteins influencing apoptosis, but also due to the passive withdrawal of cytokines and antigen.

1.9 Cell cycle

The cell cycle is controlled by the cyclin-dependent kinase (CDK) family of proteins. In mammalian cells the main members of this family are CDK1, 2, 4 and 6. The activity of these kinases is regulated at multiple levels: cyclin expression at the transcriptional level, abundance of CDK inhibitors such as p21 and p27, and by their phosphorylation status which is regulated by CDC25 phosphatases and the Wee1 kinase (Figure 7.

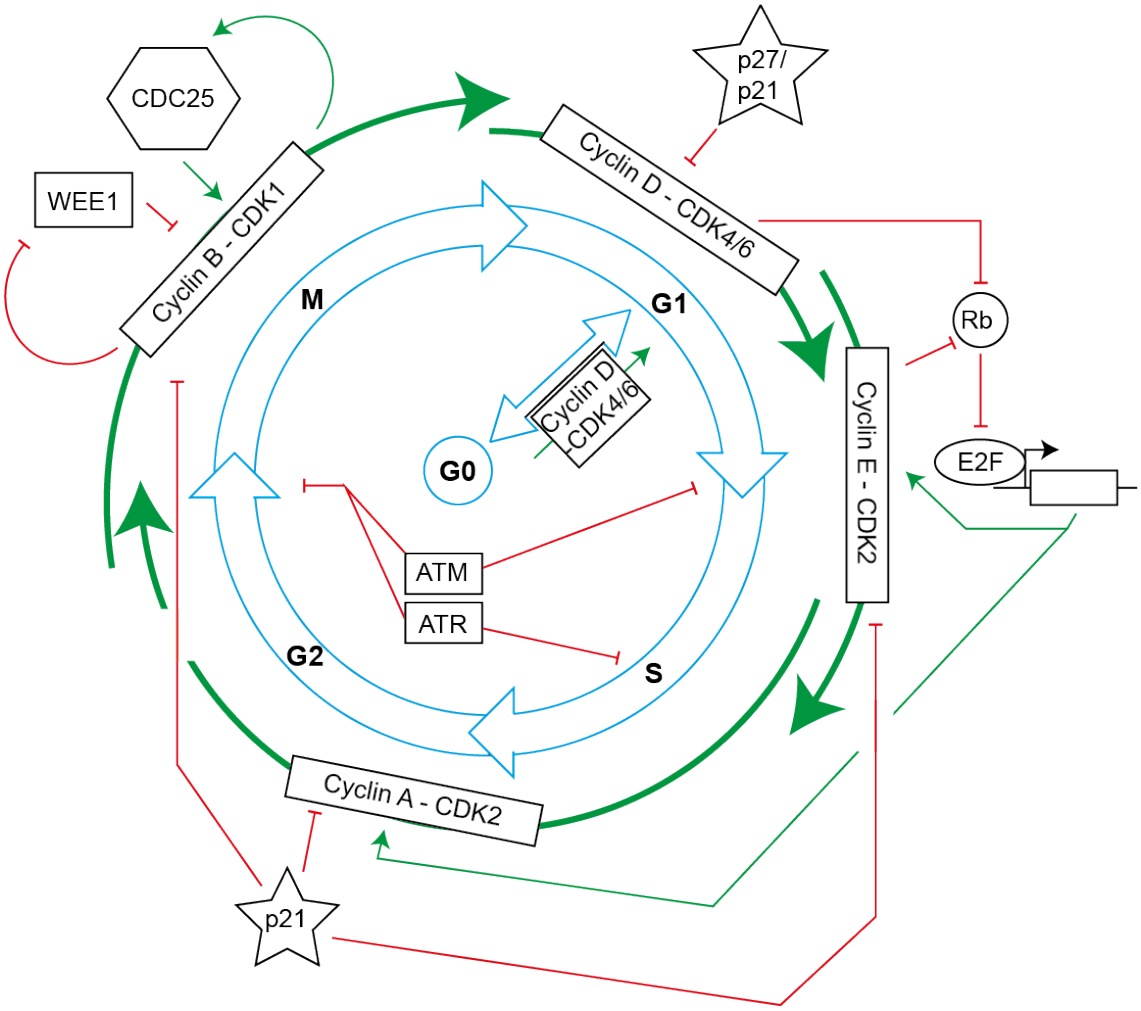

Figure 7. The mammalian cell cycle. Quiescent cells, such as naïve CD4$^+$ T cells, reside in G0 phase. Upon mitogenic stimulation these cells enter G1 phase and subsequently progress through the cell cycle ultimately producing two daughter cells upon completion of mitosis (M). The ordered progression through the distinct phases of the cell cycle is controlled by CDK activity. CDK activity is controlled through the sequential expression of cyclins which bind to and activate CDKs. The G1/S and G2/M transitions are controlled by feedback circuits. The G1/S circuit requires sufficient levels of cyclin D and E to accumulate to induce E2F transcriptional activity. The G2/M transition requires sufficient cyclin B to accumulate to overcome WEE1-dependent inhibition of CDK1. This inhibition is mediated through phosphorylation of CDK1. CDK inhibitors, such as p21 and p27, provide an additional layer of CDK regulation. ATM and ATR detect genotoxic stress and activate cell cycle checkpoints which block cell cycle progression at the indicated points.

1.9.1 G0/G1

Naïve T cells are quiescent and reside in the G0 phase of the cell cycle. Entry into G1 by CD4+ T cells is induced by TCR and CD28 signalling in addition to cytokine signals such as that of IL-2, which is considered to be the most potent T cell mitogen. While stimulation of the TCR in combination with CD28 is sufficient to induce cell

cycle progression *in vitro*, this process is greatly augmented by IL-2-dependent STAT5 signalling, particularly under conditions in which costimulation is limited (Moriggl et al., 1999; Shi et al., 2009). Other cytokines, such as IL-4, are also able to support proliferation due to fact that receptors for these cytokines share the γ_c subunit that is able to initiate STAT transcription factor activation (Lin et al., 1995).

The G0-G1 transition and progression through G1 requires the activity of the cyclin D-CDK4/6 complex whereas navigation through the G1/S transition (restriction point) requires both the activity of cyclin D-CDK4/6 and cyclin E-CDK2 complexes. The activity of these complexes is regulated at the level of cyclin expression, but also by the CDK inhibitor $p27^{Kip1}$, which is expressed at high levels in naïve T cells and must be degraded for G1 progression (Appleman et al., 2000). It has been shown that TCR stimulation alone, in the absence of costimulation, is sufficient to induce expression of cyclin D and E and CDKs. This TCR-dependent regulation is completely dependent on ERK signalling (Appleman et al., 2002a). Conversely, $p27^{Kip1}$ degradation exclusively requires CD28-dependent PI3K signalling which mediates this process via inhibition of GSK-3, an AKT substrate (Appleman et al., 2002b). G1 entry is also associated with a dramatic increase in cell size in response to antigen, a process known as blastogenesis. This increase in cell size reflects the massive metabolic demands placed on a $CD4^+$ T cell during division as each cell divides every ~6-16hrs, which is among the fastest cell cycles known in mammalian biology (Gudmundsdottir et al., 1999).

mTORC1 is a considered to be the master regulator of catabolism and anabolism and therefore instrumental in regulating blastogenesis and G1 entry (Inoki et al., 2002). mTORC1 is able to integrate signals from mitogenic stimuli, nutrient availability, cellular energy levels and oxygen levels to authorise division only in permissive conditions. Mitogenic stimulation, such as signals from the TCR and costimulation receptors, activates mTORC1 via the PI3K-AKT and ERK-RSK pathways. PI3K activates AKT which directly phosphorylates and inactivates TSC1/2. TSC1/2 is a RHEB GTPase activating protein (GAP) which induces GTP hydrolysis by RHEB resulting in RHEB inactivation. Inhibition of TSC2 therefore activates RHEB which in turn activates mTORC1. Phosphorylation of 4E-BP1 by mTORC1 abrogates its ability to bind to the eukaryotic initiation factor 4E (eIF4E). Release of eIF4E allows it to bind to the 5'-cap of mRNAs and initiate cap-dependent translation (Qin et al., 2016). p70S6K is another major mTORC1 substrate, which phosphorylates S6, a

component of the 40S ribosomal subunit. There is also a MEK-dependent mechanism for mTORC1 activation and S6 phosphorylation in naïve T cells downstream of the TCR and CD28 receptors (Lin et al., 2012). Studies using cancer cell lines have established a mechanism by which ERK and its substrate RSK induce mTORC1 activity by mediating TSC2 phosphorylation as well as phosphorylation of the mTORC1 complex itself (Figure 8) (Carrière et al., 2008; Carriere et al., 2011; Ma et al., 2005; Miyazaki and Takemasa, 2017). Additionally, ERK can phosphorylate S6 via RSK in an mTORC1-independent manner (Roux et al., 2007). Myers et al. reported that RASGRP1 signalling during tonic TCR signalling in naïve $CD4^+$ T cells is able to activate mTORC1 in an RSK-independent manner, possibly via another ERK-dependent mechanism (Myers et al., 2019).

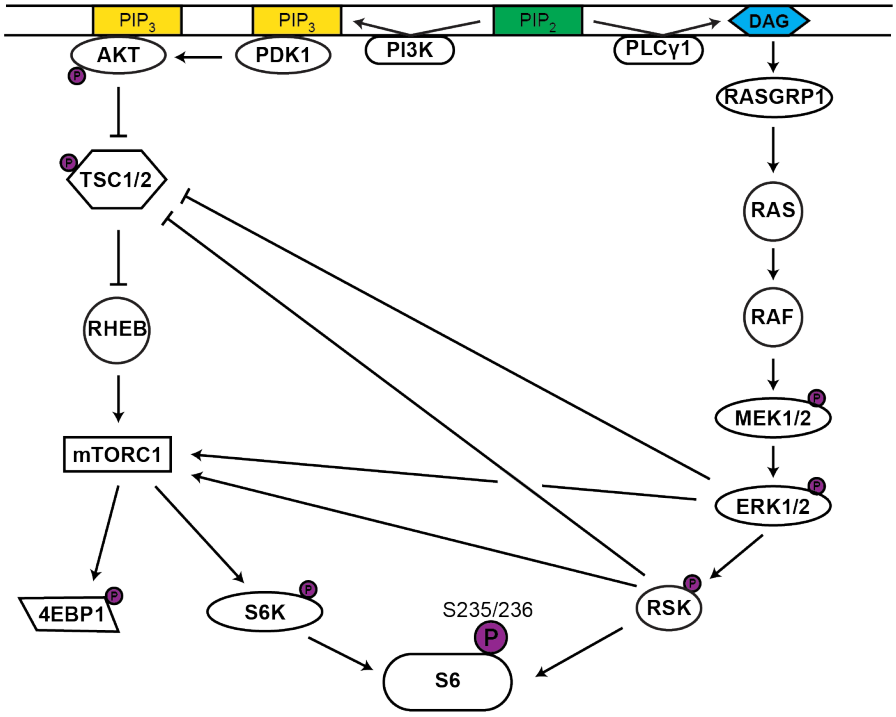

Figure 8. Cross-talk between ERK and mTORC1 signalling pathways. ERK and RSK have been reported to stimulate signalling through the mTORC1 pathway by phosphorylating and inhibiting TSC proteins as well as by phosphorylating and activating the mTORC1 complex directly. Additionally, ERK is able to induce S6 S235/236 phosphorylation via RSK in an mTORC1-independent manner.

A critical role for mTORC1 function in blastogenesis and proliferation is illustrated by the extreme reduction in cell growth and proliferation observed in RAPTOR-deficient cells (Yang et al., 2013). RAPTOR is a component of the mTORC1 complex and is essential for mTORC1 function. The inability of RAPTOR-

deficient cells to proliferate was predominantly due to a defect in G1 entry caused by reduced expression of cyclin D2 and E, as well as CDK2, 4 and 6. This also lead to an almost complete block of Rb phosphorylation illustrating an inability of RAPTOR-deficient cells to pass the G1 restriction point. Interestingly, deletion of RAPTOR or mTORC1 inhibition at later timepoints during activation *in vitro* had much less of an effect on the proliferative capacity of the $CD4^+$ T cells. Altogether these data show that mTORC1 activity is critical for entry into G1, but not cell cycle progression of cycling cells. The G1 entry defect in RAPTOR-deficient cells was associated with reduced lipid biosynthesis, glutaminolysis and glycolysis. mTORC1 regulates the upregulation of glycolysis, at least in part, by stabilising the C-MYC transcription factor. mTORC1-dependent regulation of fatty acid metabolism seems to be at the post-transcriptional level as the protein levels, but not transcription, of SREBP1 and SREBP2 are dysregulated in RAPTOR-deficient cells. SREBP transcription factors regulate the expression of genes involved in lipid biosynthesis (Espenshade and Hughes, 2007). mTORC-dependent regulation of global metabolic pathways is likely to be responsible, at least in part, for blastogenesis and may be required for G1 entry. Interestingly the induction of anabolic pathways during G1 activation seems to be coupled to CDK activity as inhibition of CDK by transduction of naïve $CD4^+$ cells with a TAT-$p16^{INK4A}$ fusion protein prevented cell growth and entry into G1 (Lea et al., 2003).

ERK signalling also induces the accumulation of C-MYC (Sears et al., 2000). C-MYC-dependent upregulation of glycolysis and glutaminolysis is critical for $CD4^+$ T cell blastogensis and proliferation in response to TCR and CD28 stimulation (Wang et al., 2011b). C-MYC achieves this switch from oxidative phosphorylation to glycolytic/glutaminolytic metabolism by inducing the transcription of enzymes/transporters involved in these pathways. The glycolytic switch allows the cell to rapidly increase its metabolic capacity but also provides substrate for the pentose phosphate pathway which generates precursors for many biosynthetic pathways involved in blastogenesis. mTORC1 signalling is clearly required for C-MYC activity but NFκB signalling has also been found to play an essential role (Grumont et al., 2004). This mechanism was elucidated by Grumont et al. using total splenic T cells activated *in vitro* with anti-CD3 and anti-CD28 antibodies. They found that PKCθ induced under these conditions was responsible for NFAT-dependent transcription of *c-rel* and nuclear import of RELA. These proteins perform redundant

roles in this setting by binding to NFκB transcription factors and inducing C-MYC induction. In the absence of these proteins C-MYC expression is completely ablated and T cells fail to undergo blastogenesis and entry into S phase. Overexpression of C-MYC in these double mutant cells is able to rescue cell growth.

In addition to NFκB and mTORC1 activity, calcineurin-dependent activation of the SLC7A5/SLC3A2 system L1 amino acid transporter has been implicated in C-MYC expression at the post-transcriptional level during activation of $CD8^+$ T cells (Sinclair et al., 2013). This mechanism of C-MYC regulation was found to be mTORC1-independent as the addition of Rapamycin did not affect C-MYC induction through this pathway. This is surprising as the SLC7A5/SLC3A2 antiporter is particularly important in regulating mTORC1 activity as it mediates the exchange of intracellular glutamine for extracellular leucine and mTORC1 is robustly inhibited in the absence of leucine.

C-MYC does not solely regulate metabolic changes for G1 entry. In fact, MYC is incredibly promiscuous in its activities and by one estimate exhibits high affinity for 11% of all promoters in the human genome, although it is not sufficient for transcription initiation at these sites (Fernandez et al., 2003; Frank et al., 2001).

1.9.2 S phase

E2F transcription factors are thought to be key regulators of the G1/S transition. Once again C-MYC has been found to induce the expression of, and enhance the transactivation activity of, these transcription factors providing a link between cell growth and division (Fernandez et al., 2003; Leung et al., 2008). During G0 and early G1 the retinoblastoma (Rb) family of proteins, known as “pocket” proteins, bind and regulate E2F transcription factors thereby acting as gatekeepers for the G1/S restriction point. Rb binds to E2F1, 2 and 3 and inhibits their transactivation activity (Lees et al., 1993). Concurrently, p107 and p130 pocket proteins bind to E2F4 and 5, trapping them in the nucleus where they repress expression of E2F-responsive genes (Balciunaite et al., 2005). An increase in the activity of Cyclin D-CDK4/6 complexes during G1 results in Rb protein phosphorylation which leads to the release of E2F1, 2 and 3, exclusion of E2F4 and 5 from the nucleus, and the expression of genes required for S phase entry (Takahashi et al., 2000).

Among this set of E2F-responsive genes are cyclin E and A. Cyclin E binds to CDK2 inducing its activity. This complex is responsible for completing the hyperphosphorylation of Rb proteins, leading to a further increase in E2F-dependent transcription and the formation of a positive feedback loop. E2F transcription factors also induce their own expression providing another mechanism of positive feedback (Leung et al., 2008). Full Rb hyperphosphorylation results in passage through the G1/S restriction point and initiation of S phase. The E2F-Rb feedback loop at the restriction point acts as a bistable switch for S phase entry and cell cycle progression past this point is independent of mitogenic signalling (Yao et al., 2008). After the G1/S transition has been completed negative feedback loops supress E2F-dependent transcription of G1/S transcripts. E2F transcriptional activators induce the expression of E2F6-8 repressors which accumulate and displace E2F activators from promoters (Giangrande et al., 2004). Additionally the E2F-dependent increase in CDK2-cyclin A/E activity results in phosphorylation and inactivation of E2F1 forming a second negative feedback loop (Xu et al., 1994).

The genome is replicated in S phase. This process is tightly regulated by CDK and Dbf4-dependent CDC7 kinase activity to ensure the genome is faithfully replicated once per cell cycle (Yeeles et al., 2015). DNA replication is initiated from multiple replication origins that are co-ordinated to maintain genome stability. These origins are licenced during late G1 phase. Initially the origin replication complex (ORC) binds to these origins licencing them by facilitating the loading of the MCM2-7 helicase (Coster et al., 2014). Firing of origins occurs when CDC45 and GINS proteins are loaded onto the origin under the control of CDK2 and CDC7 kinases to generate the CDC45-MCM-GINS (CMG) helicase complex (Pacek et al., 2006). CDK2- and CDC7-dependent phosphorylation of MCM4 activates the MCM2-7 helicase resulting in DNA unwinding, formation of the replisome containing DNA polymerases α, δ and ε, and a pair of bi-directional replication forks (Ilves et al., 2010; Sheu and Stillman, 2010). ~10% of licenced origins fire in a temporally ordered sequence during an unperturbed S phase, however in the presence of replication stress dormant origins can be fired to ensure complete genome replication (Ge et al., 2007).

Origin firing is regulated spatially as well as temporally. Clusters of 2-5 origins are fired simultaneously during S phase. These clusters are further organised into a higher order structure known as a replication factory that contains ~6-12 replicons

(Gillespie and Blow, 2010). Early firing factories are located in the centre of the nucleus whereas later firing factories are located at the periphery. These factories initiate in a synchronised manner at various times during S phase in a CDK-dependent manner. Replication stress, characterised by slowing or stalling of replication forks, results in an increase in the number of replication forks in active factories but a reduction in the total number of factories (Ge and Blow, 2010).

1.9.3 G2/M

Entry into M phase is controlled at the level of CDK1 activity. Once a threshold level of activity has been reached this kinase induces chromosome condensation, segregation and cell division. Like the other CDK proteins CDK1 requires a cyclin cofactor for activity, in this case cyclin B, although during S and G2 phases it is bound to cyclin A. Cyclin B accumulates under the control of CDK2 and E2F activity during S phase (Lukas et al., 1999). However, the kinase activity of MYT1 and WEE1 inhibit premature activity of the CDK1-cyclin B complex by phosphorylating CDK1 at T14 and Y15 (Figure 9) (Norbury et al., 1991). The dual specificity CDC25 phosphatase opposes this inhibition by dephosphorylating T14 and Y15, thereby activating CDK1 (Gautier et al., 1991). Modification of these residues is the foundation for a second node of G2/M regulation that, similar to the G1/S transition, forms a bistable switch (Rata et al., 2018). This ensures that the cell does not enter M prematurely and cannot revert back to S phase once the M phase sequence has been initiated. Once sufficient Cyclin B has accumulated, active CDK1 is able to phosphorylate CDC25 and WEE1, activating and inhibiting their respective activities. This circuit therefore forms a positive feedback loop resulting in the rapid accumulation of dephosphorylated CDK1-cyclin B complexes that are able to drive progression through mitosis (Solomon et al., 1990). This mechanism of regulation is not unique to CDK1 at the G2/M transition as it is conserved between the CDKs and thus can be used to regulate progression through multiple stages of the cell cycle (Welburn et al., 2007).

An additional layer of regulation of G2/M transition is exerted by the GWL-ENSA-PP2A-B55 pathway which makes the bistability of the system even more robust (Figure 9) (Mochida et al., 2016). In fact, the G2/M transition can be mediated

by this pathway alone. CDK1-dependent phosphorylation of WEE1, CDC25 and other M phase substrates is counteracted by the activity of the PP2A phosphatase bound to its B55 regulatory subunit. This complex is also subject to autoregulation via a positive feedback loop composed of the GWL kinase and its substrates - ENSA and ARPP19 - which are potent inhibitors of PP2A. PP2A-B55 is able to dephosphorylate GWL, inactivating it and its substrates and thus maintaining PP2A-B55 in its inactive state. These two loops are also connected by the ability of CDK1-Cyclin B to phosphorylate and activate GWL resulting in mutual antagonism.

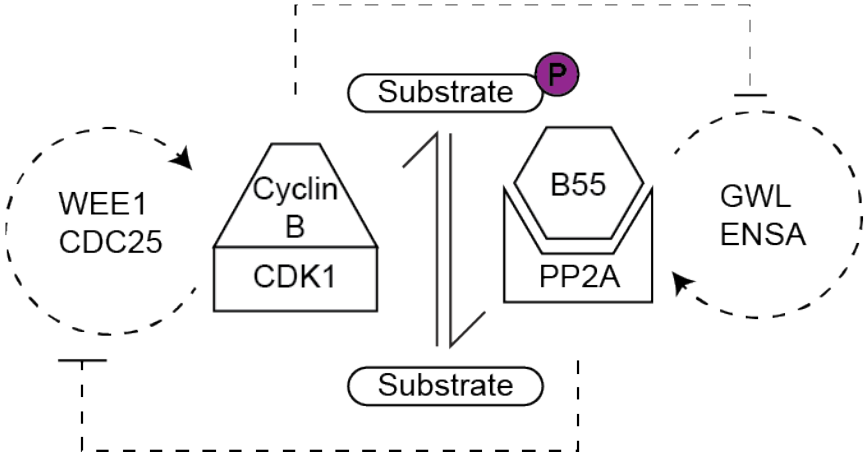

Figure 9. The G2/M transition is mediated by two bistable switches. The G2/M transition is highly regulated to prevent inappropriate entry into M phase and subsequent mitotic catastrophe. Phosphorylation of M phase substrates by CDK1-Cyclin B promotes the G2/M transition whereas dephosphorylation of these substrates by PP2A-B55 prevents it. Each complex is regulated by a positive feedback loop as well as mutual antagonism by the other complex. This circuitry ensures that the transition into M phase occurs rapidly once sufficient cyclin B has accumulated and is irreversible. It also provides a mechanism by which cell cycle checkpoints can exert their effects. Adapted from (Rata et al., 2018).

1.9.4 Cell cycle checkpoints

There are a number of checkpoints that the cell must satisfy to progress through the cell cycle. The principal function of these checkpoints is to protect the cell against genomic instability. A number of them, positioned at G1/S, S and G2/M, are controlled by ATM and ATR kinases (Maréchal and Zou, 2013). ATM is activated by double strand breaks (DSBs) in DNA, whereas ATR is activated by single strand breaks (SSBs). Other cellular stresses are also able to influence the activity of these kinases. ATM and ATR mediate cell cycle arrest, recruit DNA damage repair

machinery to the sites of damage and can influence cell fate decisions by inducing apoptosis or senescence.

Replication stress is a major cause of SSBs. Replication stress is classified as a reduction in the efficiency of DNA replication during S phase and can be caused by a multitude of factors including depletion of DNA polymerase substrates, DNA damage, and impairment of replisome function. Replication stress leads to fork stalling. Fork stalling results in the dissociation of the CMG helicase from the polymerase and formation of single-stranded DNA (ssDNA)/double-stranded DNA (dsDNA) junctions (Byun et al., 2005). ssDNA/dsDNA junctions can also be formed as intermediates during DNA damage repair and also after DSB end resection (Jazayeri et al., 2006). These ssDNA/dsDNA junctions form the basic substrate for ATR recruitment and activation. However, before this takes place ssDNA is recognised and bound by RPA, and the 9-1-1 clamp is loaded onto dsDNA at the dsDNA/ssDNA junction (Ellison and Stillman, 2003; Zou et al., 2003). This structure acts as the scaffold for the nucleation of the ATR signalling complex by recruiting ATRIP, ATR and TOPBP1 (Lee et al., 2007; Kumagai et al., 2006) This signalling complex induces ATR kinase activity and the phosphorylation of an array of substrates including its main effector - CHK1 - at S317 and S345 (Liu et al., 2000).

CHK1 carries out a multitude of functions to enforce the block in cell cycle progression and protect against genome instability. In particular CHK1 phosphorylates CDC25 triggering its degradation. This skews the CDK Y15 equilibrium towards phosphorylation rendering CDKs inactive (Sørensen et al., 2003). It also appears that CHK1 can inhibit origin firing during S phase by inhibiting CDC7 activity (Moiseeva et al., 2017). Interestingly CHK1 blocks all origin firing in inactive replication factories but allows dormant origins to fire in currently active factories, redirecting replication activity to regions encountering stress (Anglana et al., 2003; Ge et al., 2007; Yekezare et al., 2013). It is unclear how this level of regulation is enforced although even in unperturbed cells ATR signalling is required to limit late origin firing. A mechanism has been proposed in which ATR blocks CDK1-dependent phosphorylation of RIF1 thereby facilitating PP1 recruitment to chromatin and the antagonism of CDC7 and CDK2 signalling required for origin firing (Moiseeva et al., 2019). Additionally, ATR-dependent phosphorylation of MCM2 results in the recruitment of PLK1 which is thought to promote firing of local origins but also the local inhibition of CHK1 (Trenz et al., 2008). This suggests a possible mechanism in

which ATR activity at sites of damage induces origin firing while inhibiting CHK1 activity locally. Whereas once CHK1 diffuses away from these sites it regains activity in the absence of local PLK activity and blocks origin firing.

The ATR pathway also stabilises stalled forks, preventing their collapse and further genome instability. By inhibiting origin firing ATR prevents exhaustion of RPA, which binds to ssDNA and prevents the formation of DSBs at these sites (Toledo et al., 2013). ATR modulates the activity the chromatin remodeller SMARCAL1 which is recruited to the stalled fork and catalyses fork reversal, preventing DSB formation by aberrant fork processing (Couch et al., 2013). ATR-dependent phosphorylation limits SMARCAL 1 activity thereby preventing excessive reversal and fork collapse. Direct phosphorylation by ATR is also required for the recruitment of a range of other chromatin remodellers to the stalled fork that are required for its stabilisation and repair, including WRN and BLM (Ammazzalorso et al., 2010; Davies et al., 2004). There is also evidence that ATR signalling stabilises the replisome itself at stalled forks (Dungrawala et al., 2015). CHK1 activity can also limit DNA damage during replication stress by relieving inhibition of E2F-depenent transcription during S phase by phosphorylating and inactivating the E2F6 transcriptional repressor (Bertoli et al., 2013). This maintains expression of multiple factors required for stalled fork processing and restart.

ATR also participates in the recruitment of DNA damage repair machinery to sites of damage. For example, ATR-dependent phosphorylation of FANCD2 and XPA, which are members of the inter-strand crosslink repair and nucleotide excision repair pathways respectively, facilitates their recruitment to sites of damage (Wu et al., 2007; Andreassen et al., 2004). Persistently stalled replication forks can decay to form DSBs. Additionally, ATM-dependent resection of dsDNA ends results in the recruitment and activation of ATR at the site of damage while progressively reducing ATM activity (Jazayeri et al., 2006; Shiotani and Zou, 2009). This explains the requirement for ATM and MRE11 during activation of the ATR pathway in response to ionising radiation but not UV or hydroxyurea (HU) treatment (Myers and Cortez, 2006) ATR is instrumental in assembling homologous recombination repair (HRR) machinery at sites of DSB. ATR-dependent phosphorylation of XRCC3, a RAD51 paralog, after end resection is essential for RAD51 loading (Somyajit et al., 2013). ATR-dependent RPA phosphorylation also facilitates the recruitment of factors required for HRR. For example, phospho-RPA is responsible for the recruitment of

PALB2 and BRCA2 which in turn facilitate RAD51 filament formation (Murphy et al., 2014). In parallel, CHK1 phosphorylates RAD51 at T309 recruiting it to form foci at DSBs facilitating HRR (Sørensen et al., 2005).

ATM is activated by the presence of DSBs. ATM is recruited to dsDNA blunt ends and those with small ssDNA overhangs (Shiotani and Zou, 2009; You et al., 2007). Its recruitment appears to be mediated by the MRN complex which can directly bind dsDNA ends and also seems to be sufficient for ATM activation (Lee and Paull, 2005). The mechanism for ATM activation by MRN is unclear as ablation of MRN's nuclease activity does not affect ATM activation. However, interaction between the two proteins in the presence of dsDNA ends results in dissociation of ATM into active monomers and phosphorylation of downstream targets (Buis et al., 2008; Lee and Paull, 2007). One well known target of ATM is the H2AX histone. The S139-phosphorylated form of this protein is known as γH2AX which spreads over large chromatin domains flanking the sites of damage and mediates the recruitment of chromatin remodellers and repair machinery (Kinner et al., 2008). Co-immunoprecipitation experiments have shown that γH2AX can bind to ATM indirectly via MDC1 which could facilitate the propagation of γH2AX across large chromatin domains (Lou et al., 2006; Savic et al., 2009). Interestingly, ATR is also able to phosphorylate γH2AX, and TOPBP1 is able to interact with MDC1, providing a possible mechanism of cross-talk between pathways (Ward and Chen, 2001; Wang et al., 2011a). There are multiple additional layers of overlap between ATM and ATR pathways. For example, ATM activity promotes the recruitment of TOPBP1 and its interaction with ATR whereas ATR can directly phosphorylate ATM at S1981 promoting activation (Yoo et al., 2007; Stiff et al., 2006). Nevertheless, the main form of interaction between the pathways is likely to be interconversion of DNA damage intermediates, discussed above.

ATM mediates homologous recombination repair in S and G2. ATM promotes CTIP-dependent resection of dsDNA ends which results in RPA binding (Gao et al., 2020). RPA is later displaced by RAD51 under the activities of BRCA1 and 2 (Davies et al., 2001). RAD51 filaments then facilitate strand invasion of the homologous sister chromatid to enable HRR. ATM additionally prevents toxic non-homologous end joining (NHEJ) during S and G2 by stimulating CTIP to displace Ku, another blunt end dsDNA-recognising protein which recruits DNA-PKcs. DNA-PKcs orchestrates

the recruitment of the NHEJ machinery (Chanut et al., 2016). Outside of S and G2 phases the vast majority of DSBs are repaired by NHEJ independently of ATM, although there seems to be a small proportion that require ATM activity possibly to facilitate end-processing via ARTEMIS (Beucher et al., 2009). Interestingly, the requirement for ATM in this small fraction of DSBs seems to be alleviated by the deletion of its substrate KAP-1 (Goodarzi et al., 2008). KAP-1 is a transcriptional repressor that may play a role in the perturbation of heterochromatin during the repair of DSBs (Ziv et al., 2006).

CHK2 constitutes a major signalling node downstream of ATM and carries out set of functions that overlap with those of CHK1. For example, CHK2 also phosphorylates CDC25 resulting in its degradation and cell cycle arrest (Falck et al., 2001; Matsuoka et al., 1998). Another major substrate of both of these kinases is p53. p53 is a prominent tumour suppressor that regulates a plethora of transcriptional changes during the DNA damage response, reinforcing cell cycle arrest and ultimately determining cell fate. ATR-CHK1 and ATM-CHK2 pathways induce an extensive set of post-translational modifications on p53 via direct and indirect routes (Shiloh and Ziv, 2013). These modifications lead to an increase in stability and induction of p53-depednent transcription. One well characterised mechanism for activation is the phosphorylation of S15 and S20 by ATM/ATR and CHK1/CHK2 respectively which is reported to protect p53 from ubiquitination by MDM2 and subsequent degradation (Chehab et al., 2000). Deletion of these serine residues reduced p53 stability and transactivation activity in response to genotoxic stress although phosphorylation of these residues is likely not sufficient for induction of p53 activities (Chao et al., 2006). CHK1/CHK2 phosphorylation of the C-terminal domain of p53 is also thought to modulate its acetylation status. Thish is known to control its stability and transactivation activity (Ou et al., 2005). ATM- and ATR- dependent regulation of MDM2 abundance is another important mechanism for p53 regulation (Meulmeester et al., 2005).

p53 reinforces cell cycle arrest through multiple mechanisms. One of the more famous examples is the p53-dependent upregulation of p21, a CDK inhibitor. p21 binds to CDK-cyclin complexes and sterically disrupts interactions with substrates such as CDC25 and Rb preventing their phosphorylation (Chen et al., 1996). p21 can also bind PCNA at a site which interferes with DNA polymerase δ activity thereby directly blocking DNA replication (Rousseau et al., 1999). This pathway is essential

for proper cell cycle arrest following genotoxic insult (Brugarolas et al., 1995). Other well characterised mechanisms for p53-dependent cell cycle arrest are transcriptional repression of CDC25 and cyclin B expression (Clair et al., 2004; Innocente et al., 1999).

As previously mentioned, p53 is central to cell fate decisions in response to DNA damage (Hafner et al., 2019). If DNA is not repaired properly then p53 induces apoptosis or senescence to prevent propagation of mutations to new generations of cells. Kinetics, abundance, and trasnsactivation activity of p53 are the major determinants that control cell fate. For example, low doses of IR result in transient p53 accumulation, DNA repair and ultimately restart of the cell cycle, whereas if p53 stability is enhanced by addition of an MDM2 inhibitor the cell enters senescence (Purvis et al., 2012). p21 is critical for inducing senescence as well as negatively regulating apoptosis (Zhang et al., 2011b; Muñoz-Espín et al., 2013). Acetylation patterns and the oligomerisation state of p53 are thought to mediate transactivation activity towards pro-apoptotic genes. This was shown using the separation-of-function mutants - K117R and E117R - which interfere with acetylation and oligomerisation respectively. Cells from these mice were not able to induce apoptosis despite cell cycle arrest, whereas induction of senescence in response to DNA damage was normal (Timofeev et al., 2013; Li et al., 2012).

So far in this section the cell cycle checkpoint pathways have been discussed in the context of DNA damage as this is an extensively studied subject. However, a recent study by Kumar et al. show that ATR can be activated independently of DNA damage by mechanical perturbation of the nuclear envelope, including by hypertonic shock (Kumar et al., 2014). Another pair of studies has shown that CHK1 is phosphorylated at S345 in nIMCD3 cells submitted to a severe hypertonic shock but only once returned to isotonicity (Dmitrieva et al., 2003; Dmitrieva et al., 2004). However, Dmitrieva et al. found a concomitant induction of γH2AX suggesting DNA damage was present in these conditions. A crucial difference between these studies is that the latter pair used NaCl whereas the former used sorbitol to generate the hypertonic environment. Kultz et al. used the neutral comet assay to show that in fact high NaCl hypertonicity causes DSBs whereas high urea hypertonicity does not, suggesting a NaCl-specific mechanism of DNA damage (Kültz and Chakravarty, 2001). Zhang et al. extended this work by showing that urea did however induce ROS-mediated DNA lesions whereas sorbitol did not, supporting the idea that DNA

damage in these conditions is dependent on the identity of the osmolyte rather than hypertonicity (Zhang et al., 2004). Yet another study found that high sorbitol hypertonic shock induced both γH2AX and DNA double strand breaks in primary corneal epithelial cells suggesting the cell type may influence outcome of osmotic shock as well as osmolyte identity (Wang et al., 2014).

Multiple studies have found hypertonicity results in cell cycle arrest, but different mechanisms have been reported most likely due to differences in osmolyte, cell type and the extent of the hypertonic shock. Without exception the authors of these studies subject cells to extreme increases in hypertonicity which are unlikely to be physiological. One study found that caffeine, reported to be an ATR and ATM inhibitor, reversed reduced EdU incorporation rate under high NaCl conditions (Dmitrieva et al., 2001). Another reported p38 to at least partially mediate G2/M checkpoint activation in response to high NaCl conditions but that ATR and ATM signalling did not play a role (Dmitrieva et al., 2002).

1.10 Osmoregulation

Mammalian cells can be exposed to range of extracellular tonicities during their lifetime, particularly if they are highly migratory like $CD4^+$ T cells. The tissue fluids of the lymphoid tissues, skin, liver and kidney, to name a few, are hypertonic relative to serum (Go et al., 2004; Titze, 2014). For context, serum osmolarity is humans and rodent models is around 290-310 mOsm/L whereas interstitial fluid in the kidney medulla, for example, can reach 1,700 mOsm/L (Aramburu and López-Rodríguez, 2019; Marsh and Azen, 1975). There are also many pathological conditions that alter plasma osmolarity. For example, severe burns can increase plasma osmolarity to as high as 430mOsm/L and profound dehydration caused by sweating and diarrhoea during infection can also increase plasma osmolarity (Meyers, 2009; Inglis et al., 1995). Hyperglycemia associated with diabetes also increases the tonicity of plasma (Stookey, 2005). Additionally, individuals over the age of 50 have also been found to have an increased risk of having hyperosmolar plasma.

The fact that cell membranes are highly permeable to water means that imbalances in intracellular and extracellular tonicity can rapidly induce volume changes due to movement of water across the membrane down the osmotic

pressure gradient. These volume changes exert a significant stress on the cell by causing protein misfolding and DNA damage (Kuznetsova et al., 2014). Additionally, intracellular molecular crowding effects can cause major disruptions to homeostatic processes such as transcription (Delarue et al., 2018). Cells have therefore evolved multiple mechanisms to restore the osmotic equilibrium across the membrane thereby protecting themselves from the profound defects caused by volume changes. Cells activate regulatory volume increase (RVI) mechanisms in response to water efflux and regulatory volume decrease (RVD) mechanisms in response to water influx. These responses are mediated by rapid changes in enzyme activity, ion channel transduction and solute transporter activity, but also long-term changes in transcription.

Hypotonic challenge results in the activation of many ion transporters at the cell membrane, many of which have likely not been characterised. These channels predominantly mediate efflux of K^+ and Cl^- ions to reduce intracellular tonicity to restore the osmotic equilibrium. An increase in permeability to K^+ results in diffusion of these ions down their electrochemical gradient, out of the cell. In particular the voltage-dependent Kv1.3 and Kv1.5 K^+ channels are among those activated in T cells in response to cell swelling (Deutsch and Chen, 1993). K^+ efflux is coupled to Cl^- by the electroneutral K^+-Cl^- (KCC) cotransporters (de Los Heros et al., 2014b). The efflux of K^+ hyperpolarises the cell membrane forcing Cl^- out of the cell. Cl^- efflux is mediated by multiple anion transporters, such as the VRAC channels, which are activated by cell swelling (Grinstein et al., 1982). Additionally, a number of other abundant organic osmolytes, such as taurine, are released from the cell during swelling, particularly under long-term hypotonic shock.

The acute RVI response to hypertonic shock is also mediated by changes to the activity of transporters at the plasma membrane. Under hypertonic conditions there is a net influx of Na^+, K^+, and Cl^- ions into the cell mediated mainly by the Na^+-K^+-Cl^- (NKCC) contransporters, Na^+-Cl^- (NCC) cotransporters, Na^+/H^+ exchangers (NHE), and Cl^-/HCO_3^- anion exchangers (AE) (Figure 10). Ion movement mediated by these transporters is driven by the movement of Na^+ and Cl^- ions down their electrochemical gradient into the cell. The activity of NHEs is coupled to the activity of AEs to ensure ion influx is electroneutral. The H^+ and HCO_3^- lost from the cell due to activity of the NHE and AE exchangers are osmotically irrelevant as they are replenished by carbonic anhydrase using CO_2 as a substrate which freely diffuses

into the cell. Importantly both the NHE/AE and NKCC pathways have been shown to be active in T cells (Grinstein et al., 1983; Köchl et al., 2016).

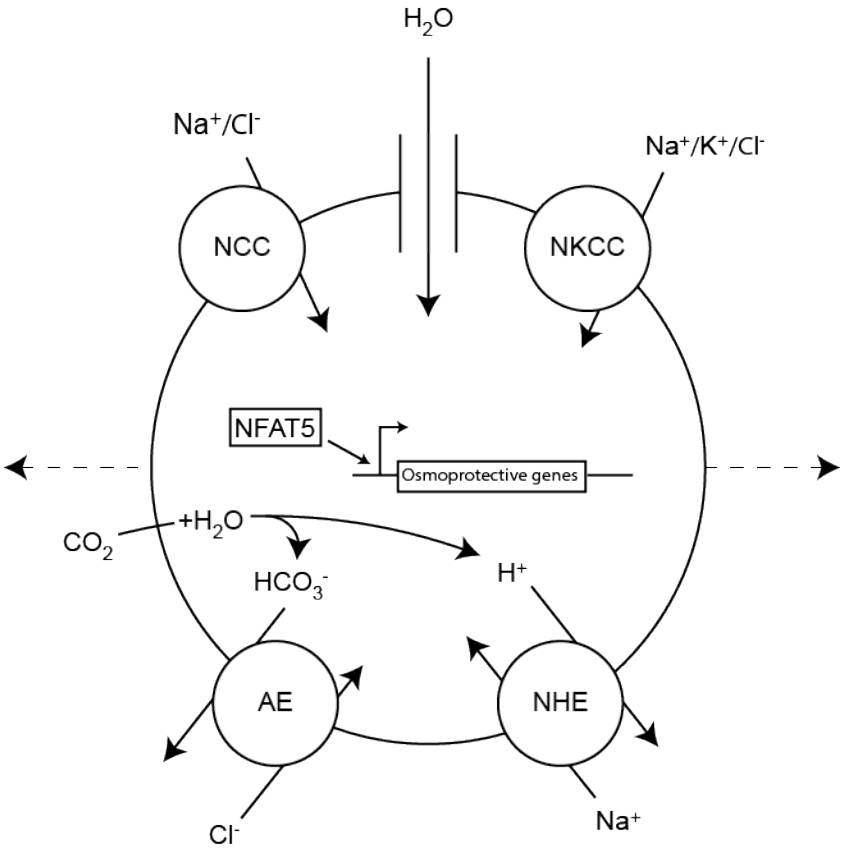

Figure 10. Regulatory volume increase (RVI) response. Under hypertonic conditions the cell activates a range of plasma membrane ion channels to facilitate net ion influx into the cell. This results in the passive movement of water into the cell through osmosis and an accompanying increase in cell volume. Additionally, transcriptional changes predominantly mediated by NFAT5 result in the expression of genes required for long-term adaption to hypertonic conditions including those responsible for osmolyte synthesis.

A large increase in ion concentration is detrimental to the cell as the structure and function of macromolecules, including proteins, can be altered under these conditions. Abolition of ion gradients across the membrane can also have major deleterious effects on cell homeostasis. For example, Na^+ movement into the cell is coupled to the uptake of many essential nutrients such as amino acids and nucleosides (Mailliard and Kilberg, 1990; Young et al., 2013). Therefore, the cell initiates the synthesis of uncharged organic osmolytes, such as sorbitol, that increase intracellular tonicity but are compatible with cellular processes. Osmolytes

are in fact able to stabilise macromolecules. However, osmolyte accumulation takes hours to complete and therefore is a long-term solution to hypertonic shock.

Many of the long-term adaptive responses during RVI, including osmolyte synthesis, are mediated at the transcriptional level by the NFAT5 transcription factor. NFAT5 is a unique member of the NFAT family of transcription factors as it is the only member that is responsive to changes in tonicity. NFAT5 activity is regulated at multiple levels in response to hypertonic shock in T cells. There is an increase in NFAT5 protein expression levels in response to hypertonic shock, as well as an increase in NFAT5 phosphorylation and nuclear translocation (López-Rodríguez et al., 2001). The threshold for NFAT5 activation in Jurkat cells was found to be >360 mOsm/L (Morancho et al., 2008). NFAT5 binds to TonE regulatory elements at promoters and enhancers to regulate transcription of a wide range of genes. A major set of NFAT5 targets are osmoprotective genes such as aldose reductase (AR), Na^+/Cl^--coupled betaine/GABA transporter (BGT1), Na^+-dependent myo-inositol transporter (SMIT), Na^+ and Cl^-dependent taurine transporter (TauT) and HSP70 (Jeon et al., 2006). These proteins serve to increase the intracellular concentration of osmolytes or to stabilise proteins during hypertonic shock. The importance of this NFAT5 function is exemplified in NFAT5-deficient mice which exhibit an increase in serum osmolarity and atrophy of the renal medulla caused by impaired expression of osmoprotective genes (Berga-Bolaños et al., 2010; López-Rodríguez et al., 2004).

Interestingly, expression of NFAT5 is also increased in $CD4^+$ T cells during activation in a calcineurin-dependent manner. This differs from the expression of NFAT5 in $CD4^+$ T cells in response to hypertonic shock, which is calcineurin-independent (López-Rodríguez et al., 2001). NFAT5 is required for $CD4^+$ T cell survival and proliferation *in vivo* in response to hypertonic conditions (Berga-Bolaños et al., 2010). The osmoprotective function of NFAT5 prevents DNA damage, as measured by γH2AX accumulation, and S and G2/M cell cycle arrest in T cells in response to hypertonic stress (Drews-Elger et al., 2009). Curiously, despite the increased incidence of DNA damage in NFAT5-deficient T cells in response to hypertonic stress, the cell cycle arrest exhibited by these cells was found to be independent of DNA damage as γH2AX-negative cells were also blocked at the G2/M transition. In the absence of NFAT5, cell cycle arrest is mediated by downregulation of cyclins and p21, and p53 induction. Interestingly, NFAT5 is also responsible for inducing the expression of cytokines during $CD4^+$ T cell activation under hypertonic

conditions. For example, NFAT5 induces the expression of IL-2 when $CD4^+$ T cells are activated in 420mOsm/L media (Alberdi et al., 2017).

Two complementary studies showed that hypertonic stress-induced IL-2 expression by T cells is dependent on PANX1-mediated ATP release. Extracellular ATP subsequently signals in an autocrine manner by activating the ATP-gated P2X channels which mediate Ca^{2+} influx into the cell and induce p38 activation (Loomis et al., 2003; Woehrle et al., 2010). A further study has shown that p38 is a critical mediator of NFAT5 in splenocytes (Kino et al., 2009). Collectively the evidence from these studies supports the existence of signalling circuit that could facilitate NFAT5-dependent IL-2 expression in hypertonic conditions. NFAT5 has also been found to be responsible for TNFα expression in hypertonic conditions and has been shown to directly bind to the promoter in T cells (López-Rodríguez et al., 2001). NFAT5 activity has also been attributed to expression of many other cytokines in other cell types in response to high salt conditions including IL-1β, IL-6 and IL-8 as well as chemokines such as CCL2 (Berry et al., 2017; Ma et al., 2019). Intriguingly, NFAT5 is also involved in the expression and activation of the NLRP3 inflammasome in response to hypertonic shock in endothelial cells. NFAT5 is also capable of inducing RORγt expression in high salt, non-polarising conditions (Alberdi et al., 2017). This is in line with the finding that high salt diets drive T_H17 differentiation and experimental autoimmune encephalomyelitis (EAE) *in vivo* via p38, NFAT5 and SGK1 (Kleinewietfeld et al., 2013).

Additional to the Ca^{2+}-dependent mechanism described above, p38 can be activated directly by osmotic shock-induced changes to the actin cytoskeleton. These changes result in the nucleation of a complex containing the scaffolding protein OSM, RAC, MEKK3, and MKK3, which activates p38 (Uhlik et al., 2003). As previously mentioned, one of the major roles of p38 activation is to induce NFAT5 transcriptional activity. However, it also mediates acute RVI responses by regulating ion transporter activity at the plasma membrane, including that of NHE antiporters (Pederson et al., 2002). Another p38-dependent adaption to hypertonic stress is the inhibition of the proteasome (Lee et al., 2010). Finally, in addition to mediating cell cycle arrest as discussed in Chapter 1.9.4, p38 can also induce apoptosis in response to osmotic shock (Thiemicke and Neuert, 2021). Interestingly this appears to be dependent on the rate of change of tonicity.

1.11 WNK1

The NKCC, KCC and NCC ion co-transporters are regulated by the With-No-Lysine (WNK) family of kinases. These kinases derive their name from their atypical kinase active site which is missing an invariant catalytic lysine residue in subdomain II involved in ATP-binding and phosphoryl transfer. This catalytic lysine residue is instead situated in subdomain I. In addition to its kinase domain WNK1 has several coiled-coiled domains and an autoinhibitory domain.

There are 4 members of the WNK kinase family in mammals (WNK1-4). Their role in ion transport was discovered when mutations in *Wnk1* and *Wnk4* were shown to cause pseudohypoaldosteronism type II (PHA-II) in humans (Wilson et al., 2001). PHA-II patients exhibit hypertension due to defective renal handling of Na^+, Cl^- and K^+. The PHA-II-causing mutations in *Wnk1* are intronic and result in increased expression of WNK1. Mutations within a *Wnk1* exon (*HSN2*) expressed specifically within the nervous system have been shown to cause hereditary sensory and autonomic neuropathy type II (HSAN2), which is characterised by a loss of pain, touch and heat perception. Subsequently, a mouse model was used to show that the HSN2-containing WNK1 splice variant contributes to Cl^- homeostasis in neurons by inhibiting KCC2 activity and that this opposes γ-aminobutyric acid (GABA)-mediated inhibition of neuronal activity (Kahle et al., 2016). WNK1 is ubiquitously expressed and, importantly, the only paralogue expressed in T cells. There are multiple tissue-specific isoforms of WNK1 including one lacking a kinase domain which is expressed in the kidney (Delaloy et al., 2003). WNK2, 3 and 4 have more tissue-specific expression patterns, for example in the heart, brain, colon, kidney and epithelium (Kahle et al., 2004; Verissimo and Jordan, 2001).

1.11.1 WNK1 in osmoregulation

WNK1 is rapidly activated in response to hypertonic stress in a process which requires transautophosphorylation of a conserved T-loop serine residue (S382 in humans) (Zagorska et al., 2007). Intriguingly its activation is associated with rapid redistribution to vesicular structures. A study by Naguro et al. showed that upstream signals required for WNK1 activation under hypertonic conditions are provided by the ASK3 kinase (Naguro et al., 2012). This kinase is a bidirectional sensor of

intracellular tonicity as it is activated by hypotonic stress but inactivated by hypertonic stress in a protein phosphatase 6 (PP6)-dependent manner (Watanabe et al., 2018). Under hypertonic conditions PP6 dephosphorylates and inactivates ASK3, which then releases WNK1 facilitating phosphorylation of downstream targets (Figure 11). Under hypotonic conditions PP6 is inactivated resulting in ASK3 activation. Activated ASK3 inhibits WNK1 through an unknown mechanism thought to require the kinase activity of ASK3. ASK3-deficient (*Map3k15*$^{-/-}$) mice exhibit hypertension associated with elevated STK39 and OXSR1 activation in the kidney supporting a role for this mechanism of WNK1 regulation *in vivo* (Naguro et al., 2012). It is worth noting that T cells express very low amounts of *Map3k15* RNA, however these cells express high levels of *Ppp6c*.

A study from our lab showed for the first time that WNK1 signalling is activated upon CCL21 chemokine stimulation as well as CD3 cross-linking in naïve CD4^{+} T cells (Köchl et al., 2016). WNK1 kinase activation in this setting was shown to be dependent on PI3K and AKT signalling as PI-103 and MK2206, which inhibit PI3K and AKT respectively, blocked WNK1-dependent phosphorylation of OXSR1 (S325) in response to these stimuli (Figure 11). These inhibitors did not however reduce OXSR1 phosphorylation to the same extent as genetic ablation of WNK1 kinase activity, which may indicate there is an alternative mechanism for homeostatic regulation of WNK1. The mechanism by which AKT activates WNK1 kinase activity is unknown. AKT-dependent phosphorylation of WNK1 at T58 has been well documented in a number of cell types but the significance of this modification remains unclear as mutation of this residue does not affect WNK1 kinase activity *in vitro* or its intracellular localisation (Vitari et al., 2004). Of note WNK1 T58 phosphorylation has been associated with WNK1-dependent activation of SGK1, a process that does not require WNK1 kinase activity (Xu et al., 2005b).

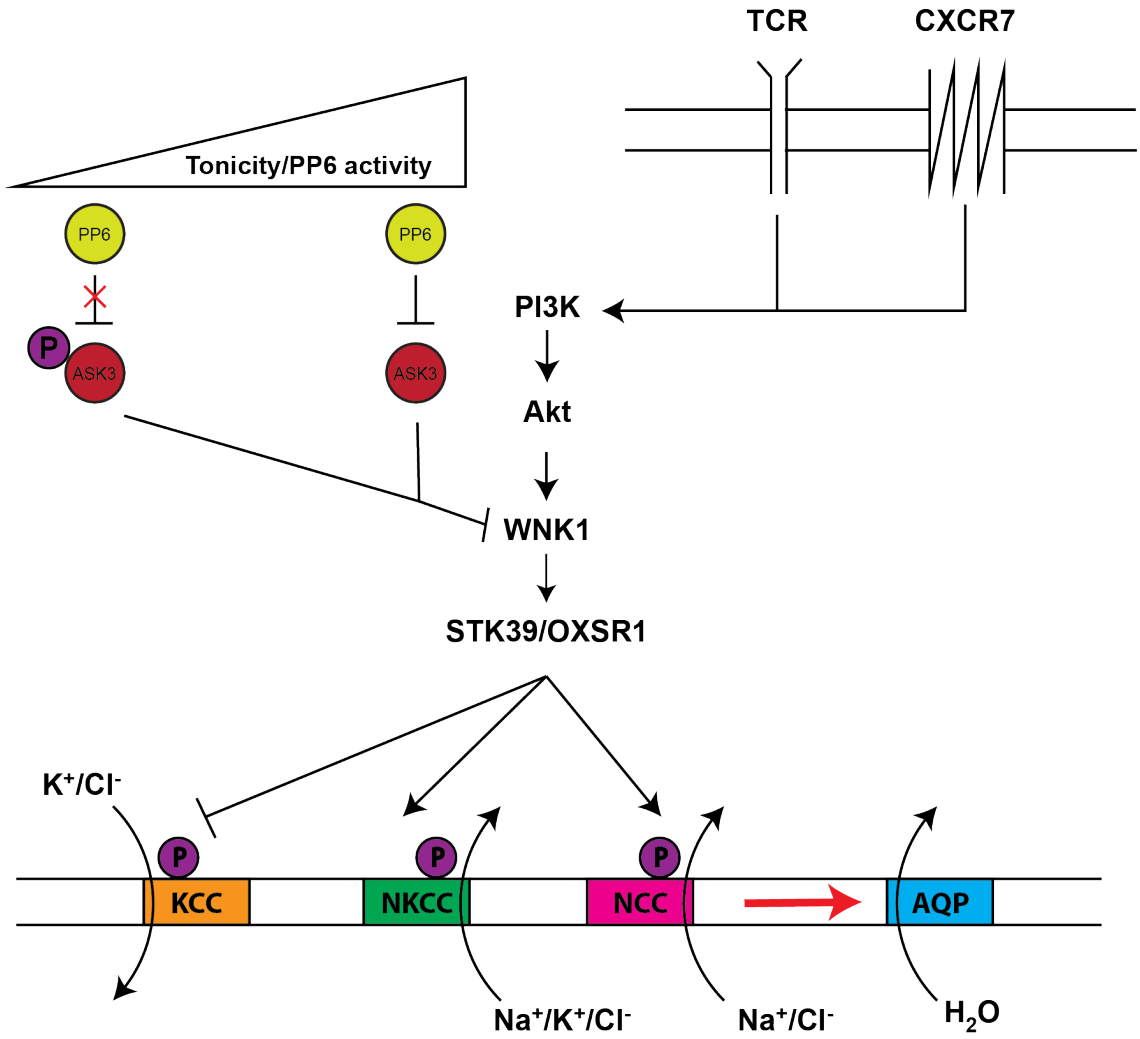

Figure 11. WNK1 regulation and downstream signalling. WNK1 is regulated at the post-transcriptional level by ASK3 and PI3K signalling. ASK3 is responsive to changes in tonicity which are detected by the PP6 phosphatase. Under hypertonic conditions PP6 becomes active and inhibits ASK3. This relieves inhibition of WNK1 and induces downstream signalling via STK39 and OXSR1 which facilitate the net influx of ions into the cell and therefore water through passive osmosis. TCR and chemokine receptor signalling is also able to induce WNK1 activity via PI3K and AKT similarly inducing downstream signalling via STK39 and OXSR1.

It has been shown that WNK1 kinase activity can be directly regulated by intracellular Cl^- concentration ($[Cl^-]_i$). Crystalographic studies revealed a Cl^--binding site within the kinase domain (Piala et al., 2014). Cl^--binding is proposed to stabilise the inactive conformation preventing T-loop S382 phosphorylation *in vitro*. The IC_{50} for Cl^--dependent inhibition of WNK1 activity *in vitro* has been reported as between ~20mM and ~200mM, depending on the precise conditions and substrate used.

(Terker et al., 2016). For context, T cells have an estimated $[Cl^-]_i$ of ~50mM (Pilas and Durack, 1997). The functional relevance of this mechanism of WNK1 regulation *in vivo* is therefore unclear as the effect of Cl^- on WNK1 activity depends on the actual IC_{50} *in vivo*. Mutation of the leucine residues responsible for chelating Cl^- ions (via their backbone amides) increases WNK1 kinase activity in HEK293 which have a reported $[Cl^-]_i$ of 40mM, suggesting that this mechanism of regulation may be physiologically relevant. Indeed, Cl^--mediated regulation would be consistent with reports that hypotonic low Cl^- conditions can activate WNK1 as this causes a reduction in intracellular Cl^- concentration (de Los Heros et al., 2014b). However, the author is not convinced that this Cl^--dependent mechanism of WNK1 regulation is physiological as increasing NaCl concentrations also inhibited other non-Cl^--sensitive kinases to a similar extent as WNK1 and the mutations introduced to ablate the putative Cl^--binding site are within the active site making interpretation of their effects impossible (Piala et al., 2014). Additionally, the backbone amides which are proposed to bind the Cl^- ion would also be present in the mutant generated. Finally, Cl^--dependent regulation would compromise the ability of WNK1 to mediate RVI as hypertonic stress results in an increase in $[Cl^-]_I$ due to cell shrinkage.

Strong evidence exists for a degradation-dependent mechanism of WNK1 regulation by the CUL3-KLHL3 E3 ubiquitin ligase as mutations in these two components were identified in families with PHA-II that did not have mutations in *Wnk* genes (Boyden et al., 2012). The CUL3-KLHL3 complex was subsequently found to bind WNK isoforms and mediate their ubiquitination and PHA-II associated mutations in these proteins resulted in loss of WNK-binding capacity (Ohta et al., 2013). The signals that regulate the activity of this E3 ubiquitin ligase towards WNK proteins have not been elucidated. WNK1 expression has also been shown to be supressed by the microRNA miR-192 (Elvira-Matelot et al., 2010).

Once activated, WNK1 phosphorylates its two canonical targets – STK39 and OXSR1 – at a threonine residue located in the T-loop (STK39 T233 and OXSR1 T185 in humans) inducing their activation (Figure 11). STK39 and OXSR1 have a conserved C-terminal (CCT) docking domain that mediates interactions with proteins containing a RFXV/I motif including WNK, NKCC and NCC proteins (Vitari et al., 2006). This CCT-mediated interaction is essential for STK39/OXSR1 activation by WNK1 as well as targeting these proteins to downstream substrates. STK39 and OXSR1 kinase activity is enhanced by interaction with the MO25 scaffold proteins

(Filippi et al., 2011). STK39 and OXSR1 phosphorylate a cluster of threonine residues at the N-terminus of NCC and NKCC co-transporters resulting in their activation (Pacheco-Alvarez et al., 2006; Richardson et al., 2008; Thastrup et al., 2011). OXSR1 and STK39 also inactivate KCC cotransporters by phosphorylating multiple threonine residues in their C-terminal domain. Inactivation of KCC channels requires an additional C-terminal threonine phosphorylation event through a less well defined WNK-dependent, OXSR1/STK39-independent mechanism resulting in inactivation of these transporters (de Los Heros et al., 2014a). The OXSR1/STK39 pathway has also been shown to influence the activity of other channels, for example STK39 was shown to phosphorylate and stimulate the internalisation of the Na^+/HCO_3^- cotransporter NBCe1-B and the Cl^-/HCO_3^- channel CFTR in HeLa cells (Hong et al., 2013).

In addition to the canonical OXSR1/STK39 pathway, WNK1 can regulate ion transport by activating the SGK1 kinase in a kinase-independent manner. This regulation may be achieved by modulating the activity of the PI3K-AKT pathway towards SGK1 (Xu et al., 2005b). Through its interactions with SGK1, WNK1 has been shown to positively regulate the activity of the ENaC Na^+ channel by blocking its ubiquitination by the E3 ubiquitin ligase NEDD4L and thus preventing it from degradation (Xu et al., 2005a). Additionally, WNK1-dependent SGK1 activity has been shown to inhibit the ROMK (Kv1.1) voltage-gated K^+ channel by promoting its endocytosis (Cheng and Huang, 2011). Neither of these transporters are expressed in T cells, although other members of the voltage gated K^+ channel are, such as Kv1.3. By regulating this array of ion transporters, WNK1 activation under hypertonic conditions results in net influx of Na^+, K^+ and Cl^- ions into the cell and an increase in cell volume.

There are conflicting reports regarding the regulation of WNK1 activity under hypotonic conditions. Some studies report an increase in WNK1 activity whereas others report no induction of activity (Lenertz et al., 2005; Zagorska et al., 2007). A complicating factor is that hypotonic conditions in these studies are generated by diluting culture media. This results in an increase in water concentration but also a decrease in concentration of all media components meaning it is difficult to delineate which factor is responsible for stimulating WNK1 activity. It may also be due to cell type specific functions of WNK1. However, from basic principles it would seem that WNK1 activity would be detrimental to the cell during hypotonic shock because it

would result in the net influx of Na^+, K^+, and Cl^- into the cell. This in turn would result in the net influx of water by osmosis and thus result in increased swelling of the cell.

1.11.2 Other downstream signalling pathways

WNK1 was initially identified through a screen used to identify MAPKs. Xu et al. showed that WNK1 is able to induce ERK5 phosphorylation via MEKK2/3 in an overexpression system in HeLa cells (Xu et al., 2004). The authors of this study also showed that knock-down of WNK1 resulted in attenuation of IGF-stimulated ERK5 activation. WNK1-dependent regulation of ERK5 activity was supported in a subsequent paper that showed WNK1 knock-down reduced EGF-induced ERK5 phosphorylation in neuronal progenitor cells (Sun et al., 2006). Interestingly, a reduction in EGF-induced ERK1/2 phosphorylation was also seen in these WNK1-deficient neuronal stem cells. A study of WNK1 regulation of MAPK signalling *in vivo* is needed to determine whether this function of WNK1 is physiologically relevant.

1.11.3 Other functions of WNK1

WNK1 has been reported to perform a plethora of functions in mammalian cells. It is not clear whether any of them are linked to its osmoregulatory function or whether they are regulated via distinct mechanisms. Soon after its discovery WNK1 was shown to be essential in mouse embryogenesis. Homozygous knock-out of the *Wnk1* allele is embryonic lethal and mice die at E12.5 due to defects in cardiac development and angiogenesis (Zambrowicz et al., 2003). This was shown to be due to an absolute requirement for WNK1-OXSR1 signalling in the embryonic endothelium as animals with endothelial-specific knock-out of *Wnk1* or *Oxsr1* phenocopied constitutive *Wnk1* knock-out animals. Furthermore, endothelial-specific expression of *Wnk1* or constitutively active *Oxsr1* transgenes was sufficient to rescue early embryonic lethality of *Wnk1*$^{-/-}$ mice (Xie et al., 2013; Xie et al., 2009). However, these “rescued mice” exhibited increased perinatal mortality and growth retardation showing that WNK1 activity in other tissues is required for normal development.

WNK1 has been shown to act as both a positive and a negative regulator of proliferation. siRNA-mediated knock-down of WNK1 in 3T3 preadipocytes increased insulin-dependent and -independent proliferation, whereas knock-down of WNK1 in

C17.2 neural progenitor cells reduced proliferation ~80% in the presence of serum and almost completely ablated proliferation in response to EGF (Sun et al., 2006; Jiang et al., 2005). A more recent study by Zhang et al. showed that WNK1 positively regulates proliferation of vascular smooth muscle cells in response to hypotonic challenge by inducing expression of cyclin D and supressing CDK inhibitor (p21/p27) expression (Zhang et al., 2018). These data suggest that WNK1-dependent regulation of proliferation may be stimulus- or cell type-specific. AKT S473 phosphorylation was induced downstream of WNK1 during smooth muscle cell proliferation, whereas WNK1-dependent suppression of insulin-stimulated preadipocyte proliferation was not associated with changes to AKT S473 phosphorylation suggesting a possible divergence in WNK1-dependent signalling that may explain its apparently opposing functions. From these studies it is unclear whether WNK1-dependent regulation of proliferation is physiologically relevant *in vivo* and whether this process is linked to WNK1-dependent osmoregulation.

A number of studies have shown that WNK1 positively regulates migration. Knock-down of WNK1 impairs EGF-stimulated neural progenitor cell migration and serum-induced PC12 cell migration (Yang et al., 2017; Sun et al., 2006). Interestingly, OXSR1 heterozygous bone marrow-derived dendritic cells fail to migrate in response to LPS suggesting a possible role for the WNK1-OXSR1 signalling pathway in these cells (Pasham et al., 2012).

1.11.4 The role of WNK1 in the T cell lineage

Our lab has shown that WNK1 positively regulates migration of naive $CD4^+$ T cells in response to CCL21 chemokine stimulation *in vitro* (Köchl et al., 2016). This role of WNK1 was validated *in vivo* using intravital microscopy which showed that *Wnk1*$^{-/-}$ naive $CD4^+$ T cell intranodal migration was dramatically reduced compared to *Wnk1*$^{+/-}$ controls. This migration defect was also observed in the presence of integrin-blocking antibodies showing that WNK1 regulates migration independently of integrin activity. This study by our lab also provided evidence that WNK1 signals via the canonical OXSR1/STK39 pathway to ion transporters, such as SLC12A2, to promote migration. Additionally, WNK1-deficient naïve $CD4^+$ T cells were found to have a hyperadhesive phenotype characterised by increased ICAM-1-binding in response to CCL21 stimulation or CD3 crosslinking. Further work revealed that WNK1

negatively regulates naïve $CD4^+$ T cell adhesion by inhibiting Rap1-dependent inside-out integrin signalling. This function of WNK1 was independent of OXSR1/STK39 signalling.

A role for WNK1 during T cell development has recently been elucidated by our lab. Köchl et al. show that WNK1 is required for transit through the β-selection checkpoint as a significant drop in cell numbers from the DN3 stage onwards was observed in WNK1-deficient thymocytes (Köchl et al., 2020). *Oxsr1*$^{-/-}$/*Stk39*$^{T243A/T243A}$ cells phenocopied *Wnk1*$^{-/-}$ cells in this respect suggesting WNK1 signalling via these kinases is required for progression past the β-selection checkpoint. The block in development was accompanied by a reduction in cell size and rate of entry into S phase, which was explained by a reduction in MYC abundance in WNK1-deficient cells. Accordingly, forced expression of MYC brought the numbers of WNK1-deficient DN4 cells to levels comparable to control cells.

1.12 Aims

WNK1 has predominantly been studied in the kidney and central nervous system where its role in human disease has been well characterised. In both tissues its main reported function is to regulate ion transport. A study from our lab showed that WNK1 also plays a major role in T cell biology (Köchl et al., 2016). Köchl et al. showed that WNK1 is activated via PI3K-AKT signalling downstream of the TCR and CCR7 chemokine receptor. This study also showed that WNK1 positively regulates $CD4^+$ T cell migration and negatively regulates $CD4^+$ T cell integrin-mediated adhesion. More recently our lab published a paper which shows that WNK1 regulates progression through the β-selection checkpoint during T cell development (Köchl et al., 2020). In this context WNK1 is required for pre-TCR-induced proliferation and continued T cell development to the DN4 stage. Finally, while working in the Tybulewicz lab Harald Hartweger found that T cells require WNK1 to support a class-switched antibody response (unpublished data). In light of these findings, the main aim of this project was to answer the following questions:

- Is WNK1 important for T-dependent immune responses because of its role in $CD4^+$ T cell adhesion and migration?
- Is WNK1 required for $CD4^+$ T cell activation and differentiation?
- Is WNK1 required for mature $CD4^+$ T cell proliferation?
- If WNK1 is required, through what mechanism does it regulate these processes?

- In particular, does WNK1-dependent osmoregulation play a role?

Chapter 2. Materials & Methods

2.1 Mice

Mice with a conditional allele of *Wnk1* containing LoxP sites flanking exon 2 (*Wnk1*^{tm1Clhu},*Wnk1*^{fl}) (Xie et al., 2009), with a knock-out allele of *Wnk1* (*Wnk1*^{tm1Clhu}, *Wnk1*$^{-}$), with a conditional allele of *Oxsr1* containing LoxP sites flanking exons 9 and 10 (*Oxsr1*$^{tm1.1Ssy}$, *Oxsr1*^{fl}) (Lin et al., 2011), with a kinase-inactive allele of *Wnk1* (*Wnk1*$^{tm1.1Tyb}$, *Wnk1*^{D368A}) (Köchl et al., 2016), with a tamoxifen-inducible Cre in the ROSA26 locus (Gt(ROSA)26Sor$^{tm1(Cre/ESR1)Thl}$, ROSA26-CreERT2, RCE) (de Luca et al., 2005), with a knock-in allele of *Stk39* (*Stk39*$^{tm1.1Arte}$, *Stk39*^{T243A}) (Rafiqi et al., 2010) that cannot be activated by WNK1, with a knock-out allele of *Rag1* (*Rag1*^{tm1Mom}, *Rag1*$^{-}$) (Mombaerts et al., 1992), with transgenes encoding TCRα and TCRβ chains specific for chicken ovalbumin residues 323-339 (Tg($^{TcraTcrb)425Cbn}$,OT-II) (Barnden et al., 1998) have been described before. All mice were maintained on a C57BL/6J background, were housed in specific pathogen free conditions at the Francis Crick institute and given food and water *ad libitum*. All experiments were carried out under the authority of a Project Licence granted by the UK Home Office.

2.2 Bone marrow chimeras

Sex-matched 8-12 week old RAG1-deficient recipient mice were irradiated with 1 dose of 5Gy from a ^{137}Cs source. Bone marrow from the hind limbs of sex-matched donor mice were harvested and treated with ammonium-chloride-potassium (ACK) lysis buffer for 3 min at room temperature, washed and resuspended in PBS. At least 10^6 cells were transferred intravenously into irradiated recipient mice which were maintained on 0.02% enrofloxacin (Baytril, Bayer Healthcare) for 4 weeks. The haematopoietic compartment was allowed to reconstitute for at least 8 weeks after bone marrow transfer before mice were used for any further studies.

2.3 *In vivo* deletion of floxed alleles

To delete floxed alleles of *Wnk1* or *Oxsr1*, mice were injected intraperitoneally with 2 mg tamoxifen (Sigma-Aldrich) in 100 μL of corn oil (Sigma-Aldrich) on 3 (*Wnk1*^{fl})

or 5 (*Oxsr1*^{fl}) consecutive days. Mice were sacrificed 7 d (*Wnk1*^{fl}) or 21 d (*Oxsr1*^{fl}) after initial tamoxifen injection unless indicated otherwise.

2.4 NP-CGG immunisation and ELISA

These experiments were performed by Harald Hartweger to measure the size of antigen-specific antibody responses. Mice were injected intraperitoneally with 50 μg of 4-hydroxy-3-nitrophenylacetyl (NP) in PBS + 25% Alum (Thermo Fisher Scientific). Blood was collected from the lateral tail vein at the indicated time points and allowed to clot for 30 min at room temperature. Blood samples were then centrifuged at 17,000 xg for 10 min at room temperature. The supernatant was collected and centrifuged again at 17,000 xg for 10 min. The supernatant was stored at -80°C prior to analysis.

5 μg/mL NP_{20}-BSA (Santa Cruz Biotechnology) was used to coat 96-well Maxisorp Immunoplates (Nalge Nunc International Corporation) overnight at 4 °C. Plates were washed 5 times with PBS + 0.01% Tween-20 and blocked with 3% BSA in PBS for 2 hours at room temperature. PBS + 0.01 % Tween-20 was used to wash the plates 2 further times. Sera were diluted by a factor of 100 for IgM ELISAs and 1,000 for IgG1 ELISA. 2-fold serial dilutions were then performed and the resulting serum solutions were incubated on the NP-coated plates overnight at 4 °C. Plates were washed 3 times with PBS + 0.01 % Tween-20 and then incubated with 1.6 μg/mL biotin-conjugated goat anti-mouse IgM (Thermo Fisher Scientific) or 4 μg/mL biotin-conjugated goat anti-mouse IgG1 (Thermo Fisher Scientific) for 2 h at room temperature. Plates were then washed with PBS + 0.01 % Tween-20 3 times and incubated with 1 μg/mL peroxidase-labelled streptavidin (Vector laboratories) for 2 h at room temperature. Plates were washed 5 times with PBS-T and incubated with 1x TMB ELISA substrate solution (Thermo Fisher Scientific). The reaction was stopped with 2 N H_2SO_4. Absorption at 450 nm was measured using the SpectraMax 190 (Molecular Devices LLC.). Serum concentrations, in arbitrary units (a.u.), of NP-specific IgG and IgM antibodies were calculated from the linear section of the response curves.

2.5 Preparation of single cells suspensions

Blood was harvested from live mice by cutting the lateral tail vein and collecting in a heparin-coated tube. Peripheral lymph nodes, mesenteric lymph nodes and spleens were harvested from mice sacrificed using a schedule 1 killing (S1K) method and dissociated into single cell suspensions by mashing through a 70 μm filter. Bone marrow from the hind limbs was harvested by flushing femurs and tibias with air-buffered Iscove's modified Dulbecco's medium (AB-IMDM) + 5 % foetal calf serum (FCS, Biosera). Blood, bone marrow, and spleen samples were treated with ACK for 3 min at room temperature, washed and resuspended in PBS. ACK treatment was repeated twice for blood samples.

2.6 Naïve CD4+ T cell isolation by negative depletion

Lymph node cell suspensions were resuspended in a mixture of biotinylated antibodies against CD8, CD11b, CD11c, B220, CD19, CD25, CD44, and GR-1 in AB-IMDM + 5 % FCS for 20 min at 4 °C (Table 1). Cells were incubated with streptavidin-coated Dynabeads (Thermo Fisher Scientific, Inc) in magnetic-activated cell sorting (MACS) buffer or AB-IMDM + 5 % FCS for 20 min at 4 °C. Cell/bead suspensions were placed on a magnet for 2 min at room temperature and the bead-depleted fraction was collected.

Table 1. List of biotinylated antibodies used for negative depletion.

Antigen	Clone	Supplier	Dilution
B220	RA3-6B2	Biolegend	1:200
CD11b	M1/70	Biolegend	1:200
CD11c	N418	Biolegend	1:200
CD19	1D3	BD Biosciences	1:200
CD25	PC61.5	ThermoFisher Scientific	1:400

CD44	IM7	ThermoFisher Scientific	1:400
CD8	53-6.7	Biolegend	1:200
GR-1	RB6-8C5	Biolegend	1:400

2.7 RNA isolation and quantitative reverse transcription-quantitative polymerase chain reaction (RT-qPCR)

These experiments were carried out according to the manufacturer's instructions and used to determine the abundance of specific RNA species per cell. RNA was purified from at least 5 x 10^4 CD4+ T cells using the RNeasy Micro kit (Quiagen). cDNA was synthesised using the SuperScript™VILO™cDNA synthesis kit (Invitrogen). Taqman™ Gene Expression Assays (Thermo Fisher Scientific) were used to measure *Wnk1* (exon boundary 1-2, Mm01184006_m1)*, Hprt* (exon boundary 2-3, Mm03024075_m1)*,* and *Il2* (exon boundary 2-3, Mm00434256_m1) expression. Fluorescence was measured using a QuantStudio 3 or QuantStudio 5 qPCR machine (Thermo Fisher Scientific). Technical duplicates or triplicates were performed for each assay. The relative amount of each RNA species was calculated relative to *Hprt* using the following formula:

$$\text{Relative expression} = 2^{-(C_{t(Gene\ of\ interest)} - C_{t\ (Hprt)})}$$

2.8 Adoptive transfer of OT-II CD4+ T cells

CD45.1$^-$/CD45.2$^+$ OT-II T cells were isolated from peripheral and mesenteric lymph nodes. Cells were labelled with 5 μM CellTrace Violet (CTV, ThermoFisher, Chapter 2.10). 1x10^6 (for day 3 analysis) or 35x10^3 (for day 7 analysis) labelled OT-II T cells were injected into the tail vein of CD45.1$^+$/CD45.2$^+$ C57BL/6J. 24 h later (day 0) mice were immunised with 50 μg (day 3 analysis) or 100 μg (day 7 analysis) chicken ovalbumin (OVA) protein (Invivogen) in PBS + 25 % Alum (Thermo Fisher Scientific) via the intraperitoneal route. Peripheral and

mesenteric lymph nodes were harvested at day 3. Mesenteric lymph nodes, spleen and blood were harvested at day 7.

2.9 *In vitro* activation

Naïve CD4+ T cells were isolated from peripheral and mesenteric lymph nodes and cultured in RPMI+ media (Table 8) at 37 °C unless otherwise stated.

2.9.1 Co-culture

To generate bone marrow-derived antigen presenting cells (APCs), bone marrow was isolated from the hind limbs of sex matched wild type C57BL/6J mice at day -10. Bone marrow was incubated in ACK buffer for 1 min at room temperature. Cells were resuspended in DC medium (Table 8) at $10x10^6$ cells/mL. Bone marrow suspensions were then diluted 10-fold by gently dropping 200μL into the centre of a well (6-well plate) containing 2ml DC medium with 20ng/mL GM-CSF (Peprotech). Cells were incubated for 10 days at 37 °C. At day -7 2 mL of DC medium containing 20ng/mL GM-CSF was added to each well. 2ml of each well was replenished with new DC medium containing 20ng/mL GM-CSF on day -5 and day -3. Bone marrow-derived APCs were harvested at day 0 and adjusted to 500,000 cells/mL. Naïve $CD4^+$ OT-II T cells were isolated by negative depletion, resuspended in DC medium and adjusted to 500,000 cells/mL. 50,000 OT-II T cells and 50,000 bone marrow-derived APCs were co-cultured in a round-bottomed well (96-well plate) in the presence of indicated concentrations of $OVA_{323-339}$ (Sigma) for the indicated times.

2.9.2 Activation of T cells with plate-bound anti-CD3 and anti-CD28

125 μL (48-well), 250 μL (24-well), 500 μL (12-well) or 1 mL (6-well) of PBS containing anti-CD3 and anti-CD28 antibodies at 4 μg/mL was dispensed into each well of a flat-bottomed cell culture plate (Corning) and incubated overnight at 4 °C. Naïve CD4+ T cells were cultured at $1x10^6$ cells/mL in 250 μL (48-well), 500 μL (24-well), 1 mL (12-well) or 2 mL (6-well) RPMI+ at 37 °C for the indicated time points. Cells were activated in the presence of 2.5 μM WNK463 (MedChem Express) in DMSO or the equivalent amount of DMSO (Sigma-Aldrich) where indicated. 1μM

ATRi (AZD6738) in DMSO or the equivalent amount of DMSO was added at 36 h where indicated. 4mM hydroxyurea (HU, Sigma-Aldrich) in PBS was added to samples at 70 h for 2 h where indicated.

For 1 h stimulations cells were incubated in the presence of 2.5 μM WNK463 in DMSO, 1μM MEKi (Selleckchem) in DMSO or the equivalent amount of DMSO at 4 °C for 30 min in RPMI+. Cells were transferred into RPMI+ medium containing 2.5 μM WNK463 in DMSO, 1μM MEKi (Selleckchem) in DMSO or the equivalent amount of DMSO with indicated amounts of NaCl and L-glucose and centrifuged onto cell culture plates at 340xg for 30 s prior to incubation 37 °C. After 1 h at 37 °C the cell culture medium was aspirated off and cells were resuspended in pre-chilled PBS.

2.9.3 Soluble stimulation

Naïve CD4+ T cells were incubated in IMDM + 0.5% FCS for 1 h at 37°C. Cells at $15x10^6$ cells/mL were aliquoted into 100μL samples. Samples were cooled at 4°C for 10 min. Cells were resuspended in RPMI + 0.5% FCS medium containing 10 μg/mL anti-CD3 and 10 μg/mL anti-CD28 antibodies (Table 2) in the presence of 2.5μM WNK463 (MedChem Express) in DMSO, 100nM SRCi (Sigma-Aldrich) in DMSO or the equivalent amount of DMSO and incubated at 4 °C for 30 min. Unstimulated (0 min) samples were incubated in the presence of relevant inhibitors but without anti-CD3 or anti-CD28 antibodies. Cells were warmed to 37°C for 15 min. Cells were stimulated with the addition of 80 μg/mL anti-Armenian hamster IgG (Antibodies-online.com). Activation was stopped at the indicated time point with the addition of 2% PFA.

Table 2. List of antibodies used for *in vitro* activation of $CD4^+$ T cells

Antigen	Clone	Supplier	Dilution
CD3	145-2C11	Tonbo Biosciences	1:125 (plate-bound stimulation) 1:50 (soluble stimulation)
CD28	37.51	Biolegend	1:250 (plate-bound stimulation) 1:100 (soluble stimulation)
Hamster IgG (H&L chain)	Polyclonal (#ABIN101378)	Antibodies-online.com	1:25 (soluble stimulation)

Table 3. List of inhibitors used for *in vitro* activation experiments

Target	Name (abbreviation)	Supplier	Concentration
WNK kinases	WNK463	MedChem Express	2.5μM
MEK kinases	PD 0325901 (MEKi)	Selleckchem	1μM
SRC kinases	Dasatinib (SRCi)	Sigma-Aldrich	100nM
ATR	AZD6738 (ATRi)	Selleckchem	1μM

2.10 CTV labelling of CD4+ T cells

CTV labelling was used to measure the number of divisions each cell underwent. Naïve CD4+ T cells were incubated in PBS with 5 μM (for OT-II T cell experiments) or 2.5 μM (for polyclonal T cell experiments) CTV for 10 minutes at 37°C. Pre-warmed RPMI+ media was added to the cells for 7 min. Cells were then pelleted and resuspended in the appropriate media.

2.11 Flow cytometry

2.11.1 Activation marker and proliferation analysis

This method was used to identify live, single, CD4+, and PD-1+ populations and measure the abundance of certain activation markers on the surface of individual cells. Cells were stained in PBS containing fluorophore-conjugated antibodies (see Table 4) and LIVE/DEAD™ Near-IR dye (Thermo Fisher Scientific) (diluted 1:500) at 4 °C for 20 min. Cells were then washed, resuspended in fluorescence-activated cell sorting (FACS) buffer and run on the flow cytometer. For cell counting, a known number of BD Calibrate APC beads (BD biosciences) were added to the sample in FACS buffer. Samples were analysed on BD LSRFortessa™ (BD biosciences) flow cytometers.

2.11.2 CXCR5 staining

This method was used to measure the abundance of CXCR5 on the surface of individual cells. Staining of CXCR5 was achieved by incubating cells in PBS + 2 % FCS containing biotinylated anti-CXCR5 antibody (BD Biosciences) at 37 °C for 30 min. Cells were then washed, incubated with fluorophore-conjugated streptavidin for 15 min at room temperature, washed, resuspended in FACS buffer, and run on the flow cytometer.

2.11.3 Phospho-ERK/S6/CD3ζ/ZAP-70 staining

This method was used to measure the abundance of certain phospho-proteins on a per cell basis. Cells were fixed in 2 % paraformaldehyde (PFA) at 4 °C for 15 min and permeabilised with 90 % methanol overnight at -20 °C. Cells were washed 3 times and then incubated with relevant primary antibody (Table 4) in PBS + 2 % FCS for 30 min at room temperature. To detect the primary antibody, cells were subsequently stained with the relevant secondary antibody (Table 5) in PBS + 2 % FCS for 30 min at room temperature. Samples were then washed, resuspended in FACS buffer, and analysed on the flow cytometer.

2.11.4 Cell cycle analysis

This method was used to measure the proportion of cells in each of the cell cycle phases as well as measuring the rate of S phase progression. Cells were stained with LIVE/DEAD™ Near-IR dye (Thermo Fisher Scientific) for 15 min at 4 °C. Cells were fixed in 4 % PFA for 15 min at 4 °C. Cells were stained with fluorophore-conjugated antibodies in BD Perm/Wash™ buffer (BD biosciences) containing 2 % FCS for 30 min at room temperature. Cells were washed with BD Perm/Wash™ buffer and resuspended in BD Perm/Wash™ buffer containing 1 μg/mL FxCycle™ Violet stain (Thermo Fisher Scientific) and incubated at room temperature for 30 min. Samples were then analysed on the flow cytometer.

For EdU incorporation analysis, 10 μM EdU (Thermo Fisher Scientific) was added to the cell culture medium for 10 min after ther cells had been activated for 72 h on anti-CD3 and anti-CD28-coated cell culture plates. EdU was detected using the Click-

iT™ EdU Alexa Fluor™ 488 Flow Cytometry Assay Kit (Thermo Fisher Scientific) according to the manufacturer's instructions.

Table 4. List of primary antibodies used for flow cytometry.

Antigen	Clone	Supplier	Dilution
CD25	PC61.5	ThermoFisher Scientific	1:200
CD4	GK1.5	ThermoFisher Scientific	1:200
CD44	IM7	ThermoFisher Scientific	1:200
CD45.1	A20	ThermoFisher Scientific	1:100
CD45.2	104	Biolegend	1:100
CD69	H1.2F3	Biolegend	1:200
CXCR5	2G8	BD Biosciences	1:100
Ki67	SolA15	ThermoFisher Scientific	1:100
p-CD3ζ (Y142)	K25-407.69	BD Biosciences	1:400 (1.25μg/mL)
p-ERK1 (T202/Y204)	Polyclonal (#9101)	Cell Signaling Technology	1:50
p-ERK2 (T185/Y187)	Polyclonal (#9101)	Cell Signaling Technology	1:50
p-MPM2 (S/TP motif)	MPM-2	Merck Millipore	1:100
p-S6 (S235/236)	D57.2.2E	Cell Signaling Technology	1:50
p-ZAP-70 (Y319)	65E4	Cell Signaling Technology	1:400
PD-1	29F.1A12	Biolegend	1:100

Table 5. List of secondary antibodies used for flow cytometry.

Antigen	Conjugate	Species	Supplier	Dilution
Mouse IgG (H&L chain)	Alexa Fluor 488	Donkey (highly cross-adsorbed)	ThermoFisher Scientific	1:500
Rabbit IgG (H&L chain)	Alexa Fluor 647	Goat (highly cross-adsorbed)	ThermoFisher Scientific	1:500

Streptavidin	APC		ThermoFisher Scientific	1:500

2.12 Luminex assay

The Cytokine & Chemokine 36-Plex Mouse ProcartaPlex™ Panel 1A (Thermo Fisher Scientific) was used to measure the concentration of 36 cytokines (IFNγ, GM-CSF, IL-1β, IL-12p70, IL-13, IL-18, IL-2, IL-4, IL-5, IL-6, TNFα, ENA-78, G-CSF, IFNα, IL-1α, IL-15, IL-28, IL-3, IL-31, LIF, M-CSF, IL-10, IL-17A, IL-22, IL-23, IL-27, IL-9, Eotaxin, GROα, IP-10, MCP-1, MCP-3, MIP-1α, MIP-1β, MIP-2, and RANTES) in the cell culture media according to the manufacturer's instructions. Cell culture media was harvested at the indicated time points, frozen at -80 °C prior to analysis, and analysed using the Luminex® 100 system (Biorad).

2.13 Immunoblot

Immunoblot experiments were carried out to measure the abundance of certain proteins or phospho-proteins in bulk cell lysates. Cell pellets were thawed at room temperature and lysed using RIPA buffer. Samples were centrifuged for 15 min at 4 °C and the supernatant was collected. The protein concentration of each sample was determined using the Pierce™ BCA protein assay kit (Thermo Fisher Scientific) according to the manufacturer's instructions. Samples were then mixed with sodium dodecyl sulphate (SDS) sample buffer (Sigma-Aldrich) and loaded into NuPAGE™ 4-12 % Bis-Tris precast polyacrylamide gels (Thermo Fisher Scientific) with the volume of each sample adjusted to ensure equal protein amounts per well. Electrophoresis was carried out at 200 V for 53 min in NuPAGE™ MOPS SDS running buffer (Thermo Fisher Scientific). Proteins were transferred to a methanol-activated polyvinylidene difluoride (PVDF) membrane in NuPAGE™ transfer buffer (Thermo Fisher Scientific) at 30 V for 65 min. Membranes were blocked with Odyssey® blocking buffer (LI-COR) for 1 h at room temperature. Membranes were then incubated with primary antibody (see

Table 6) in Odyssey® blocking buffer overnight at 4 °C. Membranes were washed 3 times with TBS-T and then incubated with fluorophore-conjugated secondary antibody (Table 7) in Odyssey® blocking buffer for 1 h at room temperature. Membranes were washed 3 times with TBS-T and imaged using the Odyssey® CLx (LI-COR). Image Studio Lite (LI-COR) was used to quantify intensities of bands. The region above and below each band was used to calculate background intensity.

Table 6. List of primary antibodies used for immunoblot.

Antigen	Clone	Supplier	Dilution
ERK	3A7	Cell Signaling Technology	1:1000
OXSR1	Polyclonal	MRC PPU Reagents and services	1:1000
p-CHK1 (S345)	133D3	Cell Signaling Technology	1:1000
p-KAP (S824)	Polyclonal (#A300-767A)	Bethyl Laboratories	1:1000
p-OXSR1 (S325)	Polyclonal	MRC PPU Reagents and Services	1:1000
p-RPA32 (S4/8)	Polyclonal (#A300-245A)	Bethyl Laboratories	1:1000
α-Tubulin	TAT-1	Cell Services STP, Crick	1:15000
γH2AX (S139)	JBW301	Merck Millipore	1:10000

Table 7. List of secondary antibodies used for immunoblot.

Antigen	Conjugate	Supplier	Dilution
Mouse IgG	IRDye® 800CW	LI-COR Biosciences	1:4000
Mouse IgG	Alexa Fluor 680	ThermoFisher Scientific	1:4000

Rabbit IgG	IRDye® 800CW	LI-COR Biosciences	1:4000
Rabbit IgG	Alexa Fluor 680	ThermoFisher Scientific	1:4000
Sheep IgG	Alexa Fluor 680	ThermoFisher Scientific	1:4000

2.14 Solutions, buffers and media

Table 8. List of solutions, media and buffers used

Name	Formulation
PBS	136.89 mM NaCl, 3.35 mM KCl, 10.12 mM Na_2HPO_4, 1.84 mM KH_2PO_4
TBS-T	50 mM Tris, 150 mM NaCl, 0.05 % Tween 20
FACS	PBS, 0.5 % bovine serum albumin (BSA)
MACS	PBS, 0.5 % BSA, 2 mM EDTA
ACK	155 mM NH_4Cl, 10 mM $KHCO_3$, 0.1 mM Na_2EDTA
AB-IMDM	35.93 mM NaCl, 0.18 mM Penicillin, 0.17 mM Streptomycin, IMDM powder (Gibco™; Thermo Fisher Scientific), adjusted to pH 7.2
RPMI+	RPMI-1640 (Gibco™; Thermo Fisher Scientific), 100 μM non-essential amino acids (Gibco™; Thermo Fisher Scientific), 20 mM HEPES (Gibco™; Thermo Fisher Scientific), 10 % FCS, 100 U/mL Penicillin (Sigma-Aldrich), 100 μg/mL Streptomycin (Sigma-Aldrich), 2 mM L-glutamine (Sigma-Aldrich) and 100 μM 2-mercaptoethanol (Sigma-Aldrich).

RPMI+ (292mOsm/L)	RPMI+, NaCl concentration (+L-glucose concentration where applicable) adjusted to make total osmolarity 292mOsm/L, osmolarity measured on an osmometer (Model 3250, Thermo Fisher Scientific)
RPMI+ (250mOsm/L)	RPMI+, NaCl concentration adjusted to make total osmolarity 250mOsm/L, osmolarity measured on an osmometer (Model 3250, Thermo Fisher Scientific)
RPMI+ (169mOsm/L)	RPMI+, NaCl concentration adjusted to make total osmolarity 169mOsm/L, osmolarity measured on an osmometer (Model 3250, Thermo Fisher Scientific)
DC medium	RPMI-1640 (Gibco™; Thermo Fisher Scientific), 10 % FCS, 100 U/mL Penicillin (Sigma-Aldrich), 100 μg/mL Streptomycin (Sigma-Aldrich), 2 mM L-glutamine (Sigma-Aldrich)
RIPA	50 mM Tris, 150 mM NaCl, 50 mM NaF, 2 mM EDTA, 2 mM $Na_4P_2O_7$, 1 mM Na_3VO4, 1 % Triton X-100, 0.5 % deoxycholate, 0.1 % SDS, 1 mM PMSF, 1x complete EDTA-free protease inhibitor cocktail (Roche), 1x Phostop (Roche)

2.15 Quantification and statistical analysis

The non-parametric Mann-Whitney U-test was used to analyse the difference between groups as it was not possible to determine whether populations were normally distributed due to the limiting n numbers in the majority of experiments. In cases where n numbers were sufficient to make this calculation popluations did not always follow normal distributions. Statistical tests were carried out using GraphPad Prism 8. The abundance of (modified) proteins measured by immunoblot was calculated using densitometry on LI-COR ImageStudio™ Lite. Flow cytometry populations were analysed using FlowJo 9 and 10.

Chapter 3. CD4$^+$ T cells require WNK1 to support an immune response *in vivo*

In light of the fact that our lab had previously shown that WNK1 plays a critical role in CD4$^+$ T cell adhesion and migration I endeavoured to determine whether CD4$^+$ T cells require WNK1 to respond to antigen *in vivo*.

3.1 Deletion of *Wnk1* in naïve CD4$^+$ T cells

In order to study the role of WNK1 in naïve CD4+ T cells it was necessary to use a conditional allele of *Wnk1* because constitutive deletion of *Wnk1* is embryonic lethal (Xie et al., 2009; Zambrowicz et al., 2003). Furthermore, data from our laboratory has shown that deletion of *Wnk1* during T cell development results in a block at the DN3 to DN4 transition (Köchl et al., 2020). The Cre-LoxP system was used to facilitate tamoxifen-inducible deletion of *Wnk1*. Mice were generated with a *Wnk1* allele containing LoxP sites inserted either side of exon 2 (*Wnk1*^{fl}) and a transgene encoding a CRE recombinase-oestrogen receptor fusion protein (CreER^{T2}) inserted into the Rosa26 locus (Gt(ROSA)26Sor$^{tm1(cre/ERT2)Thl}$, RCE) (Figure 12A) (de Luca et al., 2005; Xie et al., 2009). The oestrogen receptor ligand-binding domain of this construct (ER^{T2}) contains mutations that confer sensitivity to tamoxifen but not 17β-estradiol (Feil et al., 1997). The ER^{T2} domain binds to Hsp90 which sequesters the construct in the cytoplasm. Tamoxifen binding induces the dissociation of ER^{T2} and HSP90 and the subsequent translocation of CreER^{T2} into the nucleus where Cre activity results in site-specific recombination of LoxP sites (Figure 12A). The LoxP sites in the *Wnk1*^{fl} allele were arranged as direct repeats and so recombination results in excision of the intervening DNA. This excision event results in the loss of exon 2, which encodes part of the kinase domain, and a frame shift in the *Wnk1* gene, which introduces a premature stop codons into the coding sequence (*Wnk1*$^-$). The *Wnk1*^{fl} allele and RCE transgene were combined with *Wnk1*$^+$, *Wnk1*$^-$ or *Wnk1*^{D368A} (kinase-dead) alleles through mouse breeding to generate *Wnk1*$^{fl/+}$/RCE, *Wnk1*$^{fl/-}$/RCE, and *Wnk1*$^{fl/D368A}$/RCE animals. *Wnk1* mutant alleles and the RCE transgene were limited to the haematopoietic compartment by generating bone marrow chimeric mice (Figure 12B). Sub-lethally irradiated *Rag1*$^{-/-}$ mice were used as bone marrow recipients to ensure that *Wnk1* mutant alleles and RCE were present in all

lymphocytes but absent in most cells of all other haematopoietic lineages. After allowing reconstitution to occur for at least 8 weeks, tamoxifen was administered via the intraperitoneal route on 3 consecutive days and naive $CD4^+$ T cells were analysed 7 d after the initial injection (Figure 12B). This strategy facilitated the generation of *Wnk1*$^{+/-}$, *Wnk1*$^{-/-}$ and *Wnk1*$^{D368A/-}$ T cells.

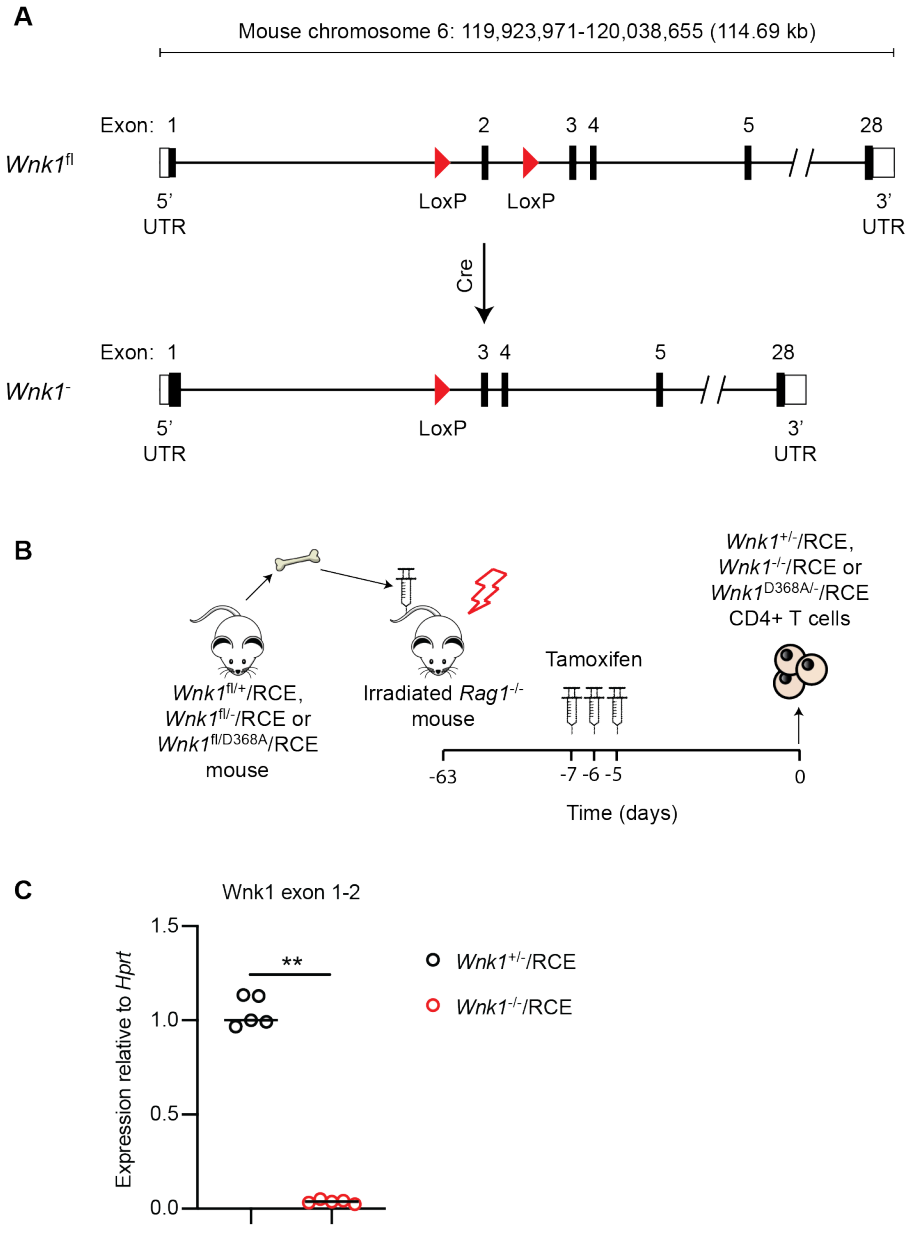

Figure 12. Cre-LoxP mediated deletion of exon 2 of *Wnk1* in CD4$^+$ T cells. (**A**) Schematic showing LoxP sites flanking exon 2 of *Wnk1* and the product of Cre recombinase activity. (**B**) Experimental design: irradiated RAG1-deficient mice were reconstituted with bone marrow from *Wnk1*$^{fl/+}$/RCE, *Wnk1*$^{fl/-}$/RCE or *Wnk1*$^{fl/D368A}$/RCE mice. At least 8 weeks later mice were treated with tamoxifen for 3 days to induce the deletion of the floxed *Wnk1* allele. 7 days after the first injection naïve CD4$^+$ T cells (CD25^{lo}/CD44^{lo}) were isolated from lymph nodes by negative depletion. (**C**) Expression of *Wnk1* (exons 1-2) mRNA in CD4+ T cells at day 0 normalised to the amount of *Hprt* mRNA measured by RT-qPCR (n=5). Each point represents a single mouse; horizontal lines show median. Data shown representative of 2 independent experiments. Statistical analysis carried out using the Mann-Whitney U test. ** $0.001 < p < 0.01$.

To test the deletion efficiency of the *Wnk1*^{fl} allele *in vivo* I used reverse transcription-quantitative PCR (RT-qPCR) to measure the relative amount of *Wnk1* RNA (exons 1-2) expressed in naïve CD4$^+$ T cells at day 0 as we could not identify any antibodies against WNK1 that worked on immunoblots. I found that the tamoxifen regime described above was sufficient to reduce the abundance of *Wnk1* RNA (exons 1-2) in *Wnk1*$^{-/-}$/RCE samples to ~4% of that in *Wnk1*$^{+/-}$/RCE control samples (Figure 12C). I concluded that this tamoxifen-inducible system deletes *Wnk1* exon 2 in naïve CD4$^+$ T cells with high efficiency and thus could be used to study the role of WNK1 in CD4$^+$ T cell function.

3.2 CD4$^+$ T cell requirement for WNK1 during an immune response

Our laboratory has shown that WNK1 regulates CD4$^+$ T cell migration and adhesion *in vitro* and *in vivo*. Subsequent to this discovery Harald Hartweger, also from our lab, endeavoured to determine whether WNK1 is required by CD4$^+$ T cells to support an immune response. To do this he generated mixed bone marrow chimeras by reconstituting sub-lethally irradiated *Rag1*$^{-/-}$ mice with a 4:1 mixture of *Tcr*$\alpha^{-/-}$ and *Wnk1*$^{fl/+}$/RCE or *Wnk1*$^{fl/-}$/RCE bone marrow, respectively (Figure 13A). He then immunised these mice with NP-CGG (a model antigen) in alum (an adjuvant) and monitored the NP-specific antibody response by ELISA. This experimental design was used to ensure that *Wnk1*^{fl}, *Wnk1*$^{-}$, and RCE alleles were present in all T cells, but absent in most cells of all other haematopoietic lineages, including B lymphocytes. This allowed Harald Hartweger to study the role of WNK1 in T cells specifically, during an immune response.

The only significant difference in NP-specific IgM concentrations between the two genotypes was in naïve animals at day -7 ($p=0.029$) (Figure 13B). At this timepoint *Wnk1*$^{-/-}$/RCE animals had an average reduction in NP-specific IgM levels of ~40%. However, because the animals were antigen-inexperienced at this timepoint this signal was background and most likely due to cross-reactivity from IgM antibodies present in the blood plasma prior to immunisation. There was also a significant drop in NP-specific IgM antibodies between day -7 and day 0 in *Wnk1*$^{+/-}$ /RCE animals suggesting that tamoxifen administration affected IgM production, at

least in the control animals, and therefore the increase in NP-specific IgM concentration after day 0 could be, at least in part, attributed to recovery from the effects of tamoxifen. Therefore, I used the concentration of NP-specific IgM at day -7 as the baseline. There was a significant increase in plasma levels of NP-specific IgM between day -7 and 21, which is the peak of the response, in mice with both *Wnk1*$^{+/-}$/RCE (p=0.024) and *Wnk1*$^{-/-}$/RCE (p=0.0198) T cells. There was no significant difference in NP-specific IgM titres between the two genotypes from day 0 onward. These data suggest that *Wnk1*$^{-/-}$/RCE T cells can support a normal IgM response to antigen. However, the high background signal, significant difference in background signal between genotypes, and potent effects of tamoxifen on IgM levels made it hard to base firm conclusions on these data.

Wnk1$^{-/-}$/RCE T cells were able to support a small, but significant increase in NP-specific IgG1 levels between day -7 and day 7 (p=0.016) (Figure 13C). However, the median concentration of NP-specific IgG1 in the plasma of *Wnk1*$^{-/-}$/RCE animals was significantly reduced to ~7% of that in *Wnk*$^{+/-}$/RCE animals at day 21, the peak of the response (Figure 13C). It is worth noting that the small IgG response in *Wnk1*$^{-/-}$/RCE animals may be mediated by escapee T cells in which the *Wnk1*^{fl} allele had not been deleted. This profound, if not complete, block in the generation of antigen-specific IgG showed that *Wnk1*$^{-/-}$/RCE T cells are severely defective and that therefore there is a strong requirement for WNK1 in T cells during an immune response, presumably in CD4^{+} T cells. However, it is unclear at what point during the adaptive immune response *Wnk1*$^{-/-}$/RCE T cells fail to carry out their function. Therefore, I investigated whether CD4^{+} T cells require WNK1 for activation, proliferation, and survival *in vivo*.

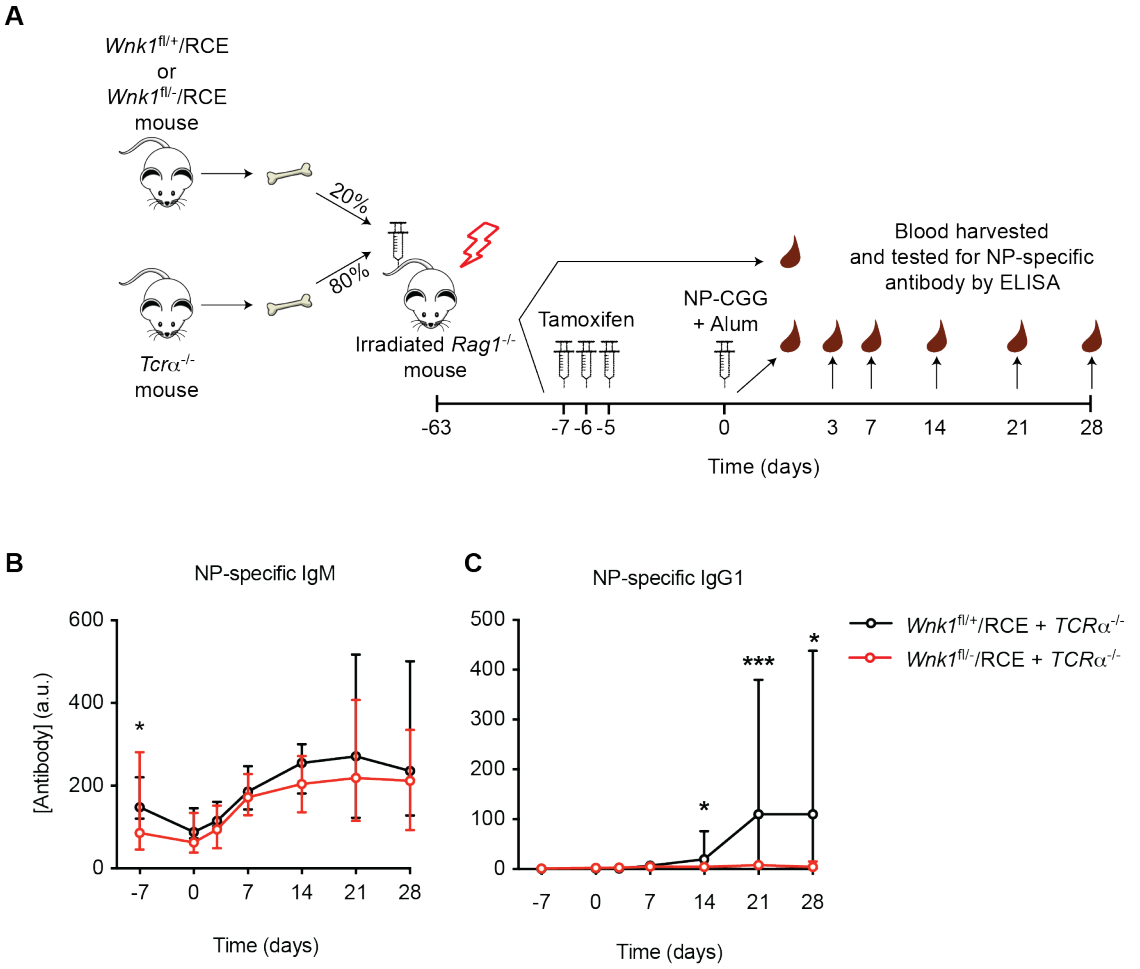

Figure 13. CD4⁺ T cells require WNK1 to support a class-switched antibody response. (**A**) Experimental design: Mixed bone marrow chimeras were generated by reconstituting irradiated RAG1-deficient mice with bone marrow from *Tcrα* $^{-/-}$ mice (80%) and bone marrow from *Wnk1*$^{fl/+}$/RCE or *Wnk1*$^{fl/-}$/RCE mice (20%). At least 8 weeks later mice were treated with tamoxifen for 3 days to induce the deletion of the floxed *Wnk1* allele. 7 days after the first tamoxifen treatment mice were immunised with NP-CGG in alum. Blood was collected from mice on the days indicated and analysed for NP-specific antibodies by ELISA. (**B, C**) NP-specific IgM (B) and IgG1 (C) antibodies quantified by ELISA at time points indicated (n=10-18). Each data point represents the median±95% confidence interval antibody titre as measured in arbitrary units (a.u.) for the indicated genotype at each timepoint. Data shown pooled from 2 independent experiments. Statistical analysis carried out using the Mann-Whitney U test. * $0.01 < p < 0.05$; ** $0.001 < p < 0.01$; *** $0.0001 < p < 0.001$. These experiments were carried out by Harald Hartweger.

3.3 WNK1-deficient CD4$^+$ T cells successfully upregulate activation markers *in vivo*

An early event in the adaptive immune response is CD4$^+$ T cell activation marker expression. TCR engagement with cognate p-MHC-II molecules induces downstream signalling and ultimately a change to the gene expression program of CD4$^+$ T cells, including the upregulation of *Il2ra, Cd44,* and *Cd69*. I sought to determine whether WNK1 is required for the expression of IL-2Rα (CD25), CD44 and CD69 activation markers by CD4$^+$ T cells in response to antigen. To do this, I adoptively transferred *Wnk1*$^{+/-}$/OT-II/RCE or *Wnk1*$^{-/-}$/OT-II/RCE T cells (CD45.1$^-$/CD45.2$^+$) into a wild type recipient mouse (CD45.1$^+$/CD45.2$^+$) and immunised with chicken ovalbumin (OVA) protein in alum (Figure 14A). OT-II T cells express an MHC II I-A^b-restricted T cell receptor specific for a peptide from chicken ovalbumin extending from amino acid 323 to 339 (OVA$_{323-339}$) (Barnden et al., 1998). This approach allowed me to restrict *Wnk1*$^-$, and RCE alleles to CD4$^+$ T cells and follow the response of naïve, antigen-specific cells to antigen *in vivo*.

Wnk1$^{-/-}$/OT-II/RCE cells, along with heterozygous controls, upregulated the expression of CD25, CD44 and CD69 after 3 days post-immunisation (Figure 14B-G). In fact, relative to controls, *Wnk1*$^{-/-}$/OT-II/RCE cells had elevated levels of CD25 and CD69 on their surface at this time point and equivalent levels of CD44. This suggested that *Wnk1*$^{-/-}$/OT-II/RCE cells are able to engage cognate p-MHC-II complexes *in vivo* and transduce signals from the TCR to induce changes in gene expression. However, I could not exclude the possibility that these changes in protein expression were antigen-independent as OT-II T cells could not be detected at day 3 in the absence of immunisation, a condition that would be needed to determine the contribution of the adoptive transfer process on activation marker expression. Data in chapter 4.1 addresses this issue by using an *in vitro* activation system.

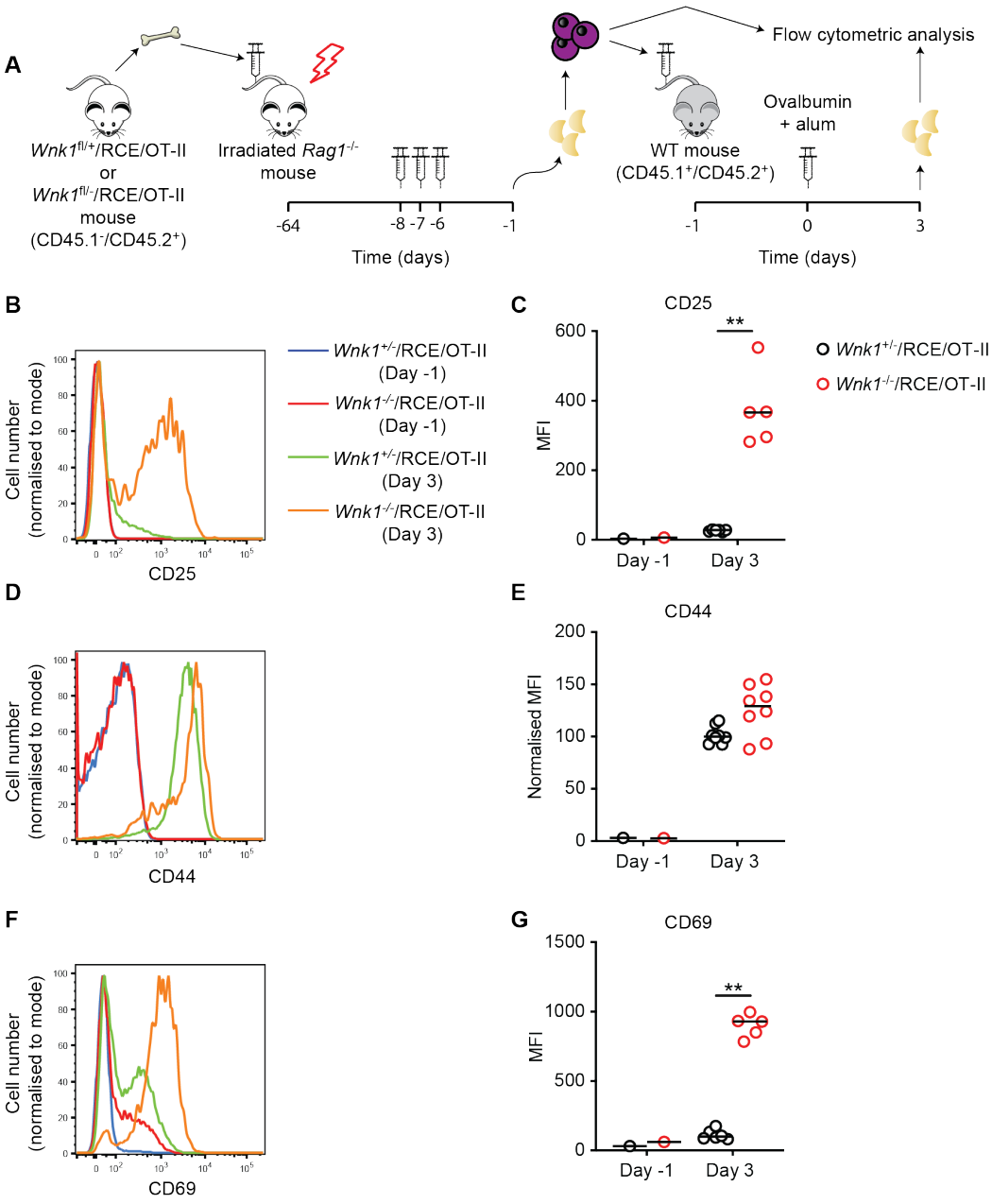

Figure 14. WNK1-deficient cells express abnormally high levels of activation markers in response to antigen *in vivo*. (**A**) Experimental design: *Wnk1*$^{+/-}$/RCE/OT-II and *Wnk1*$^{-/-}$/RCE/OT-II T cells (CD45.1^{-}/CD45.2^{+}) were generated as described in Chapter 3.1. Naïve CD4^{+} T cells (CD25^{-}/CD44^{-}) were isolated from lymph nodes, labelled with CTV, and transferred into (B6xB6.SJL) F1 mice (CD45.1^{+}/CD45.2^{+}) which were immunised the following day with ovalbumin in alum and analysed 3 later. Data shown from live, single, CD4^{+} CD45.1^{-} CD45.2^{+} T cells. (**B-G**) Surface expression levels of CD25 (B, C), CD44 (D, E) and CD69 (F, G) on *Wnk1*$^{+/-}$/RCE/OT-II and *Wnk1*$^{-/-}$/RCE/OT-II (CD4^{+} CD45.1^{-} CD45.2^{+}) cells at indicated time points showing example histograms (B, D, F) and graphs (C, E, G) of the median florescent intensity (MFI) (n=5-8). MFI values in (E) were normalised to the median value of *Wnk1*$^{+/-}$/RCE/OT-II samples at day 3 (set to 100). Each point represents a single mouse; horizontal lines show median. Data shown from 2 independent experiments (E) or from 1 experiment representative of 2 (B-D, F, G) independent experiments. Statistical analysis carried out using Mann-Whitney U test. * $0.01 < p < 0.05$; ** $0.001 < p < 0.01$.

The elevated levels of CD25 and CD69 may show that WNK1 is required for suppression of the expression of these proteins. However, a more comprehensive time course is required to exclude the possibility that control *Wnk1*$^{+/-}$/RCE/OT-II cells upregulated these proteins to equivalent levels, but only transiently, and in fact the expression of activation markers by *Wnk1*$^{-/-}$/RCE /OT-II T cells is delayed. Data in Chapter 4.1 clarifies this issue by measuring activation marker expression at a number of time points during activation *in vitro*. Despite these caveats I think it is fair to conclude that WNK1-deficient cells are able to upregulate activation marker expression *in vivo*, albeit in a dysregulated manner. This suggested that these cells are able to transduce signals from the TCR and induce at least some of the transcriptional changes required for activation *in vivo*. Defects in this stage of CD4$^+$ T cell activation are therefore unlikely to be responsible for the failure of WNK1-deficient cells to support a class-switched antibody response.

3.4 Defective antigen-induced proliferation, survival and T_{FH} differentiation of WNK1-deficient CD4$^+$ T cells

After activation marker upregulation CD4+ T cells rapidly proliferate in a process known as clonal expansion in order to generate a large population of antigen-specific cells capable of orchestrating an immune response. I used the adoptive transfer method described in chapter 3.3 to study the role of WNK1 during clonal expansion (Figure 15A). OT-II T cells were labelled with CTV – a cell tracker dye - prior to injection into the wild type mouse. CTV is an amine-reactive dye that indiscriminately labels cellular proteins. The amount of CTV per cell is diluted by ~50% during successive divisions and thus can be used to determine the number of divisions each individual cell has undergone. WNK1-deficient CD4$^+$ T cells exhibited dramatically reduced CTV dilution, and thus proliferation, in response to antigen *in vivo* at day 3 post-immunisation (Figure 15B). This defective proliferation could be characterised as a reduction in both the percentage of cells that had undergone at least one division, and the average number of divisions completed by cells that had undergone at least one division (proliferation index), relative to control *Wnk1*$^{+/-}$/OT-II/RCE cells (Figure 15C, D). These data showed that WNK1 is required for CD4$^+$ T cell proliferation *in vivo*.

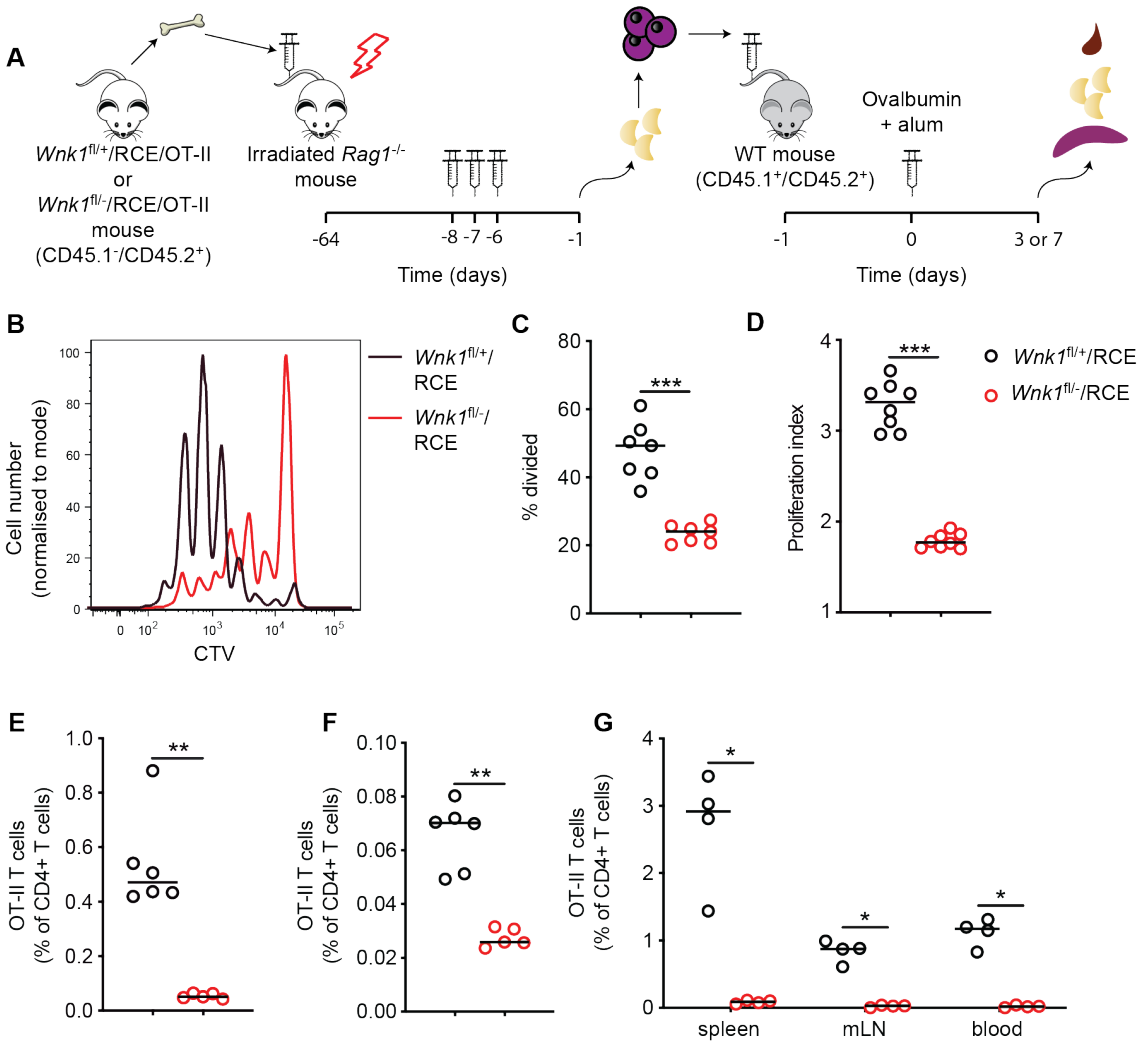

Figure 15. Defective antigen-induced proliferation and survival of WNK1-deficient CD4⁺ T cells *in vivo*. (**A**) Experimental design: *Wnk1*$^{+/-}$/RCE/OT-II and *Wnk1*$^{-/-}$/RCE/OT-II T cells (CD45.1^{-}/CD45.2^{+}) were generated as described in Chapter 3.1. Naïve CD4^{+} T cells (CD25^{lo}/CD44^{lo}) were isolated from lymph nodes, labelled with CTV, and transferred into (B6xB6.SJL) F1 mice (CD45.1^{+}/CD45.2^{+}) which were immunised the following day with OVA in alum and analysed at day 3 or 7 post-immunisation. Data shown from live, single, CD4^{+} CD45.1^{-} CD45.2^{+} T cell population. (**B-G**) Analysis of CD4^{+} OT-II T cells at day 3 (B-F) and at day 7 (G). (**B**) CTV intensity as a measure of proliferation. (**C**) Percentage of cells that had divided (n=7). (**D**) Proliferation index (average number of divisions by dividing cells, n=8). (**E**) CD4^{+} OT-II T cells as a percentage of all CD4^{+} cells in peripheral and mesenteric lymph nodes (n=5-6). (**F**) As in E but taking out the effect of division. (**G**) CD4+ OT-II T cells as a percentage of all CD4^{+} T cells in spleen, mesenteric lymph nodes (mLN) and blood at day 7 post-immunisation (n=4). Each point represents a single mouse; horizontal lines show median. Data shown from 2 independent experiments (C-D) or from 1 experiment representative of 2 (E, F) or 3 (G) independent experiments. Statistical analysis carried out using Mann-Whitney U test. * 0.01 < p < 0.05; ** 0.001 < p < 0.01; *** 0.0001 < p < 0.001.

As previously mentioned, clonal expansion is needed to generate a large pool of antigen-specific CD4$^+$ T cells. The number of *Wnk1*$^{-/-}$/OT-II/RCE cells was, on average, ~9-fold lower than the number of *Wnk1*$^{+/-}$/OT-II/RCE cells at day 3 (Figure 15E). Reduced proliferation by *Wnk1*$^{-/-}$/OT-II/RCE cells must have contributed to the reduction in population size at day 3 but altered viability of these cells may also have played a role. In order to deconvolute these two factors the number of cells that would be present at day 3 if no proliferation took place was calculated by fitting a model to the CTV dilution profile (Figure 15B) and dividing the cell number in each peak by the value indicated in Figure 16.

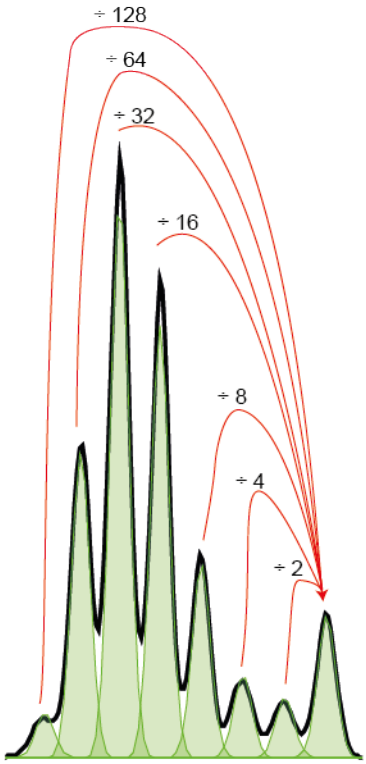

Figure 16. Calculation to remove effect of division. The number of cells in each peak was calculated by fitting a model (green) to the curves. The number of cells that would be present if no cell division had taken place was then calculated by dividing the number of cells in each peak by the number indicated.

Removing the effect of proliferation, there was a ~3-fold reduction in the number of *Wnk1*$^{-/-}$/OT-II/RCE cells relative to *Wnk1*$^{+/-}$/OT-II/RCE cells at day 3, which could have been due to a survival and/or homing defect (Figure 15F). It is difficult to examine the relative contributions of survival and homing as one cannot analyse OT-II T cell population in all tissues in the mouse. Measuring the total number of CD4$^+$ T

cell using bioluminescence might be one approach to overcome this issue. Nevertheless, these data showed that WNK1 is required for both $CD4^+$ T cell proliferation and survival/homing *in vivo*, and that defects in these processes contributed roughly equal amounts to the reduction in the population of *Wnk1*$^{-/-}$/OT-II/RCE cells at day 3 post immunisation.

The decrease in the population size of *Wnk1*$^{-/-}$/OT-II/RCE cells relative to *Wnk1*$^{+/-}$/OT-II/RCE cells at day 3 was amplified by day 7 post immunisation. As shown in Figure 15G, there was a dramatic reduction in the *Wnk1*$^{-/-}$/OT-II/RCE cell population in the spleen, mesenteric lymph nodes (mLN) and blood at day 7, where the median population size of *Wnk1*$^{-/-}$/OT-II/RCE cells was ~1.5-3% of the *Wnk1*$^{+/-}$/OT-II/RCE cells at day 7. This increase in severity of the population size defect was most likely due to the continued effects of WNK1-deficiency on survival/homing and proliferation, particularly as proliferation results in exponential population expansion. The equivalent reduction in the number of *Wnk1*$^{-/-}$/OT-II/RCE cells in the spleen, mLN and blood suggested that a survival defect contributes more to the WNK1-deficient phenotype than a homing defect, unless WNK1-deficient cells were homing to, and accumulating in, the mucosa-associated lymphoid tissue, or non-secondary lymphoid tissues.

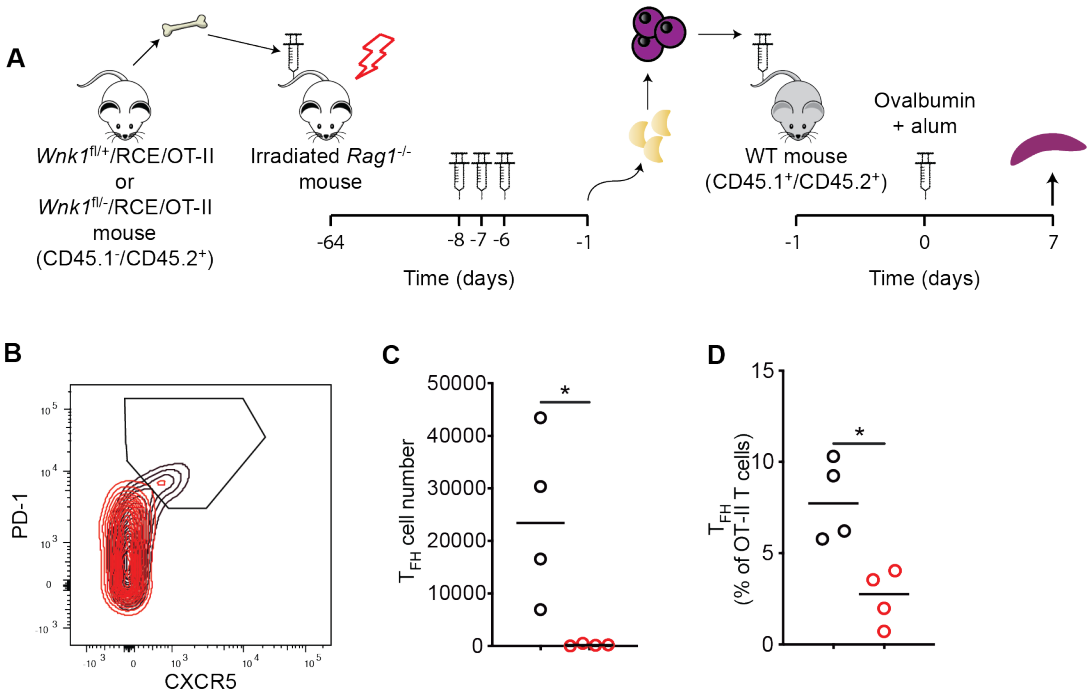

Figure 17. WNK1-deficient CD4$^+$ T cells exhibit defective T$_{FH}$ differentiation and fail to produce a large population of antigen-specific T$_{FH}$ cells. (**A**) Experimental design: *Wnk1*$^{+/-}$/RCE/OT-II and *Wnk1*$^{-/-}$/RCE/OT-II T cells (CD45.1$^-$/CD45.2$^+$) were generated as described in Chapter 3.1. Naïve CD4$^+$ T cells (CD25^{lo}/CD44^{lo}) were isolated from lymph nodes and transferred into (B6xB6.SJL) F1 mice (CD45.1$^+$/CD45.2$^+$) which were immunised the following day with OVA in alum and analysed at day 7 post-immunisation. Data shown from live, single, CD4$^+$ CD45.1$^-$ CD45.2$^+$ T cell population. (**B**) PD-1 and CXCR5 levels on splenic (CD45.1$^-$CD45.2$^+$) *Wnk1*$^{fl/+}$/RCE/OT-II (black) and *Wnk1*$^{fl/-}$/RCE/OT-II (red) CD4$^+$ T cells. Gate indicates T$_{FH}$ cells. (**C**) T$_{FH}$ cell numbers in the spleen (n=4). (**D**) T$_{FH}$ cells as a percentage of all OT-II T cells in the spleen (n=4). Data shown from 1 experiment representative of 3 independent experiments. Statistical analysis carried out using Mann-Whitney U test. * $0.01 < p < 0.05$.

After activation, some CD4$^+$ T cells differentiate into T$_{FH}$ cells and migrate to the follicular border to provide help to B lymphocytes, supporting their activation. T$_{FH}$ cells then migrate into the follicle where they participate in the germinal centre reaction in which activated B cells undergo somatic hypermutation and class-switch recombination to generate high affinity B cell receptors of an isotype relevant to the class of invading pathogen (Berek et al., 1991; Jacob et al., 1991). The germinal centre reaction generally begins around day 7 post-immunisation, after which activated B cells begin to differentiate into memory B cells or plasma cells, which are responsible for the generation of antigen-specific, class-switched antibodies present in the blood plasma. I measured the number of OT-II T$_{FH}$ cells (PD1$^+$/CXCR5$^+$, Figure 17B-D) at day 7 to determine whether there was a sufficiently sized population to

support a germinal centre reaction. As shown in Figure 17C, there was an almost complete absence of *Wnk1*$^{-/-}$/OT-II/RCE T_{FH} cells (~190 cells on average) in the spleen at day 7 post-immunisation. This was predominantly due to defective proliferation and survival/homing, but these defects were compounded by a reduction in the proportion of *Wnk1*$^{-/-}$/OT-II/RCE cells that differentiate into T_{FH} cells (Figure 17D).

The population of *Wnk1*$^{-/-}$/OT-II/RCE T_{FH} cells at day 7 was unlikely to be able to support B cell activation or the germinal centre reaction. Therefore, I concluded that the inability of WNK1-deficient cells to support a class-switched antibody response was because of a failure to generate a sufficient population of antigen-specific $CD4^+$ T cells to support a germinal centre response. This failure was mainly due to a reduction in antigen-induced proliferation and survival/homing, with a further contribution from impaired T_{FH} differentiation.

Chapter 4. WNK1 is required for CD4$^+$ T cell activation *in vitro*

I used *in vitro* activation systems in which the WNK1-deficient phenotype was faithfully replicated to further define the role of WNK1 and downstream signalling proteins during CD4$^+$ T cell activation and proliferation.

4.1 WNK1 supresses antigen-dependent and antigen-independent activation marker expression *in vitro*

In order to further characterise the role of WNK1 in CD4$^+$ T cells, I endeavoured to determine whether I could replicate the WNK1-deficient phenotype using an *in vitro* activation system. Initially I cultured control or WNK1-deficient OT-II T cells with bone marrow-derived antigen presenting cells (APCs) in the presence, or absence, of $OVA_{323-339}$ peptide (Figure 18A) (Helft et al., 2015). I found that WNK1-deficient cells are able to upregulate the surface expression of CD25, CD44 and CD69 in response to antigen *in vitro* (Figure 18B-G). At almost all concentrations of $OVA_{323-339}$ peptide I found that *Wnk1*$^{-/-}$/OT-II/RCE cells expressed higher levels of CD25, CD44 and CD69 on their surface than *Wnk1*$^{+/-}$/OT-II/RCE cells at day 5. However, data from additional timepoints are needed to determine the effect of WNK1 on activation marker expression dynamics. From a single timepoint it was unclear whether WNK1-deficient cells have elevated activation marker expression throughout activation *in vitro* or whether they upregulate activation markers in a temporally delayed manner while at day 5 control cells are in fact downregulating activation marker expression.

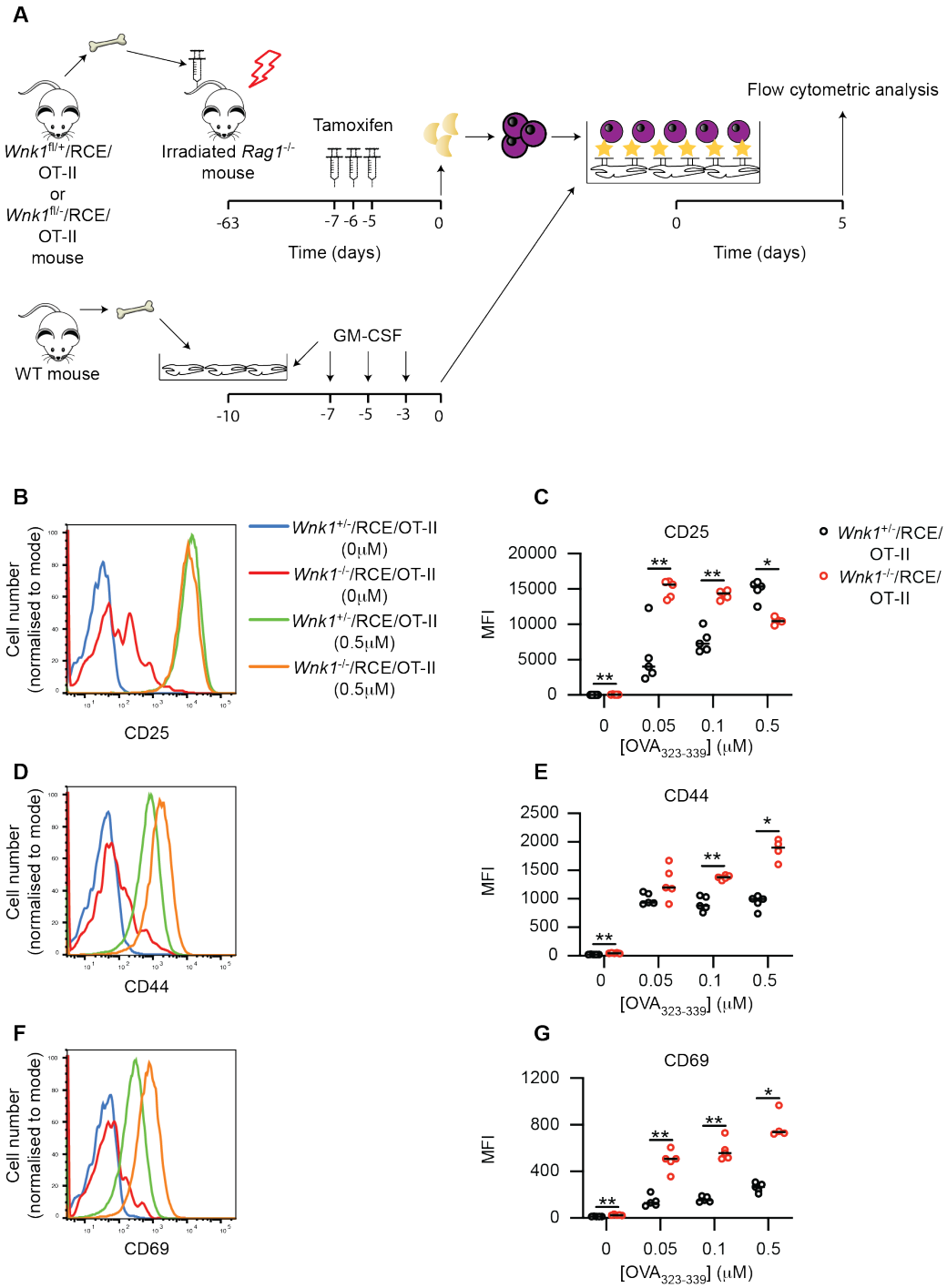

Figure 18. WNK1-deficient cells express abnormally high levels of activation markers in response to antigen *in vitro*. (**A**) Experimental design: *Wnk1*$^{+/-}$/RCE/OT-II and *Wnk1*$^{-/-}$/RCE/OT-II T cells (CD45.1^{-}/CD45.2^{+}) were generated as described in Chapter 3.1. Naïve CD4^{+} T cells (CD25^{lo}/CD44^{lo}) were isolated from lymph nodes and co-cultured GM-CSF-bone marrow culture-derived APCs in the presence of $OVA_{323-339}$ peptide. Data shown from live, single, CD11c^{-} CD4^{+} T cells. (**B-G**) Surface expression levels of CD25 (B, C), CD44 (D, E) and CD69 (F, G) on *Wnk1*$^{+/-}$/RCE/OT-II or *Wnk1*$^{-/-}$/RCE/OT-II T cells at day 5 in the presence of indicated $OVA_{323-339}$ peptide concentrations showing example histograms (B, D, F) and graphs (C, E, G) of the median florescent intensity (MFI, n=4-5). Each point represents a single mouse; horizontal lines show median. Data from 1 experiment representative of 2 independent experiments. Statistical analysis carried out using Mann-Whitney U test. * $0.01 < p < 0.05$; ** $0.001 < p < 0.01$.

Incorporation of activation marker cell surface expression data from the OT-II T cells at day 0 and day 3 revealed that WNK1 does in fact supress expression of activation markers during activation *in vitro* (Figure 19). This conclusion was made under the assumption that expression between the timepoints measured followed a roughly linear trajectory. Interestingly, even in the absence of antigen, *Wnk1*$^{-/-}$/OT-II/RCE cells expressed elevated levels of CD25 and CD69 when compared to *Wnk1*$^{+/-}$/OT-II/RCE cells (Figure 19A, C, D). CD25 was upregulated in WNK1-deficient cells during culture *ex vivo* in the absence of antigen. CD69 expression was elevated in naïve *Wnk1*$^{-/-}$/OT-II/RCE cells at day 0 showing that upregulation of this protein occurs during *Wnk1* deletion *in vivo*. This may also be the case for CD25 or CD44, but depletion of CD25^{hi}CD44^{hi} cells during naïve CD4^{+} T cell isolation would result in their removal from the samples at day 0. These observations showed that WNK1 suppresses the expression of activation markers in the absence, and presence, of antigen. Whether these two processes are regulated by the same WNK1-dependent mechanism will require further study.

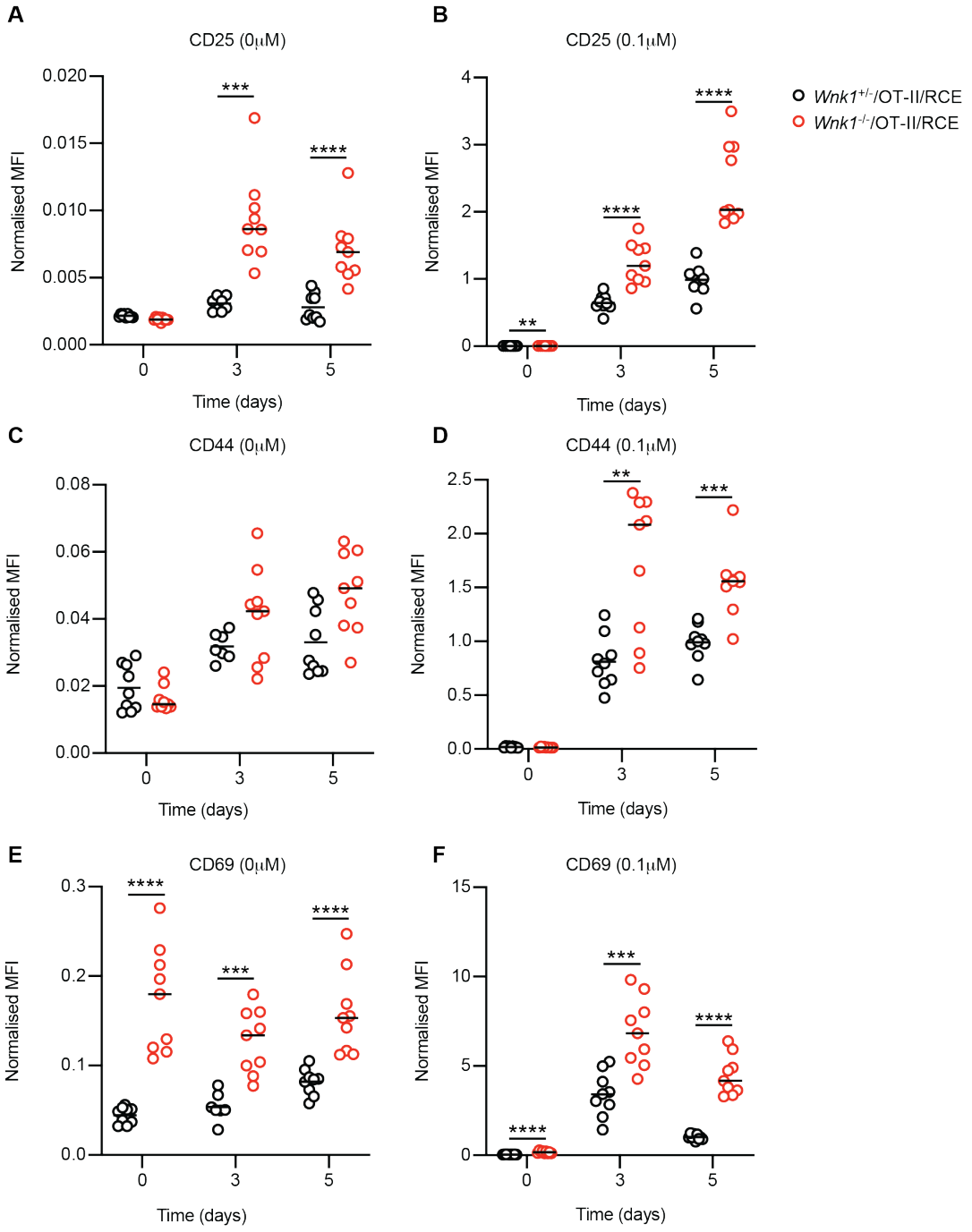

Figure 19. WNK1 supresses antigen-dependent and -independent activation marker expression *in vitro.* (**A-F**) Time course of surface expression of CD25 (A,B), CD44 (C,D) and CD69 (E,F) on *Wnk1*$^{+/-}$/RCE/OT-II or *Wnk1*$^{-/-}$/RCE/OT-II T cells in the presence of 0μM (A,C,E) or 0.1μM (B,D,F) $OVA_{323-339}$ peptide concentrations (n=7-9). MFI values normalised to median of *Wnk1*$^{+/-}$/RCE/OT-II samples at day 5 with 0.1μM $OVA_{323-339}$ peptide (set to 1). Each point represents a single mouse; horizontal lines show median. Data pooled from 2 independent experiments. Statistical analysis carried out using Mann-Whitney U test. * 0.01 < p < 0.05; ** 0.001 < p < 0.01; ***0.0001<p<0.001; ****p<0.0001.

4.2 WNK1 kinase activity supresses activation marker expression during activation with anti-CD3 and anti-CD28 antibodies *in vitro*

In order to determine whether the WNK1-deficient phenotype could be observed in CD4+ T cells activated in the simplest possible *in vitro* system I used plate-bound anti-CD3 and anti-CD28 antibodies to activate *Wnk1*$^{+/-}$/RCE and *Wnk1*$^{-/-}$/RCE cells. These antibodies cross-link the cell surface receptors to which they are specific and induce downstream signalling. Since APCs are not needed, this method reduces the complexity of the cellular environment while providing TCR and costimulation signals which are the minimal requirement for activation.

Wnk1$^{-/-}$/RCE cells also express elevated levels of CD25, CD44 and CD69 relative to controls during activation with immobilised anti-CD3 and anti-CD28 antibodies *in vitro* at almost all timepoints (Figure 20B-G). These data show that we can recapitulate the WNK1-deficient activation marker phenotype seen *in vivo* and *in vitro* co-culture using this system, and that this phenotype is unlikely to be related to the migration defect exhibited by WNK1-deficient cells as activation in this system does not require migration for antigen encounter (Köchl et al., 2016).

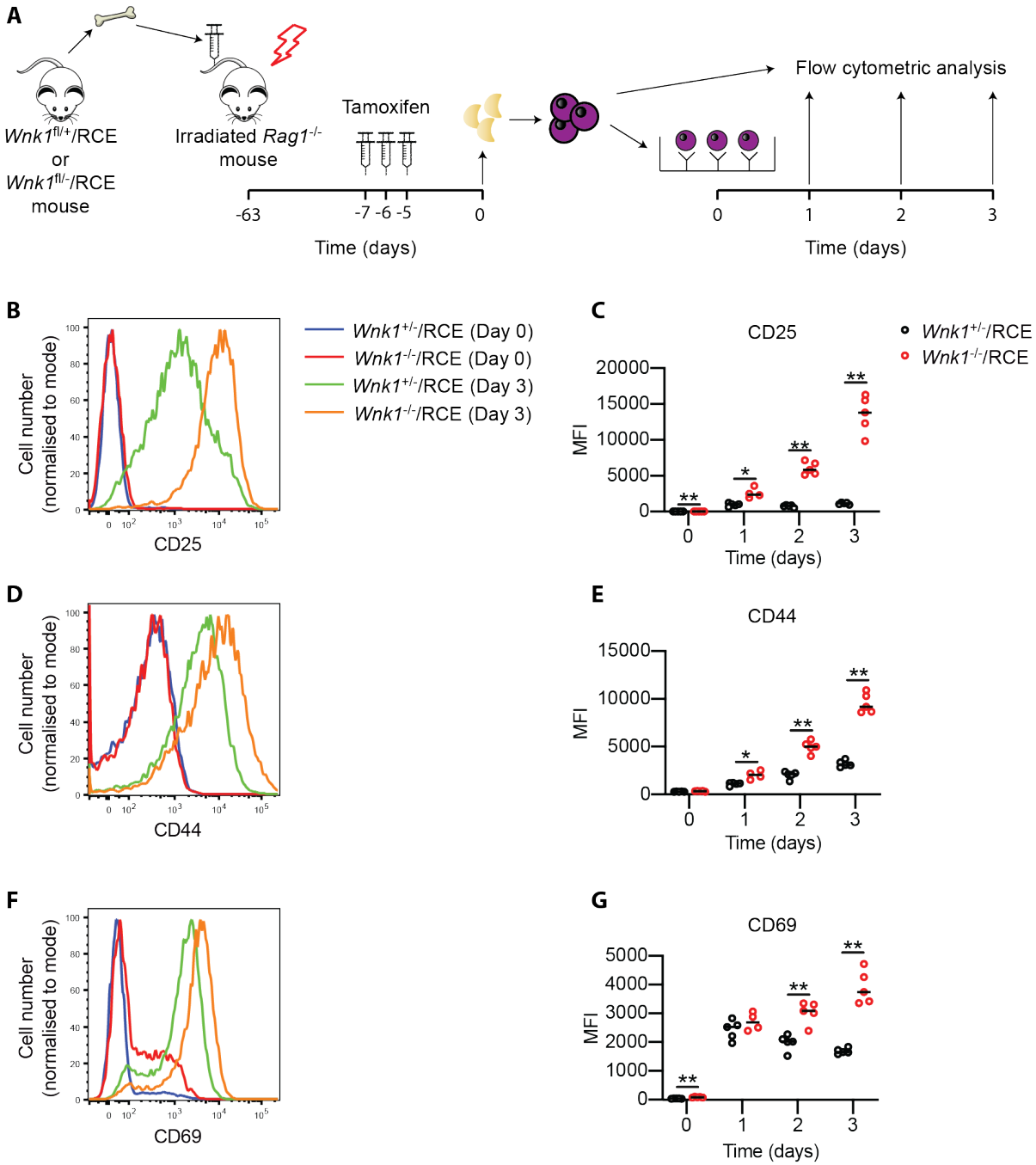

Figure 20. WNK1-deficient CD4⁺ T cells express abnormally high levels of activation markers during activation *in vitro* with anti-CD3 and anti-CD28 antibodies. (**A**) Experimental design: *Wnk1*$^{+/-}$/RCE and *Wnk1*$^{-/-}$/RCE T cells were generated as described in Chapter 3.1. Naïve CD4⁺ T cells (CD25^{lo}/CD44^{lo}) were isolated from lymph nodes and cultured on plate-bound anti-CD3 and anti-CD28 antibodies. Data shown from live, single, CD4⁺ T cells. (**B-G**) Surface expression levels of CD25 (B, C), CD44 (D, E) and CD69 (F, G) on *Wnk1*$^{+/-}$/RCE and *Wnk1*$^{-/-}$/RCE CD4⁺ T cells at indicated time points showing example histograms (B, D, F) and graphs (C, E, G) of the median florescent intensity (MFI) (n=5). Each point represents a single mouse; horizontal lines show median. Data from 1 experiment representative of 4 independent experiments. Statistical analysis carried out using Mann-Whitney U test. * $0.01 < p < 0.05$; ** $0.001 < p < 0.01$.

WNK1 is known to have kinase-dependent and independent functions (Friedel et al., 2015; Yamada et al., 2016). To determine whether WNK1 kinase activity is required for the suppression of activation marker expression I used mice carrying an allele of *Wnk1* containing a point mutation which renders the kinase domain inactive (*Wnk1*^{D368A}). This allele was combined with the *Wnk1*^{fl} and RCE alleles to generate *Wnk1*$^{D368A/fl}$/RCE mice. Bone marrow chimeras were once again used to restrict these alleles to the haematopoietic compartment. Tamoxifen-inducible deletion of the *Wnk1*^{fl} allele facilitated the generation of *Wnk1*$^{D368A/-}$/RCE T cells that could be used to study the role of WNK1 kinase activity during CD4^{+} T cell activation.

Wnk1$^{D368A/-}$/RCE CD4^{+} T cells phenocopied the elevated activation marker expression seen on *Wnk1*$^{-/-}$/RCE CD4^{+} T cells during activation *in vitro* (Figure 21B-G). The increase in activation marker surface expression seen on CD4^{+} T cells of these genotypes relative to controls was roughly equivalent in magnitude. These observations lead me to conclude that WNK1 kinase activity is required for suppression of activation marker expression during activation *in vitro*.

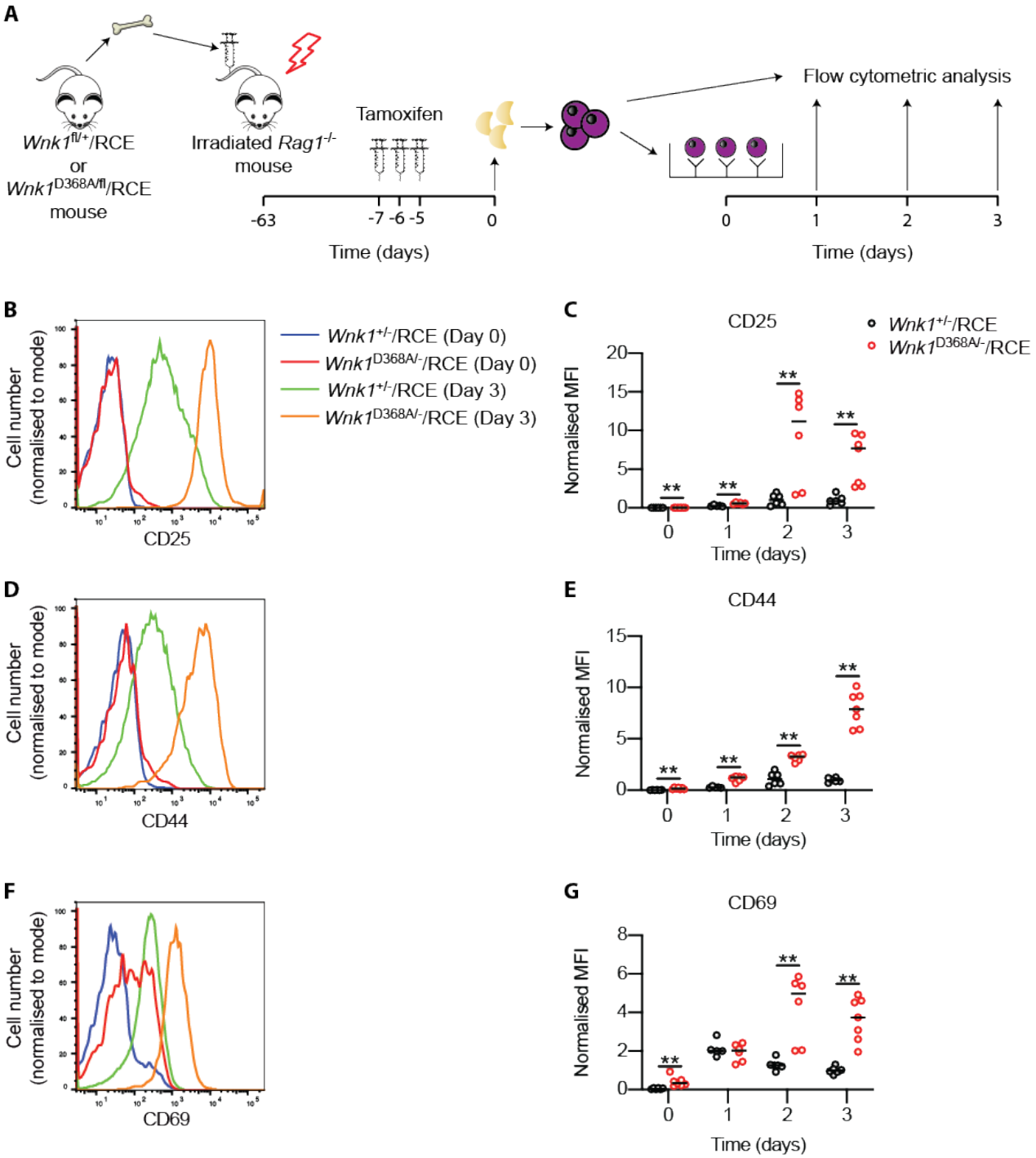

Figure 21. WNK1 kinase activity is required for normal activation marker expression during activation *in vitro.* (**A**) Experimental design: *Wnk1*$^{+/-}$/RCE and *Wnk1*$^{D368A/-}$/RCE T cells were generated as described in Chapter 3.1. Naïve CD4^{+} T cells (CD25^{lo}/CD44^{lo}) were isolated from lymph nodes and cultured on plate-bound anti-CD3 and anti-CD28 antibodies. Data shown from live, single, CD4^{+} T cells. (**B-G**) Surface expression levels of CD25 (B, C), CD44 (D, E) and CD69 (F, G) on *Wnk1*$^{+/-}$/RCE and *Wnk1*$^{D368A/-}$/RCE CD4^{+} T cells at indicated time points showing example histograms (B, D, F) and graphs (C, E, G) of the median florescent intensity (MFI) (n=5-7). MFI normalised to the median value of *Wnk1*$^{+/-}$/RCE samples at day 3 (set to 1). Each point represents a single mouse; horizontal lines show median. Data pooled from 2 independent experiments. Statistical analysis carried out using Mann-Whitney U test. * $0.01 < p < 0.05$; ** $0.001 < p < 0.01$.

The approach I used to generate WNK1-deficient T cells requires that naive CD4$^+$ T cells exist *in vivo* for a period of time without the WNK1 protein. This raises the possibility that effects observed *ex vivo* are caused by several days of WNK1-deficiency *in vivo*. In order to address this issue, acute inhibition of WNK1 kinase activity was achieved by the addition of the pan-WNK inhibitor – WNK463 – to the cell culture media. This inhibitor takes advantage of the atypical structure of the WNK family kinase domains to provide relatively specific inhibition of these kinases (Yamada et al., 2016). An *in vitro* kinase activity screen showed that 10μM WNK463 inhibited only 2 of the 442 human kinases tested by more than 50%. The fact that naïve CD4$^+$ T cells express only the WNK1 paralog offered us an opportunity to use this inhibitor to acutely inhibit the WNK1 kinase *in vitro* with relatively high specificity.

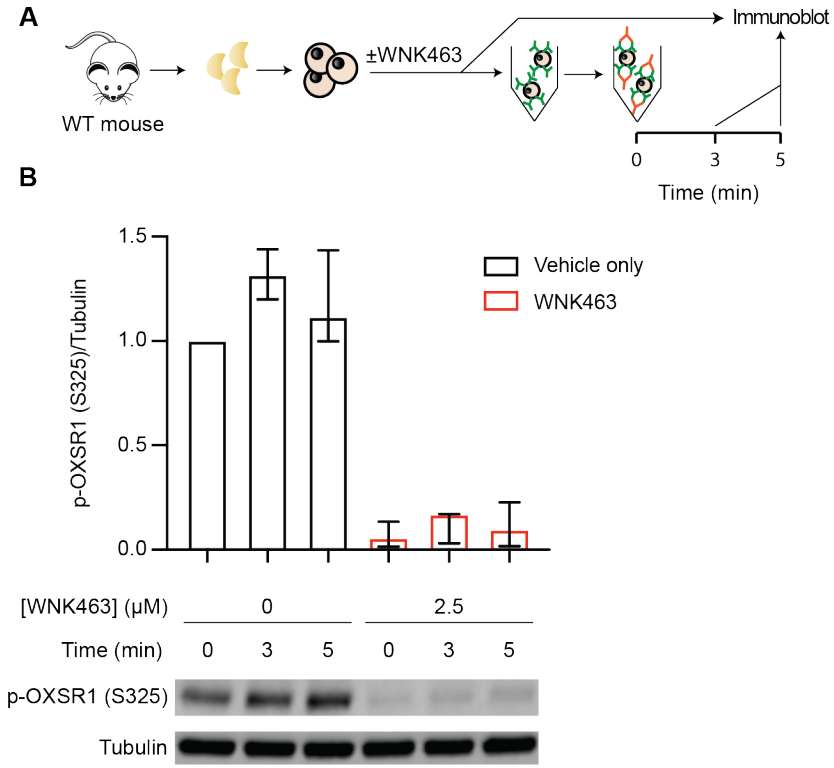

Figure 22. 2.5μM WNK463 is sufficient to inhibit homeostatic and TCR-induced WNK1 activity. (**A**) WT naïve CD4$^+$ T cells (CD25^{lo}/CD44^{lo}) were isolated from lymph nodes and incubated with anti-CD3 and anti-CD28 antibodies in the presence of 2.5μM WNK463 or equivalent amount of DMSO for 30 min at 4 °C. Cells were then washed, warmed to 37°C, and stimulated using cross-linking antibody (± WNK463) for indicated times. (**B**) Graph and example immunoblot of p-OXSR1 and tubulin abundance in WNK463-treated and vehicle only-treated cell extracts after stimulation for the indicated times (n=3). Each bar represents the median±95% confidence interval of relative band intensity. Data pooled from 3 independent experiments. Relative band intensity normalised to vehicle-treated samples at 0 min (set to 1).

Preincubation of naïve $CD4^+$ T cells with 2.5μM WNK463 for 30 min at 4°C was sufficient to almost completely abolish WNK1 activity, as measured by p-OXSR1 (S325) abundance, in both the presence and absence of TCR and CD28 costimulation (Figure 22A, B). Although this WNK463-mediated WNK1 inhibition was experimentally reproducible, as it was observed in 3 independent experiments, a lack of sufficient biological repeats meant that it was not possible to determine whether this was a statistically significant effect. Nevertheless, I concluded that WNK463 could be used to acutely inhibit WNK1 kinase activity in $CD4^+$ T cells in culture.

$CD4^+$ T cells activated *in vitro* with immobilised anti-CD3 and anti-CD28 antibodies in the presence of WNK463 expressed elevated surface levels of CD25, CD44 and CD69 relative to control samples treated with vehicle only (DMSO) by day 3 or earlier (Figure 23). This elevation of activation marker expression was not as large as that seen on *Wnk1*$^{-/-}$/RCE and *Wnk1*$^{D368A/-}$/RCE cells during activation *in vitro*. The extended period of WNK1-deficiency experienced by *Wnk1*$^{-/-}$/RCE and *Wnk1*$^{D368A/-}$/RCE cells *in vivo* or off-target activity by WNK463 may account for the differences in the magnitude of the defect. Nonetheless, because WNK463-treatment qualitatively produced the same effect as genetic deletion of WNK1 kinase activity I conclude that WNK1 kinase activity is acutely required for suppression of activation marker surface expression *in vitro*.

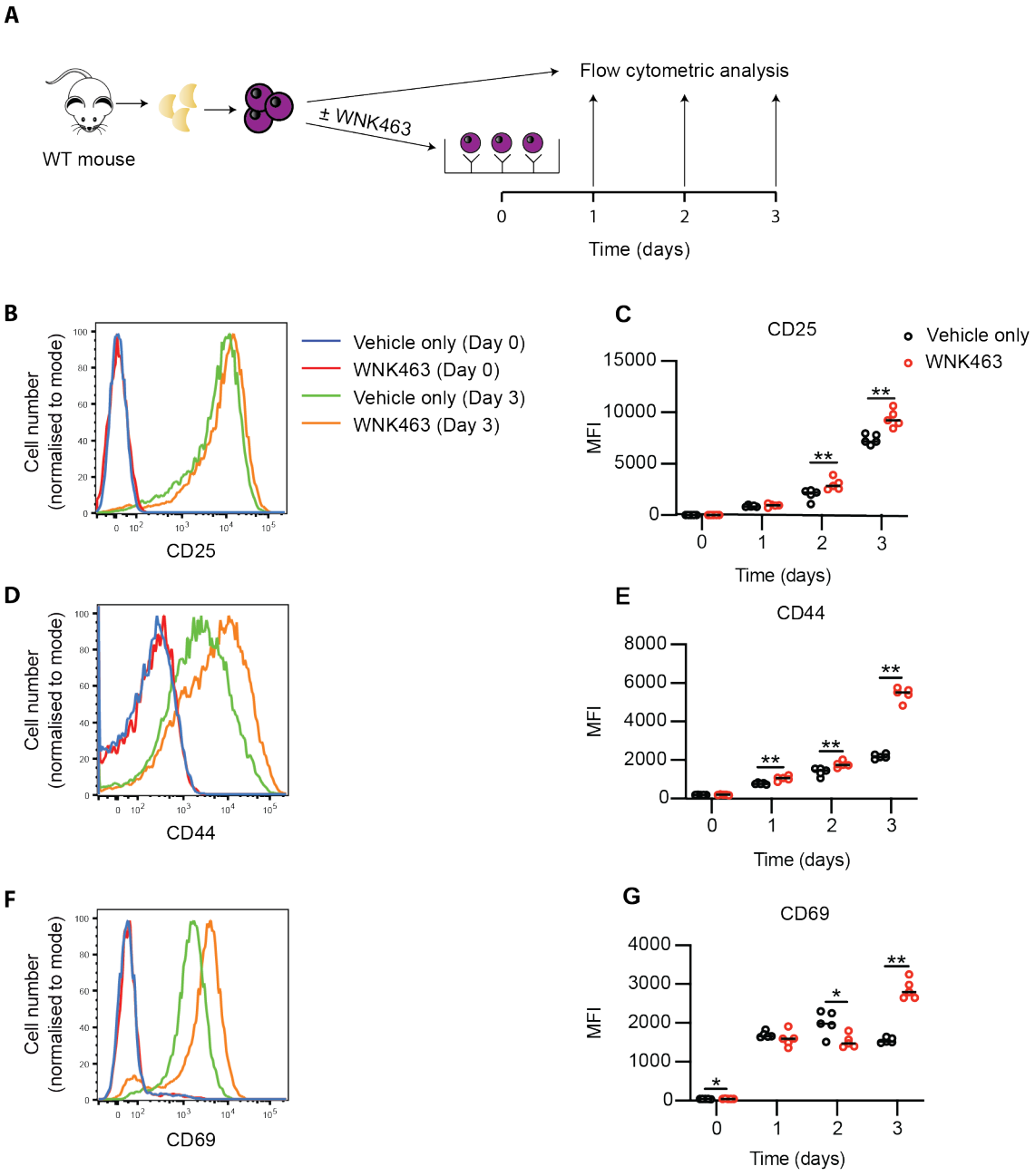

Figure 23. CD4⁺ T cells treated with the WNK inhibitor - WNK463 - express activation markers at aberrantly high levels during activation *in vitro.* (**A**) WT naïve CD4⁺ T cells ($CD25^{lo}/CD44^{lo}$) were isolated from lymph nodes and cultured on plate-bound anti-CD3 and anti-CD28 antibodies in the presence of vehicle only or WNK463. Data shown from live, single, CD4⁺ T cell population. (**B-G**) Surface expression levels of CD25 (B, C), CD44 (D, E) and CD69 (F, G) on vehicle only and WNK463-treated CD4⁺ cells at indicated time points showing example histograms (B, D, F) and graphs (C, E, G) of the median florescent intensity (MFI) (n=5). Each point represents a single mouse; horizontal lines show median. Data from 1 experiment representative of 2 independent experiments. Statistical analysis carried out using Mann-Whitney U test. * $0.01 < p < 0.05$; ** $0.001 < p < 0.01$

4.3 Deletion of *Oxsr1* in naïve CD4$^+$ T cells

WNK1 is known to directly phosphorylate and activate the OXSR1 kinase which in turn regulates the activity of a number of ion channels at the plasma membrane (Figure 11) (Vitari et al., 2005). To determine whether OXSR1 is required for CD4+ T cell function I used a conditional allele of *Oxsr1* because constitutive deletion of this gene is embryonic lethal (Xie et al., 2013). This allele had LoxP sites inserted around exons 9 and 10, which encode for a section of the kinase domain (*Oxsr1*^{fl}) (Figure 24A) (Lin et al., 2011). This allele was combined with the RCE transgene to facilitate tamoxifen-inducible excision of exons 9 and 10 and a concomitant frame shift resulting in the introduction of premature stop codons into the coding region of the gene. The STK39 kinase is also directly phosphorylated and activated by WNK1 and regulates the activity of many of the same ion transporters as OXSR1 (Figure 11). This functional redundancy may allow STK39 to compensate for the loss of OXSR1 from naïve CD4$^+$ T cells. The *Oxsr1*^{fl} allele was therefore combined with a mutant allele of *Stk39* that encodes for a STK39 protein that cannot be phosphorylated and activated by WNK1 (*Stk39*^{T243A}) (Rafiqi et al., 2010; Vitari et al., 2005).

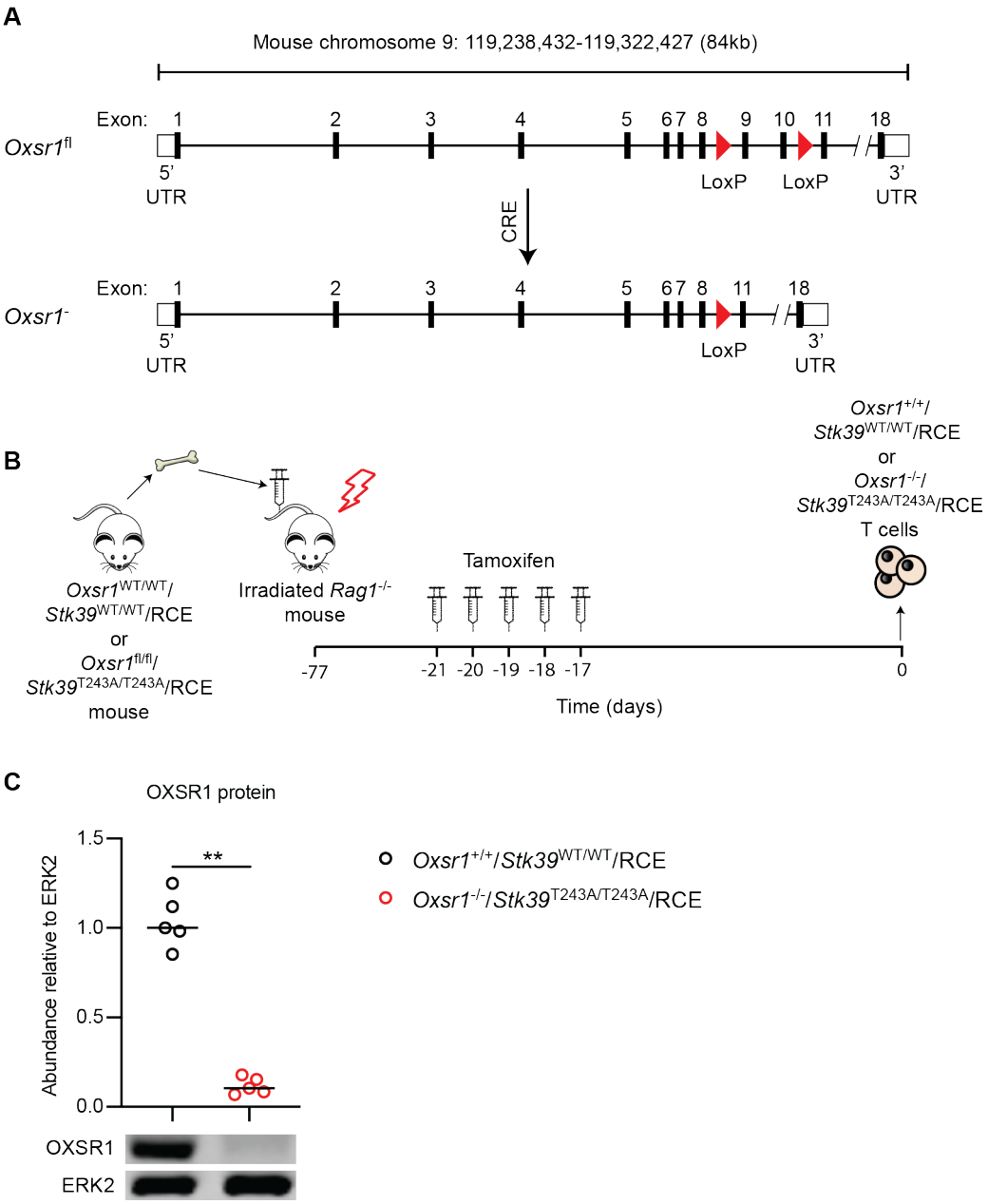

Figure 24. Cre-LoxP mediated deletion of exons 9 and 10 of *Oxsr1* in CD4$^+$ T cells. (**A**) Schematic showing LoxP sites flanking exons 9 and 10 of *Oxsr1* and the product of Cre recombinase activity. (**B**) Experimental design: irradiated RAG1-deficient mice were reconstituted with bone marrow from *Oxsr1*$^{+/+}$/*Stk39*$^{+/+}$/RCE or *Oxsr1*$^{fl/fl}$/*Stk39*$^{T243A/T243A}$/RCE mice. At least 8 weeks later mice were treated with tamoxifen for 5 days to induce the deletion of the floxed *Oxsr1* allele. 21 days after the initial injection naive CD4$^+$ T cells (CD25^{lo}/CD44^{lo}) were isolated from lymph nodes by negative depletion. (**C**) Graph shows OXSR1 abundance in *Oxsr1*$^{+/+}$/*Stk39*$^{+/+}$/RCE and *Oxsr1*$^{-/-}$/*Stk39*$^{T243A/T243A}$/RCE naïve CD4+ T cells determined by immunoblotting cell extracts with antibodies against OXSR1 and ERK proteins (n=5); an example immunoblot is shown below. Each point represents a single mouse; horizontal lines show median. Data from 1 experiment representative of 2 independent experiments. Statistical analysis carried out using the Mann-Whitney U test. ** 0.001 < p < 0.01.

Bone marrow chimeras were generated using sub-lethally irradiated Rag1-deficient recipient mice to restrict these mutations to the haematopoietic compartment and mainly to lymphocytes. Mice were injected with tamoxifen via the intraperitoneal route for 5 consecutive days (Figure 24B). 21 days after the first injection lymph nodes were harvested and the OXSR1 protein content of naïve $CD4^+$ T cells was analysed by immunoblot (Figure 24C). The tamoxifen regime described above was sufficient to reduce the abundance of OXSR1 in *Oxsr1*$^{fl/fl}$/Stk39$^{T243A/T243A}$/RCE samples to ~10% of that found in the *Oxsr1*$^{+/+}$/*Stk39*$^{+/+}$/RCE samples. I concluded that this inducible deletion system is sufficiently efficient to study the role of OXSR1 in naïve CD4+ T cells.

4.4 OXSR1- and STK39-dependent signalling is required for suppression of activation marker expression during activation *in vitro*

The canonical signalling pathway downstream of WNK1 requires phosphorylation and activation of OXSR1 and STK39 kinases by WNK1. Activated OXSR1 and STK39 kinases regulate the activity of NKCC, KCC and NCC ion channels by directly phosphorylating these proteins. Therefore, in order to determine whether this canonical pathway is required for suppression of activation marker expression I used mice carrying a conditional allele of *Oxsr1* (*Oxsr1*^{fl}, see chapter **Error! Reference source not found.**), RCE and a point mutation in *Stk39* that prevents WNK1-dependent phosphorylation and activation of this protein (*Stk39*^{T243A}). The combination of these conditional and point mutant alleles allowed me to prevent signalling through the canonical pathway and removed any possible effects of redundancy between the OXSR1 and STK39 kinases. Once again, bone marrow chimeras were used to restrict the mutant alleles to the haematopoietic compartment. However, in contrast to deletion of the *Wnk1*^{fl} allele, mice were administered with tamoxifen on 5 consecutive days and naïve $CD4^+$ T cells were harvested 21 days after the initial injection to ensure robust deletion of the *Oxsr1*^{fl} allele and loss of OXSR1. The tamoxifen regime used for *Wnk1*^{fl} deletion did not efficiently reduce OXSR1 protein levels.

Oxsr1$^{-/-}$/*Stk39*$^{T243/T243}$/RCE cells exhibited elevated expression of CD25, CD44 and CD69 activation markers during activation *in vitro* relative to

Oxsr1$^{+/+}$/*Stk39*$^{+/+}$/RCE cells (Figure 25B-G). However, the increase in expression was not as large as that seen in *Wnk1*$^{-/-}$/RCE and *Wnk1*$^{D368A/-}$/RCE cells. It is worth noting that naïve *Oxsr1*$^{-/-}$/*Stk39*$^{T243/T243}$/RCE CD4^{+} T cells would have existed without wild-type STK39 throughout development and without functional signalling via the canonical WNK1 pathway for an unknown period of time *in vivo* following loss of OXSR1. These differences in the experimental setup used to delete the *Wnk1*^{fl} allele may also have been, at least partially, responsible for differences in the defects observed. Nevertheless, from these data I concluded that OXSR1 and STK39 kinases supress activation marker expression. The similarity between the phenotypes of *Oxsr1*$^{-/-}$/*Stk39*$^{T243/T243}$/RCE and *Wnk1*$^{-/-}$/RCE CD4^{+} T cells is consistent with WNK1 signalling via OXSR1 and STK39 to regulate expression of activation markers.

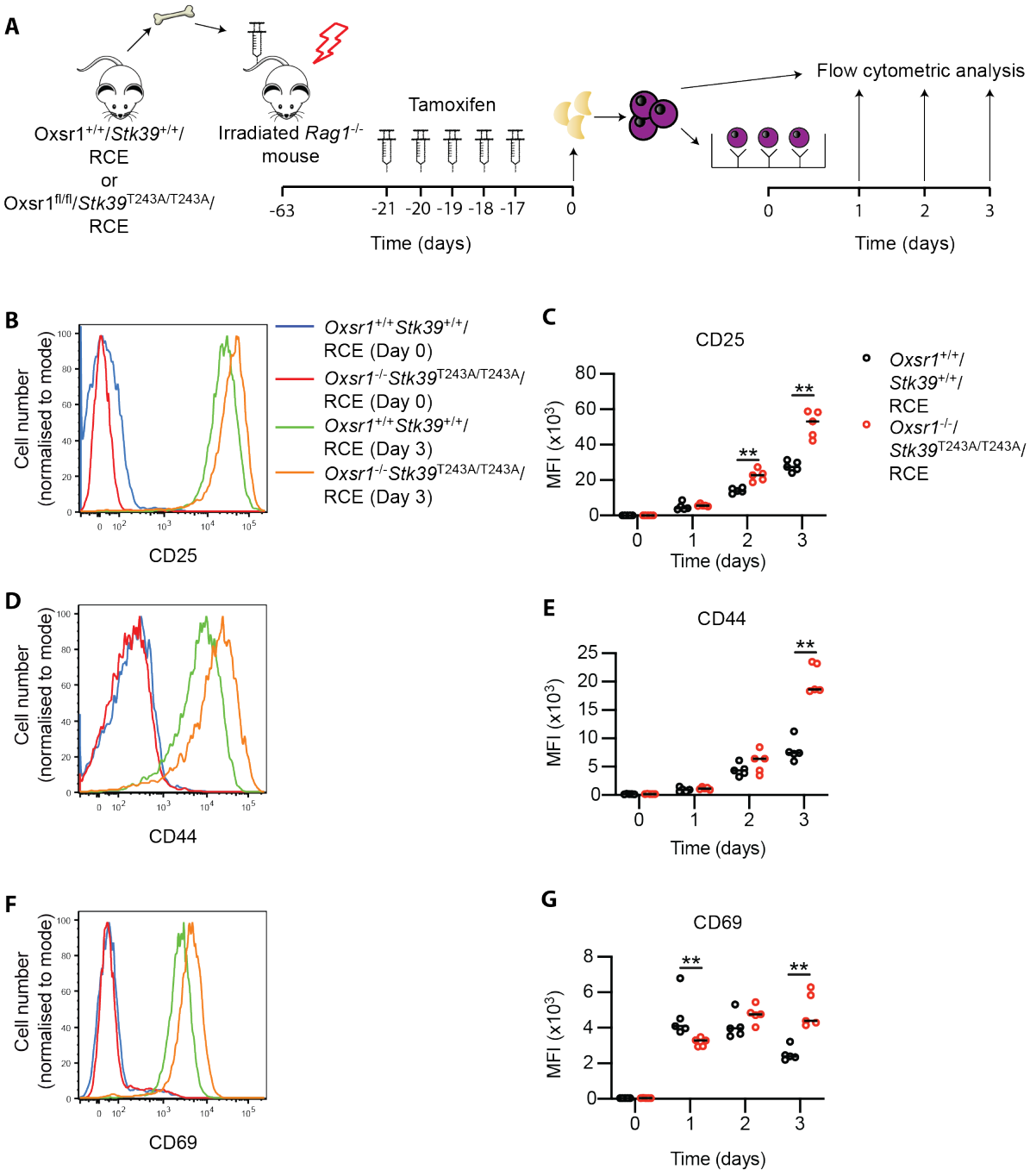

Figure 25. OXSR1 and STK39 are required for normal activation marker expression during activation *in vitro*. (**A**) Experimental design: *Oxsr1*$^{+/+}$/*Stk39*$^{+/+}$/RCE or *Oxsr1*$^{-/-}$/*Stk39*$^{T243A/T243A}$/RCE T cells were generated as described in Chapter **Error! Reference s ource not found.**. Naïve CD4^{+} T cells (CD25^{lo}/CD44^{lo}) were isolated from lymph nodes and cultured on plate-bound anti-CD3 and anti-CD28 antibodies. Data shown from live, single, CD4^{+} T cells. (**B-G**) Surface expression levels of CD25 (B, C), CD44 (D, E) and CD69 (F, G) on *Oxsr1*$^{+/+}$/*Stk39*$^{+/+}$/RCE and *Oxsr1*$^{-/-}$/*Stk39*$^{T243A/T243A}$/RCE CD4^{+} T cells at indicated time points showing example histograms (B, D, F) and graphs (C, E, G) of the median florescent intensity (MFI) (n=5). Each point represents a single mouse; horizontal lines show median. Data from 1 experiment representative of 2 experiments. Statistical analysis carried out using Mann-Whitney U test. * 0.01 < p < 0.05; ** 0.001 < p < 0.01.

It is tempting to hypothesise that suppression of activation marker expression is therefore, at least in part, mediated by net ion influx into the cell through SLC12A-family ion transporters, which are substrates of OXSR1 and STK39. However, further experiments in which the activities of these transporters are manipulated would be needed to confirm this hypothesis. Additionally, it would be interesting to investigate whether an additional non-canonical, OXSR1/STK39-independent pathway downstream of WNK1 contributes to the regulation of activation marker expression as this could explain the difference in the severity of the *Oxsr1*$^{-/-}$/*Stk39*$^{T243/T243}$/RCE and *Wnk1*$^{-/-}$/RCE phenotypes.

4.5 WNK1 supresses cytokine expression *in vitro*

Cytokine secretion is a key characteristic of CD4^{+} T cell activation and is required for many aspects of an immune response including clonal expansion and differentiation of lymphocytes, class-switching by B lymphocytes and regulation of innate immune cell function. To analyse the expression and secretion of cytokines by *Wnk1*$^{-/-}$/RCE CD4^{+} T cells during activation *in vitro* I used RT-qPCR and Luminex assays to measure the amounts of cellular *Il-2* RNA and cytokine protein secreted into the cell culture medium, respectively (Figure 26A). *Wnk1*$^{-/-}$/RCE CD4^{+} T cells expressed elevated levels of *Il2* RNA relative to controls from day 1 of activation *in vitro* (Figure 26B). At day 3 expression was ~10-fold higher showing that these cells were capable of increasing cytokine gene expression and that WNK1 is required to supress *Il2* transcription. This increase in *Il2* gene transcription was reflected by an increase in IL-2 protein secreted into the cell culture medium (Figure 26C) showing that both transcription, translation and secretion of this protein was increased in *Wnk1*$^{-/-}$/RCE CD4^{+} T cells.

Wnk1$^{-/-}$/RCE CD4^{+} T cells also secreted elevated levels of IL-4, IL-18 and TNFα into the cell culture media (Figure 26D-F) showing that WNK1 is also required to supress the expression/secretion of these cytokines. It is tempting to speculate that these increases in cytokine secretion were also due to an increase in the transcription of these genes, although further analysis of cellular RNA content would be needed to conclude this. IFNγ abundance was significantly increased in *Wnk1*$^{-/-}$/RCE CD4^{+} T cell media at day 1 relative to controls, however this difference between the genotypes was not maintained across day 2 and 3 *in vitro* (Figure 26G). This

suggests that the suppression of cytokine expression by WNK1 could be restricted to a certain subset of cytokines.

Measuring total cytokine concentration in the cell culture medium is not an ideal measure of expression as the amount of cytokine produced per cell cannot be calculated. In Chapter 4.7 I show that that *Wnk1*$^{-/-}$/RCE CD4^{+} T cells have reduced proliferation and survival when compared to *Wnk1*$^{+/-}$/RCE CD4^{+} T cells and are therefore present in lower numbers by day 2 *in vitro*. This means that *Wnk1*$^{-/-}$/RCE CD4^{+} T cells actually expressed higher levels of cytokine on a per cell basis than that represented in Figure 26. Staining and detection of intracellular cytokine would be required to measure cytokine expression on a per cell basis. The *in vitro* activation system used in these experiments is also not ideal to measure cytokine expression because cytokine expression *in vivo* is determined by the CD4+ T cell subset, which is in turn determined by the cytokine environment already present in the mouse tissue that the CD4+ T cells are activated in. This cytokine environment is of course not present *in vitro*. An analysis of cytokine expression by T cells in lymphoid tissues during an immune response would be required to address this issue.

Nevertheless, from these data I conclude that WNK1 supresses the expression of certain cytokines, including IL-2. An inability of *Wnk1*$^{-/-}$/RCE CD4^{+} T cells to express IL-2 is therefore unlikely to be the reason for the reduced proliferation exhibited by these cells.

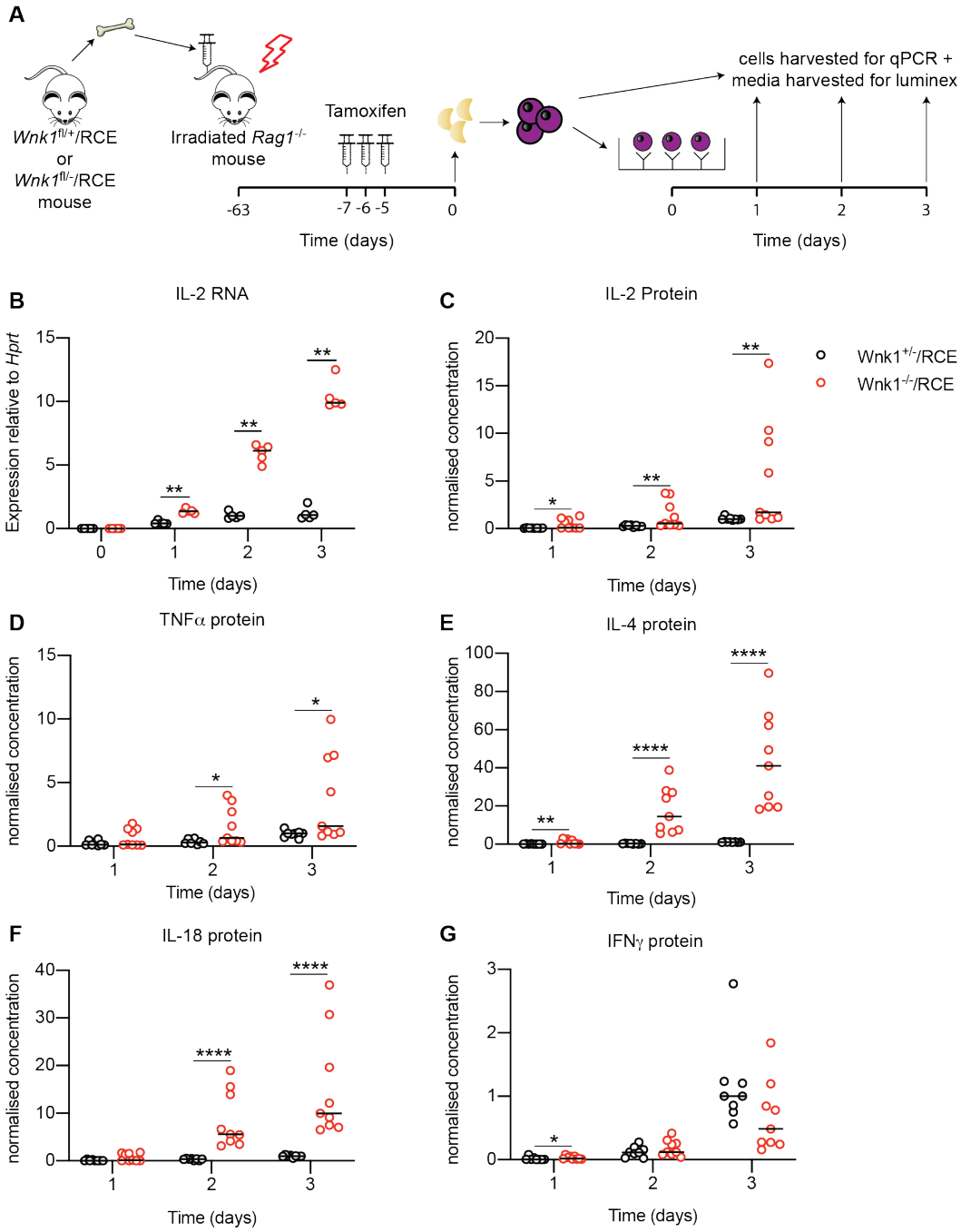

Figure 26. WNK1-deficient cells express and secrete elevated levels of cytokines during activation *in vitro* relative to controls. (**A**) Experimental design: *Wnk1*$^{+/-}$/RCE and *Wnk1*$^{-/-}$/RCE T cells were generated as described in Chapter 3.1. Naïve CD4^{+} T cells (CD25^{lo}/CD44^{lo}) were isolated from lymph nodes and cultured on plate-bound anti-CD3 and anti-CD28 antibodies. Cells were collected at indicated timepoints and IL-2 RNA was quantified by RT-qPCR. Media was collected at the indicated time points and cytokine content was analysed by Luminex assay. (**B**) Expression of *Il2* mRNA relative to the amount of *Hprt* mRNA in cells at the indicated time points (n=5). (**C-G**) Amount of IL-2 (C), IFNγ (D), IL-4 (E), IL-18 (F), and TNFα (G) protein in media at the indicated time points (n=8-9). Values normalised to median of *Wnk1*$^{+/-}$/RCE cells at day 3 (set to 1). Each point represents a single mouse; horizontal lines show median. Data from one experiment representative of 2 independent experiments (B) or pooled from 2 independent experiments (C-G). Statistical analysis carried out using Mann-Whitney U test. * 0.01 < p < 0.05; ** 0.001 < p < 0.01; ***0.0001<p<0.001; ****p<0.0001.

4.6 WNK1 is required for proliferation during activation *in vitro*

One of the likely reasons that WNK1-deficient T cells are unable to support an antigen-specific, class-switched antibody response is that they fail to undergo the rapid cell division required for clonal expansion in response to antigen. To further study this defect I sought to determine whether this phenotype could be recapitulated using an *in vitro* system for activation. Initially I used the co-culture system described in chapter 4.1 in which naïve OT-II $CD4^+$ T cell are cultured with bone-marrow derived APCs in the presence, or absence, of $OVA_{323-339}$ peptide (Figure 27A). OT-II T cells were labelled with CTV so that I could follow the number of divisions completed by each cell over time. *Wnk1*$^{-/-}$/OT-II/RCE cells had undergone fewer divisions than *Wnk1*$^{+/-}$/OT-II/RCE cells at day 3 and 5 and at all concentrations of $OVA_{323-339}$ (Figure 27B). This difference could be quantified by both a reduction in the percentage of cells that had undergone at least one division as well as a reduction in the proliferation index (Figure 27C-D). These data show that WNK1 is required for proliferation in response to antigen *in vitro*.

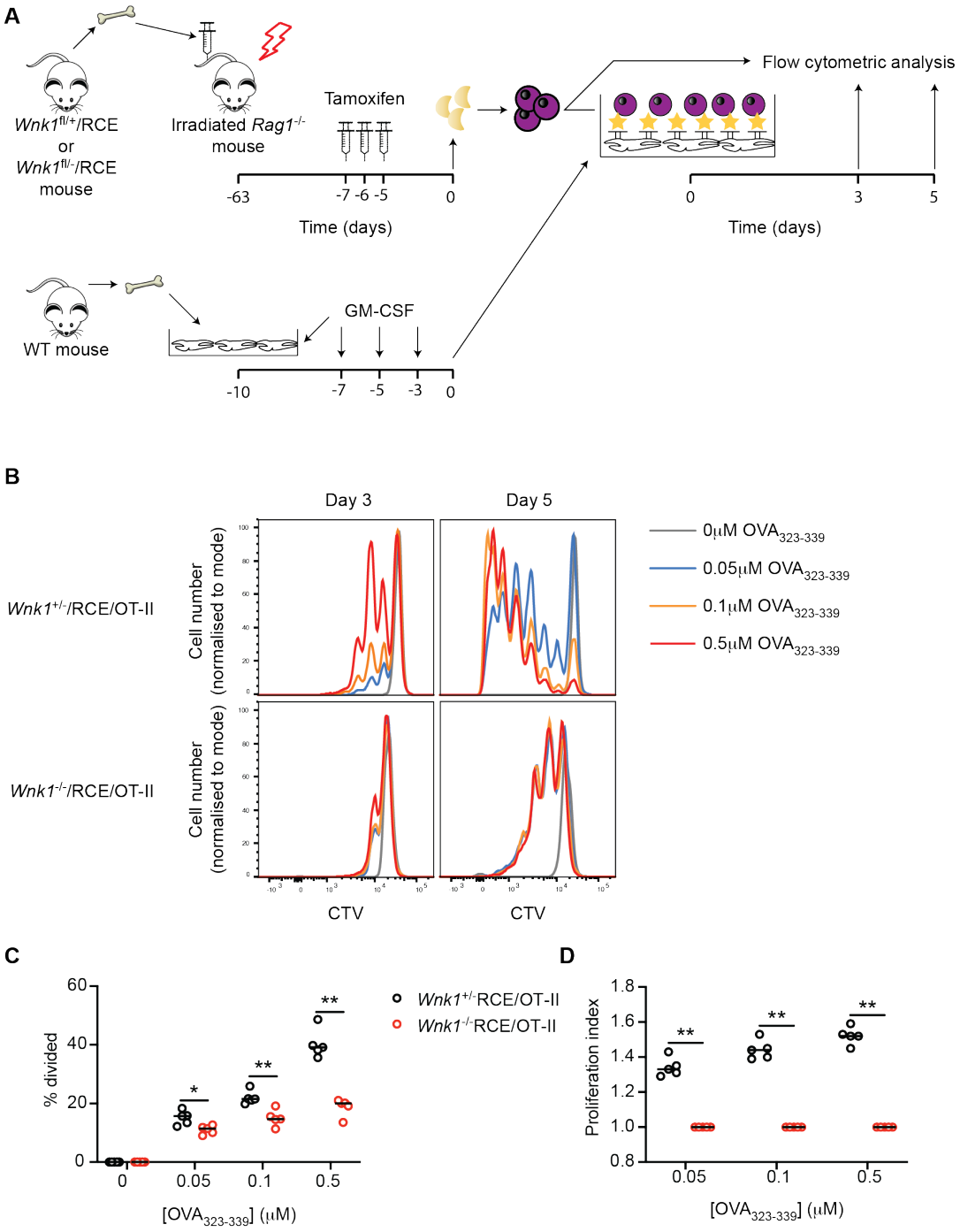

Figure 27. WNK1 is required for CD4⁺ T cell proliferation in response to antigen *in vitro*. (**A**) Experimental design: *Wnk1*$^{+/-}$/RCE/OT-II and *Wnk1*$^{-/-}$/RCE/OT-II T cells (CD45.1^{-}/CD45.2^{+}) were generated as described in Chapter 3.1. Naïve CD4^{+} T cells (CD25^{lo}/CD44^{lo}) were isolated from lymph nodes, stained with CTV, and co-cultured with GM-CSF-induced bone marrow-derived APCs in the presence of OVA$_{323-339}$ peptide. Data shown from live, single, CD11c^{-} CD4^{+} T cells. (**B**) CTV intensity as a measure of proliferation. (**C**) Percentage of OT-II cells that had divided at day 3 in the presence of indicated OVA$_{323-339}$ peptide concentrations (n=5). (**D**) Proliferation index (average number of divisions by dividing cells) of OT-II cells at day 3 in the presence of indicated OVA$_{323-339}$ peptide concentrations (n=5). Each point represents a single mouse; horizontal lines show median. Data from 1 experiment representative of 2 independent experiments. Statistical analysis carried out using Mann-Whitney U test. * 0.01 < p < 0.05; ** 0.001 < p < 0.01.

4.7 WNK1 kinase activity is required for CD4$^+$ T cell proliferation and survival during activation *in vitro* with anti-CD3 and anti-CD28 antibodies

In order to further characterise the requirement for WNK1 during CD4$^+$ T cell activation, I investigated whether proliferation phenotype of WNK1-deficient T cells could be recapitulated during activation *in* vitro with immobilised anti-CD3 and anti-CD28 antibodies. Naïve CD4$^+$ T cells were labelled with CTV prior to culturing in the presence of anti-CD3 and anti-CD28 antibodies in order to track the proliferation of individual cells over time (Figure 28A). *Wnk1*$^{-/-}$/RCE also proliferated less in response to this form of stimulation *in vitro* relative to *Wnk1*$^{+/-}$/RCE cells (Figure 28B). Similarly to antigen-dependent activation, this reduction in proliferation was due to a reduction in the percentage of *Wnk1*$^{-/-}$/RCE cells that have undergone at least one division as well as proliferation index (Figure 28C, D). These data showed that using anti-CD3 and anti-CD28 antibody-dependent activation *in vitro* it is possible to recapitulate the WNK1-deficient proliferation phenotype seen using antigen and APCs to stimulate T cells.

It was possible to remove the contribution of cell division from the total cell count at each timepoint by fitting a model to the CTV dilution profile and calculating the number of cells that would be present in the absence of division (Figure 28B). As shown in Figure 28E, there was a small but significant reduction in the number of *Wnk1*$^{-/-}$/RCE cells at day 3 relative to *Wnk1*$^{+/-}$/RCE samples if no proliferation had taken place showing that WNK1 is required for survival as well as proliferation *in vitro*. The use of this *in vitro* activation system allowed me to explicitly show that *Wnk1*$^{-/-}$/RCE cells exhibited a small survival defect and from this it is tempting to hypothesise that WNK1-dependent survival also plays a role during immune responses *in vivo*.

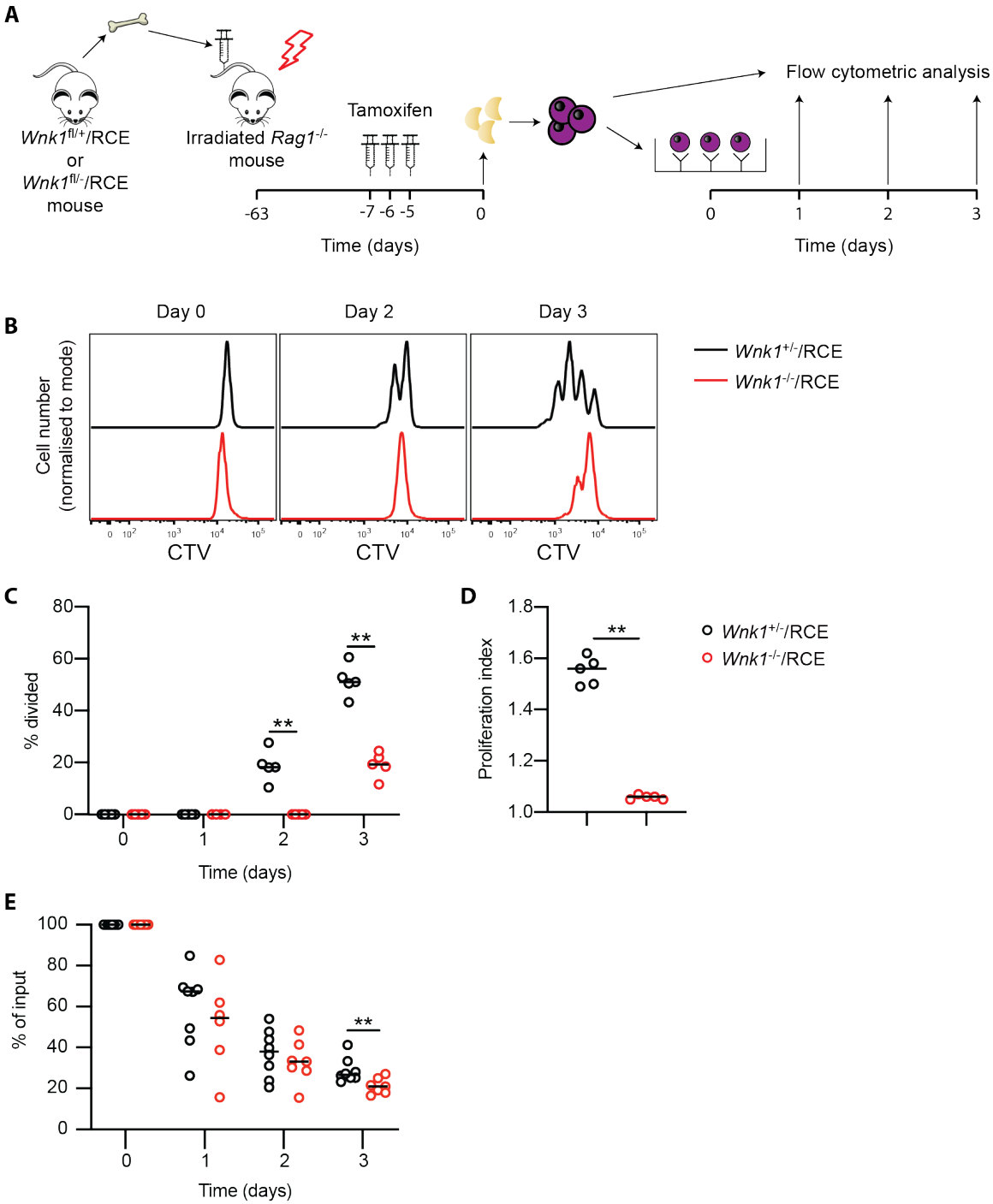

Figure 28. WNK1 is required for CD4+ T cell proliferation and survival in response to TCR and CD28 cross-linking in vitro. (**A**) Experimental design: *Wnk1*$^{+/-}$/RCE and *Wnk1*$^{-/-}$/RCE T cells were generated as described in Chapter 3.1. Naïve CD4+ T cells (CD25lo/CD44lo) were isolated from lymph nodes and cultured on plate-bound anti-CD3 and anti-CD28 antibodies. Data shown from live, single, CD4+ T cells. (**B**) CTV intensity as a measure of proliferation. (**C**) Percentage of Wnk1+/-/RCE and Wnk1-/-/RCE cells that had divided at the indicated timepoints (n=5). (**D**) Proliferation index (average number of divisions by dividing cells) of Wnk1+/-/RCE and Wnk1-/-/RCE cells at day 3 (n=5). (**E**) Cell number (as a percentage of the input population) adjusted to remove the effect of proliferation. Each point represents a single mouse; horizontal lines show median. Data pooled from 2 independent experiments (E) or from 1 experiment representative of 3 independent experiments (B-D). Statistical analysis carried out using Mann-Whitney U test. * $0.01 < p < 0.05$; ** $0.001 < p < 0.01$.

In order to determine whether WNK1 kinase activity is required for proliferation *in vitro* I used cells expressing a kinase dead form of WNK1 (*Wnk1*^{D368A}) (Figure 29A). *Wnk1*$^{D368A/-}$/RCE cells exhibited a reduction in proliferation equivalent to that shown by *Wnk1*$^{-/-}$/RCE during activation *in vitro* (Figure 29B-D). This allowed me to conclude that WNK1 kinase activity is required for CD4^{+} T cell proliferation *in vitro*.

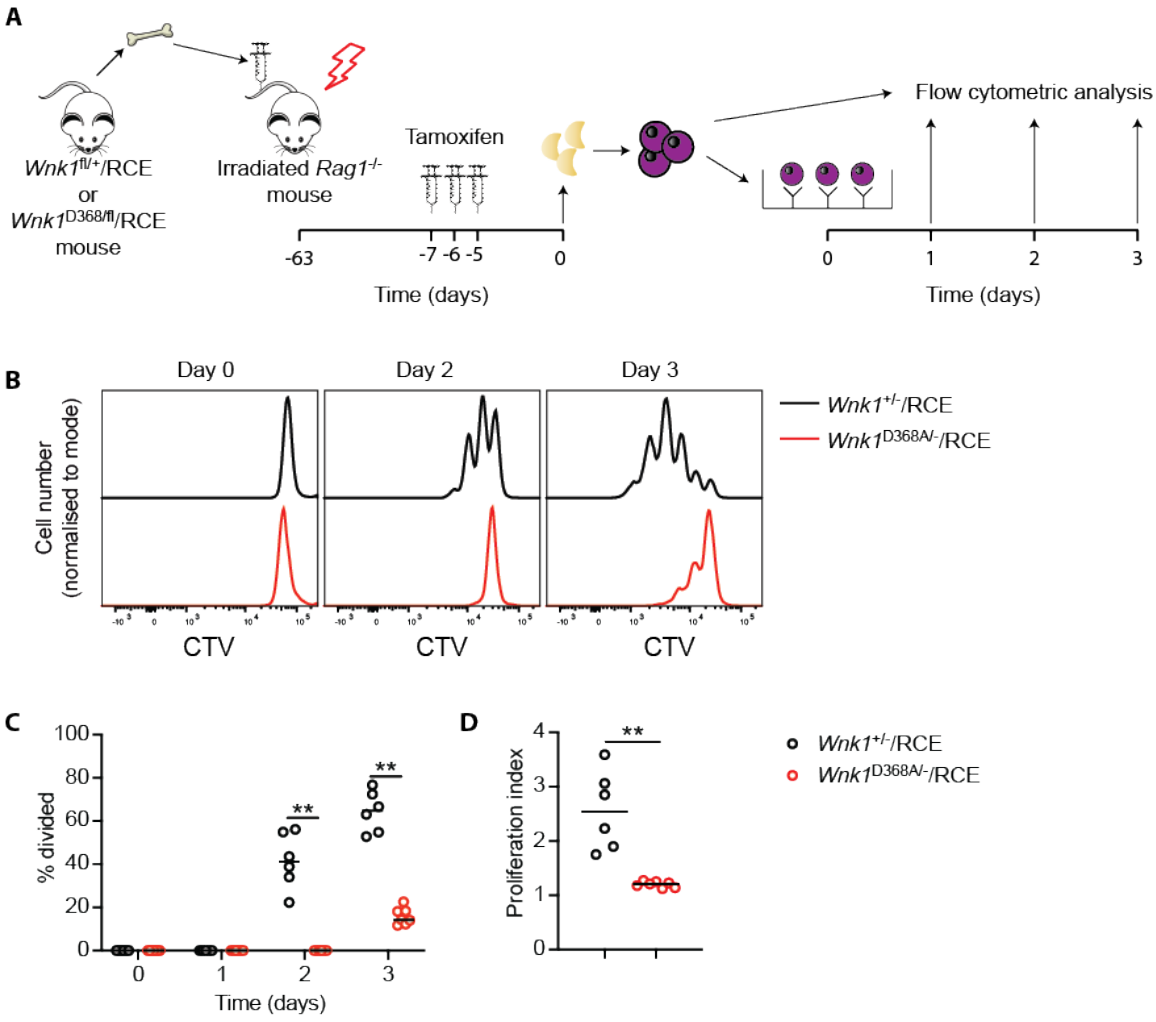

Figure 29. WNK1 kinase activity is required for CD4^{+} T cell proliferation during activation *in vitro*. (**A**) Experimental design: *Wnk1*$^{+/-}$/RCE and *Wnk1*$^{D368A/-}$/RCE T cells were generated as described in Chapter 3.1. Naïve CD4^{+} T cells (CD25^{lo}/CD44^{lo}) were isolated from lymph nodes and cultured on plate-bound anti-CD3 and anti-CD28 antibodies. Data shown from live, single, CD4^{+} T cells. (**B**) CTV intensity as a measure of proliferation. (**C**) Percentage of *Wnk1*$^{+/-}$/RCE and *Wnk1*$^{D368A/-}$/RCE cells that had divided at the indicated timepoints (n=5-7). (**D**) Proliferation index (average number of divisions by dividing cells) of *Wnk1*$^{+/-}$/RCE and *Wnk1*$^{D368A/-}$/RCE cells at day 3 (n=6-7). Each point represents a single mouse; horizontal lines show median. Data pooled from 2 independent experiments. Statistical analysis carried out using Mann-Whitney U test. * $0.01 < p < 0.05$; ** $0.001 < p < 0.01$.

The proliferative defect of *Wnk1*$^{-/-}$/RCE and *Wnk1*$^{D368A/-}$/RCE T cells may be due to the extended absence of WNK1 activity these cells experience *in vivo* prior to culture *ex vivo*. To exclude this possibility, I activated cells in the presence of the pan-WNK inhibitor – WNK463 (Figure 30A). As naïve CD4^{+} T cells do not express WNK isoforms other than WNK1 this inhibitor could be used to specifically inhibit WNK1 in an acute fashion *in vitro*. CD4^{+} T cells activated in the presence of WNK463 exhibited a reduction in proliferation equivalent to that observed in *Wnk1*$^{-/-}$/RCE and *Wnk1*$^{D368A/-}$/RCE cells (Figure 30B-D). Taken together these data showed that WNK1 kinase activity is acutely required for CD4^{+} T cell proliferation during activation *in vitro* and that the WNK1-deficient proliferation phenotype can be recapitulated by activating cells *in vitro* using anti-CD3 and anti-CD28 antibodies in the presence of WNK463.

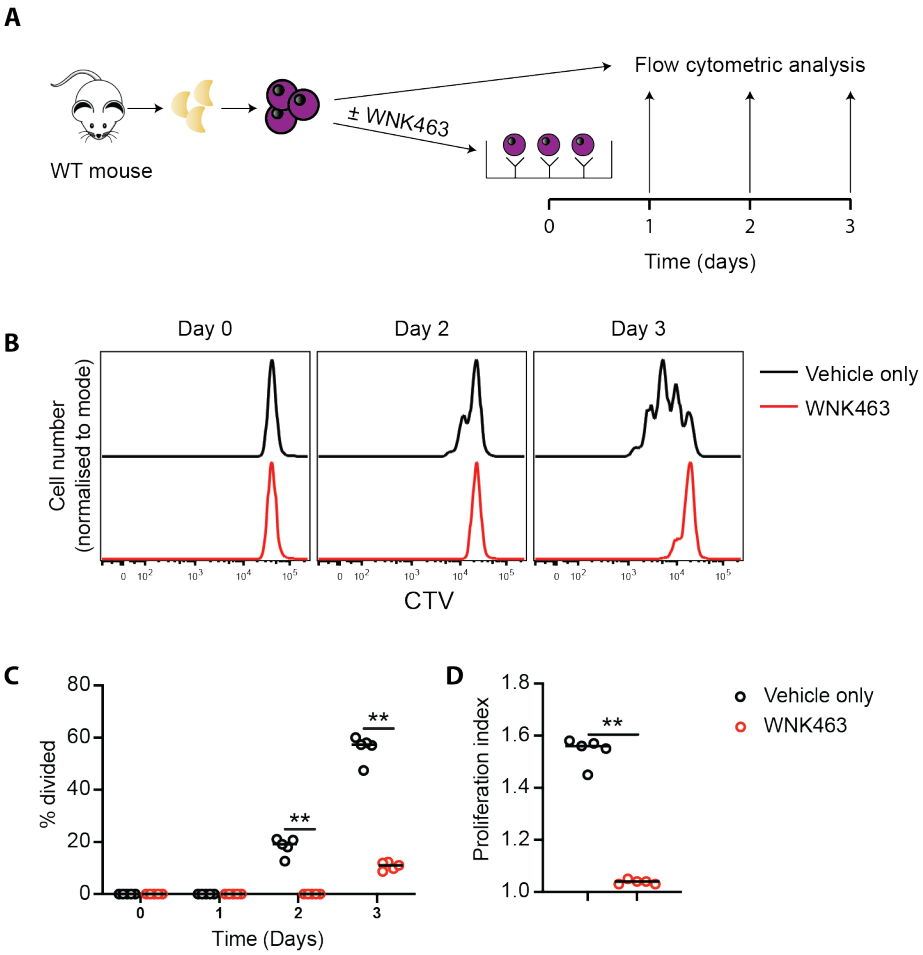

Figure 30. WNK1 kinase activity is acutely required for CD4$^+$ T cell proliferation during activation *in vitro*. (**A**) WT Naïve CD4$^+$ T cells (CD25^{lo}/CD44^{lo}) were isolated from lymph nodes and cultured on plate-bound anti-CD3 and anti-CD28 antibodies in the presence of vehicle only or WNK463. Data shown from live, single, CD4$^+$ T cells. (**B**) CTV intensity as a measure of proliferation. (**C**) Percentage of vehicle only- or WNK463-treated cells that had divided at the indicated timepoints (n=5). (**D**) Proliferation index (average number of divisions by dividing cells) of vehicle only- or WNK463- treated cells at day 3 (n=5). Each point represents a single mouse; horizontal lines show median. Data from 1 experiment representative of 2 independent experiments. Statistical analysis carried out using Mann-Whitney U test. * $0.01 < p < 0.05$; ** $0.001 < p < 0.01$.

4.8 OXSR1- and STK39-dependent signalling is required for CD4$^+$ T cell proliferation during activation *in vitro*

Immediately downstream of WNK1 kinase activity are the OXSR1 and STK39 kinases. As discussed in Chapter 1.11.1 these kinases regulate the activity of numerous ion transporters at the plasma membrane. In order to investigate the role of these kinases in CD4$^+$ T cell proliferation *in vitro*, I activated cells carrying the *Oxsr1*^{fl}, RCE and *Stk39*^{T243A} alleles using plate-bound anti-CD3 and anti-CD28 antibodies (Figure 31A). These cells exhibited a reduction in proliferation both at the level of proliferation index and the percentage of cells undergoing division when compared to *Oxsr1*$^{+/+}$/*Stk39*$^{+/+}$/RCE cells (Figure 31B-D). When compared to *Wnk1*$^{-/-}$/RCE and *Wnk1*$^{D368A/-}$/RCE T cells however, the proliferation defect was not as severe. In contrast to WNK1-deficient T cells, a proportion of *Oxsr1*$^{-/-}$/*Stk39*$^{T243A/T243A}$/RCE T cells underwent division by day 2 *in vitro*. *Oxsr1*$^{-/-}$/*Stk39*$^{T243A/T243A}$/RCE cells also completed more divisions on average at day 3 than *Wnk1*$^{-/-}$/RCE or *Wnk1*$^{D368A/-}$/RCE cells. The reduced proliferation of *Oxsr1*$^{-/-}$/*Stk39*$^{T243A/T243A}$/RCE cells showed that OXSR1 and/or STK39 are required for proliferation during activation *in vitro* and suggested that WNK1 may signal via the canonical OXSR1-STK39 pathway to positively regulate proliferation during activation *in vitro*. The partial phenotype exhibited by *Oxsr1*$^{-/-}$/*Stk39*$^{T243A/T243A}$/RCE cells may suggest that WNK1 also signals via another non-canonical, OXSR1/STK39-independent pathway to regulate this process. However, from these data it is once again impossible to rule out the possibility that the partial phenotype is due to the longer period of time in which the canonical signalling pathway is absent from *Oxsr1*$^{-/-}$/*Stk39*$^{T243A/T243A}$/RCE cells (21 d) compared to *Wnk1*$^{-/-}$/RCE or *Wnk1*$^{D368A/-}$/RCE cells (7 d). Ideally a specific inhibitor would be used to acutely inhibit OXSR1 and STK39 activity to allow for a direct comparison between the proliferative capacity of OXSR1/STK39-inhibited and WNK1-inhibited cells. STOCK1S-50699 could be used for this purpose as it abolishes OXSR1 and STK39 activity by inhibiting interactions between the C-terminal domain of these proteins and WNK1 as well as downstream proteins (de Los Heros et al., 2014a).

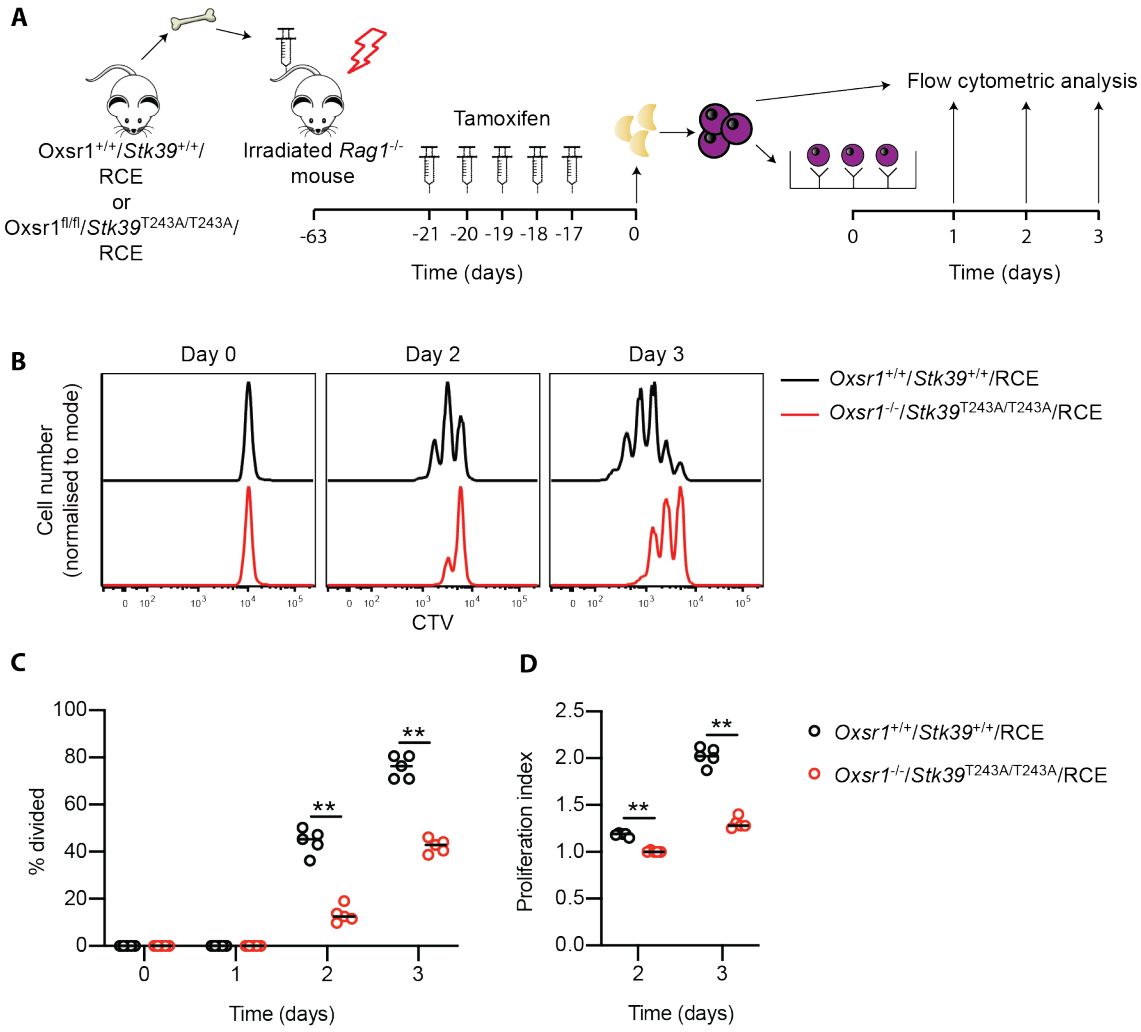

Figure 31. Cells harbouring mutations in *Oxsr1* and *Stk39* mimic the proliferation defect exhibited by WNK1-deficient cells during activation *in vitro*. (**A**) Experimental design: *Oxsr1*$^{+/+}$/*Stk39*$^{+/+}$/RCE or *Oxsr1*$^{-/-}$/*Stk39*$^{T243A/T243A}$/RCE T cells were generated as described in Chapter **Error! Reference source not found.**. Naïve CD4^{+} T cells (CD25^{lo}/CD44^{lo}) were isolated from lymph nodes and cultured on plate-bound anti-CD3 and anti-CD28 antibodies. Data shown from live, single, CD4^{+} T cells. (**B**) CTV intensity as a measure of proliferation. (**C**) Percentage of *Oxsr1*$^{+/+}$/*Stk39*$^{+/+}$ and *Oxsr1*$^{-/-}$/*Stk39*$^{T243A/T243A}$/RCE cells that had divided at the indicated timepoints (n=?). (**D**) Proliferation index (average number of divisions by dividing cells) of *Oxsr1*$^{+/+}$/*Stk39*$^{+/+}$ and *Oxsr1*$^{-/-}$/*Stk39*$^{T243A/T243A}$/RCE cells at day 3 (n=5). Each point represents a single mouse; horizontal lines show median. Data from 1 experiment representative of 2 independent experiments. Statistical analysis carried out using Mann-Whitney U test. * 0.01 < p < 0.05; ** 0.001 < p < 0.01; ***0.0001<p<0.001; ****p<0.0001.

Chapter 5. WNK1 is required for TCR signalling and cell cycle progression

Having found that WNK1 is required for $CD4^+$ T cell proliferation I investigated its role in more detail during early TCR signalling events and during progression through individual phases of the cell cycle.

5.1 WNK1 is required for entry into G1 during activation *in vitro*

In order to further investigate how WNK1 regulates proliferation I endeavoured to determine the requirement for WNK1 during progression through the different phases of the cell cycle using the *in vitro* activation system (Figure 32A). Naïve $CD4^+$ T cells are quiescent and reside in the G0 phase of the cell cycle. TCR and costimulation signalling induces the activity of the CDK6/4-cyclin D2 complex which mediates the transition into the G1 phase of the cell cycle (Lea et al., 2003). Ki67 expression is increased during the transition between G0 and G1 and maintained at a high level throughout the S, G2 and M phases of the cell cycle. It plays a role in heterochromatin organisation during interphase and prevents condensed chromosome aggregation during mitosis, however in this study we will use it as a marker for cell cycle entry (Sun and Kaufman, 2018).

The frequency of Ki67+ cells during activation *in vitro* is dependent on the number of cells entering the cell cycle from G0, the number of cells undergoing division, and the relative viability of Ki67- and Ki67+ populations. By fitting a model to the CTV dilution profile of cell populations at each time point, an example of which is shown in Figure 28B, it was possible to calculate the proportion of Ki67+ cells in each population in the absence of cell division.

After adjusting for proliferation there was a reduced frequency of Ki67+ *Wnk1*$^{-/-}$/RCE cells at day 1 and 2 during activation *in vitro* compared to controls (Figure 32B, C). This difference was unlikely to be due to any effects of WNK1 on viability because *Wnk1*$^{-/-}$/RCE cell numbers are normal at these timepoints during activation *in vitro* (Figure 28E). These data therefore showed that *Wnk1*$^{-/-}$/RCE cells enter the cell cycle in a delayed manner. This can at least in part explain the reduced proliferation exhibited by *Wnk1*$^{-/-}$/RCE cells following TCR and CD28 costimulation. By day 3

however, the frequency of Ki67+ cells was equivalent between the two genotypes. From these observations I can conclude that WNK1 positively regulates entry into the cell cycle but is not absolutely required for this process.

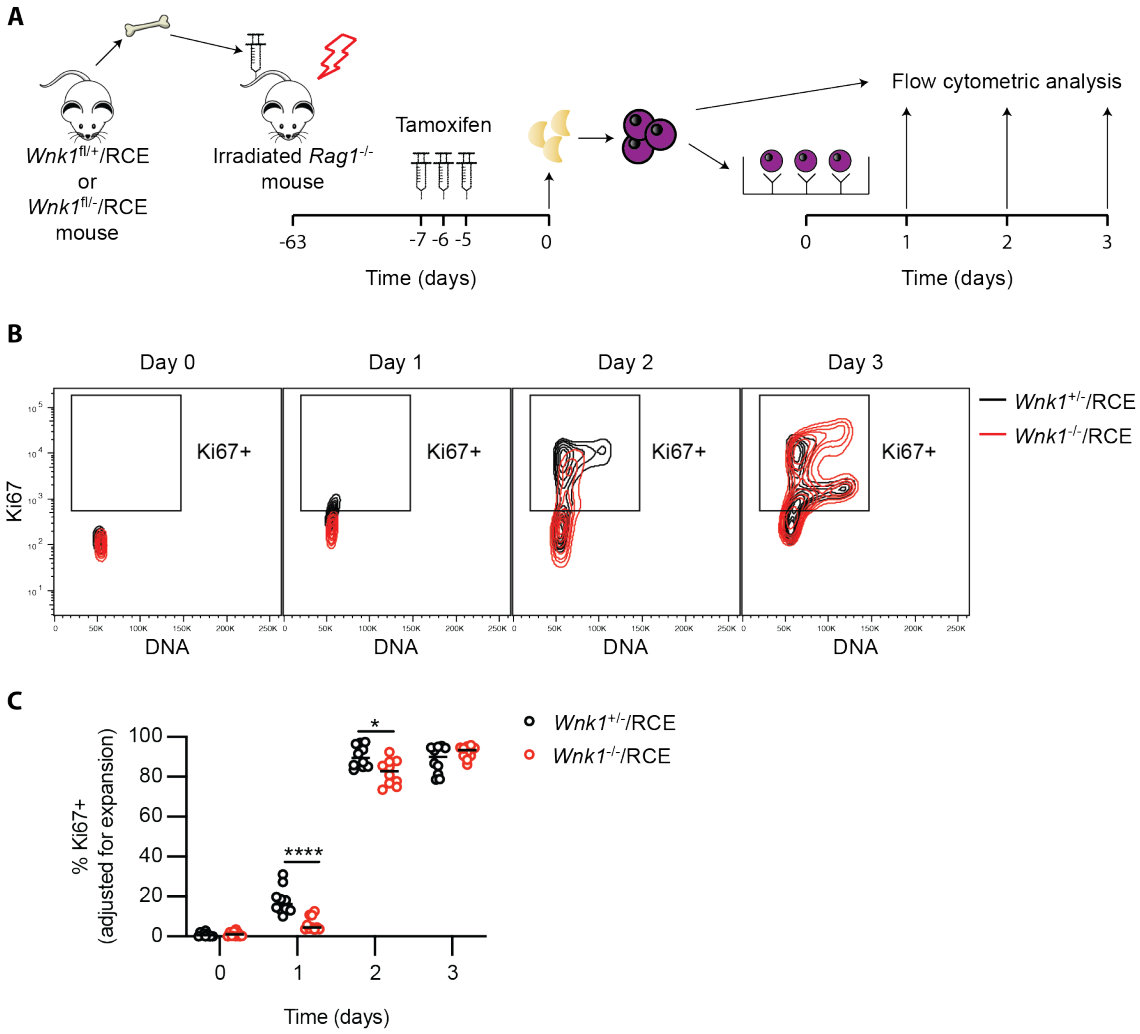

Figure 32. WNK1-deficient cells exhibit delayed entry into G1 during activation *in vitro*. (**A**) Experimental design: *Wnk1*$^{+/-}$/RCE and *Wnk1*$^{-/-}$/RCE T cells were generated as described in Chapter 3.1. Naïve CD4^{+} T cells (CD25^{lo}/CD44^{lo}) were isolated from lymph nodes and cultured on plate-bound anti-CD3 and anti-CD28 antibodies. Data shown from live, single, CD4^{+} T cells. (**B**) Density plots of Ki67 expression vs DNA content of *Wnk1*$^{+/-}$/RCE and *Wnk1*$^{-/-}$/RCE cells at indicated time points. (**C**) Percentage of *Wnk1*$^{+/-}$/RCE and *Wnk1*$^{-/-}$/RCE cells that were Ki67+ cells at the indicated time points adjusted to remove the effect of proliferation (n=10). Each point represents a single mouse; horizontal lines show median. Data pooled from 2 independent experiments. Statistical analysis carried out using Mann-Whitney U test. * 0.01 < p < 0.05; ** 0.001 < p < 0.01; ***0.0001<p<0.001; ****p<0.0001.

5.2 WNK1-dependent osmoregulation is required for TCR signalling

G1 entry by $CD4^+$ T cells is induced by TCR and costimulation signalling, in particular via ERK and mTORC1 pathways. I investigated whether TCR signalling is intact in WNK463-treated $CD4^+$ T cells in response to TCR cross-linking using soluble antibodies (Figure 33A). I used a flow cytometry-based method to measure phosphorylation of CD3ζ (Y142), ZAP-70 (Y319), ERK1 (T202/Y204) and ERK2 (T185/Y187) in order to assess upstream and downstream signalling events. (For the purposes of clarity phosphorylated residues will be referred to by their position in human proteins.) I found that treatment of $CD4^+$ T cells with the WNK463 inhibitor had no effect on TCR/CD28-induced CD3ζ (Y142) phosphorylation (p-CD3ζ) but ZAP-70 (Y319) phosphorylation (p-ZAP-70) was reduced compared to controls (Figure 33B-E). These data suggested that WNK1 positively regulates ZAP-70 Y319 phosphorylation in response to TCR activation. However, this conclusion needs to be verified by using *Wnk1*$^{D368A/-}$/RCE cells and an immunoblot-based detection method to exclude the possibility that the observed defects are due to off-target effects of WNK463 or to artefacts of the flow cytometry-based method. Indeed, an inducible p-CD3ζ signal could be detected in SRCi-treated samples suggesting that the anti-p-CD3ζ (Y142) antibody may not be specific. Alternatively, SRC inhibition could have been incomplete or CD3ζ could have been phosphorylated at Y142 in an SRC-independent manner. ERK1 (T202/Y204) and ERK2 (Y185/Y187) phosphorylation (p-ERK) was also reduced in WNK463-treated cells compared to control cells (Figure 33F, G). This was likely to be, at least in part, due to the defective signalling at the level of ZAP-70 Y319 phosphorylation. The difference in p-ERK levels between WNK463+SRCi-treated and SRCi-treated cells may have been due to a positive regulatory role of WNK1 on SRC-independent ERK phosphorylation. Alternatively, the presence of WNK463 could have lead to differences in non-specific background staining.

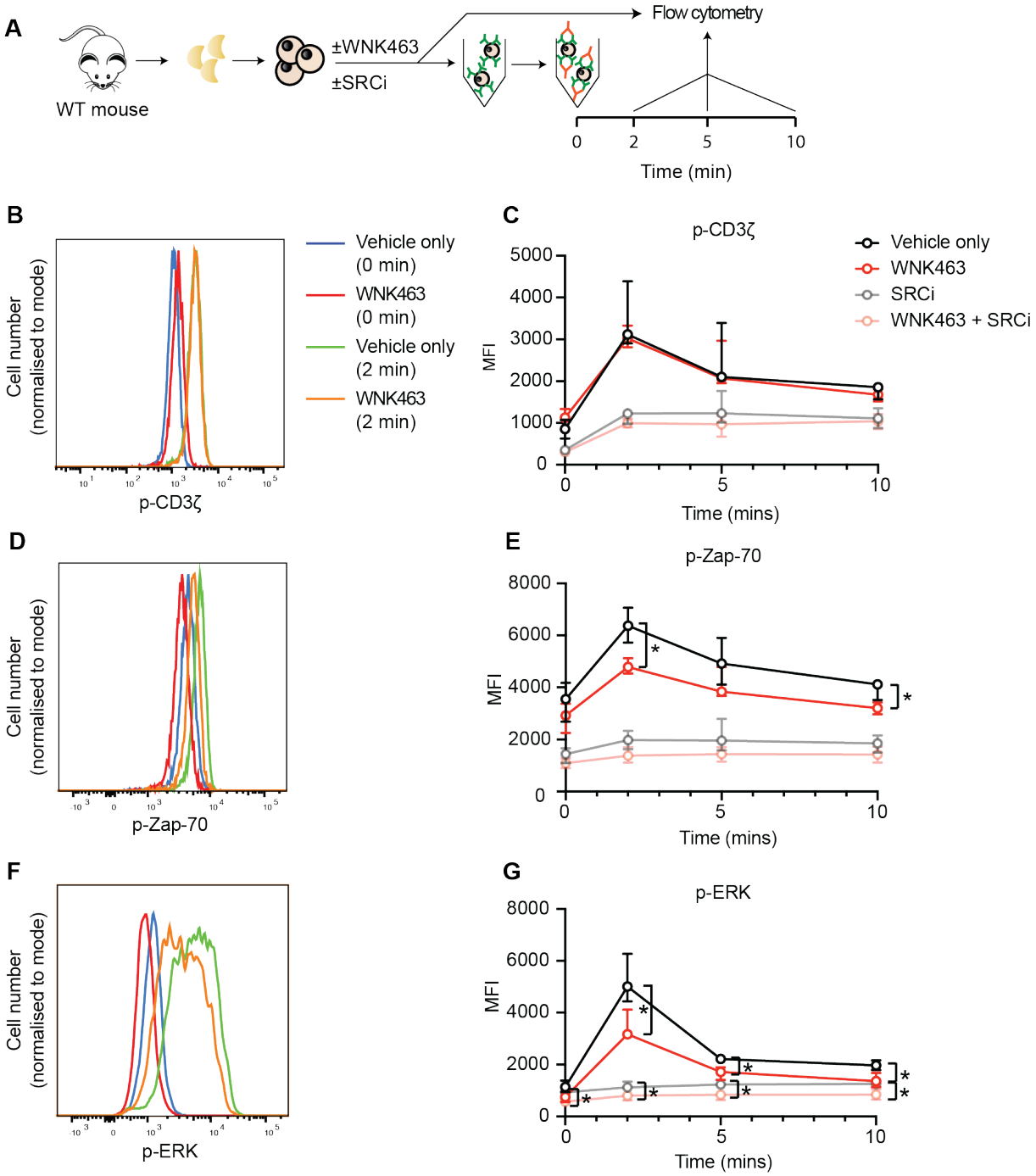

Figure 33. CD4$^+$ T cells treated with WNK463 exhibit defective TCR signalling. (**A**) WT Naïve CD4$^+$ T cells (CD25^{lo}/CD44^{lo}) were isolated from lymph nodes, rested for 60 min at 37°C, and incubated with anti-CD3 and anti-CD28 antibodies in the presence of indicated combinations of vehicle only, WNK463 or SRCi for 30 min at 4°C. Cells were then washed, warmed to 37°C, and stimulated using cross-linking antibody (± inhibitors). Data shown from single, CD4$^+$ T cells. (**B**-**G**) Amount of p-CD3ζ (B, C), p-ZAP-70 (D, E) and p-ERK (F, G) after stimulation for the indicated times and in the presence of indicated inhibitors showing example histograms (B, D, F) and graphs (C, E, G) of median fluorescence intensity (MFI, n=4). Each data point represents the median±95% confidence interval of MFI. Data pooled from 2 independent experiments. Statistical analysis carried out using the Mann-Whitney U test. * 0.01 < p < 0.05.

I measured p-ERK levels in $CD4^+$ T cells expressing a kinase-dead mutant of WNK1 (D368A) in order to determine whether defective TCR signalling in the presence of WNK463 was due to off-target effects of the inhibitor. Plate-bound anti-CD3 and anti-CD28 antibodies were used to activate the *Wnk1*$^{D368A/-}$/RCE $CD4^+$ T cells for 1 h to investigate whether the TCR signalling defect persisted for periods longer than 10 min and to recapitulate the activation conditions under which the other WNK1-deficient phenotypes were found (Figure 34A).

A lower frequency of *Wnk1*$^{D368A/-}$/RCE cells had high levels of p-ERK after 1 h of stimulation with plate-bound anti-CD3 and anti-CD28 antibodies (Figure 34B, C). This showed that WNK1 kinase activity is required for TCR-dependent ERK activation. The specificity of the anti-p-ERK antibody was tested by the addition of a MEK inhibitor (MEKi) to the media to block ERK phosphorylation downstream of TCR activation. No p-ERK signal was observed in cells activated in the presence of MEKi. This was consistent with the anti-p-ERK antibody being specific (Figure 34B, C).

As discussed in Chapter 1.11.1, the most well characterised kinase-dependent function of WNK1 is to maintain osmotic homeostasis across the plasma membrane, and activation of WNK1 results in the net influx of Na^+, K^+ and Cl^- ions and water into the cell. Therefore, we hypothesised that a reduction in water influx, or a net efflux of water from the cell, may be responsible for the ERK signalling defect displayed by *Wnk1*$^{D368A/-}$/RCE cells. To test this, we activated these cells under hypotonic conditions (169mOsm/L) by lowering the concentration of NaCl in the medium, which resulted in a substantial increase in the frequency of *Wnk1*$^{D368A/-}$/RCE cells with high levels of ERK phosphorylation. The frequency of p-ERK+ *Wnk1*$^{+/-}$ /RCE cells also increased under these conditions but by a very small amount. This partial rescue of p-ERK levels in WNK1-deficient cells may be caused by the lowered osmolarity or by the reduced amount of NaCl in the medium. To distinguish between these two possibilities we activated the cells in an isotonic medium which had the same reduced levels of NaCl as the hypotonic medium, but osmolarity was made up to isotonic levels with L-glucose. L-glucose was used as a compensatory osmolyte as cells are specific for the D-stereoisomer of glucose and thus L-glucose is biologically inert. p-ERK signalling in *Wnk1*$^{D368A/-}$/RCE cells was not rescued when cells were activated under these conditions, demonstrating that the rescue of p-ERK levels was caused by the reduction in osmolarity not the reduced NaCl concentration (Figure 34C). Taken together these data showed that WNK1 kinase activity facilitates

TCR-dependent ERK activation, at least in part by controlling water movement across the cell membrane. The fact that the frequency of p-ERK+ *Wnk1*$^{D368A/-}$/RCE cells remained below the level of *Wnk1*$^{+/-}$/RCE cells during activation under hypotonic conditions suggested that WNK1 regulates other cellular processes required for TCR-dependent ERK activation. One known function of WNK1 that would not be compensated for by activation in hypotonic medium is the influx of ions into the cell, which may account for the incomplete rescue. It is also worth noting that WNK1-dependent osmoregulation may be temporally regulated during activation and reducing medium tonicity by a set amount for the entire activation process would not replicate such kinetics.

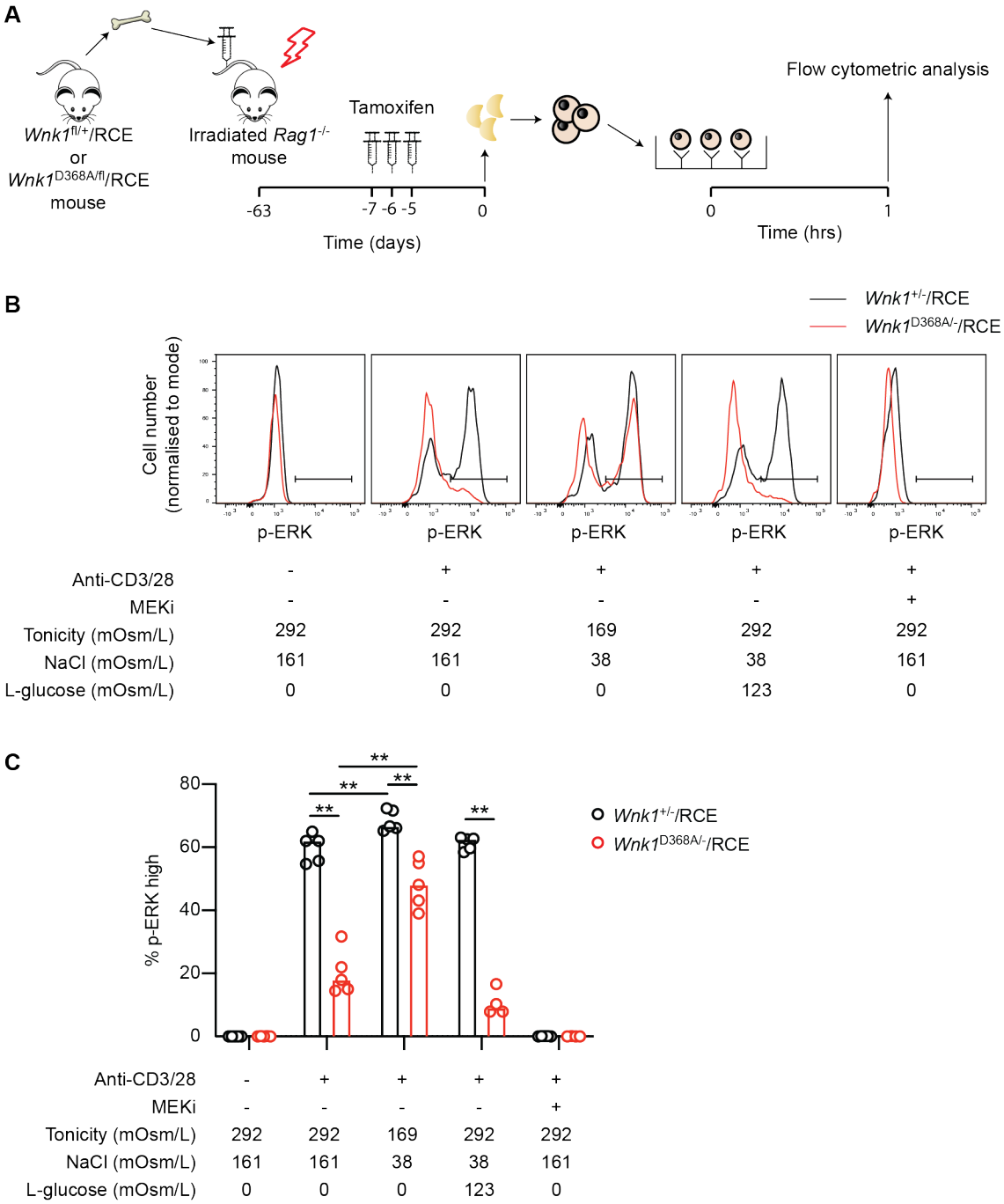

Figure 34. WNK-dependent water influx is required for TCR-dependent ERK activation. (A) Experimental design: *Wnk1*$^{+/-}$/RCE and *Wnk1*$^{D368A/-}$/RCE T cells were generated as described in Chapter 3.1. Naïve CD4^{+} T cells (CD25^{lo}/CD44^{lo}) were isolated from lymph nodes and cultured in the presence of immobilised anti-CD3 and anti-CD28 antibodies for 1 h. Data from single CD4^{+} T cells. (**B**) Histograms of p-ERK abundance in *Wnk1*$^{+/-}$/RCE and *Wnk1*$^{D368A/-}$/RCE cells activated in the indicated conditions. Gate used to identify p-ERK high cells is shown. (**C**) Percentage of *Wnk1*$^{+/-}$/RCE and *Wnk1*$^{D368A/-}$/RCE cells that were p-ERK high after activation in the indicated conditions (n=5). Each point represents a single mouse; horizontal lines show median. Data are from 1 experiment representative of 2 independent experiments. Statistical analysis carried out using Mann-Whitney U test. * 0.01 < p < 0.05; ** 0.001 < p < 0.01.

In order to determine whether WNK1 activity is acutely required for TCR-dependent ERK activation I measured the effect of WNK463 on ERK phosphorylation during T cell activation *in vitro* (Figure 35A). WNK463-treated $CD4^+$ T cells exhibited a ~6-fold reduction in p-ERK+ frequency compared to cells treated with vehicle only (Figure 35B, C). This reduction in ERK signalling could be completely rescued by activating these cells in hypotonic medium (169mOsm/L), containing 123mOsm/L less NaCl (Figure 35B, C). Activation of WNK463-treated cells in media where this missing NaCl had been replaced with L-glucose did not rescue the ERK signalling defect in WNK463-treated cells. These data showed that WNK1-dependent water homeostasis is acutely required for TCR-dependent ERK activation. The complete rescue of p-ERK signalling suggested that this is the only function of WNK1 required for TCR-dependent ERK activation. The discrepancies between experiments using WNK463-treated and *Wnk1*$^{D368A/-}$/RCE cells may be explained by the extended period in which *Wnk1*$^{D368A/-}$/RCE cells experience WNK1-deficiency *in vivo*, or to off-target effects of WNK463.

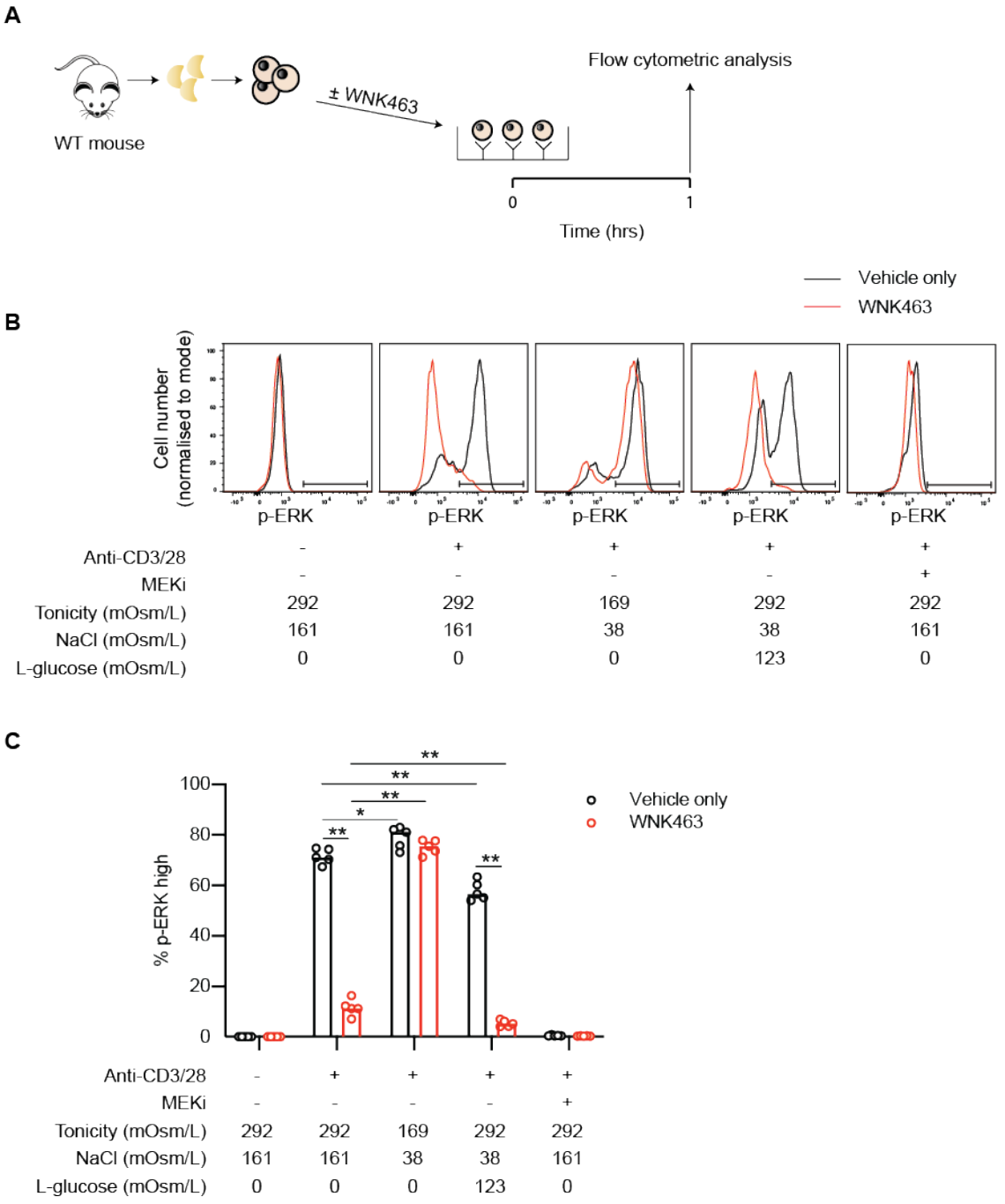

Figure 35. WNK1-dependent osmoregulation is acutely required for TCR-induced ERK activation. (**A**) WT Naïve CD4$^+$ T cells (CD25^{lo}/CD44^{lo}) were isolated from lymph nodes and cultured on plate-bound anti-CD3 and anti-CD28 antibodies in the presence of vehicle only or WNK463 for 1 h. Data from single, CD4$^+$ T cell population. (**B**) Histograms of p-ERK (Thr201/Tyr203) abundance in vehicle only- and WNK463-treated cells activated in the indicated conditions. Gate used to identify p-ERK high cells is shown. (**C**) Percentage of vehicle only- and WNK463-treated cells that were p-ERK high after activation in the indicated conditions (n=5). Each point represents a single mouse; horizontal lines show median. Data are from 1 experiment representative of 2 independent experiments. Statistical analysis carried out using Mann-Whitney U test. * $0.01 < p < 0.05$; ** $0.001 < p < 0.01$.

ERK and mTORC1 signalling pathways are critical for G1 entry during $CD4^+$ T cell activation. ERK activity induces phosphorylation of the S6 ribosomal protein at S235/236 via mTORC1 and RSK pathways (Figure 8). PI3K signalling via AKT is also able to induce S6 (S235/236) phosphorylation (p-S6) via the mTORC1 pathway in an ERK-independent manner. S6 phosphorylated at S235/236 (p-S6) can therefore be used as a measure of ERK and mTORC1 signalling flux. A MEK inhibitor (MEKi) and Rapamycin (Rapa), which inhibits mTORC1, were used to determine the contribution of individual pathways to S6 phosphorylation. The addition of both MEKi and Rapamycin blocked all p-S6 signal induced by TCR and CD28 stimulation showing that no other pathways contribute to this phosphorylation event.

Naïve $CD4^+$ T cells were activated using immobilised anti-CD3 and anti-CD28 antibodies for 3 h or 20 h and the amount of intracellular p-S6 was measured using flow cytometry (Figure 36A). The proportion of p-S6 high *Wnk1*$^{-/-}$/RCE cells was reduced compared to control cells after 3 and 20 h of stimulation (Figure 36B, C). This difference was predominantly due to MEK-dependent, mTORC1-independent signalling at the 3 h timepoint presumably indicating defective ERK-RSK signalling in *Wnk1*$^{-/-}$/RCE cells. Conversely mTORC1-dependent, MEK-independent S6 phosphorylation at 3 h, presumably mediated by PI3K-AKT-mTORC1 signalling, was unaffected by loss of WNK1. S6 phosphorylation at 20h was dependent on MEK signalling via mTORC1, assuming MEK is upstream of mTORC1. These data supported the previous findings that ERK signalling downstream of TCR and CD28 costimulation is defective in WNK1-deficient cells. This defect was still apparent even after 20 h of TCR and CD28 costimulation. It was not possible to carry out non-parametric statistical tests on these data as this experiment contained only 2-3 biological repeats of each condition. Additionally, the experiment was not repeated. Therefore, additional experiments are required to show that the effects of WNK1 on S6 phosphorylation are statistically significant and reproducible.

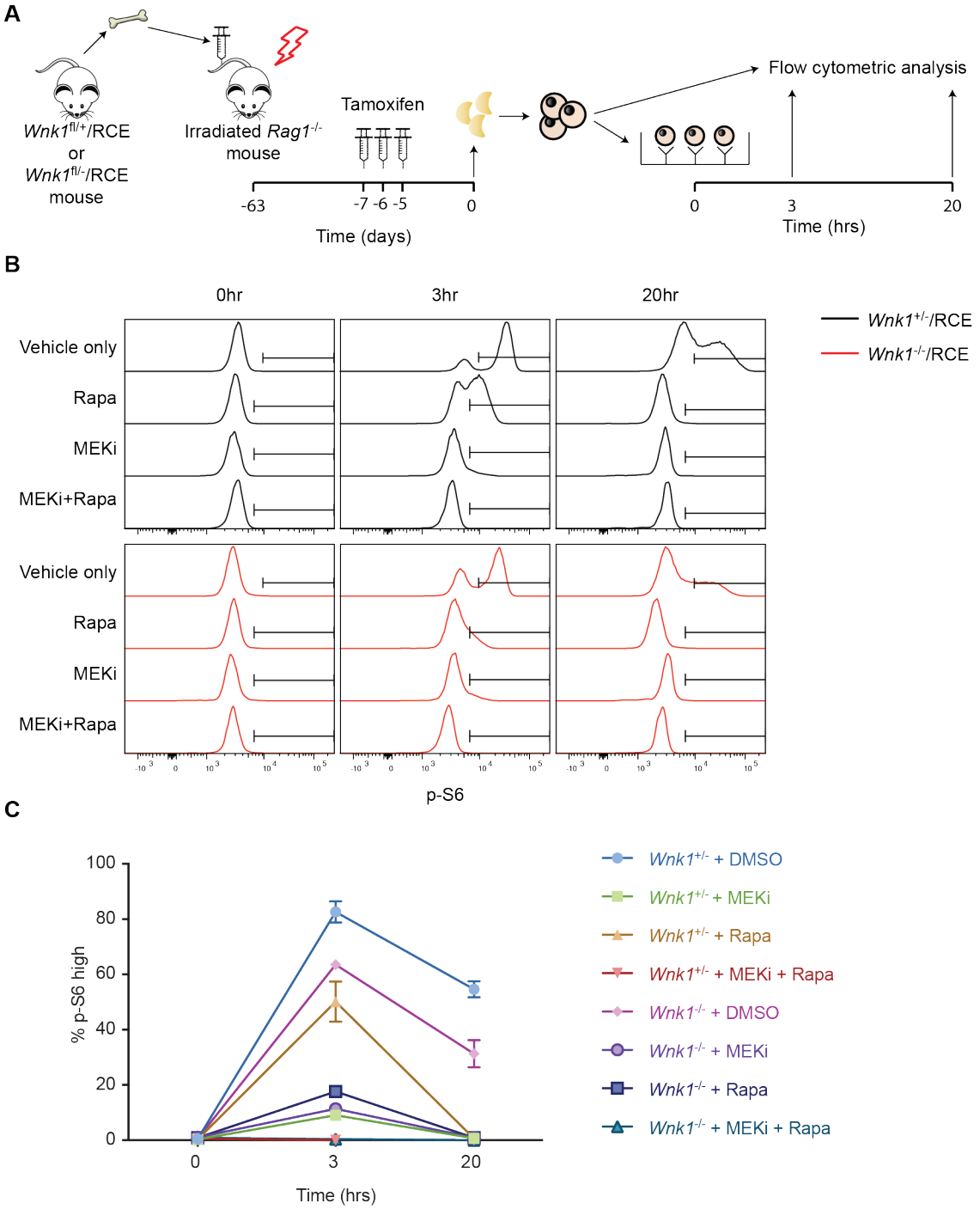

Figure 36. WNK1-deficient cells have defective MEK-dependent S6 phosphorylation. (**A**) Experimental design: *Wnk1*$^{+/-}$/RCE and *Wnk1*$^{-/-}$/RCE T cells were generated as described in Chapter 3.1. Naïve CD4^{+} T cells (CD25^{lo}/CD44^{lo}) were isolated from lymph nodes and cultured on plate-bound anti-CD3 and anti-CD28 antibodies for the indicated time points. Data from live, single, CD4^{+} T cells. (**B**, **C**) Example histograms (B) and graph (C) of p-S6 (S235/236) abundance in *Wnk1*$^{+/-}$/RCE and *Wnk1*$^{-/-}$/RCE cells activated for the indicated amount of time in the presence of the inhibitors indicated (n=2-3). Gates used to identify p-S6+ population are indicated. Graph shows median ±range. Data from 1 experiment.

5.3 WNK1-dependent osmoregulation is required for entry into G1 phase of the cell cycle

In light of the fact that WNK1-dependent water homeostasis is required for TCR signalling we investigated whether this process was also required for G1 entry. To address this question we activated WNK463-treated cells in hypotonic media (250mOsm/L) and measured the proportion of that had exited G0 and entered the cell cycle by day 2 *in vitro*, using Ki67 expression and DNA content to identify this population (Figure 37A, B). As discussed in Chapter 5.1, the effect of cell division on the frequency of Ki67+ cells was removed by fitting a model to the CTV dilution profile of cell populations in each condition, an example of which is shown in Figure 37B, and calculating the proportion of Ki67+ cells that would be present in the absence of division.

A 42mOsm/L reduction in culture medium tonicity was sufficient to rescue the decrease in cell cycle entry rate exhibited by WNK463-treated cells (Figure 37C). This rescue was not observed when WNK463-treated cells were activated in isotonic medium containing 42mOsm/L L-glucose used to replace the reduced NaCl in the hypotonic medium. This experiment showed that WNK1-dependent osmoregulation is required for G1 entry during $CD4^+$ T cell activation.

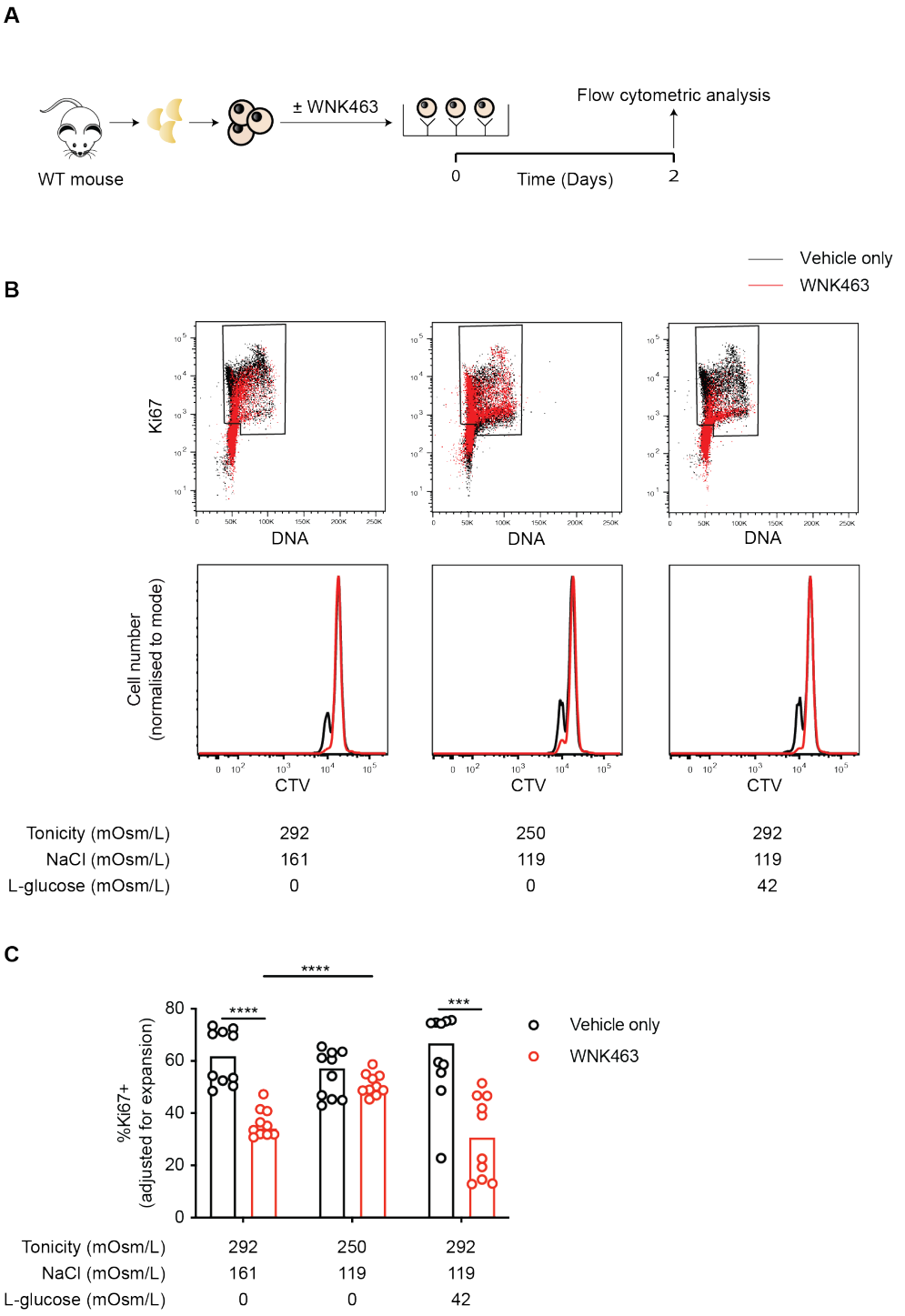

Figure 37. WNK1-dependent osmoregulation is required for entry into G1. (**A**) WT Naïve CD4$^+$ T cells (CD25^{lo}/CD44^{lo}) were isolated from lymph nodes and cultured on plate-bound anti-CD3 and anti-CD28 antibodies in the presence of vehicle only or WNK463 for 2 days. Data from live, single, CD4$^+$ T cells. (**B**) Dot plots of Ki67 expression vs DNA content (upper panels) and CTV dilution profiles (lower panels) of vehicle only- and WNK463-treated cells at day 2 of activation in the indicated conditions. Gate displayed in upper panels used to identify cells Ki67$^+$ cells. (**C**) Percentage of Ki67+ cells after adjusting for proliferation (n=10). Each point represents a single mouse; horizontal lines show median. Data pooled from 2 independent experiments. Statistical analysis carried out using Mann-Whitney U test. ***0.0001<p<0.001; ****p<0.0001.

5.4 WNK1-deficiency results in altered cell cycle dynamics

Although WNK1 is required for G1 entry, WNK1-deficient cells are able to enter the cell cycle, albeit in a delayed manner. To investigate the possibility that WNK1 is required for progression through the other phases of the cell cycle I studied the cell cycle dynamics of Ki67+ cells after 72 h of activation *in vitro* (Figure 38A). DNA content can be used to distinguish cells in G1, S and G2/M phases of the cell cycle. MPM2 phosphorylation status can be incorporated to distinguish between cells in G2 and M phases giving a fully resolved picture of the cell cycle profile for a population of cells. *Wnk1*$^{-/-}$/RCE cells had a dramatically altered cell cycle profile when compared to *Wnk1*$^{+/-}$/RCE cells, which was characterised by a reduction in the proportion of cells in G1 and M phases but an increase of cells in S and G2 phases (Figure 38B, C). These data showed that WNK1 is required for cell cycle regulation however it was unclear whether WNK1-deficiency is associated with an increase in speed through G1 and M phases or a reduction in speed through S and G2 phases of the cell cycle.

To determine the speed of S phase progression I measured the rate of 5-ethynyl-2'-deoxyuridine (EdU) incorporation. EdU is a thymidine analogue that is incorporated into DNA during synthesis (Figure 38A). EdU incorporation rate was determined by calculating the difference between the mean EdU MFI of S phase cells and the mean EdU MFI of cells in G1 and G2/M phases (∆MFI) (Figure 38D). *Wnk1*$^{-/-}$/RCE cells incorporated ~3.5-fold less EdU than *Wnk1*$^{+/-}$/RCE cells during a 10-minute pulse. This suggested that DNA replication, and thus S phase, occured at ~30% efficiency in *Wnk1*$^{-/-}$/RCE cells. It is likely therefore that *Wnk1*$^{-/-}$/RCE cells were experiencing severe replication stress and the increase in G2 phase length may have been due to the activation of cell cycle checkpoint pathways in response to this. Alternatively, the reduced EdU incorporation rate in *Wnk1*$^{-/-}$/RCE cells may have been due to reduced nucleoside uptake. Further experiments are needed to determine exactly how WNK1 regulates nucleoside incorporation into DNA during S phase.

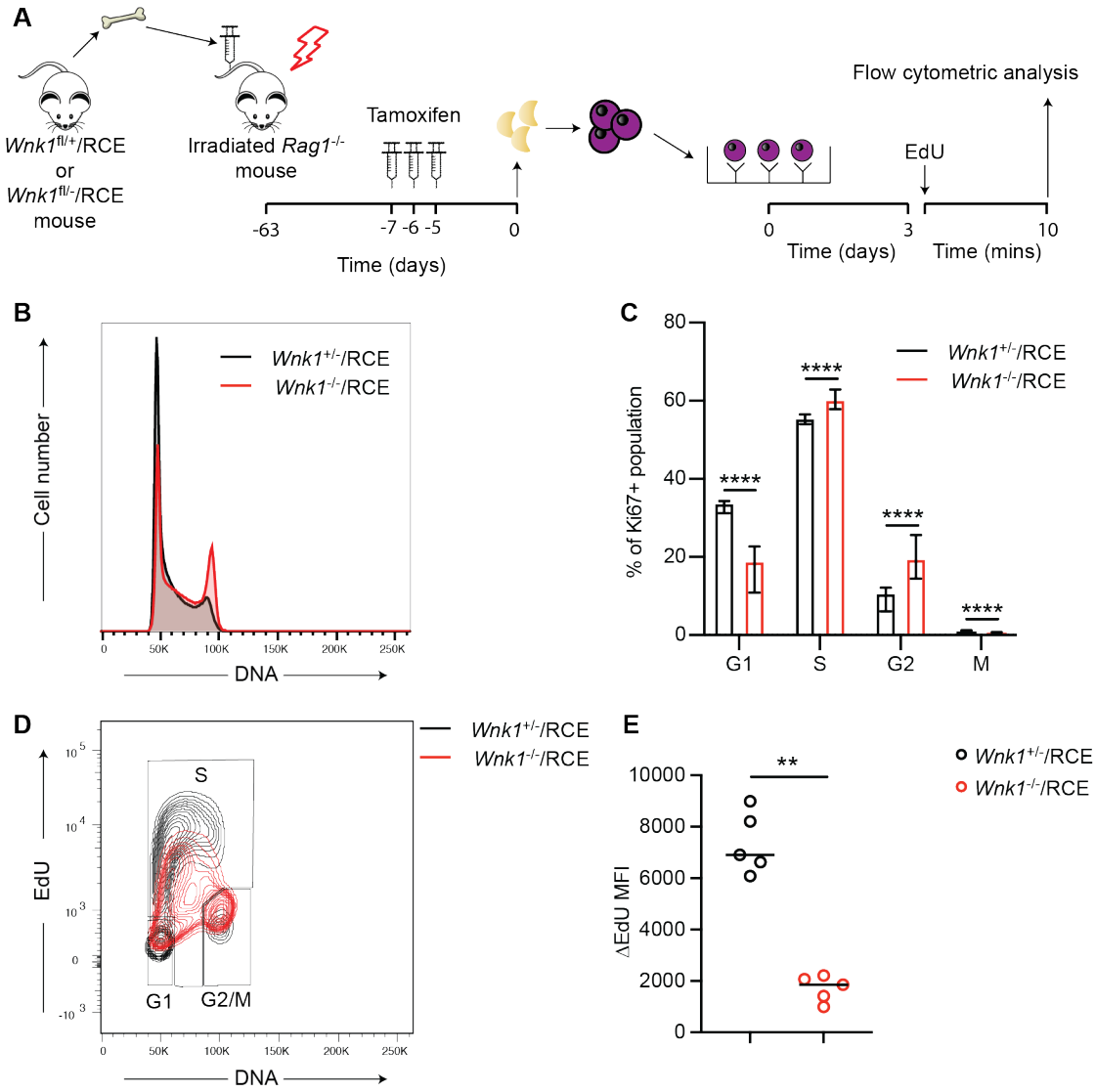

Figure 38. WNK1 is required for progression through the cell cycle. (**A**) Experimental design: *Wnk1*$^{+/-}$/RCE and *Wnk1*$^{-/-}$/RCE T cells were generated as described in Chapter 3.1. Naïve CD4^{+} T cells (CD25^{lo}/CD44^{lo}) were isolated from lymph nodes and cultured on plate-bound anti-CD3 and anti-CD28 antibodies. After 72 h EdU was added to the cell media for 10 min. Data from live, single, Ki67^{+} CD4^{+} T cells (**B**) DNA content of *Wnk1*$^{+/-}$/RCE and *Wnk1*$^{-/-}$/RCE cells at day 3. (**C**) Percentage of Ki67+ cells in each of the cell cycle phases at day 3 quantified from DNA histograms using the Watson model (n=8-9). (**D**) Contour plots of EdU incorporation vs DNA content of *Wnk1*$^{+/-}$/RCE and *Wnk1*$^{-/-}$/RCE cells after 10 min pulse of EdU at day 3. Gates used to identify S, G1 and G2/M phase cells. (**E**) ΔMFI of EdU in *Wnk1*$^{+/-}$/RCE and *Wnk1*$^{-/-}$/RCE cells in S phase (n=5). Bars or horizontal lines show median; each point represents a single mouse (E); error bars show 95% confidence intervals (C). Data pooled from 2 independent experiments (C) or from 1 experiment representative of 2 independent experiments (E). Statistical analysis carried out using Mann-Whitney U test. * 0.01 < p < 0.05; ** 0.001 < p < 0.01; ***0.0001<p<0.001; ****p<0.0001.

5.5 WNK1-deficiency results in ATR checkpoint activation

A reduction in DNA replication efficiency, and an accompanying block at the G2/M phase transition, is characteristic of cell cycle checkpoint activation. ATR and ATM kinases mediate cell cycle arrest in response to a range of cellular stresses, although their role in responding to DNA damage is the best characterised. These kinases mediate cell cycle arrest via multiple mechanisms including the acute inhibition of CDK-cyclin complexes by indirectly regulating the tyrosine phosphorylation status of CDK proteins via CDC25 phosphatases. ATR and ATM checkpoint activation are also accompanied by an increase in the expression of the CDK inhibitor p21, providing an additional layer of CDK regulation. In order to investigate the possibility that WNK1-deficient cells were undergoing ATR- or ATM-mediated cell cycle arrest I used immunoblotting to measure phosphorylation of Chk1 (S345) and KAP1 (Ser824) as a readout for ATR and ATM activity, respectively (Figure 39A).

WNK463-treated cells exhibited a ~3-fold increase in Chk1 (S345) phosphorylation but no difference in KAP1 (S824) phosphorylation (Figure 39B, C). This suggests that the ATR, but not the ATM, cell cycle checkpoint is activated in the absence of WNK1 activity. Hydroxyurea (HU) and ATR-inhibition enhanced and depleted the p-Chk1 signal, respectively, suggesting that our detection method was specific. Interestingly ATR-inhibition induced ATM activation in vehicle only-treated cells to a greater extent than in WNK463-treated cells. ATR is involved in stabilising and restarting stalled replication forks and in its absence these decay to double strand breaks, which activate ATM. One possible reason for a difference in ATM activation in the presence of an ATR inhibitor would be a decreased number of replication forks present in WNK463-treated cells, although the number of replication forks would need to be directly quantified to determine whether this is the case.

To determine whether activation of the ATR pathway was responsible for the S and G2/M block observed in WNK-deficient cells, I added an ATR inhibitor (ATRi) to the culture medium at 36 h (Figure 39A) and measured its effect on the cell cycle profile of samples after 72 h of activation *in vitro* using flow cytometry. ATR-inhibition significantly reduced the proportion of WNK463-treated cells in G2, although the proportion of cells in S phase was unchanged. This suggested that ATR mediates at least part of the G2/M arrest observed in WNK463-treated cells. ATR inhibition reduced the proportion of vehicle only-treated cells in S phase but not G2 phase. A

possible explanation for this is that ATR inhibits firing of some replication origins during an unpeturbed S phase and so inhibition of this kinase would result in an increase in the number of origins firing and an equivalent reduction in the time required for replication of the entire genome assuming substrates are not limiting. It is interesting that ATR inhibition didn't produce the same reduction in the proportion of S phase cells in WNK463-treated samples suggesting DNA synthesis may not have been limited by ATR in these cells.

The major drawback of this experiment was that the data could not be used to determine the rate of progression through individual phases of the cell cycle. This is because the proportional nature of the data collected means that values for the cell cycle phases are entirely interdependent. For example, the proportion of cells in S phase depends on the rate of S phase progression but also the rate of progression through each of the other cell cycle phases. The functionally opposing roles of ATR during fork slowing and restart also complicates the conclusions one can draw from these data. Finally, the experiment was not repeated so it was unclear whether the effect of ATR on the cell cycle is reproducible. Time course experiments measuring cell cycle rates could shed more light on the function of the ATR pathway in the absence of WNK1 activity by providing additional information about cell cycle kinetics.

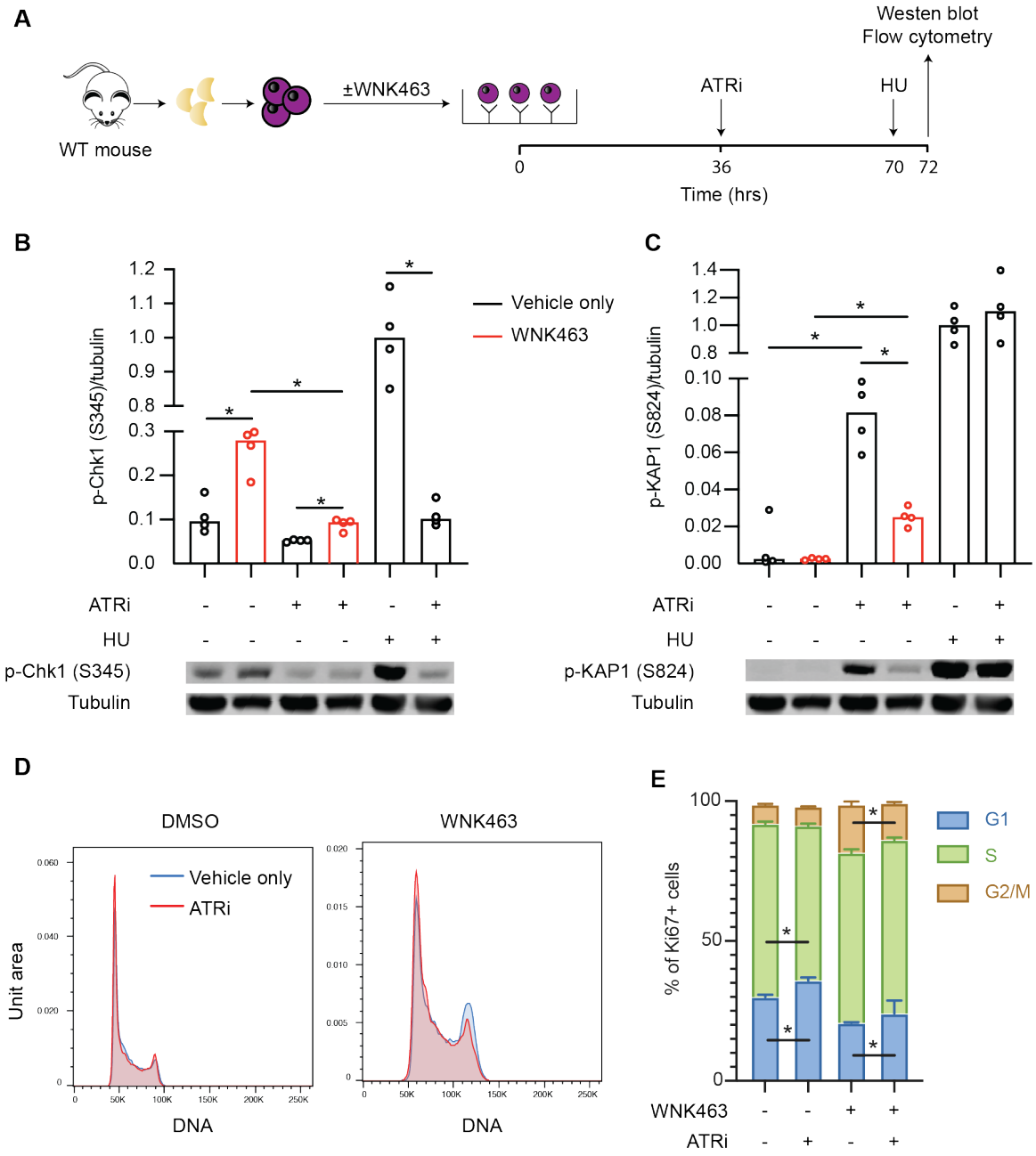

Figure 39. Cells treated with WNK463 activate the ATR-mediated cell cycle checkpoint. (**A**) WT naïve CD4$^+$ T cells (CD25^{lo}/CD44^{lo}) were isolated from lymph nodes and cultured on plate-bound anti-CD3 and anti-CD28 antibodies in the presence of vehicle only or WNK463 for 72 h. At 36 h ATR-inhibitor (ATRi) was added to the media of the indicated samples. 4mM hydroxyurea (HU) was added to the media of indicated samples at 70 h to induce replication fork stalling (**B**-**C**) Immunoblots of cells at 72 h with antibodies against p-Chk1 (S345) (B), p-KAP1 (S824) (C), and tubulin (B, C). (**D**) DNA content of (live, single, Ki67$^+$ CD4$^+$) cells in vehicle only- and WNK463-treated cells in the presence or absence of ATRi at 72 h (**E**) Proportion of (live, single, Ki67$^+$ CD4$^+$) cells in each phase of the cell cycle at 72 h. Quantified from DNA histograms using the Watson model (n=4). Horizontal lines show median; each point represents a single mouse (B-C); Error bars show interquartile range (E). Data from 1 experiment representative of 3 experiments (B, C) or from 1 unrepeated experiment (D, E). Statistical analysis carried out using Mann-Whitney U test. * 0.01 < p < 0.05.

ATR is activated by the presence of ssDNA formed during replication stress or DSB resection. DNA damage markers were quantified by Western blot to determine whether DNA damage was occurring during $CD4^+$ T cell activation in the absence of WNK1 activity (Figure 40A). γH2AX can be generated by both ATM and ATR signalling pathways, whereas RPA32 is phosphorylated at S4/8 (p-RPA32) by DNA-PKcs in response to a number of types of DNA damage. Neither of these markers were significantly increased in WNK463-treated cells at day 3 of activation *in vitro* (Figure 40B, C). In contrast, treatment of the cells with hydroxyurea (HU), a chemical that induces replication stress and subsequently DNA damage, for the final 2 h of culture resulted in a large increase in γH2AX and p-RPA32. These data suggest that DNA damage is not occurring in WNK1-deficient cells. However, a more comprehensive analysis of replication stress in these cells is required to show this conclusively. For example, DNA fibre assays could be used to measure multiple aspects of replication fork dynamics in the absence of WNK1 activity. Increased statistical power may also be needed to reveal small increases in DNA damage in the absence of WNK1 activity.

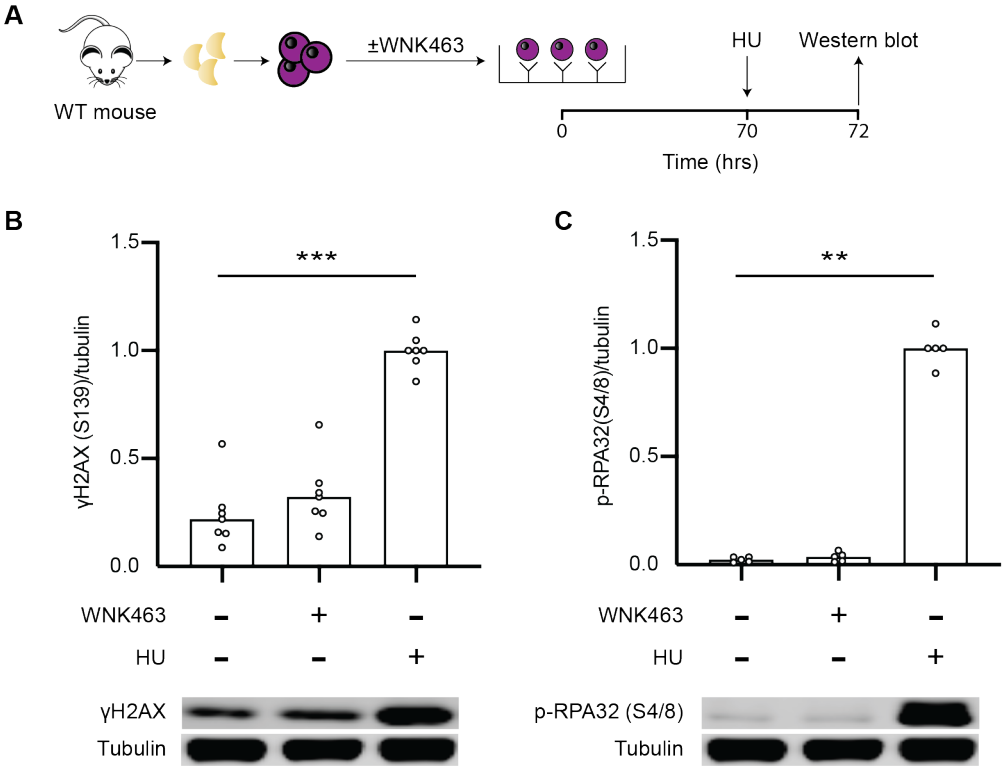

Figure 40. WNK1 inhibition does not promote γH2AX or p-RPA32 (S4/8) accumulation during activation *in vitro*. (**A**) WT naïve CD4$^+$ T cells (CD25^{lo}/CD44^{lo}) were isolated from lymph nodes and cultured on plate-bound anti-CD3 and anti-CD28 antibodies in the presence of vehicle only or WNK463 for 72 h. 4mM hydroxyurea (HU) was added to the media of indicated samples at 70 h to induce replication fork arrest and subsequent DNA damage. (**B**-**C**) Immunoblots of vehicle only- and WNK463-treated cells at 72 h with antibodies against p-RPA32 (S4/8) (B), γH2AX (S139) (C), and tubulin (B, C) (n=5-7). Bars show median; each point represents a single mouse. Data pooled from 3 independent experiments. Statistical analysis carried out using Mann-Whitney U test. ** 0.001 < p < 0.01; ***0.0001<p<0.001.

Chapter 6. Discussion

There is a nearly absolute requirement for WNK1 expression in $CD4^+$ T cells during a T-dependent, class-switched antibody response. This requirement for WNK1 activity can be observed even at the earliest stage of $CD4^+$ T cell activation – TCR signal transduction. WNK1 inhibition did not affect TCR-induced phosphorylation of CD3ζ on Y142, suggesting that LCK activity and localisation are undisturbed. However, TCR-induced phosphorylation of ZAP-70 at Y319 is substantially reduced in the absence of WNK1 kinase activity. This implies that ZAP-70 activity is also reduced as phosphorylation of Y319 is critical for ZAP-70 activation and signalling to downstream signalling intermediates including SLP76 and ERK proteins (Di Bartolo et al., 1999b). These profound effects on downstream signalling are exemplified by the dramatic decrease in the proportion of p-ERK+ WNK1-deficient cells after an hour of stimulation *in vitro*. WNK1 is also required for $CD4^+$ T cell entry into G1 in response to TCR and CD28 stimulation as well as progression through the cell cycle.

It is possible that defective ZAP-70 Y319 phosphorylation is solely responsible for the p-ERK and G1 entry defects exhibited by WNK1-deficient cells. The similar magnitude of the p-ZAP-70 and p-ERK defects observed in WNK1-inhibited cells during stimulation using soluble antibodies, for example, is consistent with this although feedback circuits and amplification effects in the ZAP-70 signalling pathway make it impossible to draw a conclusion on this matter. Based on the evidence presented in this thesis therefore, the possibility that the TCR signal and activation process are being interrupted at multiple points downstream of ZAP-70 in WNK1-deficient cells cannot be excluded. An inducible, constitutively active form of ZAP-70 could be used to address this question. Additionally, confirmation of the ZAP-70 signalling defect by immunoblotting *Wnk1*$^{D368A/-}$ cell extracts is needed to confirm that the ZAP-70 Y319 phosphorylation defect is not an artefact of the flow cytometric method nor a result of off-target effects of WNK463.

Given that ZAP-70 Y319 phosphorylation is the earliest event in $CD4^+$ T cell activation that was found to be affected by WNK1 activity, I will focus this part of the discussion on possible mechanisms by which WNK1 could influence this process. One possibility is that WNK1 regulates ZAP-70 Y319 phosphorylation by modulating the LFA-1-dependent adhesion of $CD4^+$ T cells, a function of WNK1 that was previously reported by our lab (Köchl et al., 2016). The fact that the ZAP-70 signalling

defect can be observed when WNK1-inhibited cells are stimulated *in vitro* using anti-CD3 and anti-CD28 antibodies suggests that WNK1-dependent regulation of LFA-1 activity does not play a role in ZAP-70 Y319 phosphorylation because unlike during T cell activation *in vivo* this type of stimulation does not require integrin-mediated adhesion. However, ICAM-1 molecules decorate the surface of all the $CD4^+$ T cells in culture providing possible ligands for LFA-1 during activation *in vitro* with anti-CD3 and anti-CD28 antibodies. As LFA-1 has been shown to induce ZAP-70 Y319 phosphorylation upon binding to ICAM-1, and has well characterised costimulatory effects *in vivo*, it would be surprising if increased LFA-1 activity in WNK1-deficient cells inhibited ZAP-70 Y319 phosphorylation (Evans et al., 2011; Kandula and Abraham, 2004). However, a study by Jankowska et al. showed that the addition of ICAM-1 during T cell activation with immobilised anti-CD3 antibodies reduced ZAP-70 Y319 phosphorylation, at least in part by reducing actin flow (Jankowska et al., 2018). This observation provides a possible mechanism by which WNK1 could regulate ZAP-70 Y319 phosphorylation via LFA-1. To exclude the possibility that impaired TCR signalling in WNK1-inhibited cells is due to increased integrin-dependent adhesion, activation could be analysed in the presence of integrin inhibitors.

A second possibility that could explain effects of WNK1 activity on ZAP-70 Y319 phosphorylation is that LCK activity specifically towards ZAP-70 has been altered in WNK1-inhibited cells. However, phosphorylation of LCK S59 and Y192, which are the two most well characterised post-translational modifications that are able to modulate LCK substrate specificity, are not good candidates for explaining the defect in ZAP-70 Y319 phosphorylation. Phosphorylation of LCK Y192 is thought to dramatically alter ligand binding but not towards ZAP-70. LCK S59 phosphorylation affects LCK activity itself, as measured by Y394 phosphorylation, suggesting it would affect activity towards CD3ζ as well, which is not the case in WNK1-inhibited cells (Dutta et al., 2017; Granum et al., 2014). Moreover, Dutta *et al.* show that calcineurin activity, which modulates LCK substrate specificity in part through dephosphorylation of LCK S59, reduces ZAP-70 Y493 phosphorylation but does not affect ZAP-70 Y319 phosphorylation. Other mechanisms of post-translational LCK regulation cannot be excluded, however alternative explanations exist.

A third possibility is that ZAP-70 recruitment to the membrane is disrupted in WNK1-inhibited cells. ZAP-70 membrane recruitment is mediated predominantly through co-operative interactions between the ZAP-70 tandem SH2 domains and doubly phosphorylated ITAMs on the intracellular tail of CD3ζ (Iwashima et al., 1994). Additionally, interactions between the C-terminal SH2 domain and phosphoinositides, such as PIP_2 and PIP_3, on the inner leaflet of the plasma membrane appear to be very important for ZAP-70 recruitment and function (Park et al., 2016). LCK-mediated phosphorylation and/or autophosphorylation of ZAP-70 Y319 is tightly coupled to ITAM binding and thus if ZAP-70 recruitment to the membrane were to be perturbed then ZAP-70 Y319 phosphorylation would also be affected. It would therefore be interesting to measure TCR-induced ZAP-70 recruitment to the membrane in WNK1-inhibited cells, possibly using total internal reflection fluorescence (TIRF) microscopy (Yokosuka et al., 2005). If ZAP-70 membrane recruitment is found to be defective, then the role of this process in ZAP-70 Y319 phosphorylation and downstream signalling could be tested using a gain-of-function ZAP-70 mutant – D184K – which has a higher membrane affinity. Expression of this mutant in WNK1-deficient T cells could restore ZAP-70 activation and downstream signalling if it is the case that defective ZAP-70 membrane recruitment is responsible for the TCR signalling defects observed in these cells.

TCR-induced phosphorylation of CD3ζ at Y142, which is located within an ITAM motif, is normal in WNK1-deficient cells. Therefore, it is likely that bi-phosphorylated CD3ζ ITAMs, which form the binding site for ZAP-70, are present in normal amounts in WNK1-inhibited cells during TCR and CD28 costimulation. Thus, if ZAP-70 membrane recruitment is impaired it is unlikely to be due to reduced CD3ζ phosphorylation but may be due to other factors. One such possibility is that WNK1 inhibition alters the abundance of phosphoinositides, such as PIP_3 and PIP_2, at the plasma membrane, because these lipids play a major role in ZAP-70 recruitment (Park et al., 2016). It would therefore be interesting to measure the abundance of these lipids using fluorescent reporters in WNK1-deficient cells during TCR and CD28 costimulation (Balla and Várnai, 2009).

A fourth possibility that could explain the ZAP-70 Y319 phosphorylation defect is a change in the dephosphorylation kinetics of Y319. The phosphorylation status of ZAP-70 Y319 is governed by an equilibrium between LCK-dependent

phosphorylation or autophosphorylation and phosphatase-dependent dephosphorylation. In this case the most well characterised phosphatases that act on Y319 are the STS family. As discussed in Section 0, STS phosphatases depend on ubiquitination of ZAP-70 for dephosphorylation. Thus, it would be interesting to measure ubiquitination of ZAP-70 in WNK463-treated cells as this post-translational modification could plausibly be responsible for altering the equilibrium towards Y319 dephosphorylation. The role of phosphatases could be further examined by using inhibitors, although specificity may present a problem as small molecule inhibitors of these enzymes are not generally very specific. Additionally, phosphatases themselves tend to be highly promiscuous towards their substrates when compared to kinases and it is therefore hard to delineate their effects for specific substrates. Nevertheless, two studies have found that the SHP-1 inhibitor – PHPS1 – can be used to potently inhibit STS activity and sulfonated azo dyes, such as Congo red, inhibit STS1 with a selectivity index of >20 compared to PTP-1B and SHP-1. If treatment with an STS inhibitor abolished the difference in TCR-induced ZAP-70 Y319 phosphorylation between WNK1-inhibited and control cells this would suggest that WNK1 promotes ZAP-70 Y319 phosphorylation by supressing STS phosphatase activity.

The fact that the defect in TCR-induced ERK phosphorylation in WNK1-inhibited cells can be reversed by activating these cells under hypotonic conditions shows that it is the osmoregulatory function of WNK1 that is required for this process. If the p-ERK defect in WNK1-inhibited cells is caused by defective ZAP-70 Y319 phosphorylation, this would suggest that WNK1-dependent osmoregulation is needed for ZAP-70 Y319 phosphorylation. However, rescue of the p-ZAP-70 defect in WNK1-inhibited cells by activation in hypotonic medium needs to be demonstrated to formally show this. It cannot be excluded that hypotonic treatment in fact induces ERK signalling independently of the TCR in WNK1-deficient cells. To test this possibility, ERK phosphorylation needs to be measured under hypotonic treatment in the absence of TCR stimulation. However, the fact that there is only a very small increase in the proportion of p-ERK high control cells when activated under hypotonic conditions is consistent with WNK1-dependent osmoregulation being required for TCR-dependent ERK signalling, which requires ZAP-70 Y319 phosphorylation.

As discussed in Chapter 1.11.1, under hypertonic conditions WNK1 signals to NKCC, KCC and NCC ion transporter family members via OXSR1 and STK39

kinases resulting in a net influx of ions and water into the cell. Additionally, this pathway is partially activated under steady-state conditions to maintain a constant cell volume as well as being induced downstream of the TCR (Köchl et al., 2016). In the absence of WNK1 activity, constitutive KCC activity will lead to a net efflux of ions from the cell and TCR stimulation will fail to induce water influx. This would result in a reduction in cell volume and a failure to increase volume in response to TCR stimulation. The lack of WNK1 likely means that these cells also have a compromised RVI response to this shrinkage. Hypotonic treatment will reverse these aspects of WNK1-deficiency.

The mechanism by which cell volume could regulate TCR signalling, in particular ZAP-70 Y319 phosphorylation, is unclear. Macromolecular crowding effects are a major consequence of cell shrinkage. An increase in crowding reduces diffusion rates. Additionally, the volume exclusion effect of increased crowding makes protein-protein interactions more energetically favourable. This is due to the fact that, when crowding is increased, unbound interactors incur a greater entropic cost to the solution than bound interactors, because bound interactors exclude less volume from cosolutes (Minton, 1983). The intracellular space is highly crowded. Even in unperturbed conditions, it is estimated that macromolecules occupy up to 40% of cellular volume (Ellis, 2001). ZAP-70 phosphorylation, for example, requires diffusion, binding to p-CD3ζ, a conformational change, and finally interaction and phosphorylation by LCK. Theoretically, increased molecular crowding could influence many of these steps in both positive and negative manners. For example, the diffusion coefficient of ZAP-70 could be reduced as a consequence of cell shrinkage thus reducing the efficiency of its recruitment to the membrane. This crowding-dependent reduction in diffusion rates has been illustrated experimentally by the fact that hypertonic shock reduces the diffusion coefficient of GFP in CHO cells as measured by FRAP (Swaminathan et al., 1997). ZAP-70 is several times larger than GFP meaning it would be influenced to a greater extent by changes to cell volume. However, the volume exclusion effects of cell shrinkage would promote interactions between ZAP-70 and CD3ζ and LCK and thus Y319 phosphorylation. Then again this is also true for interactions between ZAP-70 and STS phosphatases. Volume exclusion effects could also affect the favourability of ZAP-70 conformational changes required for Y319 phosphorylation. The direction of the effect would depend on the relative sphericity of the “closed” and “primed/active” species as sphericity

determines the volume that each ZAP-70 molecule excludes from cosolutes. The effect of cell shrinkage on ZAP-70 Y319 phosphorylation therefore depends on which step in the process is rate-limiting. Additionally, the extent of cell shrinkage needs to be quantified to determine the plausibility of the mechanism. The fact that maximal hypotonic rescue of ERK signalling in WNK1-deficient cells requires the removal of 123mM of NaCl suggests that the WNK1 activity accounts for ~40% of intracellular tonicity and therefore cell shrinkage in its absence could be profound. Molecular crowding is difficult to manipulate other than through osmotic means. However, Delarue et al. show that ribophagy induced by Rapamycin-dependent inhibition of mTORC dramatically reduces the excluded volume of the cytoplasm (Delarue et al., 2018). Hence, WNK1-deficient T cells could be treated with Rapamycin to determine if a reduction in molecular crowding rescues TCR signalling defects. However, treatment with Rapamycin is likely to cause many other changes to cell physiology, making the interpretation of such an experiment difficult.

Above, I proposed that changes to phosphatase activity could be the cause of reduced ZAP-70 phosphorylation in WNK1-deficient cells. The ability of cell shrinkage to activate phosphatases is illustrated beautifully by Watanabe *et al*. who show that PP6 is activated under hypertonic conditions and induces WNK1 activity via ASK3 inhibition as discussed in Chapter 1.11.1 (Naguro et al., 2012; Watanabe et al., 2018). This shows that osmotic changes have the potential to regulate phosphatases. However, PP6 itself is a Ser/Thr phosphatase and thus cannot be directly responsible for ZAP-70 dephosphorylation. Interestingly, PP6 has nonetheless been shown to regulate TCR signalling (Ye et al., 2015). Deletion of PP6 using the CRE recombinase under the control of the *Lck* promoter results in reduced TCR expression, reduced TCR-proximal signalling, but elevated downstream signalling from at least the level of C-RAF onwards. There is no evidence that the STS phosphatases, which are well known for dephosphorylating ZAP-70, are regulated by cell volume changes.

A TCR-proximal defect as seen in WNK1-deficient cells would be expected to have profound effects on T cell activation as most, if not all, pathways downstream of the TCR may well be affected by the absence of WNK1 activity. One of the earliest effects of T cell activation which would be predicted to be altered by WNK1-deficiency is activation marker and cytokine expression because these processes are heavily dependent on TCR signalling and in some cases can be used as a marker

for TCR signalling flux. Unexpectedly, WNK1-deficient cells display a “hyperactivated” cell surface phenotype as activation marker expression is elevated in these cells relative to controls during activation *in vitro*. A similar effect is seen in the production of cytokines, a large number of which have increased expression levels in WNK1-deficient cells. At least in the case of IL-2 this is at both the transcriptional and translational level. A defect at the level of ZAP-70 activation would be expected to negatively impact all TCR-induced transcription factor and translation activity. For example, CD69 is one of the earliest activation markers to be expressed and is highly dependent on ERK activity. It is clear that ERK phosphorylation at T202/Y204, and thus activation, is heavily downmodulated in WNK1-deficient cells between 0-1hr of activation *in vitro*. Additionally, ERK-dependent S6 phosphorylation is also reduced in WNK1-deficient cells at least until 20 h of activation *in vitro*. CD69 expression on the other hand is normal at day 1 and elevated at day 2 in WNK1-deficient cells activated *in vitro*. CD44, which is highly sensitive to mTORC1 activity, is also expressed at super-physiological levels in WNK1-defiicent cells from day 1 onwards. We also know that mTORC1 activity is reduced in WNK1-deficient cells at least until 20 h of stimulation. It is hard to reconcile these contradictory observations. A decoupling of TCR signalling and activation marker/cytokine expression may have occurred in WNK1-deficient cells. This is supported by the fact that *Wnk1*$^{-/-}$/OT-II/RCE cells display elevated CD25 and CD69 compared to controls even in the absence of antigen although the addition of antigen does dramatically increase activation marker expression in WNK1-deficient cells suggesting it still plays a central role. It is unclear which signalling pathways and transcription factors could be responsible for substituting for TCR signalling to induce activation marker expression.

The osmoregulatory function of WNK1 may once again provide an answer for at least some of the observed effects. The NFAT5 transcription is activated in response to cell shrinkage. This transcription factor has been shown to directly induce TNFα transcription and a putative binding site in the IL-18 promoter has been identified (Neuhofer, 2010). Additionally, NFAT5 was shown to promote IL-2 expression in CD4^{+} T cells under hypertonic conditions (Alberdi et al., 2017). Activation of *Il2* expression in response to hypertonic shock seems to be regulated through an unusual mechanism requiring ATP release and autocrine/paracrine signalling via P2X7 receptor to p38 (Loomis et al., 2003). This provides a means by which these cytokines could be upregulated in the absence of full TCR signalling in

WNK1-deficient cells. IL-2 signalling is known to be sufficient for *Il4* expression meaning that NFAT5-dependent expression of IL-2 could also have a knock-on effect of inducing the elevated levels of IL-4 observed in WNK1-deficient cells (Cote-Sierra et al., 2004). IL-4 in turn is known to antagonise T_H1 differentiation possibly explaining the drop in IFNγ expression by WNK1-deficient cells. Elevated IL-4 expression could also be explained by supressed ERK signalling in the absence of WNK1 activity. As previously discussed, low levels of ERK signalling during activation decrease the ratio of fos-jun/jun-jun AP1 dimer DNA binding activity resulting in activation of *Il4* transcription (Li et al., 1999). Additionally, elevated autocrine/paracrine IL-2 signalling could contribute to the super-physiological levels of CD25 expressed on WNK1-deficient cells as STAT5 mediates a positive feedback loop enhancing *Cd25* expression (John et al., 1999).

OXSR1 and/or STK39 also supress activation marker expression during $CD4^+$ T cell activation *in vitro*. It is conceivable that WNK1 signals via these kinases to supress activation marker expression. This would have to be tested using an inducible, constitutively active OXSR1 and/or STK39 construct. If induction of OXSR1 and/or STK39 activity in WNK1-deficient cells recues the activation marker defect this would show that WNK1 signals via these kinases to supress activation marker expression. It would also be interesting to determine whether the WNK1-OXSR1/STK39 signalling pathway regulates activation marker expression via its osmoregulatory function. Measuring the effect of varying medium tonicity on activation marker expression by *Wnk1*$^{-/-}$/RCE and *Oxsr1*$^{-/-}$/*Stk39*$^{T243A/T243A}$/RCE cells could address this question. The less extreme upregulation of activation markers in OXSR1/STK39-deficient cells compared to WNK1-deficient cells suggests that WNK1 may additionally regulate activation marker expression via a parallel pathway.

The transition from G0 into G1 phase of the cell cycle is another of the earliest changes in cell phenotype induced by TCR stimulation. Titration of ZAP-70 activity results in a corresponding reduction in T cell proliferation during activation *in vitro* in a dose-dependent manner (Au-Yeung et al., 2014). This is due to a reduced number of cells reaching the required threshold of TCR signalling for commitment to division. It is therefore likely that WNK1 regulates cell cycle entry through regulation of ZAP-70 signalling. This mechanism of regulation of G1 entry by WNK1 fits with the fact that WNK1-deficiency dramatically reduces ERK signalling and consequently mTORC1 activity, which are the master regulators of the G0/G1 transition as

discussed in Chapter 1.9.1. Finally, activation of WNK1-deficient cells in hypotonic media rescues the G1 entry defect, as well as the TCR signalling defect, suggesting that WNK1-dependent osmoregulation is required for ZAP-70 signalling which in turn induces G1 entry. Other possibilities cannot however be excluded. This theory could be tested using an inducible ZAP-70 kinase such as the one generated by Graef et al. which takes advantage of interactions between Rapamycin derivatives and FKBP12 in order to inducibly recruit ZAP-70 to the membrane resulting in activation (Graef et al., 1997). If the reduced rate of G1 entry by WNK1-deficient T cells is caused by limiting ZAP-70 activity, expression of such an inducibly activated ZAP-70 kinase could rescue this cell cycle defect.

The reduced rate of entry into G1 partially explains the inability of WNK1-deficient cells to expand and support a class-switched antibody response *in vivo*. However, WNK1-deficient cells also display severe defects during progression through multiple additional stages of the cell cycle. This effect is probably not due to TCR signalling defects as ZAP-70 signalling is dispensable for $CD4^+$ T cell division after 24 h of continuous signalling (Au-Yeung et al., 2014) and S, G2 and M cell cycle defects become apparent in WNK1-deficient T cells only at day 3.

The dramatically altered DNA profile of WNK1-deficient cell populations at day 3 of activation *in vitro* suggests significant dysregulation to cell cycle dynamics. The use of this readout for measuring progression through individual phases is hampered by the fact that these proportional values are entirely interdependent. EdU incorporation rate is used as a surrogate for S phase rate and shows that WNK1-deficient cells may have a ~3.5-fold reduction in DNA polymerase processivity. However, this finding is complicated by the fact that WNK1 may have effects on nucleoside uptake which could also explain reduced EdU incorporation. Total cell cycle times need to be measured by microscopy to determine empirical values for the rate of individual cell cycle phases. Nevertheless, the reduction of CTV dilution rates in WNK1-deficient cells supports the notion that there is a significant reduction to cell cycle speed in the absence of WNK1 activity.

S and G2 delays are characteristic of DNA damage checkpoint activation. However, it seems there is no significant increase in DNA damage in WNK1-inhibited cells as measured by γH2AX and p-RPA32 (S4/8). As discussed previously, γH2AX is formed in response to ATM or ATR signalling whereas RPA32 (S4/8) phosphorylation is mediated by DNA-PKcs in response to a most types of DNA

damage, including hydroxyurea-dependent replication stress (Liaw et al., 2011). Despite the apparent absence of DNA damage, increased p-CHK1 (S345) can clearly be observed in WNK463-treated cells relative controls at day 3 *in vitro* suggesting DNA damage-independent activation of ATR is taking place. Alternatively, the increased proportion of WNK1-deficient cells in S phase at day 3 *in vitro* could increase the p-CHK1 signal from these samples purely due to the fact that more background replication stress and ATR activation is observed in S phase. However, the extent in elevation of p-CHK1 signal appears much greater than the increase in the proportion of WNK1-deficient cells in S phase. It would be useful to measure other ATR-dependent phosphorylation events that are normally induced at the site of DNA damage to confirm that ATR activation is occurring in the absence of DNA damage. One attractive candidate is RPA32 (S33) phosphorylation which seems to be predominantly mediated by ATR (Toledo et al., 2013). p-KAP1 levels are unaltered in WNK463-treated cells suggesting ATM is not being activated by DSBs. Quantification of other ATM-dependent phosphorylation events, such as CHK2 phosphorylation, would be useful to support this finding.

Once again, the osmoregulatory function of WNK1 could be used to explain ATR activation and dysregulation of S and G2 progression in WNK1-deficient cells. Osmotic shock is well known to induce S and G2 arrest (Michea et al., 2000). Whether this is due to DNA damage is unclear and a number of different signalling pathways have been proposed to regulate this arrest (see Chapter 1.9.4). Kumar et al. found that osmotic stress, or other forms of mechanical stress, induced ATR activation in the absence of DNA damage (Kumar et al., 2014). This was characterised by localisation of ATR and ATRIP to the nuclear envelope. It would be interesting to image the localisation of these proteins in WNK1-deficient cells to examine the possibility that mechanical stress is activating ATR. Additionally, this hypothesis predicts that hypotonic conditions should be able to rescue these defects providing another way to investigate this possibility. ATR inhibition reduces the proportion of WNK1-deficient cells in G2 suggesting that in the absence of WNK1 activity ATR may enforce G2/M cell cycle arrest. However, direct measurement of the G2/M transition rate in the presence of ATRi would be needed to confirm this.

OXSR1 and STK39 positively regulate proliferation during $CD4^+$ T cell activation. It is tempting to speculate that WNK1 promotes cell cycle progression by activating these kinases. This possibility could be investigated using a constitutively

active OXSR1 and/or STK39 construct. If the expression of these constructs rescued the WNK1-deficient proliferation phenotype this would show that WNK1 signals via OXSR1 and STK39 to promote cell cycle progression. It would be interesting to further characterise the cell cycle phenotype of *Oxsr1*$^{-/-}$/*Stk39*$^{T243A/T243A}$/RCE cells to determine whether these kinases also play a role in G1 entry as well as cell cycle progression.

The reduced number of WNK1-deficient antigen-specific CD4^{+} T cells post-immunisation is due not only to a failure to expand properly but also reduced survival and/or homing. Defective homing *in vivo* has been clearly demonstrated by Köchl et al. and almost certainly influences the ability of WNK1-deficient cells to mount an immune response as antigen encounter in secondary lymphoid tissues is an essential step in CD4^{+} T cell activation (Köchl et al., 2016). A significant reduction in viability in WNK1-deficient cells can be observed at day 3 *in vitro* suggesting increased cell death could also play a role *in vivo*.

As discussed in Chapter 1.8, CD4^{+} T cell death during an immune response can be induced by withdrawal of cytokines or AICD, which involves the augmentation of cell death receptor signalling pathways. As there is an increased concentration of cytokines such as IL-2 and IL-4 that promote survival via γ_c chain-containing receptors it is unlikely that cytokine withdrawal is responsible for the increased cell death observed in WNK1-deficient cultures. It is possible that elevated cytokine signalling in WNK1-deficient cells may in fact increase susceptibility to AICD as IL-2 signalling has been shown to have pro-apoptotic effects during expansion including upregulating FASL and downregulating FLIP (Refaeli et al., 1998b). TNFα, which is highly upregulated in WNK1-deficient cells, can also signal in an autocrine and paracrine manner to induce AICD (Müller et al., 2009). It would be interesting to determine whether FAS and FASL are upregulated in WNK1-deficient cells during activation, particularly in light of the fact that a number of other activation-induced cell surface receptors are upregulated. Suppression of cell death receptor signalling by NFκB during the early stages of expansion could also be defective in WNK1-deficient cells as ZAP-70 signalling is required for NFκB signalling. The key NFκB family members for survival are RELA and p52 and their nuclear import could be measured to determine whether NFκB also plays a role in WNK1-mediated survival.

Alternatively, transcriptional targets such as GADD45β could be measured as a readout of NFκB transcriptional activity.

T_{FH} cell differentiation is essential for T-dependent class-switched antibody responses. The reduction in WNK1-deficient T_{FH} cells *in vivo* relative to controls is mainly due to reduced proliferation and survival as discussed above, however WNK1 also promotes T_{FH} differentiation itself. Further investigation is required to determine the precise role of WNK1 during this process. However, T_{FH} differentiation is highly dependent on changes to chemokine-dependent migration and Köchl et al. have shown that WNK1 activity is critical for this process. Therefore, it is conceivable that defective migration in response to CXCR5 signalling in WNK1-deficient cells is the reason why fewer of these cells differentiate into T_{FH} cells. This theory could be tested using immunohistochemistry of secondary lymphoid tissue in order to determine whether WNK1-deficient cells are able to migrate to the B cells zone, and into the follicle, as efficiently as their WT counterparts.

In conclusion, WNK1 is involved in a great many aspects of $CD4^+$ T cell activation and function. WNK1-dependent osmoregulation is critical for ZAP-70 activation in response to TCR stimulation and subsequent G1 entry. Furthermore, WNK1 promotes progression through the other stages of the cell cycle, in part by supressing activation of cell cycle checkpoints. Conversely, WNK1 plays a negative regulatory role during expression of cytokines and activation markers in response to TCR and CD28 costimulation. This may be because in the absence of WNK1, osmotic stress induces the expression of these proteins in a TCR-independent manner. Finally, WNK1-dependent survival, proliferation, and differentiation of T_{FH} cells is essential to generate a class-switched antibody response *in vivo*.

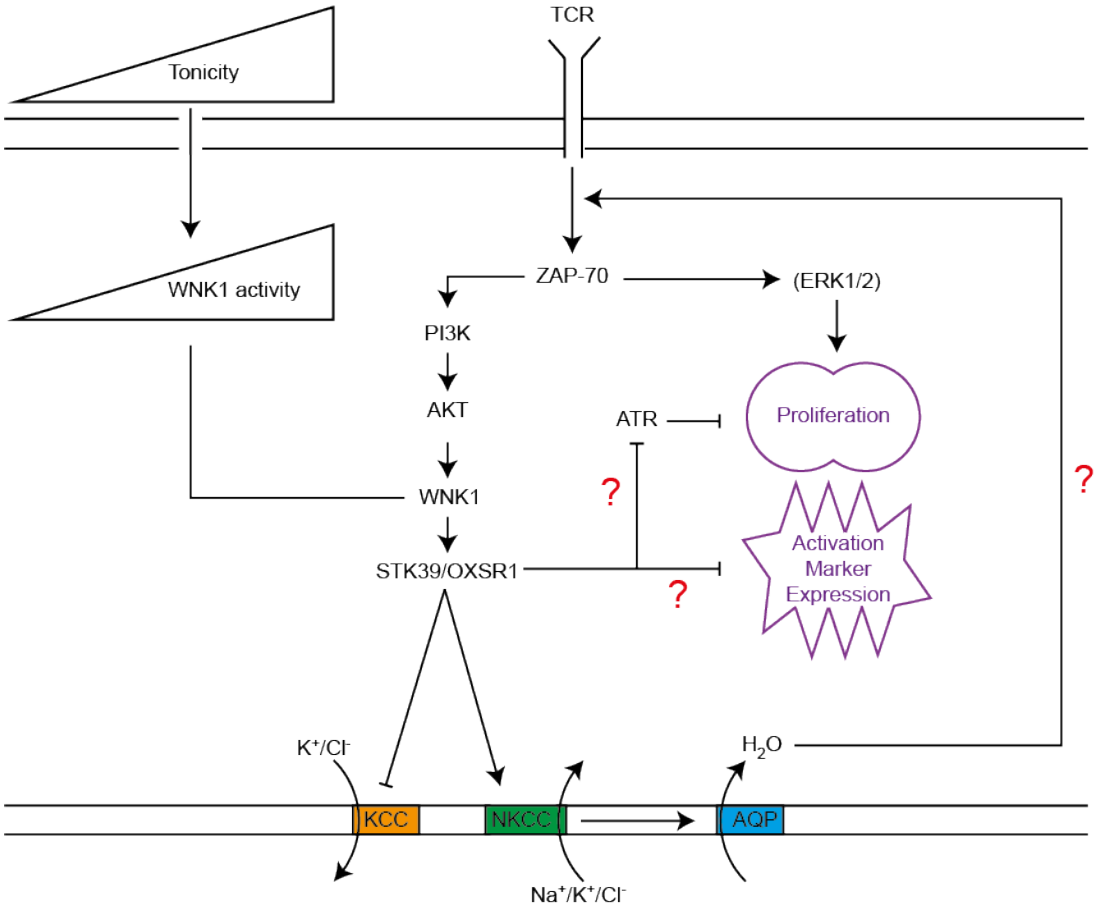

Figure 41. Model for WNK1-dependent regulation of CD4$^+$ T cell activation. WNK1 is activated by hypertonic conditions and TCR stimulation. WNK1 signals via STK39 and OXSR1 to induce ion influx and consequently passive water influx. Water influx promotes TCR-dependent ZAP-70 activation which initiates downstream signalling and ultimately proliferation. Furthermore, WNK1 activity supresses the activation of the ATR-dependent cell cycle checkpoint further facilitating proliferation. The mechanisms by which water influx promotes ZAP-70 activation and WNK1 supresses ATR activation remain major outstanding questions. In this model the author has indicated that WNK1 signalling via OXSR1 and STK39 prevents ATR activation, but additional experiments are required to show that this is the case. WNK1 signalling via STK39 and OXSR1 also suppresses activation marker expression through an unknown mechanism that requires further study.

Reference List

Afkarian, M., Sedy, J. R., Yang, J., Jacobson, N. G., Cereb, N., Yang, S. Y., Murphy, T. L. & Murphy, K. M. 2002. T-bet is a STAT1-induced regulator of IL-12R expression in naïve CD4+ T cells. *Nature Immunology,* 3**,** 549-557.

Aichinger, M., Wu, C., Nedjic, J. & Klein, L. 2013. Macroautophagy substrates are loaded onto MHC class II of medullary thymic epithelial cells for central tolerance. *The Journal of experimental medicine,* 210**,** 287-300.

Akiba, H., Takeda, K., Kojima, Y., Usui, Y., Harada, N., Yamazaki, T., Ma, J., Tezuka, K., Yagita, H. & Okumura, K. 2005. The Role of ICOS in the CXCR5⁺ Follicular B Helper T Cell Maintenance In Vivo. *The Journal of Immunology,* 175**,** 2340.

Alberdi, M., Iglesias, M., Tejedor, S., Merino, R., López-Rodríguez, C. & Aramburu, J. 2017. Context-dependent regulation of Th17-associated genes and IFNγ expression by the transcription factor NFAT5. *Immunology & Cell Biology,* 95**,** 56-67.

Allen, C. D. C., Ansel, K. M., Low, C., Lesley, R., Tamamura, H., Fujii, N. & Cyster, J. G. 2004. Germinal center dark and light zone organization is mediated by CXCR4 and CXCR5. *Nature Immunology,* 5**,** 943-952.

Almeida, A. R. M., Legrand, N., Papiernik, M. & Freitas, A. A. 2002. Homeostasis of Peripheral CD4⁺ T Cells: IL-2Rα and IL-2 Shape a Population of Regulatory Cells That Controls CD4⁺ T Cell Numbers. *The Journal of Immunology,* 169**,** 4850.

Ammazzalorso, F., Pirzio, L. M., Bignami, M., Franchitto, A. & Pichierri, P. 2010. ATR and ATM differently regulate WRN to prevent DSBs at stalled replication forks and promote replication fork recovery. *The EMBO journal,* 29**,** 3156-3169.

Andreassen, P. R., D'andrea, A. D. & Taniguchi, T. 2004. ATR couples FANCD2 monoubiquitination to the DNA-damage response. *Genes & Development,* 18**,** 1958-1963.

Anglana, M., Apiou, F., Bensimon, A. & Debatisse, M. 2003. Dynamics of DNA replication in mammalian somatic cells: nucleotide pool modulates origin choice and interorigin spacing. *Cell,* 114**,** 385-94.

Appleby, M. W., Gross, J. A., Cooke, M. P., Levin, S. D., Qian, X. & Perlmutter, R. M. 1992. Defective T cell receptor signaling in mice lacking the thymic isoform of p59fyn. *Cell,* 70**,** 751-763.

Appleman, L. J., Berezovskaya, A., Grass, I. & Boussiotis, V. A. 2000. CD28 Costimulation Mediates T Cell Expansion Via IL-2-Independent and IL-2-Dependent Regulation of Cell Cycle Progression. *The Journal of Immunology,* 164**,** 144.

Appleman, L. J., Van Puijenbroek, A. A., Shu, K. M., Nadler, L. M. & Boussiotis, V. A. 2002. CD28 costimulation mediates down-regulation of p27kip1 and cell cycle progression by activation of the PI3K/PKB signaling pathway in primary human T cells. *J Immunol,* 168**,** 2729-36.

Aramburu, J. & López-Rodríguez, C. 2019. Regulation of Inflammatory Functions of Macrophages and T Lymphocytes by NFAT5. *Frontiers in Immunology,* 10.

Ardouin, L., Bracke, M., Mathiot, A., Pagakis, S. N., Norton, T., Hogg, N. & Tybulewicz, V. L. J. 2003. Vav1 transduces TCR signals required for LFA-1 function and cell polarization at the immunological synapse. *European Journal of Immunology,* 33**,** 790-797.

Asselin-Paturel, C., Brizard, G., Chemin, K., Boonstra, A., O'garra, A., Vicari, A. & Trinchieri, G. 2005. Type I interferon dependence of plasmacytoid dendritic cell activation and migration. *J Exp Med,* 201**,** 1157-67.

Au-Yeung, B. B., Zikherman, J., Mueller, J. L., Ashouri, J. F., Matloubian, M., Cheng, D. A., Chen, Y., Shokat, K. M. & Weiss, A. 2014. A sharp T-cell antigen receptor signaling threshold for T-cell proliferation. *Proceedings of the National Academy of Sciences,* 111**,** E3679.

Baaten, B. J., Li, C. R., Deiro, M. F., Lin, M. M., Linton, P. J. & Bradley, L. M. 2010. CD44 regulates survival and memory development in Th1 cells. *Immunity,* 32**,** 104-15.

Bachmann, M. F., Mckall-Faienza, K., Schmits, R., Bouchard, D., Beach, J., Speiser, D. E., Mak, T. W. & Ohashi, P. S. 1997. Distinct roles for LFA-1 and CD28 during activation of naive T cells: adhesion versus costimulation. *Immunity,* 7**,** 549-57.

Bajenoff, M., Egen, J. G., Koo, L. Y., Laugier, J. P., Brau, F., Glaichenhaus, N. & Germain, R. N. 2006. Stromal cell networks regulate lymphocyte entry, migration, and territoriality in lymph nodes. *Immunity,* 25**,** 989-1001.

Balciunaite, E., Spektor, A., Lents, N. H., Cam, H., Te Riele, H., Scime, A., Rudnicki, M. A., Young, R. & Dynlacht, B. D. 2005. Pocket Protein Complexes Are Recruited to Distinct Targets in Quiescent and Proliferating Cells. *Molecular and Cellular Biology,* 25**,** 8166.

Balla, T. & Várnai, P. 2009. Visualization of cellular phosphoinositide pools with GFP-fused protein-domains. *Current protocols in cell biology,* Chapter 24**,** Unit-24.4.

Ballek, O., Valečka, J., Manning, J. & Filipp, D. 2015. The pool of preactivated Lck in the initiation of T-cell signaling: a critical re-evaluation of the Lck standby model. *Immunology & Cell Biology,* 93**,** 384-395.

Banchereau, J., Briere, F., Caux, C., Davoust, J., Lebecque, S., Liu, Y.-J., Pulendran, B. & Palucka, K. 2000. Immunobiology of Dendritic Cells. *Annual Review of Immunology,* 18**,** 767-811.

Bancroft, G. J., Schreiber, R. D. & Unanue, E. R. 1991. Natural immunity: a T-cell-independent pathway of macrophage activation, defined in the scid mouse. *Immunol Rev,* 124**,** 5-24.

Barnden, M. J., Allison, J., Heath, W. R. & Carbone, F. R. 1998. Defective TCR expression in transgenic mice constructed using cDNA-based alpha- and beta-chain genes under the control of heterologous regulatory elements. *Immunol Cell Biol,* 76**,** 34-40.

Baumjohann, D., Okada, T. & Ansel, K. M. 2011. Cutting Edge: Distinct Waves of BCL6 Expression during T Follicular Helper Cell Development. *The Journal of Immunology,* 187**,** 2089.

Beach, D., Gonen, R., Bogin, Y., Reischl, I. G. & Yablonski, D. 2007. Dual role of SLP-76 in mediating T cell receptor-induced activation of phospholipase C-gamma1. *J Biol Chem,* 282**,** 2937-46.

Beddoe, T., Chen, Z., Clements, C. S., Ely, L. K., Bushell, S. R., Vivian, J. P., Kjer-Nielsen, L., Pang, S. S., Dunstone, M. A., Liu, Y. C., Macdonald, W. A., Perugini, M. A., Wilce, M. C., Burrows, S. R., Purcell, A. W., Tiganis, T., Bottomley, S. P., Mccluskey, J. & Rossjohn, J. 2009. Antigen ligation triggers a conformational change within the constant domain of the alphabeta T cell receptor. *Immunity,* 30**,** 777-88.

Beltman, J. B., Maree, A. F., Lynch, J. N., Miller, M. J. & De Boer, R. J. 2007. Lymph node topology dictates T cell migration behavior. *J Exp Med,* 204**,** 771-80.

Berek, C., Berger, A. & Apel, M. 1991. Maturation of the immune response in germinal centers. *Cell,* 67**,** 1121-9.

Berga-Bolaños, R., Drews-Elger, K., Aramburu, J. & López-Rodríguez, C. 2010. NFAT5 Regulates T Lymphocyte Homeostasis and CD24-Dependent T Cell Expansion under Pathologic Hypernatremia. *The Journal of Immunology,* 185**,** 6624.

Berry, M. R., Mathews, R. J., Ferdinand, J. R., Jing, C., Loudon, K. W., Wlodek, E., Dennison, T. W., Kuper, C., Neuhofer, W. & Clatworthy, M. R. 2017. Renal Sodium Gradient Orchestrates a Dynamic Antibacterial Defense Zone. *Cell,* 170**,** 860-874.e19.

Bertoli, C., Klier, S., Mcgowan, C., Wittenberg, C. & De bruin, Robertus a. M. 2013. Chk1 Inhibits E2F6 Repressor Function in Response to Replication Stress to Maintain Cell-Cycle Transcription. *Current Biology,* 23**,** 1629-1637.

Beucher, A., Birraux, J., Tchouandong, L., Barton, O., Shibata, A., Conrad, S., Goodarzi, A. A., Krempler, A., Jeggo, P. A. & Löbrich, M. 2009. ATM and Artemis promote homologous recombination of radiation-induced DNA double-strand breaks in G2. *The EMBO Journal,* 28**,** 3413-3427.

Blum, J. S., Wearsch, P. A. & Cresswell, P. 2013. Pathways of antigen processing. *Annual review of immunology,* 31**,** 443-473.

Boomer, J. S., Deppong, C. M., Shah, D. D., Bricker, T. L. & Green, J. M. 2014. Cutting edge: A double-mutant knockin of the CD28 YMNM and PYAP motifs reveals a critical role for the YMNM motif in regulation of T cell proliferation and Bcl-xL expression. *J Immunol,* 192**,** 3465-9.

Boyden, L. M., Choi, M., Choate, K. A., Nelson-Williams, C. J., Farhi, A., Toka, H. R., Tikhonova, I. R., Bjornson, R., Mane, S. M., Colussi, G., Lebel, M., Gordon, R. D., Semmekrot, B. A., Poujol, A., Valimaki, M. J., De Ferrari, M. E., Sanjad, S. A., Gutkin, M., Karet, F. E., Tucci, J. R., Stockigt, J. R., Keppler-Noreuil, K. M., Porter, C. C., Anand, S. K., Whiteford, M. L., Davis, I. D., Dewar, S. B., Bettinelli, A., Fadrowski, J. J., Belsha, C. W., Hunley, T. E., Nelson, R. D., Trachtman, H., Cole, T. R., Pinsk, M., Bockenhauer, D., Shenoy, M., Vaidyanathan, P., Foreman, J. W., Rasoulpour, M., Thameem, F., Al-Shahrouri, H. Z., Radhakrishnan, J., Gharavi, A. G., Goilav, B. & Lifton, R. P. 2012. Mutations in kelch-like 3 and cullin 3 cause hypertension and electrolyte abnormalities. *Nature,* 482**,** 98-102.

Brändle, D., Müller, C., Rülicke, T., Hengartner, H. & Pircher, H. 1992. Engagement of the T-cell receptor during positive selection in the thymus down-regulates RAG-1 expression. *Proceedings of the National Academy of Sciences,* 89**,** 9529.

Brdicka, T., Kadlecek, T. A., Roose, J. P., Pastuszak, A. W. & Weiss, A. 2005. Intramolecular Regulatory Switch in ZAP-70: Analogy with Receptor Tyrosine Kinases. *Molecular and Cellular Biology,* 25**,** 4924.

Brogdon, J. L., Leitenberg, D. & Bottomly, K. 2002. The Potency of TCR Signaling Differentially Regulates NFATc/p Activity and Early IL-4 Transcription in Naive CD4⁺ T Cells. *The Journal of Immunology,* 168**,** 3825.

Brugarolas, J., Chandrasekaran, C., Gordon, J. I., Beach, D., Jacks, T. & Hannon, G. J. 1995. Radiation-induced cell cycle arrest compromised by p21 deficiency. *Nature,* 377**,** 552-557.

Buis, J., Wu, Y., Deng, Y., Leddon, J., Westfield, G., Eckersdorff, M., Sekiguchi, J. M., Chang, S. & Ferguson, D. O. 2008. Mre11 nuclease activity has essential roles in DNA repair and genomic stability distinct from ATM activation. *Cell,* 135**,** 85-96.

Bunnell, S. C., Hong, D. I., Kardon, J. R., Yamazaki, T., Mcglade, C. J., Barr, V. A. & Samelson, L. E. 2002. T cell receptor ligation induces the formation of dynamically regulated signaling assemblies. *Journal of Cell Biology,* 158**,** 1263-1275.

Burchill, M. A., Yang, J., Vang, K. B., Moon, J. J., Chu, H. H., Lio, C.-W. J., Vegoe, A. L., Hsieh, C.-S., Jenkins, M. K. & Farrar, M. A. 2008. Linked T Cell Receptor and Cytokine Signaling Govern the Development of the Regulatory T Cell Repertoire. *Immunity,* 28**,** 112-121.

Burkhardt, A. L., Brunswick, M., Bolen, J. B. & Mond, J. J. 1991. Anti-immunoglobulin stimulation of B lymphocytes activates src-related protein-tyrosine kinases.

Proceedings of the National Academy of Sciences of the United States of America, 88**,** 7410-7414.

Byun, T. S., Pacek, M., Yee, M. C., Walter, J. C. & Cimprich, K. A. 2005. Functional uncoupling of MCM helicase and DNA polymerase activities activates the ATR-dependent checkpoint. *Genes Dev,* 19**,** 1040-52.

Cabaniols, J.-P., Fazilleau, N., Casrouge, A., Kourilsky, P. & Kanellopoulos, J. M. 2001. Most α/β T Cell Receptor Diversity Is Due to Terminal Deoxynucleotidyl Transferase. *Journal of Experimental Medicine,* 194**,** 1385-1390.

Campi, G., Varma, R. & Dustin, M. L. 2005. Actin and agonist MHC-peptide complex-dependent T cell receptor microclusters as scaffolds for signaling. *J Exp Med,* 202**,** 1031-6.

Cannons, J. L., Qi, H., Lu, K. T., Dutta, M., Gomez-Rodriguez, J., Cheng, J., Wakeland, E. K., Germain, R. N. & Schwartzberg, P. L. 2010. Optimal Germinal Center Responses Require a Multistage T Cell:B Cell Adhesion Process Involving Integrins, SLAM-Associated Protein, and CD84. *Immunity,* 32**,** 253-265.

Carpino, N., Turner, S., Mekala, D., Takahashi, Y., Zang, H., Geiger, T. L., Doherty, P. & Ihle, J. N. 2004. Regulation of ZAP-70 Activation and TCR Signaling by Two Related Proteins, Sts-1 and Sts-2. *Immunity,* 20**,** 37-46.

Carrière, A., Cargnello, M., Julien, L.-A., Gao, H., Bonneil, É., Thibault, P. & Roux, P. P. 2008. Oncogenic MAPK Signaling Stimulates mTORC1 Activity by Promoting RSK-Mediated Raptor Phosphorylation. *Current Biology,* 18**,** 1269-1277.

Carriere, A., Romeo, Y., Acosta-Jaquez, H. A., Moreau, J., Bonneil, E., Thibault, P., Fingar, D. C. & Roux, P. P. 2011. ERK1/2 phosphorylate Raptor to promote Ras-dependent activation of mTOR complex 1 (mTORC1). *The Journal of biological chemistry,* 286**,** 567-577.

Castellanos Mdel, C., Lopez-Giral, S., Lopez-Cabrera, M. & De Landazuri, M. O. 2002. Multiple cis-acting elements regulate the expression of the early T cell activation antigen CD69. *Eur J Immunol,* 32**,** 3108-17.

Cella, M., Engering, A., Pinet, V., Pieters, J. & Lanzavecchia, A. 1997. Inflammatory stimuli induce accumulation of MHC class II complexes on dendritic cells. *Nature,* 388**,** 782-787.

Chabot, V., Martin, L., Meley, D., Sensebé, L., Baron, C., Lebranchu, Y., Dehaut, F. & Velge-Roussel, F. 2016. Unexpected impairment of TNF-α-induced maturation of human dendritic cells in vitro by IL-4. *Journal of Translational Medicine,* 14**,** 93.

Chakarov, S. & Fazilleau, N. 2014. Monocyte-derived dendritic cells promote T follicular helper cell differentiation. *EMBO Molecular Medicine,* 6**,** 590-603.

Chan, A. C., Irving, B. A., Fraser, J. D. & Weiss, A. 1991. The zeta chain is associated with a tyrosine kinase and upon T-cell antigen receptor stimulation associates with ZAP-70, a 70-kDa tyrosine phosphoprotein. *Proceedings of the National Academy of Sciences,* 88**,** 9166.

Chanut, P., Britton, S., Coates, J., Jackson, S. P. & Calsou, P. 2016. Coordinated nuclease activities counteract Ku at single-ended DNA double-strand breaks. *Nature Communications,* 7**,** 12889.

Chao, C., Herr, D., Chun, J. & Xu, Y. 2006. Ser18 and 23 phosphorylation is required for p53-dependent apoptosis and tumor suppression. *The EMBO Journal,* 25**,** 2615-2622.

Chehab, N. H., Malikzay, A., Appel, M. & Halazonetis, T. D. 2000. Chk2/hCds1 functions as a DNA damage checkpoint in G(1) by stabilizing p53. *Genes & development,* 14**,** 278-288.

Chen, C., Zhao, S., Karnad, A. & Freeman, J. W. 2018. The biology and role of CD44 in cancer progression: therapeutic implications. *J Hematol Oncol,* 11**,** 64.

Chen, J., Saha, P., Kornbluth, S., Dynlacht, B. D. & Dutta, A. 1996. Cyclin-binding motifs are essential for the function of p21CIP1. *Molecular and Cellular Biology,* 16**,** 4673.

Chen, Z., Laurence, A., Kanno, Y., Pacher-Zavisin, M., Zhu, B.-M., Tato, C., Yoshimura, A., Hennighausen, L. & O'shea, J. J. 2006. Selective regulatory function of Socs3 in the formation of IL-17-secreting T cells. *Proceedings of the National Academy of Sciences of the United States of America,* 103**,** 8137-8142.

Cheng, C.-J. & Huang, C.-L. 2011. Activation of PI3-kinase stimulates endocytosis of ROMK via Akt1/SGK1-dependent phosphorylation of WNK1. *Journal of the American Society of Nephrology : JASN,* 22**,** 460-471.

Ching, K. A., Kawakami, Y., Kawakami, T. & Tsoukas, C. D. 1999. Emt/Itk Associates with Activated TCR Complexes: Role of the Pleckstrin Homology Domain. *The Journal of Immunology,* 163**,** 6006.

Cho, Y.-L., Flossdorf, M., Kretschmer, L., Höfer, T., Busch, D. H. & Buchholz, V. R. 2017. TCR Signal Quality Modulates Fate Decisions of Single CD4⁺ T Cells in a Probabilistic Manner. *Cell Reports,* 20**,** 806-818.

Cibrian, D., Saiz, M. L., De La Fuente, H., Sanchez-Diaz, R., Moreno-Gonzalo, O., Jorge, I., Ferrarini, A., Vazquez, J., Punzon, C., Fresno, M., Vicente-Manzanares, M., Dauden, E., Fernandez-Salguero, P. M., Martin, P. & Sanchez-Madrid, F. 2016. CD69 controls the uptake of L-tryptophan through LAT1-CD98 and AhR-dependent secretion of IL-22 in psoriasis. *Nat Immunol,* 17**,** 985-96.

Ciofani, M., Knowles, G. C., Wiest, D. L., Von Boehmer, H. & Zúñiga-Pflücker, J. C. 2006. Stage-Specific and Differential Notch Dependency at the αβ and γδ T Lineage Bifurcation. *Immunity,* 25**,** 105-116.

Clair, S. S., Giono, L., Varmeh-Ziaie, S., Resnick-Silverman, L., Liu, W.-J., Padi, A., Dastidar, J., Dacosta, A., Mattia, M. & Manfredi, J. J. 2004. DNA Damage-Induced Downregulation of Cdc25C Is Mediated by p53 via Two Independent Mechanisms: One Involves Direct Binding to the cdc25C Promoter. *Molecular Cell,* 16**,** 725-736.

Coffey, F., Alabyev, B. & Manser, T. 2009. Initial Clonal Expansion of Germinal Center B Cells Takes Place at the Perimeter of Follicles. *Immunity,* 30**,** 599-609.

Comrie, W. A., Babich, A. & Burkhardt, J. K. 2015. F-actin flow drives affinity maturation and spatial organization of LFA-1 at the immunological synapse. *J Cell Biol,* 208**,** 475-91.

Cordoba, S.-P., Choudhuri, K., Zhang, H., Bridge, M., Basat, A. B., Dustin, M. L. & Van Der Merwe, P. A. 2013. The large ectodomains of CD45 and CD148 regulate their segregation from and inhibition of ligated T-cell receptor. *Blood,* 121**,** 4295-4302.

Coster, G., Frigola, J., Beuron, F., Morris, E. P. & Diffley, J. F. 2014. Origin licensing requires ATP binding and hydrolysis by the MCM replicative helicase. *Mol Cell,* 55**,** 666-77.

Cote-Sierra, J., Foucras, G., Guo, L., Chiodetti, L., Young, H. A., Hu-Li, J., Zhu, J. & Paul, W. E. 2004. Interleukin 2 plays a central role in Th2 differentiation. *Proc Natl Acad Sci U S A,* 101**,** 3880-5.

Couch, F. B., Bansbach, C. E., Driscoll, R., Luzwick, J. W., Glick, G. G., Bétous, R., Carroll, C. M., Jung, S. Y., Qin, J., Cimprich, K. A. & Cortez, D. 2013. ATR phosphorylates SMARCAL1 to prevent replication fork collapse. *Genes & development,* 27**,** 1610-1623.

Courtney, A. H., Amacher, J. F., Kadlecek, T. A., Mollenauer, M. N., Au-Yeung, B. B., Kuriyan, J. & Weiss, A. 2017. A Phosphosite within the SH2 Domain of Lck Regulates Its Activation by CD45. *Molecular Cell,* 67**,** 498-511.e6.

D'ambrosio, D., Cantrell, D. A., Frati, L., Santoni, A. & Testi, R. 1994. Involvement of p21ras activation in T cell CD69 expression. *Eur J Immunol,* 24**,** 616-20.

Daley, S. R., Coakley, K. M., Hu, D. Y., Randall, K. L., Jenne, C. N., Limnander, A., Myers, D. R., Polakos, N. K., Enders, A., Roots, C., Balakishnan, B., Miosge, L. A., Sjollema, G., Bertram, E. M., Field, M. A., Shao, Y., Andrews, T. D., Whittle, B., Barnes, S. W., Walker, J. R., Cyster, J. G., Goodnow, C. C. & Roose, J. P. 2013. Rasgrp1 mutation increases naive T-cell CD44 expression and drives mTOR-dependent accumulation of Helios(+) T cells and autoantibodies. *Elife,* 2**,** e01020.

Das, J., Ho, M., Zikherman, J., Govern, C., Yang, M., Weiss, A., Chakraborty, A. K. & Roose, J. P. 2009. Digital signaling and hysteresis characterize ras activation in lymphoid cells. *Cell,* 136**,** 337-51.

Davies, A. A., Masson, J.-Y., Mcilwraith, M. J., Stasiak, A. Z., Stasiak, A., Venkitaraman, A. R. & West, S. C. 2001. Role of BRCA2 in Control of the RAD51 Recombination and DNA Repair Protein. *Molecular Cell,* 7**,** 273-282.

Davies, S. L., North, P. S., Dart, A., Lakin, N. D. & Hickson, I. D. 2004. Phosphorylation of the Bloom's syndrome helicase and its role in recovery from S-phase arrest. *Molecular and cellular biology,* 24**,** 1279-1291.

De La Fuente, H., Cruz-Adalia, A., Martinez Del Hoyo, G., Cibrian-Vera, D., Bonay, P., Perez-Hernandez, D., Vazquez, J., Navarro, P., Gutierrez-Gallego, R., Ramirez-Huesca, M., Martin, P. & Sanchez-Madrid, F. 2014. The leukocyte activation receptor CD69 controls T cell differentiation through its interaction with galectin-1. *Mol Cell Biol,* 34**,** 2479-87.

De Los Heros, P., Alessi, D. R., Gourlay, R., Campbell, D. G., Deak, M., Macartney, T. J., Kahle, K. T. & Zhang, J. 2014. The WNK-regulated SPAK/OSR1 kinases directly phosphorylate and inhibit the K+-Cl- co-transporters. *Biochem J,* 458**,** 559-73.

De Luca, C., Kowalski, T. J., Zhang, Y., Elmquist, J. K., Lee, C., Kilimann, M. W., Ludwig, T., Liu, S. M. & Chua, S. C., Jr. 2005. Complete rescue of obesity, diabetes, and infertility in db/db mice by neuron-specific LEPR-B transgenes. *J Clin Invest,* 115**,** 3484-93.

Deford-Watts, L. M., Tassin, T. C., Becker, A. M., Medeiros, J. J., Albanesi, J. P., Love, P. E., Wulfing, C. & Van Oers, N. S. 2009. The cytoplasmic tail of the T cell receptor CD3 epsilon subunit contains a phospholipid-binding motif that regulates T cell functions. *J Immunol,* 183**,** 1055-64.

Delaloy, C., Lu, J., Houot, A. M., Disse-Nicodeme, S., Gasc, J. M., Corvol, P. & Jeunemaitre, X. 2003. Multiple promoters in the WNK1 gene: one controls expression of a kidney-specific kinase-defective isoform. *Mol Cell Biol,* 23**,** 9208-21.

Delarue, M., Brittingham, G. P., Pfeffer, S., Surovtsev, I. V., Pinglay, S., Kennedy, K. J., Schaffer, M., Gutierrez, J. I., Sang, D., Poterewicz, G., Chung, J. K., Plitzko, J. M., Groves, J. T., Jacobs-Wagner, C., Engel, B. D. & Holt, L. J. 2018. mTORC1 Controls Phase Separation and the Biophysical Properties of the Cytoplasm by Tuning Crowding. *Cell,* 174**,** 338-349.e20.

Deng, G. & Podack, E. R. 1993. Suppression of apoptosis in a cytotoxic T-cell line by interleukin 2-mediated gene transcription and deregulated expression of the protooncogene bcl-2. *Proc Natl Acad Sci U S A,* 90**,** 2189-93.

Dengjel, J., Schoor, O., Fischer, R., Reich, M., Kraus, M., Müller, M., Kreymborg, K., Altenberend, F., Brandenburg, J., Kalbacher, H., Brock, R., Driessen, C., Rammensee, H.-G. & Stevanovic, S. 2005. Autophagy promotes MHC class II presentation of peptides from intracellular source proteins. *Proceedings of the National Academy of Sciences,* 102**,** 7922.

Deutsch, C. & Chen, L. Q. 1993. Heterologous expression of specific K+ channels in T lymphocytes: functional consequences for volume regulation. *Proc Natl Acad Sci U S A,* 90**,** 10036-40.

Dhein, J., Walczak, H., Baumler, C., Debatin, K. M. & Krammer, P. H. 1995. Autocrine T-cell suicide mediated by APO-1/(Fas/CD95). *Nature,* 373**,** 438-41.

Di Bartolo, V., Mege, D., Germain, V., Pelosi, M., Dufour, E., Michel, F., Magistrelli, G., Isacchi, A. & Acuto, O. 1999. Tyrosine 319, a newly identified phosphorylation site of ZAP-70, plays a critical role in T cell antigen receptor signaling. *J Biol Chem,* 274**,** 6285-94.

Dianzani, U., Bragardo, M., Tosti, A., Ruggeri, L., Volpi, I., Casucci, M., Bottarel, F., Feito, M. J., Bonissoni, S. & Velardi, A. 1999. CD44 signaling through p56lck involves lateral association with CD4 in human CD4+ T cells. *Int Immunol,* 11**,** 1085-92.

Dienz, O., Eaton, S. M., Bond, J. P., Neveu, W., Moquin, D., Noubade, R., Briso, E. M., Charland, C., Leonard, W. J., Ciliberto, G., Teuscher, C., Haynes, L. & Rincon, M. 2009. The induction of antibody production by IL-6 is indirectly mediated by IL-21 produced by CD4+ T cells. *Journal of Experimental Medicine,* 206**,** 69-78.

Dijkers, P. F., Medema, R. H., Lammers, J. W., Koenderman, L. & Coffer, P. J. 2000. Expression of the pro-apoptotic Bcl-2 family member Bim is regulated by the forkhead transcription factor FKHR-L1. *Curr Biol,* 10**,** 1201-4.

Dinarello, C. A. 1989. Interleukin-1 and its biologically related cytokines. *Adv Immunol,* 44**,** 153-205.

Ditoro, D., Winstead, C. J., Pham, D., Witte, S., Andargachew, R., Singer, J. R., Wilson, C. G., Zindl, C. L., Luther, R. J., Silberger, D. J., Weaver, B. T., Kolawole, E. M., Martinez, R. J., Turner, H., Hatton, R. D., Moon, J. J., Way, S. S., Evavold, B. D. & Weaver, C. T. 2018. Differential IL-2 expression defines developmental fates of follicular versus nonfollicular helper T cells. *Science,* 361**,** eaao2933.

Dmitrieva, N., Michea, L. & Burg, M. 2001. p53 Protects renal inner medullary cells from hypertonic stress by restricting DNA replication. *American Journal of Physiology-Renal Physiology,* 281**,** F522-F530.

Dmitrieva, N. I., Bulavin, D. V. & Burg, M. B. 2003. High NaCl causes Mre11 to leave the nucleus, disrupting DNA damage signaling and repair. *American Journal of Physiology-Renal Physiology,* 285**,** F266-F274.

Dmitrieva, N. I., Bulavin, D. V., Fornace, A. J., Jr. & Burg, M. B. 2002. Rapid activation of G2/M checkpoint after hypertonic stress in renal inner medullary epithelial (IME) cells is protective and requires p38 kinase. *Proceedings of the National Academy of Sciences of the United States of America,* 99**,** 184-189.

Dmitrieva, N. I., Cai, Q. & Burg, M. B. 2004. Cells adapted to high NaCl have many DNA breaks and impaired DNA repair both in cell culture and <em>in vivo</em&gt. *Proceedings of the National Academy of Sciences of the United States of America,* 101**,** 2317.

Dodson, L. F., Boomer, J. S., Deppong, C. M., Shah, D. D., Sim, J., Bricker, T. L., Russell, J. H. & Green, J. M. 2009. Targeted knock-in mice expressing mutations of CD28 reveal an essential pathway for costimulation. *Mol Cell Biol,* 29**,** 3710-21.

Dong, Zheng, L., Lin, J., Zhang, B., Zhu, Y., Li, N., Xie, S., Wang, Y., Gao, N. & Huang, Z. 2019. Structural basis of assembly of the human T cell receptor-CD3 complex. *Nature,* 573**,** 546-552.

Douglass, A. D. & Vale, R. D. 2005. Single-molecule microscopy reveals plasma membrane microdomains created by protein-protein networks that exclude or trap signaling molecules in T cells. *Cell,* 121**,** 937-50.

Drews-Elger, K., Ortells, M. C., Rao, A., López-Rodriguez, C. & Aramburu, J. 2009. The transcription factor NFAT5 is required for cyclin expression and cell cycle progression in cells exposed to hypertonic stress. *PloS one,* 4**,** e5245-e5245.

Dungrawala, H., Rose, Kristie l., Bhat, Kamakoti p., Mohni, Kareem n., Glick, Gloria g., Couch, Frank b. & Cortez, D. 2015. The Replication Checkpoint Prevents Two Types of Fork Collapse without Regulating Replisome Stability. *Molecular Cell,* 59**,** 998-1010.

Dutta, D., Barr, V. A., Akpan, I., Mittelstadt, P. R., Singha, L. I., Samelson, L. E. & Ashwell, J. D. 2017. Recruitment of calcineurin to the TCR positively regulates T cell activation. *Nature Immunology,* 18**,** 196-204.

Eddahri, F., Denanglaire, S., Bureau, F., Spolski, R., Leonard, W. J., Leo, O. & Andris, F. 2009. Interleukin-6/STAT3 signaling regulates the ability of naive T cells to acquire B-cell help capacities. *Blood,* 113**,** 2426-2433.

Ellis, R. J. 2001. Macromolecular crowding: obvious but underappreciated. *Trends in Biochemical Sciences,* 26**,** 597-604.

Ellison, V. & Stillman, B. 2003. Biochemical Characterization of DNA Damage Checkpoint Complexes: Clamp Loader and Clamp Complexes with Specificity for 5′ Recessed DNA. *PLOS Biology,* 1**,** e33.

Elvira-Matelot, E., Zhou, X. O., Farman, N., Beaurain, G., Henrion-Caude, A., Hadchouel, J. & Jeunemaitre, X. 2010. Regulation of WNK1 expression by miR-192 and aldosterone. *J Am Soc Nephrol,* 21**,** 1724-31.

Espenshade, P. J. & Hughes, A. L. 2007. Regulation of Sterol Synthesis in Eukaryotes. *Annual Review of Genetics,* 41**,** 401-427.

Evans, R., Lellouch, A. C., Svensson, L., Mcdowall, A. & Hogg, N. 2011. The integrin LFA-1 signals through ZAP-70 to regulate expression of high-affinity LFA-1 on T lymphocytes. *Blood,* 117**,** 3331-3342.

Falck, J., Mailand, N., Syljuåsen, R. G., Bartek, J. & Lukas, J. 2001. The ATM–Chk2–Cdc25A checkpoint pathway guards against radioresistant DNA synthesis. *Nature,* 410**,** 842-847.

Falvo, J. V., Uglialoro, A. M., Brinkman, B. M. N., Merika, M., Parekh, B. S., Tsai, E. Y., King, H. C., Morielli, A. D., Peralta, E. G., Maniatis, T., Thanos, D. & Goldfeld, A. E. 2000. Stimulus-Specific Assembly of Enhancer Complexes on the Tumor Necrosis Factor Alpha Gene Promoter. *Molecular and Cellular Biology,* 20**,** 2239-2247.

Fan, M. Y., Low, J. S., Tanimine, N., Finn, K. K., Priyadharshini, B., Germana, S. K., Kaech, S. M. & Turka, L. A. 2018. Differential Roles of IL-2 Signaling in Developing versus Mature Tregs. *Cell Reports,* 25**,** 1204-1213.e4.

Fang, D., Cui, K., Mao, K., Hu, G., Li, R., Zheng, M., Riteau, N., Reiner, S. L., Sher, A., Zhao, K. & Zhu, J. 2018. Transient T-bet expression functionally specifies a distinct T follicular helper subset. *Journal of Experimental Medicine,* 215**,** 2705-2714.

Faroudi, M., Hons, M., Zachacz, A., Dumont, C., Lyck, R., Stein, J. V. & Tybulewicz, V. L. 2010. Critical roles for Rac GTPases in T-cell migration to and within lymph nodes. *Blood,* 116**,** 5536-47.

Fazilleau, N., Mcheyzer-Williams, L. J., Rosen, H. & Mcheyzer-Williams, M. G. 2009. The function of follicular helper T cells is regulated by the strength of T cell antigen receptor binding. *Nat Immunol,* 10**,** 375-84.

Feil, R., Wagner, J., Metzger, D. & Chambon, P. 1997. Regulation of Cre recombinase activity by mutated estrogen receptor ligand-binding domains. *Biochem Biophys Res Commun,* 237**,** 752-7.

Fernandes, R. A., Yu, C., Carmo, A. M., Evans, E. J., Van Der Merwe, P. A. & Davis, S. J. 2010. What controls T cell receptor phosphorylation? *Cell,* 142**,** 668-9.

Fernandez, P. C., Frank, S. R., Wang, L., Schroeder, M., Liu, S., Greene, J., Cocito, A. & Amati, B. 2003. Genomic targets of the human c-Myc protein. *Genes & development,* 17**,** 1115-1129.

Filippi, B. M., De Los Heros, P., Mehellou, Y., Navratilova, I., Gourlay, R., Deak, M., Plater, L., Toth, R., Zeqiraj, E. & Alessi, D. R. 2011. MO25 is a master regulator of SPAK/OSR1 and MST3/MST4/YSK1 protein kinases. *The EMBO Journal,* 30**,** 1730-1741.

Frank, S. R., Schroeder, M., Fernandez, P., Taubert, S. & Amati, B. 2001. Binding of c-Myc to chromatin mediates mitogen-induced acetylation of histone H4 and gene activation. *Genes & development,* 15**,** 2069-2082.

Fraser, J. D., Irving, B. A., Crabtree, G. R. & Weiss, A. 1991. Regulation of interleukin-2 gene enhancer activity by the T cell accessory molecule CD28. *Science,* 251**,** 313-6.

Friedel, P., Kahle, K. T., Zhang, J., Hertz, N., Pisella, L. I., Buhler, E., Schaller, F., Duan, J., Khanna, A. R., Bishop, P. N., Shokat, K. M. & Medina, I. 2015. WNK1-regulated inhibitory phosphorylation of the KCC2 cotransporter maintains the depolarizing action of GABA in immature neurons. *Science Signaling,* 8**,** ra65.

Fukuda, T., Miki, T., Yoshida, T., Hatano, M., Ohashi, K., Hirosawa, S. & Tokuhisa, T. 1995. The murine BCL6 gene is induced in activated lymphocytes as an immediate early gene. *Oncogene,* 11**,** 1657-1663.

Gagnon, E., Schubert, D. A., Gordo, S., Chu, H. H. & Wucherpfennig, K. W. 2012. Local changes in lipid environment of TCR microclusters regulate membrane binding by the CD3epsilon cytoplasmic domain. *J Exp Med,* 209**,** 2423-39.

Gao, M., Guo, G., Huang, J., Kloeber, J. A., Zhao, F., Deng, M., Tu, X., Kim, W., Zhou, Q., Zhang, C., Yin, P., Luo, K. & Lou, Z. 2020. USP52 regulates DNA end resection and chemosensitivity through removing inhibitory ubiquitination from CtIP. *Nature Communications,* 11**,** 5362.

Garçon, F. & Okkenhaug, K. 2016. PI3Kδ promotes CD4+ T-cell interactions with antigen-presenting cells by increasing LFA-1 binding to ICAM-1. *Immunology & Cell Biology,* 94**,** 486-495.

Garçon, F., Patton, D. T., Emery, J. L., Hirsch, E., Rottapel, R., Sasaki, T. & Okkenhaug, K. 2008. CD28 provides T-cell costimulation and enhances PI3K activity at the immune synapse independently of its capacity to interact with the p85/p110 heterodimer. *Blood,* 111**,** 1464-1471.

Gascoigne, N. R., Rybakin, V., Acuto, O. & Brzostek, J. 2016. TCR Signal Strength and T Cell Development. *Annu Rev Cell Dev Biol,* 32**,** 327-348.

Gaud, G., Lesourne, R. & Love, P. E. 2018. Regulatory mechanisms in T cell receptor signalling. *Nature Reviews Immunology,* 18**,** 485-497.

Gautier, G., Humbert, M., Deauvieau, F., Scuiller, M., Hiscott, J., Bates, E. E. M., Trinchieri, G., Caux, C. & Garrone, P. 2005. A type I interferon autocrine-paracrine loop is involved in Toll-like receptor-induced interleukin-12p70 secretion by dendritic cells. *The Journal of experimental medicine,* 201**,** 1435-1446.

Gautier, J., Solomon, M. J., Booher, R. N., Bazan, J. F. & Kirschner, M. W. 1991. cdc25 is a specific tyrosine phosphatase that directly activates p34cdc2. *Cell,* 67**,** 197-211.

Ge, X. Q. & Blow, J. J. 2010. Chk1 inhibits replication factory activation but allows dormant origin firing in existing factories. *J Cell Biol,* 191**,** 1285-97.

Ge, X. Q., Jackson, D. A. & Blow, J. J. 2007. Dormant origins licensed by excess Mcm2-7 are required for human cells to survive replicative stress. *Genes Dev,* 21**,** 3331-41.

Germar, K., Dose, M., Konstantinou, T., Zhang, J., Wang, H., Lobry, C., Arnett, K. L., Blacklow, S. C., Aifantis, I., Aster, J. C. & Gounari, F. 2011. T-cell factor 1 is a gatekeeper for T-cell specification in response to Notch signaling. *Proceedings of the National Academy of Sciences,* 108**,** 20060.

Ghandour, H., Cullere, X., Alvarez, A., Luscinskas, F. W. & Mayadas, T. N. 2007. Essential role for Rap1 GTPase and its guanine exchange factor CalDAG-GEFI in LFA-1 but not VLA-4 integrin mediated human T-cell adhesion. *Blood,* 110**,** 3682-3690.

Giangrande, P. H., Zhu, W., Schlisio, S., Sun, X., Mori, S., Gaubatz, S. & Nevins, J. R. 2004. A role for E2F6 in distinguishing G1/S- and G2/M-specific transcription. *Genes & Development,* 18**,** 2941-2951.

Gillespie, P. J. & Blow, J. J. 2010. Clusters, factories and domains: The complex structure of S-phase comes into focus. *Cell Cycle,* 9**,** 3218-26.

Gitlin, A. D., Shulman, Z. & Nussenzweig, M. C. 2014. Clonal selection in the germinal centre by regulated proliferation and hypermutation. *Nature,* 509**,** 637-640.

Go, W. Y., Liu, X., Roti, M. A., Liu, F. & Ho, S. N. 2004. NFAT5/TonEBP mutant mice define osmotic stress as a critical feature of the lymphoid microenvironment. *Proceedings of the National Academy of Sciences of the United States of America,* 101**,** 10673.

Godfrey, D. I., Kennedy, J., Suda, T. & Zlotnik, A. 1993. A developmental pathway involving four phenotypically and functionally distinct subsets of CD3-CD4-CD8-triple-negative adult mouse thymocytes defined by CD44 and CD25 expression. *The Journal of Immunology,* 150**,** 4244.

Goodarzi, A. A., Noon, A. T., Deckbar, D., Ziv, Y., Shiloh, Y., Löbrich, M. & Jeggo, P. A. 2008. ATM Signaling Facilitates Repair of DNA Double-Strand Breaks Associated with Heterochromatin. *Molecular Cell,* 31**,** 167-177.

Gotter, J. R., Brors, B., Hergenhahn, M. & Kyewski, B. 2004. Medullary Epithelial Cells of the Human Thymus Express a Highly Diverse Selection of Tissue-specific Genes Colocalized in Chromosomal Clusters. *Journal of Experimental Medicine,* 199**,** 155-166.

Gottschalk, R. A., Corse, E. & Allison, J. P. 2010. TCR ligand density and affinity determine peripheral induction of Foxp3 in vivo. 207**,** 1701-1711.

Govern, C. C., Paczosa, M. K., Chakraborty, A. K. & Huseby, E. S. 2010. Fast on-rates allow short dwell time ligands to activate T cells. *Proceedings of the National Academy of Sciences,* 107**,** 8724.

Graef, I. A., Holsinger, L. J., Diver, S., Schreiber, S. L. & Crabtree, G. R. 1997. Proximity and orientation underlie signaling by the non-receptor tyrosine kinase ZAP70. *The EMBO Journal,* 16**,** 5618-5628.

Granum, S., Sundvold-Gjerstad, V., Gopalakrishnan, R. P., Berge, T., Koll, L., Abrahamsen, G., Sørlie, M. & Spurkland, A. 2014. The kinase Itk and the adaptor TSAd change the specificity of the kinase Lck in T cells by promoting the phosphorylation of Tyr<sup>192</sup&gt. *Science Signaling,* 7**,** ra118.

Griffiths, E. K., Krawczyk, C., Kong, Y.-Y., Raab, M., Hyduk, S. J., Bouchard, D., Chan, V. S., Kozieradzki, I., Oliveira-Dos-Santos, A. J., Wakeham, A., Ohashi, P. S., Cybulsky, M. I., Rudd, C. E. & Penninger, J. M. 2001. Positive Regulation of T Cell Activation and Integrin Adhesion by the Adapter Fyb/Slap. *Science,* 293**,** 2260.

Grinstein, S., Clarke, C. A. & Rothstein, A. 1982. Increased anion permeability during volume regulation in human lymphocytes. *Philos Trans R Soc Lond B Biol Sci,* 299**,** 509-18.

Grinstein, S., Clarke, C. A. & Rothstein, A. 1983. Activation of Na+/H+ exchange in lymphocytes by osmotically induced volume changes and by cytoplasmic acidification. *J Gen Physiol,* 82**,** 619-38.

Grumont, R., Lock, P., Mollinari, M., Shannon, F. M., Moore, A. & Gerondakis, S. 2004. The Mitogen-Induced Increase in T Cell Size Involves PKC and NFAT Activation of Rel/NF-κB-Dependent c-myc Expression. *Immunity,* 21**,** 19-30.

Guan, H., Nagarkatti, P. S. & Nagarkatti, M. 2009. Role of CD44 in the differentiation of Th1 and Th2 cells: CD44-deficiency enhances the development of Th2 effectors in response to sheep RBC and chicken ovalbumin. *J Immunol,* 183**,** 172-80.

Gudmundsdottir, H., Wells, A. D. & Turka, L. A. 1999. Dynamics and requirements of T cell clonal expansion in vivo at the single-cell level: effector function is linked to proliferative capacity. *J Immunol,* 162**,** 5212-23.

Guha, M. & Mackman, N. 2001. LPS induction of gene expression in human monocytes. *Cellular Signalling,* 13**,** 85-94.

Guo, L., Wei, G., Zhu, J., Liao, W., Leonard, W. J., Zhao, K. & Paul, W. 2009. IL-1 family members and STAT activators induce cytokine production by Th2, Th17, and Th1 cells. 106**,** 13463-13468.

Hafner, A., Bulyk, M. L., Jambhekar, A. & Lahav, G. 2019. The multiple mechanisms that regulate p53 activity and cell fate. *Nature Reviews Molecular Cell Biology,* 20**,** 199-210.

Han, J., Luby-Phelps, K., Das, B., Shu, X., Xia, Y., Mosteller, R. D., Krishna, U. M., Falck, J. R., White, M. A. & Broek, D. 1998. Role of substrates and products of PI 3-kinase in regulating activation of Rac-related guanosine triphosphatases by Vav. *Science,* 279**,** 558-60.

Han, S., Hathcock, K., Zheng, B., Kepler, T. B., Hodes, R. & Kelsoe, G. 1995. Cellular interaction in germinal centers. Roles of CD40 ligand and B7-2 in established germinal centers. *The Journal of Immunology,* 155**,** 556.

Hardwick, J. S. & Sefton, B. M. 1995. Activation of the Lck tyrosine protein kinase by hydrogen peroxide requires the phosphorylation of Tyr-394. *Proceedings of the National Academy of Sciences,* 92**,** 4527.

Harris, T. J., Grosso, J. F., Yen, H.-R., Xin, H., Kortylewski, M., Albesiano, E., Hipkiss, E. L., Getnet, D., Goldberg, M. V., Maris, C. H., Housseau, F., Yu, H., Pardoll, D. M. & Drake, C. G. 2007. Cutting Edge: An In Vivo Requirement for STAT3 Signaling in TH17 Development and TH17-Dependent Autoimmunity. *The Journal of Immunology,* 179**,** 4313-4317.

Helft, J., Bottcher, J., Chakravarty, P., Zelenay, S., Huotari, J., Schraml, B. U., Goubau, D. & Reis E Sousa, C. 2015. GM-CSF Mouse Bone Marrow Cultures Comprise a Heterogeneous Population of CD11c(+)MHCII(+) Macrophages and Dendritic Cells. *Immunity,* 42**,** 1197-211.

Hildeman, D. A., Zhu, Y., Mitchell, T. C., Bouillet, P., Strasser, A., Kappler, J. & Marrack, P. 2002. Activated T cell death in vivo mediated by proapoptotic bcl-2 family member bim. *Immunity,* 16**,** 759-67.

Hirota, K., Turner, J.-E., Villa, M., Duarte, J. H., Demengeot, J., Steinmetz, O. M. & Stockinger, B. 2013. Plasticity of TH17 cells in Peyer's patches is responsible for the induction of T cell–dependent IgA responses. *Nature Immunology,* 14**,** 372-379.

Hoffman, E. S., Passoni, L., Crompton, T., Leu, T. M., Schatz, D. G., Koff, A., Owen, M. J. & Hayday, A. C. 1996. Productive T-cell receptor beta-chain gene rearrangement: coincident regulation of cell cycle and clonality during development in vivo. *Genes & Development,* 10**,** 948-962.

Holtz-Heppelmann, C. J., Algeciras, A., Badley, A. D. & Paya, C. V. 1998. Transcriptional regulation of the human FasL promoter-enhancer region. *J Biol Chem,* 273**,** 4416-23.

Hong, J. H., Yang, D., Shcheynikov, N., Ohana, E., Shin, D. M. & Muallem, S. 2013. Convergence of IRBIT, phosphatidylinositol (4,5) bisphosphate, and WNK/SPAK kinases in regulation of the Na+-HCO3- cotransporters family. *Proc Natl Acad Sci U S A,* 110**,** 4105-10.

Hosoya, T., Kuroha, T., Moriguchi, T., Cummings, D., Maillard, I., Lim, K.-C. & Engel, J. D. 2009. GATA-3 is required for early T lineage progenitor development. *Journal of Experimental Medicine,* 206**,** 2987-3000.

Hou, W., Zhang, Q., Yan, Z., Chen, R., Zeh Iii, H. J., Kang, R., Lotze, M. T. & Tang, D. 2013. Strange attractors: DAMPs and autophagy link tumor cell death and immunity. *Cell Death & Disease,* 4**,** e966-e966.

Houtman, J. C. D., Yamaguchi, H., Barda-Saad, M., Braiman, A., Bowden, B., Appella, E., Schuck, P. & Samelson, L. E. 2006. Oligomerization of signaling complexes by the multipoint binding of GRB2 to both LAT and SOS1. *Nature Structural & Molecular Biology,* 13**,** 798-805.

Hu, H., Wang, H., Xiao, Y., Jin, J., Chang, J.-H., Zou, Q., Xie, X., Cheng, X. & Sun, S.-C. 2016. Otud7b facilitates T cell activation and inflammatory responses by regulating Zap70 ubiquitination. *Journal of Experimental Medicine,* 213**,** 399-414.

Huang, F. P., Platt, N., Wykes, M., Major, J. R., Powell, T. J., Jenkins, C. D. & Macpherson, G. G. 2000. A discrete subpopulation of dendritic cells transports apoptotic intestinal epithelial cells to T cell areas of mesenteric lymph nodes. *J Exp Med,* 191**,** 435-44.

Huang, H., Jeon, M.-S., Liao, L., Yang, C., Elly, C., Yates, J. R. & Liu, Y.-C. 2010. K33-Linked Polyubiquitination of T Cell Receptor-ζ Regulates Proteolysis-Independent T Cell Signaling. 33**,** 60-70.

Huang, J., Brameshuber, M., Zeng, X., Xie, J., Li, Q. J., Chien, Y. H., Valitutti, S. & Davis, M. M. 2013. A single peptide-major histocompatibility complex ligand triggers digital cytokine secretion in CD4(+) T cells. *Immunity,* 39**,** 846-57.

Huang, W. Y. C., Yan, Q., Lin, W.-C., Chung, J. K., Hansen, S. D., Christensen, S. M., Tu, H.-L., Kuriyan, J. & Groves, J. T. 2016. Phosphotyrosine-mediated LAT assembly on membranes drives kinetic bifurcation in recruitment dynamics of the Ras activator SOS. *Proceedings of the National Academy of Sciences,* 113**,** 8218-8223.

Hubert, F.-X., Kinkel, S. A., Davey, G. M., Phipson, B., Mueller, S. N., Liston, A., Proietto, A. I., Cannon, P. Z. F., Forehan, S., Smyth, G. K., Wu, L., Goodnow, C. C., Carbone, F. R., Scott, H. S. & Heath, W. R. 2011. Aire regulates the transfer of antigen from mTECs to dendritic cells for induction of thymic tolerance. *Blood,* 118**,** 2462-2472.

Hui, E. & Vale, R. D. 2014. In vitro membrane reconstitution of the T-cell receptor proximal signaling network. *Nature Structural & Molecular Biology,* 21**,** 133-142.

Ilves, I., Petojevic, T., Pesavento, J. J. & Botchan, M. R. 2010. Activation of the MCM2-7 helicase by association with Cdc45 and GINS proteins. *Mol Cell,* 37**,** 247-58.

Inaba, K., Turley, S., Iyoda, T., Yamaide, F., Shimoyama, S., E Sousa, C. R., Germain, R. N., Mellman, I. & Steinman, R. M. 2000. The Formation of Immunogenic Major Histocompatibility Complex Class II–Peptide Ligands in Lysosomal Compartments of Dendritic Cells Is Regulated by Inflammatory Stimuli. *Journal of Experimental Medicine,* 191**,** 927-936.

Inglis, A., Hinnie, J. & Kinsella, J. 1995. A metabolic complication of severe burns. *Burns,* 21**,** 212-4.

Innocente, S. A., Abrahamson, J. L. A., Cogswell, J. P. & Lee, J. M. 1999. p53 regulates a G₂ checkpoint through cyclin B1. *Proceedings of the National Academy of Sciences,* 96**,** 2147.

Inoki, K., Li, Y., Zhu, T., Wu, J. & Guan, K.-L. 2002. TSC2 is phosphorylated and inhibited by Akt and suppresses mTOR signalling. *Nature Cell Biology,* 4**,** 648-657.

Iwashima, M., Irving, B. A., Van Oers, N. S., Chan, A. C. & Weiss, A. 1994. Sequential interactions of the TCR with two distinct cytoplasmic tyrosine kinases. *Science,* 263**,** 1136.

Jacob, J., Kassir, R. & Kelsoe, G. 1991. In situ studies of the primary immune response to (4-hydroxy-3-nitrophenyl)acetyl. I. The architecture and dynamics of responding cell populations. *J Exp Med,* 173**,** 1165-75.

Jankowska, K. I., Williamson, E. K., Roy, N. H., Blumenthal, D., Chandra, V., Baumgart, T. & Burkhardt, J. K. 2018. Integrins Modulate T Cell Receptor Signaling by Constraining Actin Flow at the Immunological Synapse. *Frontiers in Immunology,* 9**,** 25.

Jarrossay, D., Napolitani, G., Colonna, M., Sallusto, F. & Lanzavecchia, A. 2001. Specialization and complementarity in microbial molecule recognition by human myeloid and plasmacytoid dendritic cells. *Eur J Immunol,* 31**,** 3388-93.

Jazayeri, A., Falck, J., Lukas, C., Bartek, J., Smith, G. C. M., Lukas, J. & Jackson, S. P. 2006. ATM- and cell cycle-dependent regulation of ATR in response to DNA double-strand breaks. *Nature Cell Biology,* 8**,** 37-45.

Jenkins, M. K., Chu, H. H., Mclachlan, J. B. & Moon, J. J. 2010. On the composition of the preimmune repertoire of T cells specific for Peptide-major histocompatibility complex ligands. *Annu Rev Immunol,* 28**,** 275-94.

Jeon, U. S., Kim, J. A., Sheen, M. R. & Kwon, H. M. 2006. How tonicity regulates genes: story of TonEBP transcriptional activator. *Acta Physiologica,* 187**,** 241-247.

Jiang, Z. Y., Zhou, Q. L., Holik, J., Patel, S., Leszyk, J., Coleman, K., Chouinard, M. & Czech, M. P. 2005. Identification of WNK1 as a substrate of Akt/protein kinase B and a negative regulator of insulin-stimulated mitogenesis in 3T3-L1 cells. *J Biol Chem,* 280**,** 21622-8.

John, S., Vinkemeier, U., Soldaini, E., Darnell, J. E., Jr. & Leonard, W. J. 1999. The significance of tetramerization in promoter recruitment by Stat5. *Mol Cell Biol,* 19**,** 1910-8.

Johnston, R. J., Poholek, A. C., Ditoro, D., Yusuf, I., Eto, D., Barnett, B., Dent, A. L., Craft, J. & Crotty, S. 2009. Bcl6 and Blimp-1 Are Reciprocal and Antagonistic Regulators of T Follicular Helper Cell Differentiation. *Science,* 325**,** 1006.

Jorritsma, P. J., Brogdon, J. L. & Bottomly, K. 2003. Role of TCR-Induced Extracellular Signal-Regulated Kinase Activation in the Regulation of Early IL-4 Expression in Naive CD4+ T Cells. *The Journal of Immunology,* 170**,** 2427-2434.

Joung, I., Kim, T., Stolz, L. A., Payne, G., Winkler, D. G., Walsh, C. T., Strominger, J. L. & Shin, J. 1995. Modification of Ser59 in the unique N-terminal region of tyrosine kinase p56lck regulates specificity of its Src homology 2 domain. *Proceedings of the National Academy of Sciences,* 92**,** 5778.

Kahle, K. T., Gimenez, I., Hassan, H., Wilson, F. H., Wong, R. D., Forbush, B., Aronson, P. S. & Lifton, R. P. 2004. WNK4 regulates apical and basolateral Cl- flux in extrarenal epithelia. *Proc Natl Acad Sci U S A,* 101**,** 2064-9.

Kahle, K. T., Schmouth, J.-F., Lavastre, V., Latremoliere, A., Zhang, J., Andrews, N., Omura, T., Laganière, J., Rochefort, D., Hince, P., Castonguay, G., Gaudet, R., Mapplebeck, J. C. S., Sotocinal, S. G., Duan, J., Ward, C., Khanna, A. R., Mogil, J. S., Dion, P. A., Woolf, C. J., Inquimbert, P. & Rouleau, G. A. 2016. Inhibition of the kinase WNK1/HSN2 ameliorates neuropathic pain by restoring GABA inhibition. *Science Signaling,* 9**,** ra32.

Kahn-Perles, B., Lipcey, C., Lecine, P., Olive, D. & Imbert, J. 1997. Temporal and subunit-specific modulations of the Rel/NF-kappaB transcription factors through CD28 costimulation. *J Biol Chem,* 272**,** 21774-83.

Kanamori, M., Nakatsukasa, H., Okada, M., Lu, Q. & Yoshimura, A. 2016. Induced Regulatory T Cells: Their Development, Stability, and Applications. *Trends in Immunology,* 37**,** 803-811.

Kandula, S. & Abraham, C. 2004. LFA-1 on CD4⁺ T Cells Is Required for Optimal Antigen-Dependent Activation In Vivo. *The Journal of Immunology,* 173**,** 4443.

Katagiri, K., Hattori, M., Minato, N., Irie, S.-K., Takatsu, K. & Kinashi, T. 2000. Rap1 Is a Potent Activation Signal for Leukocyte Function-Associated Antigen 1 Distinct

from Protein Kinase C and Phosphatidylinositol-3-OH Kinase. *Molecular and Cellular Biology,* 20**,** 1956.

Katagiri, K., Imamura, M. & Kinashi, T. 2006. Spatiotemporal regulation of the kinase Mst1 by binding protein RAPL is critical for lymphocyte polarity and adhesion. *Nat Immunol,* 7**,** 919-28.

Katagiri, K., Shimonaka, M. & Kinashi, T. 2004. Rap1-mediated Lymphocyte Function-associated Antigen-1 Activation by the T Cell Antigen Receptor Is Dependent on Phospholipase C-γ1*. *Journal of Biological Chemistry,* 279**,** 11875-11881.

Katz, Z. B., Novotná, L., Blount, A. & Lillemeier, B. F. 2017. A cycle of Zap70 kinase activation and release from the TCR amplifies and disperses antigenic stimuli. *Nature Immunology,* 18**,** 86-95.

Kelly, L. M., Pereira, J. P., Yi, T., Xu, Y. & Cyster, J. G. 2011. EBI2 Guides Serial Movements of Activated B Cells and Ligand Activity Is Detectable in Lymphoid and Nonlymphoid Tissues. *The Journal of Immunology,* 187**,** 3026.

Kim, H.-P., Kim, B.-G., Letterio, J. & Leonard, W. J. 2005. Smad-dependent Cooperative Regulation of Interleukin 2 Receptor α Chain Gene Expression by T Cell Receptor and Transforming Growth Factor-β. *Journal of Biological Chemistry,* 280**,** 34042-34047.

Kim, H. P. 2002. The basis for TCR-mediated regulation of the IL-2 receptor alpha chain gene: role of widely separated regulatory elements. *The EMBO Journal,* 21**,** 3051-3059.

Kim, H. P., Imbert, J. & Leonard, W. J. 2006. Both integrated and differential regulation of components of the IL-2/IL-2 receptor system. *Cytokine Growth Factor Rev,* 17**,** 349-66.

Kim, J. E. & White, F. M. 2006. Quantitative analysis of phosphotyrosine signaling networks triggered by CD3 and CD28 costimulation in Jurkat cells. *J Immunol,* 176**,** 2833-43.

Kim, S. T., Takeuchi, K., Sun, Z. Y., Touma, M., Castro, C. E., Fahmy, A., Lang, M. J., Wagner, G. & Reinherz, E. L. 2009. The alphabeta T cell receptor is an anisotropic mechanosensor. *J Biol Chem,* 284**,** 31028-37.

Kinner, A., Wu, W., Staudt, C. & Iliakis, G. 2008. γ-H2AX in recognition and signaling of DNA double-strand breaks in the context of chromatin. *Nucleic Acids Research,* 36**,** 5678-5694.

Kino, T., Takatori, H., Manoli, I., Wang, Y., Tiulpakov, A., Blackman, M. R., Su, Y. A., Chrousos, G. P., Decherney, A. H. & Segars, J. H. 2009. Brx Mediates the Response of Lymphocytes to Osmotic Stress Through the Activation of NFAT5. *Science Signaling,* 2**,** ra5-ra5.

Klammt, C., Novotná, L., Li, D. T., Wolf, M., Blount, A., Zhang, K., Fitchett, J. R. & Lillemeier, B. F. 2015. T cell receptor dwell times control the kinase activity of Zap70. *Nature Immunology,* 16**,** 961-969.

Kleinewietfeld, M., Manzel, A., Titze, J., Kvakan, H., Yosef, N., Linker, R. A., Muller, D. N. & Hafler, D. A. 2013. Sodium chloride drives autoimmune disease by the induction of pathogenic TH17 cells. *Nature,* 496**,** 518-522.

Kliche, S., Breitling, D., Togni, M., Pusch, R., Heuer, K., Wang, X., Freund, C., Kasirer-Friede, A., Menasche, G., Koretzky, G. A. & Schraven, B. 2006. The ADAP/SKAP55 Signaling Module Regulates T-Cell Receptor-Mediated Integrin Activation through Plasma Membrane Targeting of Rap1. *Molecular and Cellular Biology,* 26**,** 7130.

Köchl, R., Thelen, F., Vanes, L., Brazao, T. F., Fountain, K., Xie, J., Huang, C. L., Lyck, R., Stein, J. V. & Tybulewicz, V. L. 2016. WNK1 kinase balances T cell adhesion versus migration in vivo. *Nat Immunol,* 17**,** 1075-83.

Köchl, R., Vanes, L., Llorian Sopena, M., Chakravarty, P., Hartweger, H., Fountain, K., White, A., Cowan, J., Anderson, G. & Tybulewicz, V. L. J. 2020. Critical role of WNK1 in MYC-dependent early mouse thymocyte development. *eLife,* 9**,** e56934.

König, R., Huang, L.-Y. & Germain, R. N. 1992. MHC class II interaction with CD4 mediated by a region analogous to the MHC class I binding site for CD8. *Nature,* 356**,** 796-798.

Kortum, R. L., Balagopalan, L., Alexander, C. P., Garcia, J., Pinski, J. M., Merrill, R. K., Nguyen, P. H., Li, W., Agarwal, I., Akpan, I. O., Sommers, C. L. & Samelson, L. E. 2013. The ability of Sos1 to oligomerize the adaptor protein LAT is separable from its guanine nucleotide exchange activity in vivo. *Sci Signal,* 6**,** ra99.

Krawczyk, C., Oliveira-Dos-Santos, A., Sasaki, T., Griffiths, E., Ohashi, P. S., Snapper, S., Alt, F. & Penninger, J. M. 2002. Vav1 Controls Integrin Clustering and MHC/Peptide-Specific Cell Adhesion to Antigen-Presenting Cells. *Immunity,* 16**,** 331-343.

Kreslavsky, T., Gleimer, M., Miyazaki, M., Choi, Y., Gagnon, E., Murre, C., Sicinski, P. & Von boehmer, H. 2012. β-Selection-Induced Proliferation Is Required for αβ T Cell Differentiation. *Immunity,* 37**,** 840-853.

Krummel, M. F. & Allison, J. P. 1995. CD28 and CTLA-4 have opposing effects on the response of T cells to stimulation. *J Exp Med,* 182**,** 459-65.

Kültz, D. & Chakravarty, D. 2001. Hyperosmolality in the form of elevated NaCl but not urea causes DNA damage in murine kidney cells. *Proceedings of the National Academy of Sciences of the United States of America,* 98**,** 1999-2004.

Kumagai, A., Lee, J., Yoo, H. Y. & Dunphy, W. G. 2006. TopBP1 Activates the ATR-ATRIP Complex. *Cell,* 124**,** 943-955.

Kumar, A., Mazzanti, M., Mistrik, M., Kosar, M., Beznoussenko, G. V., Mironov, A. A., Garrè, M., Parazzoli, D., Shivashankar, G. V., Scita, G., Bartek, J. & Foiani, M. 2014. ATR mediates a checkpoint at the nuclear envelope in response to mechanical stress. *Cell,* 158**,** 633-646.

Kuznetsova, I. M., Turoverov, K. K. & Uversky, V. N. 2014. What macromolecular crowding can do to a protein. *International journal of molecular sciences,* 15**,** 23090-23140.

Laguna, T., Notario, L., Pippa, R., Fontela, M. G., Vazquez, B. N., Maicas, M., Aguilera-Montilla, N., Corbi, A. L., Odero, M. D. & Lauzurica, P. 2015. New insights on the transcriptional regulation of CD69 gene through a potent enhancer located in the conserved non-coding sequence 2. *Mol Immunol,* 66**,** 171-9.

Lammermann, T., Bader, B. L., Monkley, S. J., Worbs, T., Wedlich-Soldner, R., Hirsch, K., Keller, M., Forster, R., Critchley, D. R., Fassler, R. & Sixt, M. 2008. Rapid leukocyte migration by integrin-independent flowing and squeezing. *Nature,* 453**,** 51-5.

Larsen, C. P., Ritchie, S. C., Pearson, T. C., Linsley, P. S. & Lowry, R. P. 1992. Functional expression of the costimulatory molecule, B7/BB1, on murine dendritic cell populations. *Journal of Experimental Medicine,* 176**,** 1215-1220.

Larsen, S. E., Bilenkin, A., Tarasenko, T. N., Arjunaraja, S., Stinson, J. R., Mcguire, P. J. & Snow, A. L. 2017. Sensitivity to Restimulation-Induced Cell Death Is Linked to Glycolytic Metabolism in Human T Cells. *J Immunol,* 198**,** 147-155.

Lauritsen, J. P. H., Wong, G. W., Lee, S.-Y., Lefebvre, J. M., Ciofani, M., Rhodes, M., Kappes, D. J., Zúñiga-Pflücker, J. C. & Wiest, D. L. 2009. Marked Induction of the Helix-Loop-Helix Protein Id3 Promotes the γδ T Cell Fate and Renders Their Functional Maturation Notch Independent. *Immunity,* 31**,** 565-575.

Lea, N. C., Orr, S. J., Stoeber, K., Williams, G. H., Lam, E. W., Ibrahim, M. A., Mufti, G. J. & Thomas, N. S. 2003. Commitment point during G0-->G1 that controls entry into the cell cycle. *Mol Cell Biol,* 23**,** 2351-61.

Lee, H. S., Lim, C. J., Puzon-Mclaughlin, W., Shattil, S. J. & Ginsberg, M. H. 2009. RIAM activates integrins by linking talin to ras GTPase membrane-targeting sequences. *J Biol Chem,* 284**,** 5119-27.

Lee, J., Kumagai, A. & Dunphy, W. G. 2007. The Rad9-Hus1-Rad1 Checkpoint Clamp Regulates Interaction of TopBP1 with ATR. *Journal of Biological Chemistry,* 282**,** 28036-28044.

Lee, J.-H. & Paull, T. T. 2005. ATM Activation by DNA Double-Strand Breaks Through the Mre11-Rad50-Nbs1 Complex. *Science,* 308**,** 551.

Lee, J. H., Katakai, T., Hara, T., Gonda, H., Sugai, M. & Shimizu, A. 2004. Roles of p-ERM and Rho-ROCK signaling in lymphocyte polarity and uropod formation. *J Cell Biol,* 167**,** 327-37.

Lee, J. H. & Paull, T. T. 2007. Activation and regulation of ATM kinase activity in response to DNA double-strand breaks. *Oncogene,* 26**,** 7741-7748.

Lee, S. H., Park, Y., Yoon, S. K. & Yoon, J. B. 2010. Osmotic stress inhibits proteasome by p38 MAPK-dependent phosphorylation. *J Biol Chem,* 285**,** 41280-9.

Lee, S. K., Rigby, R. J., Zotos, D., Tsai, L. M., Kawamoto, S., Marshall, J. L., Ramiscal, R. R., Chan, T. D., Gatto, D., Brink, R., Yu, D., Fagarasan, S., Tarlinton, D. M., Cunningham, A. F. & Vinuesa, C. G. 2011. B cell priming for extrafollicular antibody responses requires Bcl-6 expression by T cells. *Journal of Experimental Medicine,* 208**,** 1377-1388.

Lees, J. A., Saito, M., Vidal, M., Valentine, M., Look, T., Harlow, E., Dyson, N. & Helin, K. 1993. The retinoblastoma protein binds to a family of E2F transcription factors. *Molecular and Cellular Biology,* 13**,** 7813.

Lenardo, M. J. 1991. Interleukin-2 programs mouse alpha beta T lymphocytes for apoptosis. *Nature,* 353**,** 858-61.

Lenertz, L. Y., Lee, B. H., Min, X., Xu, B. E., Wedin, K., Earnest, S., Goldsmith, E. J. & Cobb, M. H. 2005. Properties of WNK1 and implications for other family members. *J Biol Chem,* 280**,** 26653-8.

Leung, J. Y., Ehmann, G. L., Giangrande, P. H. & Nevins, J. R. 2008. A role for Myc in facilitating transcription activation by E2F1. *Oncogene,* 27**,** 4172-4179.

Li, B., Tournier, C., Davis, R. J. & Flavell, R. A. 1999. Regulation of IL-4 expression by the transcription factor JunB during T helper cell differentiation. *The EMBO journal,* 18**,** 420-432.

Li, J., Lu, E., Yi, T. & Cyster, J. G. 2016. EBI2 augments Tfh cell fate by promoting interaction with IL-2-quenching dendritic cells. *Nature,* 533**,** 110-114.

Li, T., Kon, N., Jiang, L., Tan, M., Ludwig, T., Zhao, Y., Baer, R. & Gu, W. 2012. Tumor Suppression in the Absence of p53-Mediated Cell-Cycle Arrest, Apoptosis, and Senescence. *Cell,* 149**,** 1269-1283.

Liao, W., Lin, J.-X. & Leonard, Warren j. 2013. Interleukin-2 at the Crossroads of Effector Responses, Tolerance, and Immunotherapy. *Immunity,* 38**,** 13-25.

Liao, W., Schones, D. E., Oh, J., Cui, Y., Cui, K., Roh, T.-Y., Zhao, K. & Leonard, W. J. 2008. Priming for T helper type 2 differentiation by interleukin 2–mediated induction of interleukin 4 receptor α-chain expression. *Nature Immunology,* 9**,** 1288-1296.

Liaw, H., Lee, D. & Myung, K. 2011. DNA-PK-Dependent RPA2 Hyperphosphorylation Facilitates DNA Repair and Suppresses Sister Chromatid Exchange. *PLOS ONE,* 6**,** e21424.

Lin, J.-X., Migone, T.-S., Tseng, M., Friedmann, M., Weatherbee, J. A., Zhou, L., Yamauchi, A., Bloom, E. T., Mietz, J., John, S. & Leonard, W. J. 1995. The role of shared receptor motifs and common stat proteins in the generation of cytokine pleiotropy and redundancy by IL-2, IL-4, IL-7, IL-13, and IL-15. *Immunity,* 2**,** 331-339.

Lin, J. T., Stein, E. A., Wong, M. T., Kalpathy, K. J., Su, L. L., Utz, P. J., Robinson, W. H. & Fathman, C. G. 2012. Differential mTOR and ERK pathway utilization by effector CD4 T cells suggests combinatorial drug therapy of arthritis. *Clin Immunol,* 142**,** 127-38.

Lin, S. H., Yu, I. S., Jiang, S. T., Lin, S. W., Chu, P., Chen, A., Sytwu, H. K., Sohara, E., Uchida, S., Sasaki, S. & Yang, S. S. 2011. Impaired phosphorylation of Na(+)-K(+)-2Cl(-) cotransporter by oxidative stress-responsive kinase-1 deficiency manifests hypotension and Bartter-like syndrome. *Proc Natl Acad Sci U S A,* 108**,** 17538-43.

Lindemann, M. J., Benczik, M. & Gaffen, S. L. 2003. Anti-apoptotic signaling by the interleukin-2 receptor reveals a function for cytoplasmic tyrosine residues within the common gamma (gamma c) receptor subunit. *J Biol Chem,* 278**,** 10239-49.

Lindstein, T., June, C. H., Ledbetter, J. A., Stella, G. & Thompson, C. B. 1989. Regulation of lymphokine messenger RNA stability by a surface-mediated T cell activation pathway. *Science,* 244**,** 339-43.

Lissy, N. A., Davis, P. K., Irwin, M., Kaelin, W. G. & Dowdy, S. F. 2000. A common E2F-1 and p73 pathway mediates cell death induced by TCR activation. *Nature,* 407**,** 642-5.

Liu, B., Chen, W., Evavold, B. D. & Zhu, C. 2014a. Accumulation of dynamic catch bonds between TCR and agonist peptide-MHC triggers T cell signaling. *Cell,* 157**,** 357-368.

Liu, D., Xu, H., Shih, C., Wan, Z., Ma, X., Ma, W., Luo, D. & Qi, H. 2015. T–B-cell entanglement and ICOSL-driven feed-forward regulation of germinal centre reaction. *Nature,* 517**,** 214-218.

Liu, Q., Guntuku, S., Cui, X. S., Matsuoka, S., Cortez, D., Tamai, K., Luo, G., Carattini-Rivera, S., Demayo, F., Bradley, A., Donehower, L. A. & Elledge, S. J. 2000. Chk1 is an essential kinase that is regulated by Atr and required for the G(2)/M DNA damage checkpoint. *Genes & development,* 14**,** 1448-1459.

Liu, X., Chen, X., Zhong, B., Wang, A., Wang, X., Chu, F., Nurieva, R. I., Yan, X., Chen, P., Van Der Flier, L. G., Nakatsukasa, H., Neelapu, S. S., Chen, W., Clevers, H., Tian, Q., Qi, H., Wei, L. & Dong, C. 2014b. Transcription factor achaete-scute homologue 2 initiates follicular T-helper-cell development. *Nature,* 507**,** 513-518.

Liu, Y., Blanchfield, L., Ma, V. P., Andargachew, R., Galior, K., Liu, Z., Evavold, B. & Salaita, K. 2016. DNA-based nanoparticle tension sensors reveal that T-cell receptors transmit defined pN forces to their antigens for enhanced fidelity. *Proc Natl Acad Sci U S A,* 113**,** 5610-5.

Liu, Y., Gao, X., Masuda, E., Redecha, P. B., Blank, M. C. & Pricop, L. 2006. Regulated Expression of FcγR in Human Dendritic Cells Controls Cross-Presentation of Antigen-Antibody Complexes. *The Journal of Immunology,* 177**,** 8440.

Loomis, W. H., Namiki, S., Ostrom, R. S., Insel, P. A. & Junger, W. G. 2003. Hypertonic Stress Increases T Cell Interleukin-2 Expression through a Mechanism That Involves ATP Release, P2 Receptor, and p38 MAPK Activation *. *Journal of Biological Chemistry,* 278**,** 4590-4596.

López-Rodríguez, C., Antos, C. L., Shelton, J. M., Richardson, J. A., Lin, F., Novobrantseva, T. I., Bronson, R. T., Igarashi, P., Rao, A. & Olson, E. N. 2004. Loss of NFAT5 results in renal atrophy and lack of tonicity-responsive gene expression. *Proceedings of the National Academy of Sciences of the United States of America,* 101**,** 2392.

López-RodríGuez, C., Aramburu, J., Jin, L., Rakeman, A. S., Michino, M. & Rao, A. 2001. Bridging the NFAT and NFκB Families: NFAT5 Dimerization Regulates Cytokine Gene Transcription in Response to Osmotic Stress. *Immunity,* 15**,** 47-58.

Lou, Z., Minter-Dykhouse, K., Franco, S., Gostissa, M., Rivera, M. A., Celeste, A., Manis, J. P., Van Deursen, J., Nussenzweig, A., Paull, T. T., Alt, F. W. & Chen, J. 2006.

MDC1 Maintains Genomic Stability by Participating in the Amplification of ATM-Dependent DNA Damage Signals. *Molecular Cell,* 21**,** 187-200.

Love, P. E. & Hayes, S. M. 2010. ITAM-mediated signaling by the T-cell antigen receptor. *Cold Spring Harb Perspect Biol,* 2**,** a002485.

Lowenstein, E. J., Daly, R. J., Batzer, A. G., Li, W., Margolis, B., Lammers, R., Ullrich, A., Skolnik, E. Y., Bar-Sagi, D. & Schlessinger, J. 1992. The SH2 and SH3 domain-containing protein GRB2 links receptor tyrosine kinases to ras signaling. *Cell,* 70**,** 431-42.

Lu, Kristina t., Kanno, Y., Cannons, Jennifer l., Handon, R., Bible, P., Elkahloun, Abdel g., Anderson, Stacie m., Wei, L., Sun, H., O'shea, John j. & Schwartzberg, Pamela l. 2011. Functional and Epigenetic Studies Reveal Multistep Differentiation and Plasticity of In Vitro-Generated and In Vivo-Derived Follicular T Helper Cells. *Immunity,* 35**,** 622-632.

Lucas, C. L., Chandra, A., Nejentsev, S., Condliffe, A. M. & Okkenhaug, K. 2016. PI3Kdelta and primary immunodeficiencies. *Nat Rev Immunol,* 16**,** 702-714.

Lucas, P. J., Negishi, I., Nakayama, K., Fields, L. E. & Loh, D. Y. 1995. Naive CD28-deficient T cells can initiate but not sustain an in vitro antigen-specific immune response. *J Immunol,* 154**,** 5757-68.

Lukas, C., Sørensen, C. S., Kramer, E., Santoni-Rugiu, E., Lindeneg, C., Peters, J.-M., Bartek, J. & Lukas, J. 1999. Accumulation of cyclin B1 requires E2F and cyclin-A-dependent rearrangement of the anaphase-promoting complex. *Nature,* 401**,** 815-818.

Ma, L., Chen, Z., Erdjument-Bromage, H., Tempst, P. & Pandolfi, P. P. 2005. Phosphorylation and Functional Inactivation of TSC2 by Erk: Implications for Tuberous Sclerosisand Cancer Pathogenesis. *Cell,* 121**,** 179-193.

Ma, P., Zha, S., Shen, X., Zhao, Y., Li, L., Yang, L., Lei, M. & Liu, W. 2019. NFAT5 mediates hypertonic stress-induced atherosclerosis via activating NLRP3 inflammasome in endothelium. *Cell Communication and Signaling,* 17**,** 102.

Mailliard, M. E. & Kilberg, M. S. 1990. Sodium-dependent neutral amino acid transport by human liver plasma membrane vesicles. *Journal of Biological Chemistry,* 265**,** 14321-14326.

Mallick, C. A., Dudley, E. C., Viney, J. L., Owen, M. J. & Hayday, A. C. 1993. Rearrangement and diversity of T cell receptor β chain genes in thymocytes: A critical role for the β chain in development. *Cell,* 73**,** 513-519.

Manickasingham, S. P. & Reis E Sousa, C. 2001. Mature T cell seeks antigen for meaningful relationship in lymph node. *Immunology,* 102**,** 381-386.

Maréchal, A. & Zou, L. 2013. DNA damage sensing by the ATM and ATR kinases. *Cold Spring Harbor perspectives in biology,* 5**,** a012716.

Marinari, B., Costanzo, A., Marzano, V., Piccolella, E. & Tuosto, L. 2004. CD28 delivers a unique signal leading to the selective recruitment of RelA and p52 NF-kappaB subunits on IL-8 and Bcl-xL gene promoters. *Proc Natl Acad Sci U S A,* 101**,** 6098-103.

Marsh, D. J. & Azen, S. P. 1975. Mechanism of NaCl reabsorption by hamster thin ascending limbs of Henle's loop. *Am J Physiol,* 228**,** 71-9.

Martin, B., BéCourt, C., Bienvenu, B. & Lucas, B. 2006. Self-recognition is crucial for maintaining the peripheral CD4+ T-cell pool in a nonlymphopenic environment. *Blood,* 108**,** 270-277.

Matsui, K., Fine, A., Zhu, B., Marshak-Rothstein, A. & Ju, S. T. 1998. Identification of two NF-kappa B sites in mouse CD95 ligand (Fas ligand) promoter: functional analysis in T cell hybridoma. *J Immunol,* 161**,** 3469-73.

Matsuoka, S., Huang, M. & Elledge, S. J. 1998. Linkage of ATM to Cell Cycle Regulation by the Chk2 Protein Kinase. *Science,* 282**,** 1893.

Mazza, C., Auphan-Anezin, N., Gregoire, C., Guimezanes, A., Kellenberger, C., Roussel, A., Kearney, A., Van Der Merwe, P. A., Schmitt-Verhulst, A. M. & Malissen, B. 2007. How much can a T-cell antigen receptor adapt to structurally distinct antigenic peptides? *EMBO J,* 26**,** 1972-83.

Mckarns, S. C. & Schwartz, R. H. 2008. Biphasic regulation of Il2 transcription in CD4+ T cells: roles for TNF-alpha receptor signaling and chromatin structure. *Journal of immunology (Baltimore, Md. : 1950),* 181**,** 1272-1281.

Mckeithan, T. W. 1995. Kinetic proofreading in T-cell receptor signal transduction. *Proc Natl Acad Sci U S A,* 92**,** 5042-6.

Medeiros, R. B., Dickey, D. M., Chung, H., Quale, A. C., Nagarajan, L. R., Billadeau, D. D. & Shimizu, Y. 2005. Protein Kinase D1 and the β1 Integrin Cytoplasmic Domain Control β1 Integrin Function via Regulation of Rap1 Activation. *Immunity,* 23**,** 213-226.

Ménasché, G., Kliche, S., Chen, E. J. H., Stradal, T. E. B., Schraven, B. & Koretzky, G. 2007. RIAM Links the ADAP/SKAP-55 Signaling Module to Rap1, Facilitating T-Cell-Receptor-Mediated Integrin Activation. *Molecular and Cellular Biology,* 27**,** 4070.

Meulmeester, E., Maurice, M. M., Boutell, C., Teunisse, A. F. a. S., Ovaa, H., Abraham, T. E., Dirks, R. W. & Jochemsen, A. G. 2005. Loss of HAUSP-Mediated Deubiquitination Contributes to DNA Damage-Induced Destabilization of Hdmx and Hdm2. *Molecular Cell,* 18**,** 565-576.

Meyers, R. S. 2009. Pediatric fluid and electrolyte therapy. *The journal of pediatric pharmacology and therapeutics : JPPT : the official journal of PPAG,* 14**,** 204-211.

Michea, L., Ferguson, D. R., Peters, E. M., Andrews, P. M., Kirby, M. R. & Burg, M. B. 2000. Cell cycle delay and apoptosis are induced by high salt and urea in renal medullary cells. *American Journal of Physiology-Renal Physiology,* 278**,** F209-F218.

Mikhailik, A., Ford, B., Keller, J., Chen, Y., Nassar, N. & Carpino, N. 2007. A Phosphatase Activity of Sts-1 Contributes to the Suppression of TCR Signaling. *Molecular Cell,* 27**,** 486-497.

Milburn, C. C., Deak, M., Kelly, S. M., Price, N. C., Alessi, D. R. & Van Aalten, D. M. 2003. Binding of phosphatidylinositol 3,4,5-trisphosphate to the pleckstrin homology domain of protein kinase B induces a conformational change. *Biochem J,* 375**,** 531-8.

Minton, A. P. 1983. The effect of volume occupancy upon the thermodynamic activity of proteins: some biochemical consequences. *Molecular and Cellular Biochemistry,* 55**,** 119-140.

Mittal, A., Papa, S., Franzoso, G. & Sen, R. 2006. NF-kappaB-dependent regulation of the timing of activation-induced cell death of T lymphocytes. *J Immunol,* 176**,** 2183-9.

Miyazaki, M. & Takemasa, T. 2017. TSC2/Rheb signaling mediates ERK-dependent regulation of mTORC1 activity in C2C12 myoblasts. *FEBS Open Bio,* 7**,** 424-433.

Mochida, S., Rata, S., Hino, H., Nagai, T. & Novák, B. 2016. Two Bistable Switches Govern M Phase Entry. *Current biology : CB,* 26**,** 3361-3367.

Moiseeva, T., Hood, B., Schamus, S., O'connor, M. J., Conrads, T. P. & Bakkenist, C. J. 2017. ATR kinase inhibition induces unscheduled origin firing through a Cdc7-dependent association between GINS and And-1. *Nat Commun,* 8**,** 1392.

Moiseeva, T. N., Yin, Y., Calderon, M. J., Qian, C., Schamus-Haynes, S., Sugitani, N., Osmanbeyoglu, H. U., Rothenberg, E., Watkins, S. C. & Bakkenist, C. J. 2019. An ATR and CHK1 kinase signaling mechanism that limits origin firing during unperturbed DNA replication. *Proceedings of the National Academy of Sciences,* 116**,** 13374.

Molina, T. J., Kishihara, K., Siderovskid, D. P., Van Ewijk, W., Narendran, A., Timms, E., Wakeham, A., Paige, C. J., Hartmann, K. U., Veillette, A., Davidson, D. & Mak, T. W. 1992. Profound block in thymocyte development in mice lacking p56lck. *Nature,* 357**,** 161-164.

Mombaerts, P., Iacomini, J., Johnson, R. S., Herrup, K., Tonegawa, S. & Papaioannou, V. E. 1992. RAG-1-deficient mice have no mature B and T lymphocytes. *Cell,* 68**,** 869-877.

Monks, C. R., Freiberg, B. A., Kupfer, H., Sciaky, N. & Kupfer, A. 1998. Three-dimensional segregation of supramolecular activation clusters in T cells. *Nature,* 395**,** 82-6.

Morancho, B., Minguillón, J., Molkentin, J. D., López-Rodríguez, C. & Aramburu, J. 2008. Analysis of the transcriptional activity of endogenous NFAT5 in primary cells using transgenic NFAT-luciferase reporter mice. *BMC Molecular Biology,* 9**,** 13.

Moretti, J. & Blander, J. M. 2014. Insights into phagocytosis-coupled activation of pattern recognition receptors and inflammasomes. *Current opinion in immunology,* 26**,** 100-110.

Moriggl, R., Topham, D. J., Teglund, S., Sexl, V., Mckay, C., Wang, D., Hoffmeyer, A., Van Deursen, J., Sangster, M. Y., Bunting, K. D., Grosveld, G. C. & Ihle, J. N. 1999. Stat5 Is Required for IL-2-Induced Cell Cycle Progression of Peripheral T Cells. *Immunity,* 10**,** 249-259.

Müller, S., Rihs, S., Dayer Schneider, J. M., Paredes, B. E., Seibold, I., Brunner, T. & Mueller, C. 2009. Soluble TNF-α but not transmembrane TNF-α sensitizes T cells for enhanced activation-induced cell death. *European Journal of Immunology,* 39**,** 3171-3180.

Muñoz-Espín, D., Cañamero, M., Maraver, A., Gómez-López, G., Contreras, J., Murillo-Cuesta, S., Rodríguez-Baeza, A., Varela-Nieto, I., Ruberte, J., Collado, M. & Serrano, M. 2013. Programmed Cell Senescence during Mammalian Embryonic Development. *Cell,* 155**,** 1104-1118.

Murphy, A. K., Fitzgerald, M., Ro, T., Kim, J. H., Rabinowitsch, A. I., Chowdhury, D., Schildkraut, C. L. & Borowiec, J. A. 2014. Phosphorylated RPA recruits PALB2 to stalled DNA replication forks to facilitate fork recovery. *The Journal of cell biology,* 206**,** 493-507.

Myers, D. R., Norlin, E., Vercoulen, Y. & Roose, J. P. 2019. Active Tonic mTORC1 Signals Shape Baseline Translation in Naive T Cells. *Cell Reports,* 27**,** 1858-1874.e6.

Myers, J. S. & Cortez, D. 2006. Rapid Activation of ATR by Ionizing Radiation Requires ATM and Mre11. *Journal of Biological Chemistry,* 281**,** 9346-9350.

Naguro, I., Umeda, T., Kobayashi, Y., Maruyama, J., Hattori, K., Shimizu, Y., Kataoka, K., Kim-Mitsuyama, S., Uchida, S., Vandewalle, A., Noguchi, T., Nishitoh, H., Matsuzawa, A., Takeda, K. & Ichijo, H. 2012. ASK3 responds to osmotic stress and regulates blood pressure by suppressing WNK1-SPAK/OSR1 signaling in the kidney. *Nature Communications,* 3**,** 1285.

Nandi, A., Estess, P. & Siegelman, M. 2004. Bimolecular complex between rolling and firm adhesion receptors required for cell arrest; CD44 association with VLA-4 in T cell extravasation. *Immunity,* 20**,** 455-65.

Natarajan, K., Mcshan, A. C., Jiang, J., Kumirov, V. K., Wang, R., Zhao, H., Schuck, P., Tilahun, M. E., Boyd, L. F., Ying, J., Bax, A., Margulies, D. H. & Sgourakis, N. G. 2017. An allosteric site in the T-cell receptor Cbeta domain plays a critical signalling role. *Nat Commun,* 8**,** 15260.

Natkanski, E., Lee, W.-Y., Mistry, B., Casal, A., Molloy, J. E. & Tolar, P. 2013. B Cells Use Mechanical Energy to Discriminate Antigen Affinities. *Science,* 340**,** 1587-1590.

Neuhofer, W. 2010. Role of NFAT5 in inflammatory disorders associated with osmotic stress. *Current genomics,* 11**,** 584-590.

Neumeister, E. N., Zhu, Y., Richard, S., Terhorst, C., Chan, A. C. & Shaw, A. S. 1995. Binding of ZAP-70 to phosphorylated T-cell receptor zeta and eta enhances its autophosphorylation and generates specific binding sites for SH2 domain-containing proteins. *Molecular and Cellular Biology,* 15**,** 3171-3178.

Nika, K., Soldani, C., Salek, M., Paster, W., Gray, A., Etzensperger, R., Fugger, L., Polzella, P., Cerundolo, V., Dushek, O., Hofer, T., Viola, A. & Acuto, O. 2010. Constitutively active Lck kinase in T cells drives antigen receptor signal transduction. *Immunity,* 32**,** 766-77.

Norbury, C., Blow, J. & Nurse, P. 1991. Regulatory phosphorylation of the p34cdc2 protein kinase in vertebrates. *The EMBO Journal,* 10**,** 3321-3329.

Nurieva, R. I., Chung, Y., Hwang, D., Yang, X. O., Kang, H. S., Ma, L., Wang, Y.-H., Watowich, S. S., Jetten, A. M., Tian, Q. & Dong, C. 2008. Generation of T Follicular Helper Cells Is Mediated by Interleukin-21 but Independent of T Helper 1, 2, or 17 Cell Lineages. *Immunity,* 29**,** 138-149.

Nurieva, R. I., Chung, Y., Martinez, G. J., Yang, X. O., Tanaka, S., Matskevitch, T. D., Wang, Y.-H. & Dong, C. 2009. Bcl6 Mediates the Development of T Follicular Helper Cells. *Science,* 325**,** 1001.

Oh-Hora, M., Yamashita, M., Hogan, P. G., Sharma, S., Lamperti, E., Chung, W., Prakriya, M., Feske, S. & Rao, A. 2008. Dual functions for the endoplasmic reticulum calcium sensors STIM1 and STIM2 in T cell activation and tolerance. *Nature Immunology,* 9**,** 432-443.

Ohta, A., Schumacher, F.-R., Mehellou, Y., Johnson, C., Knebel, A., Thomas, Nicola, Dario & Kurz, T. 2013. The CUL3–KLHL3 E3 ligase complex mutated in Gordon's hypertension syndrome interacts with and ubiquitylates WNK isoforms: disease-causing mutations in KLHL3 and WNK4 disrupt interaction. *Biochemical Journal,* 451**,** 111-122.

Okkenhaug, K., Bilancio, A., Farjot, G., Priddle, H., Sancho, S., Peskett, E., Pearce, W., Meek, S. E., Salpekar, A., Waterfield, M. D., Smith, A. J. & Vanhaesebroeck, B. 2002. Impaired B and T cell antigen receptor signaling in p110delta PI 3-kinase mutant mice. *Science,* 297**,** 1031-4.

Oro, U., Sakaguchi, K., Appella, E. & Ashwell, J. D. 1996. Mutational analysis of Lck in CD45-negative T cells: dominant role of tyrosine 394 phosphorylation in kinase activity. *Molecular and Cellular Biology,* 16**,** 4996.

Ou, Y.-H., Chung, P.-H., Sun, T.-P. & Shieh, S.-Y. 2005. p53 C-terminal phosphorylation by CHK1 and CHK2 participates in the regulation of DNA-damage-induced C-terminal acetylation. *Molecular biology of the cell,* 16**,** 1684-1695.

Pacek, M., Tutter, A. V., Kubota, Y., Takisawa, H. & Walter, J. C. 2006. Localization of MCM2-7, Cdc45, and GINS to the site of DNA unwinding during eukaryotic DNA replication. *Mol Cell,* 21**,** 581-7.

Pacheco-Alvarez, D., Cristóbal, P. S., Meade, P., Moreno, E., Vazquez, N., Muñoz, E., Díaz, A., Juárez, M. E., Giménez, I. & Gamba, G. 2006. The Na+:Cl– Cotransporter Is Activated and Phosphorylated at the Amino-terminal Domain upon Intracellular Chloride Depletion*. *Journal of Biological Chemistry,* 281**,** 28755-28763.

Papa, I., Saliba, D., Ponzoni, M., Bustamante, S., Canete, P. F., Gonzalez-Figueroa, P., Mcnamara, H. A., Valvo, S., Grimbaldeston, M., Sweet, R. A., Vohra, H., Cockburn, I. A., Meyer-Hermann, M., Dustin, M. L., Doglioni, C. & Vinuesa, C. G. 2017. TFH-derived dopamine accelerates productive synapses in germinal centres. *Nature,* 547**,** 318-323.

Park, M.-J., Sheng, R., Silkov, A., Jung, D.-J., Wang, Z.-G., Xin, Y., Kim, H., Thiagarajan-Rosenkranz, P., Song, S., Yoon, Y., Nam, W., Kim, I., Kim, E., Lee, D.-G., Chen,

Y., Singaram, I., Wang, L., Jang, Myoung h., Hwang, C.-S., Honig, B., Ryu, S., Lorieau, J., Kim, Y.-M. & Cho, W. 2016. SH2 Domains Serve as Lipid-Binding Modules for pTyr-Signaling Proteins. *Molecular Cell,* 62**,** 7-20.

Pasham, V., Rotte, A., Yang, W., Zelenak, C., Bhandaru, M., Foller, M. & Lang, F. 2012. OSR1-sensitive regulation of Na+/H+ exchanger activity in dendritic cells. *Am J Physiol Cell Physiol,* 303**,** C416-26.

Paster, W., Bruger, A. M., Katsch, K., Grégoire, C., Roncagalli, R., Fu, G., Gascoigne, N. R. J., Nika, K., Cohnen, A., Feller, S. M., Simister, P. C., Molder, K. C., Cordoba, S.-P., Dushek, O., Malissen, B. & Acuto, O. 2015. A THEMIS:SHP1 complex promotes T-cell survival. *The EMBO journal,* 34**,** 393-409.

Pederson, S. F., Varming, C., Christensen, S. T. & Hoffmann, E. K. 2002. Mechanisms of activation of NHE by cell shrinkage and by calyculin A in Ehrlich ascites tumor cells. *J Membr Biol,* 189**,** 67-81.

Pelosi, M., Di Bartolo, V., Mounier, V., Mege, D., Pascussi, J. M., Dufour, E., Blondel, A. & Acuto, O. 1999. Tyrosine 319 in the interdomain B of ZAP-70 is a binding site for the Src homology 2 domain of Lck. *J Biol Chem,* 274**,** 14229-37.

Perona-Wright, G., Mohrs, K., Mayer, K. D. & Mohrs, M. 2010. Differential Regulation of IL-4Rα Expression by Antigen versus Cytokine Stimulation Characterizes Th2 Progression In Vivo. *The Journal of Immunology,* 184**,** 615.

Petrie, H. T., Livak, F., Schatz, D. G., Strasser, A., Crispe, I. N. & Shortman, K. 1993. Multiple rearrangements in T cell receptor alpha chain genes maximize the production of useful thymocytes. *Journal of Experimental Medicine,* 178**,** 615-622.

Pfeiffer, C. 1995. Altered peptide ligands can control CD4 T lymphocyte differentiation in vivo. 181**,** 1569-1574.

Philipsen, L., Reddycherla, A. V., Hartig, R., Gumz, J., Kästle, M., Kritikos, A., Poltorak, M. P., Prokazov, Y., Turbin, E., Weber, A., Zuschratter, W., Schraven, B., Simeoni, L. & Müller, A. J. 2017. De novo phosphorylation and conformational opening of the tyrosine kinase Lck act in concert to initiate T cell receptor signaling. *Science Signaling,* 10**,** eaaf4736.

Piala, A. T., Moon, T. M., Akella, R., He, H., Cobb, M. H. & Goldsmith, E. J. 2014. Chloride sensing by WNK1 involves inhibition of autophosphorylation. *Sci Signal,* 7**,** ra41.

Pilas, B. & Durack, G. 1997. A flow cytometric method for measurement of intracellular chloride concentration in lymphocytes using the halide-specific probe 6-methoxy-N-(3-sulfopropyl) quinolinium (SPQ). *Cytometry,* 28**,** 316-22.

Pimentel-Muinos, F. X., Mazana, J. & Fresno, M. 1994. Regulation of interleukin-2 receptor alpha chain expression and nuclear factor.kappa B activation by protein kinase C in T lymphocytes. Autocrine role of tumor necrosis factor alpha. *J Biol Chem,* 269**,** 24424-9.

Pletneva, E. V., Sundd, M., Fulton, D. B. & Andreotti, A. H. 2006. Molecular details of Itk activation by prolyl isomerization and phospholigand binding: the NMR structure of the Itk SH2 domain bound to a phosphopeptide. *J Mol Biol,* 357**,** 550-61.

Poholek, A. C., Hansen, K., Hernandez, S. G., Eto, D., Chandele, A., Weinstein, J. S., Dong, X., Odegard, J. M., Kaech, S. M., Dent, A. L., Crotty, S. & Craft, J. 2010. In Vivo Regulation of Bcl6 and T Follicular Helper Cell Development. *The Journal of Immunology,* 185**,** 313.

Ponta, H., Sherman, L. & Herrlich, P. A. 2003. CD44: from adhesion molecules to signalling regulators. *Nat Rev Mol Cell Biol,* 4**,** 33-45.

Prasad, K. V., Cai, Y. C., Raab, M., Duckworth, B., Cantley, L., Shoelson, S. E. & Rudd, C. E. 1994. T-cell antigen CD28 interacts with the lipid kinase phosphatidylinositol 3-kinase by a cytoplasmic Tyr(P)-Met-Xaa-Met motif. *Proceedings of the National Academy of Sciences,* 91**,** 2834.

Purvis, J. E., Karhohs, K. W., Mock, C., Batchelor, E., Loewer, A. & Lahav, G. 2012. p53 Dynamics Control Cell Fate. *Science,* 336**,** 1440.

Qin, X., Jiang, B. & Zhang, Y. 2016. 4E-BP1, a multifactor regulated multifunctional protein. *Cell cycle (Georgetown, Tex.),* 15**,** 781-786.

Raab, M., Lu, Y., Kohler, K., Smith, X., Strebhardt, K. & Rudd, C. E. 2017. LFA-1 activates focal adhesion kinases FAK1/PYK2 to generate LAT-GRB2-SKAP1 complexes that terminate T-cell conjugate formation. *Nature Communications,* 8**,** 16001.

Radulovic, K., Manta, C., Rossini, V., Holzmann, K., Kestler, H. A., Wegenka, U. M., Nakayama, T. & Niess, J. H. 2012. CD69 regulates type I IFN-induced tolerogenic signals to mucosal CD4 T cells that attenuate their colitogenic potential. *J Immunol,* 188**,** 2001-13.

Rafiqi, F. H., Zuber, A. M., Glover, M., Richardson, C., Fleming, S., Jovanovic, S., Jovanovic, A., O'shaughnessy, K. M. & Alessi, D. R. 2010. Role of the WNK-activated SPAK kinase in regulating blood pressure. *EMBO Mol Med,* 2**,** 63-75.

Rajarathnam, K., Schnoor, M., Richardson, R. M. & Rajagopal, S. 2019. How do chemokines navigate neutrophils to the target site: Dissecting the structural mechanisms and signaling pathways. *Cellular signalling,* 54**,** 69-80.

Rangarajan, S., He, Y., Chen, Y., Kerzic, M. C., Ma, B., Gowthaman, R., Pierce, B. G., Nussinov, R., Mariuzza, R. A. & Orban, J. 2018. Peptide-MHC (pMHC) binding to a human antiviral T cell receptor induces long-range allosteric communication between pMHC- and CD3-binding sites. *J Biol Chem,* 293**,** 15991-16005.

Ranger, A. M., Hodge, M. R., Gravallese, E. M., Oukka, M., Davidson, L., Alt, F. W., De La Brousse, F. C., Hoey, T., Grusby, M. & Glimcher, L. H. 1998. Delayed lymphoid repopulation with defects in IL-4-driven responses produced by inactivation of NF-ATc. *Immunity,* 8**,** 125-34.

Rata, S., Suarez Peredo Rodriguez, M. F., Joseph, S., Peter, N., Echegaray Iturra, F., Yang, F., Madzvamuse, A., Ruppert, J. G., Samejima, K., Platani, M., Alvarez-Fernandez, M., Malumbres, M., Earnshaw, W. C., Novak, B. & Hochegger, H. 2018. Two Interlinked Bistable Switches Govern Mitotic Control in Mammalian Cells. *Current Biology,* 28**,** 3824-3832.e6.

Razvag, Y., Neve-Oz, Y., Sajman, J., Reches, M. & Sherman, E. 2018. Nanoscale kinetic segregation of TCR and CD45 in engaged microvilli facilitates early T cell activation. *Nat Commun,* 9**,** 732.

Refaeli, Y., Van Parijs, L., London, C. A., Tschopp, J. & Abbas, A. K. 1998. Biochemical mechanisms of IL-2-regulated Fas-mediated T cell apoptosis. *Immunity,* 8**,** 615-23.

Reif, K., Ekland, E. H., Ohl, L., Nakano, H., Lipp, M., Förster, R. & Cyster, J. G. 2002. Balanced responsiveness to chemoattractants from adjacent zones determines B-cell position. *Nature,* 416**,** 94-99.

Reinhardt, R. L., Liang, H.-E. & Locksley, R. M. 2009. Cytokine-secreting follicular T cells shape the antibody repertoire. *Nature Immunology,* 10**,** 385-393.

Reis E Sousa, C., Hieny, S., Scharton-Kersten, T., Jankovic, D., Charest, H., Germain, R. N. & Sher, A. 1997. In vivo microbial stimulation induces rapid CD40 ligand-independent production of interleukin 12 by dendritic cells and their redistribution to T cell areas. *J Exp Med,* 186**,** 1819-29.

Revu, S., Wu, J., Henkel, M., Rittenhouse, N., Menk, A., Delgoffe, G. M., Poholek, A. C. & Mcgeachy, M. J. 2018. IL-23 and IL-1beta Drive Human Th17 Cell Differentiation and Metabolic Reprogramming in Absence of CD28 Costimulation. *Cell Rep,* 22**,** 2642-2653.

Reynolds, L. F., Smyth, L. A., Norton, T., Freshney, N., Downward, J., Kioussis, D. & Tybulewicz, V. L. J. 2002. Vav1 transduces T cell receptor signals to the activation of phospholipase C-gamma1 via phosphoinositide 3-kinase-dependent

and -independent pathways. *The Journal of experimental medicine,* 195**,** 1103-1114.

Ricci, M. S., Jin, Z., Dews, M., Yu, D., Thomas-Tikhonenko, A., Dicker, D. T. & El-Deiry, W. S. 2004. Direct repression of FLIP expression by c-myc is a major determinant of TRAIL sensitivity. *Mol Cell Biol,* 24**,** 8541-55.

Richardson, C., Rafiqi, F. H., Karlsson, H. K. R., Moleleki, N., Vandewalle, A., Campbell, D. G., Morrice, N. A. & Alessi, D. R. 2008. Activation of the thiazide-sensitive Na⁺-Cl[–] cotransporter by the WNK-regulated kinases SPAK and OSR1. *Journal of Cell Science,* 121**,** 675.

Ricklin, D., Hajishengallis, G., Yang, K. & Lambris, J. D. 2010. Complement: a key system for immune surveillance and homeostasis. *Nature Immunology,* 11**,** 785-797.

Riedl, S. J., Li, W., Chao, Y., Schwarzenbacher, R. & Shi, Y. 2005. Structure of the apoptotic protease-activating factor 1 bound to ADP. *Nature,* 434**,** 926-933.

Roco, J. A., Mesin, L., Binder, S. C., Nefzger, C., Gonzalez-Figueroa, P., Canete, P. F., Ellyard, J., Shen, Q., Robert, P. A., Cappello, J., Vohra, H., Zhang, Y., Nowosad, C. R., Schiepers, A., Corcoran, L. M., Toellner, K.-M., Polo, J. M., Meyer-Hermann, M., Victora, G. D. & Vinuesa, C. G. 2019. Class-Switch Recombination Occurs Infrequently in Germinal Centers. *Immunity,* 51**,** 337-350.e7.

Roose, J. P., Mollenauer, M., Ho, M., Kurosaki, T. & Weiss, A. 2007. Unusual interplay of two types of Ras activators, RasGRP and SOS, establishes sensitive and robust Ras activation in lymphocytes. *Mol Cell Biol,* 27**,** 2732-45.

Roozendaal, R., Mempel, T. R., Pitcher, L. A., Gonzalez, S. F., Verschoor, A., Mebius, R. E., Von Andrian, U. H. & Carroll, M. C. 2009. Conduits Mediate Transport of Low-Molecular-Weight Antigen to Lymph Node Follicles. *Immunity,* 30**,** 264-276.

Rousseau, D., Cannella, D., Boulaire, J., Fitzgerald, P., Fotedar, A. & Fotedar, R. 1999. Growth inhibition by CDK-cyclin and PCNA binding domains of p21 occurs by distinct mechanisms and is regulated by ubiquitin-proteasome pathway. *Oncogene,* 18**,** 4313-4325.

Roux, P. P., Shahbazian, D., Vu, H., Holz, M. K., Cohen, M. S., Taunton, J., Sonenberg, N. & Blenis, J. 2007. RAS/ERK signaling promotes site-specific ribosomal protein S6 phosphorylation via RSK and stimulates cap-dependent translation. *J Biol Chem,* 282**,** 14056-64.

Ruan, Q., Kameswaran, V., Tone, Y., Li, L., Liou, H.-C., Greene, M. I., Tone, M. & Chen, Y. H. 2009. Development of Foxp3(+) regulatory t cells is driven by the c-Rel enhanceosome. *Immunity,* 31**,** 932-940.

Samelson, L. E., Patel, M. D., Weissman, A. M., Harford, J. B. & Klausner, R. D. 1986. Antigen activation of murine T cells induces tyrosine phosphorylation of a polypeptide associated with the T cell antigen receptor. *Cell,* 46**,** 1083-1090.

Samelson, L. E., Phillips, A. F., Luong, E. T. & Klausner, R. D. 1990. Association of the fyn protein-tyrosine kinase with the T-cell antigen receptor. *Proceedings of the National Academy of Sciences,* 87**,** 4358-4362.

Saveliev, A., Vanes, L., Ksionda, O., Rapley, J., Smerdon, S. J., Rittinger, K. & Tybulewicz, V. L. J. 2009. Function of the Nucleotide Exchange Activity of Vav1 in T Cell Development and Activation. *Science Signaling,* 2**,** ra83.

Savic, V., Yin, B., Maas, N. L., Bredemeyer, A. L., Carpenter, A. C., Helmink, B. A., Yang-Iott, K. S., Sleckman, B. P. & Bassing, C. H. 2009. Formation of Dynamic γ-H2AX Domains along Broken DNA Strands Is Distinctly Regulated by ATM and MDC1 and Dependent upon H2AX Densities in Chromatin. *Molecular Cell,* 34**,** 298-310.

Scaffidi, C., Fulda, S., Srinivasan, A., Friesen, C., Li, F., Tomaselli, K. J., Debatin, K. M., Krammer, P. H. & Peter, M. E. 1998. Two CD95 (APO-1/Fas) signaling pathways. *EMBO J,* 17**,** 1675-87.

Schuh, K., Twardzik, T., Kneitz, B., Heyer, J., Schimpl, A. & Serfling, E. 1998. The interleukin 2 receptor alpha chain/CD25 promoter is a target for nuclear factor of activated T cells. *The Journal of experimental medicine,* 188**,** 1369-1373.

Schwartz, R. H. 2003. T Cell Anergy. *Annual Review of Immunology,* 21**,** 305-334.

Sears, R., Nuckolls, F., Haura, E., Taya, Y., Tamai, K. & Nevins, J. R. 2000. Multiple Ras-dependent phosphorylation pathways regulate Myc protein stability. *Genes Dev,* 14**,** 2501-14.

Sebzda, E., Bracke, M., Tugal, T., Hogg, N. & Cantrell, D. A. 2002. Rap1A positively regulates T cells via integrin activation rather than inhibiting lymphocyte signaling. *Nature Immunology,* 3**,** 251-258.

Shan, X., Czar, M. J., Bunnell, S. C., Liu, P., Liu, Y., Schwartzberg, P. L. & Wange, R. L. 2000. Deficiency of PTEN in Jurkat T cells causes constitutive localization of Itk to the plasma membrane and hyperresponsiveness to CD3 stimulation. *Mol Cell Biol,* 20**,** 6945-57.

Shen, H., Tesar, B. M., Walker, W. E. & Goldstein, D. R. 2008. Dual Signaling of MyD88 and TRIF Is Critical for Maximal TLR4-Induced Dendritic Cell Maturation. *The Journal of Immunology,* 181**,** 1849.

Sheu, Y. J. & Stillman, B. 2010. The Dbf4-Cdc7 kinase promotes S phase by alleviating an inhibitory activity in Mcm4. *Nature,* 463**,** 113-7.

Shi, J., Hou, S., Fang, Q., Liu, X., Liu, X. & Qi, H. 2018. PD-1 Controls Follicular T Helper Cell Positioning and Function. *Immunity,* 49**,** 264-274.e4.

Shi, M., Lin, T. H., Appell, K. C. & Berg, L. J. 2009. Cell cycle progression following naive T cell activation is independent of Jak3/common gamma-chain cytokine signals. *J Immunol,* 183**,** 4493-501.

Shiloh, Y. & Ziv, Y. 2013. The ATM protein kinase: regulating the cellular response to genotoxic stress, and more. *Nature Reviews Molecular Cell Biology,* 14**,** 197-210.

Shim, E. K., Jung, S. H. & Lee, J. R. 2011. Role of Two Adaptor Molecules SLP-76 and LAT in the PI3K Signaling Pathway in Activated T Cells. *The Journal of Immunology,* 186**,** 2926.

Shimonaka, M., Katagiri, K., Nakayama, T., Fujita, N., Tsuruo, T., Yoshie, O. & Kinashi, T. 2003. Rap1 translates chemokine signals to integrin activation, cell polarization, and motility across vascular endothelium under flow. *Journal of Cell Biology,* 161**,** 417-427.

Shin, S. Y., Kim, M. W., Cho, K. H. & Nguyen, L. K. 2019. Coupled feedback regulation of nuclear factor of activated T-cells (NFAT) modulates activation-induced cell death of T cells. *Sci Rep,* 9**,** 10637.

Shinkai, K., Mohrs, M. & Locksley, R. M. 2002. Helper T cells regulate type-2 innate immunity in vivo. *Nature,* 420**,** 825-9.

Shinkai, Y., Koyasu, S., Nakayama, K., Murphy, K. M., Loh, D. Y., Reinherz, E. L. & Alt, F. W. 1993. Restoration of T cell development in RAG-2-deficient mice by functional TCR transgenes. *Science,* 259**,** 822.

Shinkai, Y., Rathbun, G., Lam, K.-P., Oltz, E. M., Stewart, V., Mendelsohn, M., Charron, J., Datta, M., Young, F., Stall, A. M. & Alt, F. W. 1992. RAG-2-deficient mice lack mature lymphocytes owing to inability to initiate V(D)J rearrangement. *Cell,* 68**,** 855-867.

Shiotani, B. & Zou, L. 2009. Single-Stranded DNA Orchestrates an ATM-to-ATR Switch at DNA Breaks. *Molecular Cell,* 33**,** 547-558.

Shiow, L. R., Rosen, D. B., Brdickova, N., Xu, Y., An, J., Lanier, L. L., Cyster, J. G. & Matloubian, M. 2006. CD69 acts downstream of interferon-alpha/beta to inhibit S1P1 and lymphocyte egress from lymphoid organs. *Nature,* 440**,** 540-4.

Shulman, Z., Gitlin, A. D., Weinstein, J. S., Lainez, B., Esplugues, E., Flavell, R. A., Craft, J. E. & Nussenzweig, M. C. 2014. Dynamic signaling by T follicular helper cells during germinal center B cell selection. *Science,* 345**,** 1058.

Sinclair, L. V., Rolf, J., Emslie, E., Shi, Y.-B., Taylor, P. M. & Cantrell, D. A. 2013. Control of amino-acid transport by antigen receptors coordinates the metabolic reprogramming essential for T cell differentiation. *Nature Immunology,* 14**,** 500-508.

Singer, A., Adoro, S. & Park, J. H. 2008. Lineage fate and intense debate: myths, models and mechanisms of CD4- versus CD8-lineage choice. *Nat Rev Immunol,* 8**,** 788-801.

Sjölin-Goodfellow, H., Frushicheva, M. P., Ji, Q., Cheng, D. A., Kadlecek, T. A., Cantor, A. J., Kuriyan, J., Chakraborty, A. K., Salomon, A. R. & Weiss, A. 2015. The catalytic activity of the kinase ZAP-70 mediates basal signaling and negative feedback of the T cell receptor pathway. *Science Signaling,* 8**,** ra49.

Smith, C. W., Marlin, S. D., Rothlein, R., Toman, C. & Anderson, D. C. 1989. Cooperative interactions of LFA-1 and Mac-1 with intercellular adhesion molecule-1 in facilitating adherence and transendothelial migration of human neutrophils in vitro. *The Journal of Clinical Investigation,* 83**,** 2008-2017.

Snow, A. L., Oliveira, J. B., Zheng, L., Dale, J. K., Fleisher, T. A. & Lenardo, M. J. 2008. Critical role for BIM in T cell receptor restimulation-induced death. *Biol Direct,* 3**,** 34.

Solomon, M. J., Glotzer, M., Lee, T. H., Philippe, M. & Kirschner, M. W. 1990. Cyclin activation of p34cdc2. *Cell,* 63**,** 1013-1024.

Somyajit, K., Basavaraju, S., Scully, R. & Nagaraju, G. 2013. ATM- and ATR-Mediated Phosphorylation of XRCC3 Regulates DNA Double-Strand Break-Induced Checkpoint Activation and Repair. *Molecular and Cellular Biology,* 33**,** 1830.

Sørensen, C. S., Hansen, L. T., Dziegielewski, J., Syljuåsen, R. G., Lundin, C., Bartek, J. & Helleday, T. 2005. The cell-cycle checkpoint kinase Chk1 is required for mammalian homologous recombination repair. *Nature Cell Biology,* 7**,** 195-201.

Sørensen, C. S., Syljuåsen, R. G., Falck, J., Schroeder, T., Rönnstrand, L., Khanna, K. K., Zhou, B.-B., Bartek, J. & Lukas, J. 2003. Chk1 regulates the S phase checkpoint by coupling the physiological turnover and ionizing radiation-induced accelerated proteolysis of Cdc25A. *Cancer Cell,* 3**,** 247-258.

Soriano, S. F., Hons, M., Schumann, K., Kumar, V., Dennier, T. J., Lyck, R., Sixt, M. & Stein, J. V. 2011. In vivo analysis of uropod function during physiological T cell trafficking. *J Immunol,* 187**,** 2356-64.

Springer, T. A. & Dustin, M. L. 2012. Integrin inside-out signaling and the immunological synapse. *Curr Opin Cell Biol,* 24**,** 107-15.

Starr, T. K., Jameson, S. C. & Hogquist, K. A. 2003. Positive and negative selection of T cells. *Annu Rev Immunol,* 21**,** 139-76.

Štefanová, I., Hemmer, B., Vergelli, M., Martin, R., Biddison, W. E. & Germain, R. N. 2003. TCR ligand discrimination is enforced by competing ERK positive and SHP-1 negative feedback pathways. *Nature Immunology,* 4**,** 248-254.

Stiff, T., Walker, S. A., Cerosaletti, K., Goodarzi, A. A., Petermann, E., Concannon, P., O'driscoll, M. & Jeggo, P. A. 2006. ATR-dependent phosphorylation and activation of ATM in response to UV treatment or replication fork stalling. *The EMBO Journal,* 25**,** 5775-5782.

Stookey, J. D. 2005. High Prevalence of Plasma Hypertonicity among Community-Dwelling Older Adults: Results from NHANES III. *Journal of the American Dietetic Association,* 105**,** 1231-1239.

Su, X., Ditlev, J. A., Hui, E., Xing, W., Banjade, S., Okrut, J., King, D. S., Taunton, J., Rosen, M. K. & Vale, R. D. 2016. Phase separation of signaling molecules promotes T cell receptor signal transduction. *Science,* 352**,** 595-599.

Sun, J., Leahy, D. J. & Kavathas, P. B. 1995. Interaction between CD8 and major histocompatibility complex (MHC) class I mediated by multiple contact surfaces

that include the alpha 2 and alpha 3 domains of MHC class I. *The Journal of experimental medicine,* 182**,** 1275-1280.

Sun, X., Gao, L., Yu, R. K. & Zeng, G. 2006. Down-regulation of WNK1 protein kinase in neural progenitor cells suppresses cell proliferation and migration. *J Neurochem,* 99**,** 1114-21.

Sun, X. & Kaufman, P. D. 2018. Ki-67: more than a proliferation marker. *Chromosoma,* 127**,** 175-186.

Sun, Z., Arendt, C. W., Ellmeier, W., Schaeffer, E. M., Sunshine, M. J., Gandhi, L., Annes, J., Petrzilka, D., Kupfer, A., Schwartzberg, P. L. & Littman, D. R. 2000. PKC-theta is required for TCR-induced NF-kappaB activation in mature but not immature T lymphocytes. *Nature,* 404**,** 402-7.

Suto, A., Kashiwakuma, D., Kagami, S.-I., Hirose, K., Watanabe, N., Yokote, K., Saito, Y., Nakayama, T., Grusby, M. J., Iwamoto, I. & Nakajima, H. 2008. Development and characterization of IL-21–producing CD4+ T cells. *Journal of Experimental Medicine,* 205**,** 1369-1379.

Swaminathan, R., Hoang, C. P. & Verkman, A. S. 1997. Photobleaching recovery and anisotropy decay of green fluorescent protein GFP-S65T in solution and cells: cytoplasmic viscosity probed by green fluorescent protein translational and rotational diffusion. *Biophysical Journal,* 72**,** 1900-1907.

Szymczak, A. L., Workman, C. J., Gil, D., Dilioglou, S., Vignali, K. M., Palmer, E. & Vignali, D. A. 2005. The CD3epsilon proline-rich sequence, and its interaction with Nck, is not required for T cell development and function. *J Immunol,* 175**,** 270-5.

Tailor, P., Tsai, S., Shameli, A., Serra, P., Wang, J., Robbins, S., Nagata, M., Szymczak-Workman, A. L., Vignali, D. A. & Santamaria, P. 2008. The proline-rich sequence of CD3epsilon as an amplifier of low-avidity TCR signaling. *J Immunol,* 181**,** 243-55.

Takahashi, Y., Rayman, J. B. & Dynlacht, B. D. 2000. Analysis of promoter binding by the E2F and pRB families in vivo: distinct E2F proteins mediate activation and repression. *Genes & development,* 14**,** 804-816.

Takeuchi, O. & Akira, S. 2010. Pattern Recognition Receptors and Inflammation. *Cell,* 140**,** 805-820.

Terker, A. S., Zhang, C., Erspamer, K. J., Gamba, G., Yang, C. L. & Ellison, D. H. 2016. Unique chloride-sensing properties of WNK4 permit the distal nephron to modulate potassium homeostasis. *Kidney Int,* 89**,** 127-34.

Textor, J., Peixoto, A., Henrickson, S. E., Sinn, M., Von Andrian, U. H. & Westermann, J. 2011. Defining the quantitative limits of intravital two-photon lymphocyte tracking. *Proc Natl Acad Sci U S A,* 108**,** 12401-6.

Thastrup, Jacob o., Rafiqi, Fatema h., Vitari, Alberto c., Pozo-Guisado, E., Deak, M., Mehellou, Y. & Alessi, Dario r. 2011. SPAK/OSR1 regulate NKCC1 and WNK activity: analysis of WNK isoform interactions and activation by T-loop trans-autophosphorylation. *Biochemical Journal,* 441**,** 325-337.

Thiemicke, A. & Neuert, G. 2021. Kinetics of osmotic stress regulate a cell fate switch of cell survival. *Sci Adv,* 7.

Thieu, V. T., Yu, Q., Chang, H.-C., Yeh, N., Nguyen, E. T., Sehra, S. & Kaplan, M. H. 2008. Signal Transducer and Activator of Transcription 4 Is Required for the Transcription Factor T-bet to Promote T Helper 1 Cell-Fate Determination. *Immunity,* 29**,** 679-690.

Thompson, C. B., Lindsten, T., Ledbetter, J. A., Kunkel, S. L., Young, H. A., Emerson, S. G., Leiden, J. M. & June, C. H. 1989. CD28 activation pathway regulates the production of multiple T-cell-derived lymphokines/cytokines. *Proceedings of the National Academy of Sciences,* 86**,** 1333-1337.

Tibbitt, C., Falconer, J., Stoop, J., Van Eden, W., Robinson, J. H. & Hilkens, C. M. U. 2016. Reduced TCR-dependent activation through citrullination of a T-cell

epitope enhances Th17 development by disruption of the STAT3/5 balance. *European Journal of Immunology,* 46**,** 1633-1643.

Timofeev, O., Schlereth, K., Wanzel, M., Braun, A., Nieswandt, B., Pagenstecher, A., Rosenwald, A., Elsässer, H.-P. & Stiewe, T. 2013. p53 DNA Binding Cooperativity Is Essential for Apoptosis and Tumor Suppression In Vivo. *Cell Reports,* 3**,** 1512-1525.

Titze, J. 2014. Sodium balance is not just a renal affair. *Current Opinion in Nephrology and Hypertension,* 23**,** 101-105.

Toellner, K.-M., Luther, S. A., Sze, D. M. Y., Choy, R. K. W., Taylor, D. R., Maclennan, I. C. M. & Acha-Orbea, H. 1998. T Helper 1 (Th1) and Th2 Characteristics Start to Develop During T Cell Priming and Are Associated with an Immediate Ability to Induce Immunoglobulin Class Switching. *Journal of Experimental Medicine,* 187**,** 1193-1204.

Toledo, Luis i., Altmeyer, M., Rask, M.-B., Lukas, C., Larsen, Dorthe h., Povlsen, Lou k., Bekker-Jensen, S., Mailand, N., Bartek, J. & Lukas, J. 2013. ATR Prohibits Replication Catastrophe by Preventing Global Exhaustion of RPA. *Cell,* 155**,** 1088-1103.

Tone, Y., Furuuchi, K., Kojima, Y., Tykocinski, M. L., Greene, M. I. & Tone, M. 2008. Smad3 and NFAT cooperate to induce Foxp3 expression through its enhancer. *Nature Immunology,* 9**,** 194-202.

Touma, M., Chang, H. C., Sasada, T., Handley, M., Clayton, L. K. & Reinherz, E. L. 2006. The TCR C beta FG loop regulates alpha beta T cell development. *J Immunol,* 176**,** 6812-23.

Trenz, K., Errico, A. & Costanzo, V. 2008. Plx1 is required for chromosomal DNA replication under stressful conditions. *The EMBO Journal,* 27**,** 876-885.

Tsytsykova, A. V. & Goldfeld, A. E. 2000. Nuclear Factor of Activated T Cells Transcription Factor Nfatp Controls Superantigen-Induced Lethal Shock. *The Journal of Experimental Medicine,* 192**,** 581-586.

Tubo, N. J., Pagan, A. J., Taylor, J. J., Nelson, R. W., Linehan, J. L., Ertelt, J. M., Huseby, E. S., Way, S. S. & Jenkins, M. K. 2013. Single naive CD4+ T cells from a diverse repertoire produce different effector cell types during infection. *Cell,* 153**,** 785-96.

Ueffing, N., Schuster, M., Keil, E., Schulze-Osthoff, K. & Schmitz, I. 2008. Up-regulation of c-FLIP short by NFAT contributes to apoptosis resistance of short-term activated T cells. *Blood,* 112**,** 690-8.

Uhlik, M. T., Abell, A. N., Johnson, N. L., Sun, W., Cuevas, B. D., Lobel-Rice, K. E., Horne, E. A., Dell'acqua, M. L. & Johnson, G. L. 2003. Rac-MEKK3-MKK3 scaffolding for p38 MAPK activation during hyperosmotic shock. *Nat Cell Biol,* 5**,** 1104-10.

Van Parijs, L., Biuckians, A. & Abbas, A. K. 1998. Functional roles of Fas and Bcl-2-regulated apoptosis of T lymphocytes. *J Immunol,* 160**,** 2065-71.

Varma, R., Campi, G., Yokosuka, T., Saito, T. & Dustin, M. L. 2006. T cell receptor-proximal signals are sustained in peripheral microclusters and terminated in the central supramolecular activation cluster. *Immunity,* 25**,** 117-27.

Veillette, A., Bookman, M. A., Horak, E. M. & Bolen, J. B. 1988. The CD4 and CD8 T cell surface antigens are associated with the internal membrane tyrosine-protein kinase p56lck. *Cell,* 55**,** 301-308.

Verissimo, F. & Jordan, P. 2001. WNK kinases, a novel protein kinase subfamily in multi-cellular organisms. *Oncogene,* 20**,** 5562-9.

Vitari, A. C., Deak, M., Collins, B. J., Morrice, N., Prescott, A. R., Phelan, A., Humphreys, S. & Alessi, D. R. 2004. WNK1, the kinase mutated in an inherited high-blood-pressure syndrome, is a novel PKB (protein kinase B)/Akt substrate. *Biochem J,* 378**,** 257-68.

Vitari, A. C., Deak, M., Morrice, N. A. & Alessi, D. R. 2005. The WNK1 and WNK4 protein kinases that are mutated in Gordon's hypertension syndrome phosphorylate and activate SPAK and OSR1 protein kinases. *Biochem J,* 391**,** 17-24.

Vitari, Alberto c., Thastrup, J., Rafiqi, Fatema h., Deak, M., Morrice, Nick a., Karlsson, Håkan k. R. & Alessi, Dario r. 2006. Functional interactions of the SPAK/OSR1 kinases with their upstream activator WNK1 and downstream substrate NKCC1. *Biochemical Journal,* 397**,** 223-231.

Vivien, L., Benoist, C. & Mathis, D. 2001. T lymphocytes need IL-7 but not IL-4 or IL-6 to survive in vivo. *International Immunology,* 13**,** 763-768.

Vyas, J. M., Kim, Y.-M., Artavanis-Tsakonas, K., Love, J. C., Van Der Veen, A. G. & Ploegh, H. L. 2007. Tubulation of Class II MHC Compartments Is Microtubule Dependent and Involves Multiple Endolysosomal Membrane Proteins in Primary Dendritic Cells. *The Journal of Immunology,* 178**,** 7199.

Wabnitz, G. H., Nebl, G., Klemke, M., Schröder, A. J. & Samstag, Y. 2006. Phosphatidylinositol 3-Kinase Functions as a Ras Effector in the Signaling Cascade That Regulates Dephosphorylation of the Actin-Remodeling Protein Cofilin after Costimulation of Untransformed Human T Lymphocytes. *The Journal of Immunology,* 176**,** 1668.

Wan, Y. Y. & Degregori, J. 2003. The survival of antigen-stimulated T cells requires NFkappaB-mediated inhibition of p73 expression. *Immunity,* 18**,** 331-42.

Wang, H., Kadlecek, T. A., Au-Yeung, B. B., Goodfellow, H. E. S., Hsu, L. Y., Freedman, T. S. & Weiss, A. 2010. ZAP-70: An Essential Kinase in T-cell Signaling. *Cold Spring Harbor Perspectives in Biology,* 2**,** a002279-a002279.

Wang, H., Mccann, F. E., Gordan, J. D., Wu, X., Raab, M., Malik, T. H., Davis, D. M. & Rudd, C. E. 2004. ADAP–SLP-76 Binding Differentially Regulates Supramolecular Activation Cluster (SMAC) Formation Relative to T Cell–APC Conjugation. *Journal of Experimental Medicine,* 200**,** 1063-1074.

Wang, J., Gong, Z. & Chen, J. 2011a. MDC1 collaborates with TopBP1 in DNA replication checkpoint control. *Journal of Cell Biology,* 193**,** 267-273.

Wang, L., Dai, W. & Lu, L. 2014. Osmotic stress-induced phosphorylation of H2AX by polo-like kinase 3 affects cell cycle progression in human corneal epithelial cells. *The Journal of biological chemistry,* 289**,** 29827-29835.

Wang, R., Dillon, C. P., Shi, L. Z., Milasta, S., Carter, R., Finkelstein, D., Mccormick, L. L., Fitzgerald, P., Chi, H., Munger, J. & Green, D. R. 2011b. The transcription factor Myc controls metabolic reprogramming upon T lymphocyte activation. *Immunity,* 35**,** 871-82.

Ward, I. M. & Chen, J. 2001. Histone H2AX Is Phosphorylated in an ATR-dependent Manner in Response to Replicational Stress. *Journal of Biological Chemistry,* 276**,** 47759-47762.

Wardenburg, J. B., Fu, C., Jackman, J. K., Flotow, H., Wilkinson, S. E., Williams, D. H., Johnson, R., Kong, G., Chan, A. C. & Findell, P. R. 1996. Phosphorylation of SLP-76 by the ZAP-70 Protein-tyrosine Kinase Is Required for T-cell Receptor Function *. *Journal of Biological Chemistry,* 271**,** 19641-19644.

Watanabe, K., Umeda, T., Niwa, K., Naguro, I. & Ichijo, H. 2018. A PP6-ASK3 Module Coordinates the Bidirectional Cell Volume Regulation under Osmotic Stress. *Cell Reports,* 22**,** 2809-2817.

Weber, J. P., Fuhrmann, F., Feist, R. K., Lahmann, A., Al Baz, M. S., Gentz, L.-J., Vu Van, D., Mages, H. W., Haftmann, C., Riedel, R., Grün, J. R., Schuh, W., Kroczek, R. A., Radbruch, A., Mashreghi, M.-F. & Hutloff, A. 2015. ICOS maintains the T follicular helper cell phenotype by down-regulating Krüppel-like factor 2. *Journal of Experimental Medicine,* 212**,** 217-233.

Wei, L., Laurence, A., Elias, K. M. & O'shea, J. J. 2007a. IL-21 is produced by Th17 cells and drives IL-17 production in a STAT3-dependent manner. *The Journal of biological chemistry,* 282**,** 34605-34610.

Wei, S. H., Safrina, O., Yu, Y., Garrod, K. R., Cahalan, M. D. & Parker, I. 2007b. Ca2+ signals in CD4+ T cells during early contacts with antigen-bearing dendritic cells in lymph node. *J Immunol,* 179**,** 1586-94.

Welburn, J. P. I., Tucker, J. A., Johnson, T., Lindert, L., Morgan, M., Willis, A., Noble, M. E. M. & Endicott, J. A. 2007. How Tyrosine 15 Phosphorylation Inhibits the Activity of Cyclin-dependent Kinase 2-Cyclin A. *Journal of Biological Chemistry,* 282**,** 3173-3181.

Willerford, D. M., Chen, J., Ferry, J. A., Davidson, L., Ma, A. & Alt, F. W. 1995. Interleukin-2 receptor alpha chain regulates the size and content of the peripheral lymphoid compartment. *Immunity,* 3**,** 521-30.

Williams, J. A., Hathcock, K. S., Klug, D., Harada, Y., Choudhury, B., Allison, J. P., Abe, R. & Hodes, R. J. 2005. Regulated Costimulation in the Thymus Is Critical for T Cell Development: Dysregulated CD28 Costimulation Can Bypass the Pre-TCR Checkpoint. *The Journal of Immunology,* 175**,** 4199.

Wilson, A., De Villartay, J.-P. & Macdonald, H. R. 1996. T Cell Receptor δ Gene Rearrangement and T Early α (TEA) Expression in Immature αβ LineageThymocytes: Implications for αβ/γδ Lineage Commitment. *Immunity,* 4**,** 37-45.

Wilson, F. H., Disse-Nicodème, S., Choate, K. A., Ishikawa, K., Nelson-Williams, C., Desitter, I., Gunel, M., Milford, D. V., Lipkin, G. W., Achard, J.-M., Feely, M. P., Dussol, B., Berland, Y., Unwin, R. J., Mayan, H., Simon, D. B., Farfel, Z., Jeunemaitre, X. & Lifton, R. P. 2001. Human Hypertension Caused by Mutations in WNK Kinases. *Science,* 293**,** 1107.

Winkler, D. G., Park, I., Kim, T., Payne, N. S., Walsh, C. T., Strominger, J. L. & Shin, J. 1993. Phosphorylation of Ser-42 and Ser-59 in the N-terminal region of the tyrosine kinase p56lck. *Proceedings of the National Academy of Sciences of the United States of America,* 90**,** 5176-5180.

Woehrle, T., Yip, L., Manohar, M., Sumi, Y., Yao, Y., Chen, Y. & Junger, W. G. 2010. Hypertonic stress regulates T cell function via pannexin-1 hemichannels and P2X receptors. *Journal of Leukocyte Biology,* 88**,** 1181-1189.

Woolf, E., Grigorova, I., Sagiv, A., Grabovsky, V., Feigelson, S. W., Shulman, Z., Hartmann, T., Sixt, M., Cyster, J. G. & Alon, R. 2007. Lymph node chemokines promote sustained T lymphocyte motility without triggering stable integrin adhesiveness in the absence of shear forces. *Nat Immunol,* 8**,** 1076-85.

Worbs, T., Mempel, T. R., Bolter, J., Von Andrian, U. H. & Forster, R. 2007. CCR7 ligands stimulate the intranodal motility of T lymphocytes in vivo. *J Exp Med,* 204**,** 489-95.

Wu, J., Katrekar, A., Honigberg, L. A., Smith, A. M., Conn, M. T., Tang, J., Jeffery, D., Mortara, K., Sampang, J., Williams, S. R., Buggy, J. & Clark, J. M. 2006a. Identification of Substrates of Human Protein-tyrosine Phosphatase PTPN22. *Journal of Biological Chemistry,* 281**,** 11002-11010.

Wu, J. N., Gheith, S., Bezman, N. A., Liu, Q.-H., Fostel, L. V., Swanson, A. M., Freedman, B. D., Koretzky, G. A. & Peterson, E. J. 2006b. Adhesion- and Degranulation-Promoting Adapter Protein Is Required for Efficient Thymocyte Development and Selection. *The Journal of Immunology,* 176**,** 6681.

Wu, X., Shell, S. M., Liu, Y. & Zou, Y. 2007. ATR-dependent checkpoint modulates XPA nuclear import in response to UV irradiation. *Oncogene,* 26**,** 757-764.

Wurster, A. L., Rodgers, V. L., White, M. F., Rothstein, T. L. & Grusby, M. J. 2002. Interleukin-4-mediated protection of primary B cells from apoptosis through Stat6-dependent up-regulation of Bcl-xL. *J Biol Chem,* 277**,** 27169-75.

Xiao, S., Matsui, K., Fine, A., Zhu, B., Marshak-Rothstein, A., Widom, R. L. & Ju, S. T. 1999. FasL promoter activation by IL-2 through SP1 and NFAT but not Egr-2 and Egr-3. *Eur J Immunol,* 29**,** 3456-65.

Xie, J., Wu, T., Xu, K., Huang, I. K., Cleaver, O. & Huang, C. L. 2009. Endothelial-specific expression of WNK1 kinase is essential for angiogenesis and heart development in mice. *Am J Pathol,* 175**,** 1315-27.

Xie, J., Yoon, J., Yang, S. S., Lin, S. H. & Huang, C. L. 2013. WNK1 protein kinase regulates embryonic cardiovascular development through the OSR1 signaling cascade. *J Biol Chem,* 288**,** 8566-74.

Xu, B. E., Stippec, S., Lazrak, A., Huang, C. L. & Cobb, M. H. 2005. WNK1 activates SGK1 by a phosphatidylinositol 3-kinase-dependent and non-catalytic mechanism. *J Biol Chem,* 280**,** 34218-23.

Xu, B. E., Stippec, S., Lenertz, L., Lee, B. H., Zhang, W., Lee, Y. K. & Cobb, M. H. 2004. WNK1 activates ERK5 by an MEKK2/3-dependent mechanism. *J Biol Chem,* 279**,** 7826-31.

Xu, M., Sheppard, K. A., Peng, C. Y., Yee, A. S. & Piwnica-Worms, H. 1994. Cyclin A/CDK2 binds directly to E2F-1 and inhibits the DNA-binding activity of E2F-1/DP-1 by phosphorylation. *Molecular and Cellular Biology,* 14**,** 8420.

Xu, W., Doshi, A., Lei, M., Eck, M. J. & Harrison, S. C. 1999. Crystal Structures of c-Src Reveal Features of Its Autoinhibitory Mechanism. *Molecular Cell,* 3**,** 629-638.

Xu, W., Harrison, S. C. & Eck, M. J. 1997. Three-dimensional structure of the tyrosine kinase c-Src. *Nature,* 385**,** 595-602.

Yamada, K., Park, H.-M., Rigel, D. F., Dipetrillo, K., Whalen, E. J., Anisowicz, A., Beil, M., Berstler, J., Brocklehurst, C. E., Burdick, D. A., Caplan, S. L., Capparelli, M. P., Chen, G., Chen, W., Dale, B., Deng, L., Fu, F., Hamamatsu, N., Harasaki, K., Herr, T., Hoffmann, P., Hu, Q.-Y., Huang, W.-J., Idamakanti, N., Imase, H., Iwaki, Y., Jain, M., Jeyaseelan, J., Kato, M., Kaushik, V. K., Kohls, D., Kunjathoor, V., Lasala, D., Lee, J., Liu, J., Luo, Y., Ma, F., Mo, R., Mowbray, S., Mogi, M., Ossola, F., Pandey, P., Patel, S. J., Raghavan, S., Salem, B., Shanado, Y. H., Trakshel, G. M., Turner, G., Wakai, H., Wang, C., Weldon, S., Wielicki, J. B., Xie, X., Xu, L., Yagi, Y. I., Yasoshima, K., Yin, J., Yowe, D., Zhang, J.-H., Zheng, G. & Monovich, L. 2016. Small-molecule WNK inhibition regulates cardiovascular and renal function. *Nature Chemical Biology,* 12**,** 896-898.

Yamane, H., Zhu, J. & Paul, W. E. 2005. Independent roles for IL-2 and GATA-3 in stimulating naive CD4+ T cells to generate a Th2-inducing cytokine environment. *Journal of Experimental Medicine,* 202**,** 793-804.

Yamasaki, S., Ishikawa, E., Sakuma, M., Ogata, K., Sakata-Sogawa, K., Hiroshima, M., Wiest, D. L., Tokunaga, M. & Saito, T. 2006. Mechanistic basis of pre–T cell receptor–mediated autonomous signaling critical for thymocyte development. *Nature Immunology,* 7**,** 67-75.

Yang, J., Zhu, H., Murphy, T. L., Ouyang, W. & Murphy, K. M. 2001. IL-18–stimulated GADD45β required in cytokine-induced, but not TCR-induced, IFN-γ production. *Nature Immunology,* 2**,** 157-164.

Yang, K., Shrestha, S., Zeng, H., Karmaus, P. W., Neale, G., Vogel, P., Guertin, D. A., Lamb, R. F. & Chi, H. 2013. T cell exit from quiescence and differentiation into Th2 cells depend on Raptor-mTORC1-mediated metabolic reprogramming. *Immunity,* 39**,** 1043-56.

Yang, M., Chen, T., Li, X., Yu, Z., Tang, S., Wang, C., Gu, Y., Liu, Y., Xu, S., Li, W., Zhang, X., Wang, J. & Cao, X. 2015. K33-linked polyubiquitination of Zap70 by Nrdp1 controls CD8+ T cell activation. *Nature Immunology,* 16**,** 1253-1262.

Yang, T., Zhao, K., Shu, H., Chen, X., Cheng, J., Li, S., Zhao, Z., Kuang, Y. & Yu, S. 2017. The Nogo receptor inhibits proliferation, migration and axonal extension by transcriptionally regulating WNK1 in PC12 cells. *Neuroreport,* 28**,** 533-539.

Yang, X. O., Pappu, B. P., Nurieva, R., Akimzhanov, A., Kang, H. S., Chung, Y., Ma, L., Shah, B., Panopoulos, A. D., Schluns, K. S., Watowich, S. S., Tian, Q., Jetten, A. M. & Dong, C. 2008. T Helper 17 Lineage Differentiation Is Programmed by Orphan Nuclear Receptors RORα and RORγ. *Immunity,* 28**,** 29-39.

Yang, Y., Chang, J.-F., Parnes, J. R. & Garrison Fathman, C. 1998. T Cell Receptor (TCR) Engagement Leads to Activation-induced Splicing of Tumor Necrosis Factor (TNF) Nuclear Pre-mRNA. *Journal of Experimental Medicine,* 188**,** 247-254.

Yao, G., Lee, T. J., Mori, S., Nevins, J. R. & You, L. 2008. A bistable Rb–E2F switch underlies the restriction point. *Nature Cell Biology,* 10**,** 476-482.

Yao, S., Zhu, Y., Zhu, G., Augustine, M., Zheng, L., Goode, D. J., Broadwater, M., Ruff, W., Flies, S., Xu, H., Flies, D., Luo, L., Wang, S. & Chen, L. 2011. B7-h2 is a costimulatory ligand for CD28 in human. *Immunity,* 34**,** 729-40.

Ye, J., Shi, H., Shen, Y., Peng, C., Liu, Y., Li, C., Deng, K., Geng, J., Xu, T., Zhuang, Y., Zheng, B. & Tao, W. 2015. PP6 Controls T Cell Development and Homeostasis by Negatively Regulating Distal TCR Signaling. *The Journal of Immunology,* 194**,** 1654.

Yeeles, J. T., Deegan, T. D., Janska, A., Early, A. & Diffley, J. F. 2015. Regulated eukaryotic DNA replication origin firing with purified proteins. *Nature,* 519**,** 431-5.

Yeh, J. H., Lecine, P., Nunes, J. A., Spicuglia, S., Ferrier, P., Olive, D. & Imbert, J. 2001. Novel CD28-responsive enhancer activated by CREB/ATF and AP-1 families in the human interleukin-2 receptor alpha-chain locus. *Mol Cell Biol,* 21**,** 4515-27.

Yekezare, M., Gomez-Gonzalez, B. & Diffley, J. F. 2013. Controlling DNA replication origins in response to DNA damage - inhibit globally, activate locally. *J Cell Sci,* 126**,** 1297-306.

Yokosuka, T., Sakata-Sogawa, K., Kobayashi, W., Hiroshima, M., Hashimoto-Tane, A., Tokunaga, M., Dustin, M. L. & Saito, T. 2005. Newly generated T cell receptor microclusters initiate and sustain T cell activation by recruitment of Zap70 and SLP-76. *Nature Immunology,* 6**,** 1253-1262.

Yoo, H. Y., Kumagai, A., Shevchenko, A., Shevchenko, A. & Dunphy, W. G. 2007. Ataxia-telangiectasia Mutated (ATM)-dependent Activation of ATR Occurs through Phosphorylation of TopBP1 by ATM*. *Journal of Biological Chemistry,* 282**,** 17501-17506.

You, Z., Bailis, J. M., Johnson, S. A., Dilworth, S. M. & Hunter, T. 2007. Rapid activation of ATM on DNA flanking double-strand breaks. *Nature Cell Biology,* 9**,** 1311-1318.

Young, J. D., Yao, S. Y. M., Baldwin, J. M., Cass, C. E. & Baldwin, S. A. 2013. The human concentrative and equilibrative nucleoside transporter families, SLC28 and SLC29. *Molecular Aspects of Medicine,* 34**,** 529-547.

Yousefi, O. S., Gunther, M., Horner, M., Chalupsky, J., Wess, M., Brandl, S. M., Smith, R. W., Fleck, C., Kunkel, T., Zurbriggen, M. D., Hofer, T., Weber, W. & Schamel, W. W. 2019. Optogenetic control shows that kinetic proofreading regulates the activity of the T cell receptor. *Elife,* 8.

Yu, B., Martins, I. R., Li, P., Amarasinghe, G. K., Umetani, J., Fernandez-Zapico, M. E., Billadeau, D. D., Machius, M., Tomchick, D. R. & Rosen, M. K. 2010. Structural and energetic mechanisms of cooperative autoinhibition and activation of Vav1. *Cell,* 140**,** 246-56.

Yu, D., Rao, S., Tsai, L. M., Lee, S. K., He, Y., Sutcliffe, E. L., Srivastava, M., Linterman, M., Zheng, L., Simpson, N., Ellyard, J. I., Parish, I. A., Ma, C. S., Li, Q.-J., Parish, C. R., Mackay, C. R. & Vinuesa, C. G. 2009. The Transcriptional Repressor Bcl-6 Directs T Follicular Helper Cell Lineage Commitment. *Immunity,* 31**,** 457-468.

Yui, M. A., Feng, N. & Rothenberg, E. V. 2010. Fine-Scale Staging of T Cell Lineage Commitment in Adult Mouse Thymus. *The Journal of Immunology,* 185**,** 284.

Zagorska, A., Pozo-Guisado, E., Boudeau, J., Vitari, A. C., Rafiqi, F. H., Thastrup, J., Deak, M., Campbell, D. G., Morrice, N. A., Prescott, A. R. & Alessi, D. R. 2007. Regulation of activity and localization of the WNK1 protein kinase by hyperosmotic stress. *J Cell Biol,* 176**,** 89-100.

Zambrowicz, B. P., Abuin, A., Ramirez-Solis, R., Richter, L. J., Piggott, J., Beltrandelrio, H., Buxton, E. C., Edwards, J., Finch, R. A., Friddle, C. J., Gupta, A., Hansen, G., Hu, Y., Huang, W., Jaing, C., Key, B. W., Jr., Kipp, P., Kohlhauff, B., Ma, Z. Q., Markesich, D., Payne, R., Potter, D. G., Qian, N., Shaw, J., Schrick, J., Shi, Z. Z., Sparks, M. J., Van Sligtenhorst, I., Vogel, P., Walke, W., Xu, N., Zhu, Q., Person, C. & Sands, A. T. 2003. Wnk1 kinase deficiency lowers blood pressure in mice: a gene-trap screen to identify potential targets for therapeutic intervention. *Proc Natl Acad Sci U S A,* 100**,** 14109-14.

Zhang, H., Cordoba, S. P., Dushek, O. & Van Der Merwe, P. A. 2011a. Basic residues in the T-cell receptor zeta cytoplasmic domain mediate membrane association and modulate signaling. *Proc Natl Acad Sci U S A,* 108**,** 19323-8.

Zhang, W., Sloan-Lancaster, J., Kitchen, J., Trible, R. P. & Samelson, L. E. 1998. LAT: The ZAP-70 Tyrosine Kinase Substrate that Links T Cell Receptor to Cellular Activation. *Cell,* 92**,** 83-92.

Zhang, W., Sommers, C. L., Burshtyn, D. N., Stebbins, C. C., Dejarnette, J. B., Trible, R. P., Grinberg, A., Tsay, H. C., Jacobs, H. M., Kessler, C. M., Long, E. O., Love, P. E. & Samelson, L. E. 1999. Essential role of LAT in T cell development. *Immunity,* 10**,** 323-32.

Zhang, W., Trible, R. P., Zhu, M., Liu, S. K., Mcglade, C. J. & Samelson, L. E. 2000. Association of Grb2, Gads, and phospholipase C-gamma 1 with phosphorylated LAT tyrosine residues. Effect of LAT tyrosine mutations on T cell angigen receptor-mediated signaling. *J Biol Chem,* 275**,** 23355-61.

Zhang, Y., Gao, Y., Zhang, G., Huang, S., Dong, Z., Kong, C., Su, D., Du, J., Zhu, S., Liang, Q., Zhang, J., Lu, J. & Huang, B. 2011b. DNMT3a plays a role in switches between doxorubicin-induced senescence and apoptosis of colorectal cancer cells. *International Journal of Cancer,* 128**,** 551-561.

Zhang, Y. J., Zheng, H. Q., Chen, B. Y., Sun, L., Ma, M. M., Wang, G. L. & Guan, Y. Y. 2018. WNK1 is required for proliferation induced by hypotonic challenge in rat vascular smooth muscle cells. *Acta Pharmacol Sin,* 39**,** 35-47.

Zhang, Z., Dmitrieva, N. I., Park, J.-H., Levine, R. L. & Burg, M. B. 2004. High urea and NaCl carbonylate proteins in renal cells in culture and in vivo, and high urea causes 8-oxoguanine lesions in their DNA. *Proceedings of the National Academy of Sciences of the United States of America,* 101**,** 9491.

Zheng, L., Fisher, G., Miller, R. E., Peschon, J., Lynch, D. H. & Lenardo, M. J. 1995. Induction of apoptosis in mature T cells by tumour necrosis factor. *Nature,* 377**,** 348-51.

Zheng, L., Trageser, C. L., Willerford, D. M. & Lenardo, M. J. 1998. T cell growth cytokines cause the superinduction of molecules mediating antigen-induced T lymphocyte death. *J Immunol,* 160**,** 763-9.

Zhou, L., Lopes, J. E., Chong, M. M. W., Ivanov, I. I., Min, R., Victora, G. D., Shen, Y., Du, J., Rubtsov, Y. P., Rudensky, A. Y., Ziegler, S. F. & Littman, D. R. 2008. TGF-β-induced Foxp3 inhibits TH17 cell differentiation by antagonizing RORγt function. *Nature,* 453**,** 236-240.

Zhu, J., Min, B., Hu-Li, J., Watson, C. J., Grinberg, A., Wang, Q., Killeen, N., Urban, J. F., Jr., Guo, L. & Paul, W. E. 2004. Conditional deletion of Gata3 shows its essential function in T(H)1-T(H)2 responses. *Nat Immunol,* 5**,** 1157-65.

Zhu, J., Yamane, H. & Paul, W. E. 2010. Differentiation of effector CD4 T cell populations (*). *Annual review of immunology,* 28**,** 445-489.

Zikherman, J., Jenne, C., Watson, S., Doan, K., Raschke, W., Goodnow, C. C. & Weiss, A. 2010. CD45-Csk Phosphatase-Kinase Titration Uncouples Basal and Inducible T Cell Receptor Signaling during Thymic Development. *Immunity,* 32**,** 342-354.

Ziv, Y., Bielopolski, D., Galanty, Y., Lukas, C., Taya, Y., Schultz, D. C., Lukas, J., Bekker-Jensen, S., Bartek, J. & Shiloh, Y. 2006. Chromatin relaxation in response to DNA double-strand breaks is modulated by a novel ATM- and KAP-1 dependent pathway. *Nature Cell Biology,* 8**,** 870-876.

Zong, W. X., Edelstein, L. C., Chen, C., Bash, J. & Gelinas, C. 1999. The prosurvival Bcl-2 homolog Bfl-1/A1 is a direct transcriptional target of NF-kappaB that blocks TNFalpha-induced apoptosis. *Genes Dev,* 13**,** 382-7.

Zotos, D., Coquet, J. M., Zhang, Y., Light, A., D'costa, K., Kallies, A., Corcoran, L. M., Godfrey, D. I., Toellner, K.-M., Smyth, M. J., Nutt, S. L. & Tarlinton, D. M. 2010. IL-21 regulates germinal center B cell differentiation and proliferation through a B cell–intrinsic mechanism. *Journal of Experimental Medicine,* 207**,** 365-378.

Zou, L., Liu, D. & Elledge, S. J. 2003. Replication protein A-mediated recruitment and activation of Rad17 complexes. *Proceedings of the National Academy of Sciences,* 100**,** 13827.